4-22-2016 12:00 AM

Analysis and Design Procedure for Liquid-Filled Conical Tanks Under Seismic Loading

Ahmed Musa
The University of Western Ontario

Supervisor
Ashraf El Damatty
The University of Western Ontario

Graduate Program in Civil and Environmental Engineering
A thesis submitted in partial fulfillment of the requirements for the degree in Doctor of Philosophy
© Ahmed Musa 2016

Recommended Citation
Musa, Ahmed, "Analysis and Design Procedure for Liquid-Filled Conical Tanks Under Seismic Loading" (2016). *Electronic Thesis and Dissertation Repository*. 3724.
https://ir.lib.uwo.ca/etd/3724

This Dissertation/Thesis is brought to you for free and open access by Scholarship@Western. It has been accepted for inclusion in Electronic Thesis and Dissertation Repository by an authorized administrator of Scholarship@Western. For more information, please contact wlswadmin@uwo.ca.

Abstract

Steel conical tanks are widely used for liquid storage in North America and elsewhere. A number of those tanks collapsed in the last decades as a result of instability of the steel shells. Despite being widely used, no specific design procedure is available for conical tanks under dynamic conditions. The research conducted in the current thesis presents a simplified approach for the design of steel conical tanks when subjected to ground excitations in the form of horizontal and vertical excitations.

First, the capacity of steel conical tanks to avoid yielding and buckling of the tank vessel under hydrodynamic pressure resulting from horizontal ground excitation is evaluated using non-linear static pushover analysis. The capacity of steel conical tanks under hydrodynamic pressure resulting from vertical ground excitation is then evaluated using the same procedure. The analyses are conducted numerically using a non-linear finite element model that accounts for the effects of large deformations and geometric imperfections on the stability of steel conical tanks. Based on the obtained capacities, a design approach is proposed which is based on satisfying an interaction formula that avoids both yielding and buckling of the tank vessel. This formula is a function of the steel conical tank capacities and the seismic demands resulting from hydrodynamic pressure including both impulsive and sloshing components. Finally, this design approach is validated through comparison with the results of non-linear dynamic analysis.

The effect of the base rocking motion on the seismic behaviour of conical shaped steel tanks is then studied and a mechanical analog that simulates the forces acting on a conical tank subjected to a horizontal excitation including the effect of this base rocking motion is developed. This mechanical model takes the flexibility of the tank walls into consideration as well the hydrodynamic pressure acting on the tank base.

Keywords

Co-Authorship Statement

This thesis has been prepared in accordance with the regulations for an Integrated Article format thesis stipulated by the School of Graduate and Postdoctoral Studies at the University of Western Ontario. Statements regarding the co-authorship of individual chapters are as follows:

Chapter 2: CAPACITY OF LIQUID STEEL CONICAL TANKS UNDER HYDRODYNAMIC PRESSURE DUE TO HORIZONTAL GROUND EXCITATIONS

All the numerical work was conducted by A. Musa under close supervision of Dr. A. A. El Damatty. Drafts of Chapter 2 were written by A. Musa and modifications were done under supervision of Dr. A. A. El Damatty. A paper co-authored by A. Musa and A. A. El Damatty is published in *Thin-walled structures journal.*

Chapter 3: CAPACITY OF LIQUID-FILLED STEEL CONICAL TANKS UNDER VERTICAL EXCITATION

All the numerical work was conducted by A. Musa under close supervision of Dr. A. A. El Damatty. Drafts of Chapter 3 were written by A. Musa and modifications were done under supervision of Dr. A. A. El Damatty. A paper co-authored by A. Musa and A. A. El Damatty is published in *Thin-walled structures journal.*

Chapter 4: DESIGN PROCEDURE FOR LIQUID STORAGE STEEL CONICAL TANKS UNDER SEISMIC LOADING

All the numerical work was conducted by A. Musa under close supervision of Dr. A. A. El Damatty. Drafts of Chapter 4 were written by A. Musa and modifications were done under supervision of Dr. A. A. El Damatty. A paper co-authored by A. Musa and A. A. El Damatty is submitted to *Thin-walled structures journal.*

Chapter 5: EFFECT OF BASE ROCKING MOTION ON THE SEISMIC BEHAVIOUR OF CONICAL SHAPED STEEL LIQUID STORAGE TANKS

All the numerical work was conducted by A. Musa under close supervision of Dr. A. A. El Damatty. Drafts of Chapter 5 were written by A. Musa and modifications were done under supervision of Dr. A. A. El Damatty. A paper co-authored by A. Musa and A. A. El Damatty is submitted to *Earthquake Engineering & Structural Dynamics Journal.*

To my beloved parents *Musa Azab and Sanaa El Gendy*

To my brother *Sherief*

To my sisters *Noha, Shereen, and Maha*

For their support and encouragement

To my supervisor, *Dr. Ashraf A. El Damatty*

For offering his continuous advice and encouragement

Acknowledgments

I am eager to take this opportunity to thank everyone who helped me during my work in this research, made this thesis possible and an unforgettable experience for me

First, I would like to express my deepest sense of gratitude and appreciation to my supervisor Dr. Ashraf El Damatty for all his support, guidance, patience, and for all the knowledge he gave to me throughout the course of this thesis. I thank him for the great effort he put into training me in the scientific field. It was a great privilege to work with him.

I would also like to thank my former and current fellow graduate students, Dr. Haitham Aboshosha, Dr. Ahmed Hamada, Dr. Mahmoud Siddiqui, Ryan Jacklin , Tareq Ezabi, Mike Jolie, Amal Kamel, Mohamed Hamada, Carolina Santos, Adnan ElNajjar, Ahmed Elshaer, Joshua Rosenkrantz , Ahmed Alaadin, Fouad Yehia, Ibrahim Ibrahim, Mohamed Dawoud, Dr. Aiham Adawi, Dr. Ahmed Fahmy, Dr. Nedal Mohamed, Dr. Ahmed Dyasti, Dr. Ahmed Taha, Dr. Ahmed Alnuaim, Ahmed Suleiman, Osama Derby, Abdullah El Tawati, Maged Boshana , Hayder Al-Maamori , Mahmoud Halwagy, Papia Sultana , Ahmed Mniena, Emad Abraik, Jesus Gonzalez, Mahmoud Kassem, Mohamed Abdel Salam, Mohamed Ali, Saud Al Fayez, Yazeed Alsharedah, Ahmed Abu Hussein, Mohamed Gamal, Abdel Rhaman Fouad, and Mohamed Askar.

A special thanks to Dr. Ahmed Elansary for his support and friendship. It was a pleasure to go through my undergraduate and postgraduate studies long and enjoyable journey with you. Another special thanks goes to one of my best friends Ahmed Mansour for his support and giving me many precious memories.

A very special acknowledgment to all the lifelong friends I made here in London Ontario, specially Dr. Ahmed Soliman, Dr. Ahmed Abdel Kader, Dr. Ahmed El Attar, Dr. Khaled Shehata, Yamen Elbahy, Mohamed Diab, Mohamed Monir, Mohamed Elsherief, Moustafa Aboutabikh, Dr. Mohamed Gebril, Sherief Gaber, Mohamed Diab, Dr. Ahmed Ashmawy,

Dr. Osama Elhawary, Mohamed Abusharkh, Fabio Sammarco, and Andrea Liguori. Moreover, I would like to express my sincerest thanks to all my friends overseas in Egypt for their encouragement, belief in me and for their good spirit.

I take this opportunity to express the profound gratitude from my deep heart to my beloved parents and my siblings, the most precious people in my life, for their love and continuous support they have provided me throughout my life. I also would like to thank my cousins Mostafa, Ahmed, Maged, and Omar for their encouragement.

Table of Contents

List of Tables

List of Figures

List of Appendices

Chapter 1

1   Introduction

1.1   General

Liquid storage tanks are widely used around the world for the purpose of storing different kinds of liquids. The contained liquid might be water used for drinking and fire protection or any other fluid used in a specific industry. There are two types of liquid storage tanks depending on the required pressure head: either a ground tank, or an elevated tank supported on a steel framing system or a concrete shaft. The tank vessel is commonly constructed of either steel or reinforced concrete. The choice of the tank, whether ground or elevated, and the construction material is mainly based on the function of such tank in addition to the properties of the contained liquid. Steel tanks have the advantage of being faster in construction time and lighter in weight compared with their reinforced concrete counterparts.

Tanks are found in a variety of cross sectional shapes such as: cylindrical, rectangular, and conically-shaped which is the focus of the current study. A conical tank might consist of a pure truncated cone as shown in Fig. 1-1a or might be capped with a cylindrical part and is referred to in this case as combined conical tank as shown in Fig. 1-1b. Although such tanks whether pure or combined are commonly constructed, no specific design procedure is found for conical tanks in most liquid-tanks specifications. The only guidelines are based on treating a conical-shaped tank as a cylindrical tank with equivalent height, radius, and thickness.

The main difference between conical and cylindrical tanks in the structural behaviour is due to the inclination of the conical tank wall. For the case of hydrostatic pressure, the volume of the contained liquid can be divided into two portions: vol. 1 which represents the fluid cylinder resting on the tank base and vol.2 which represents the remaining fluid. The latter volume increases as the base of the tank is approached and is associated with a decrease in the vessel radius. This leads to the development of high compressive meridional

stresses σ_m in this region. Tensile hoop stresses σ_h are also induced circumferentially through the tank shells.
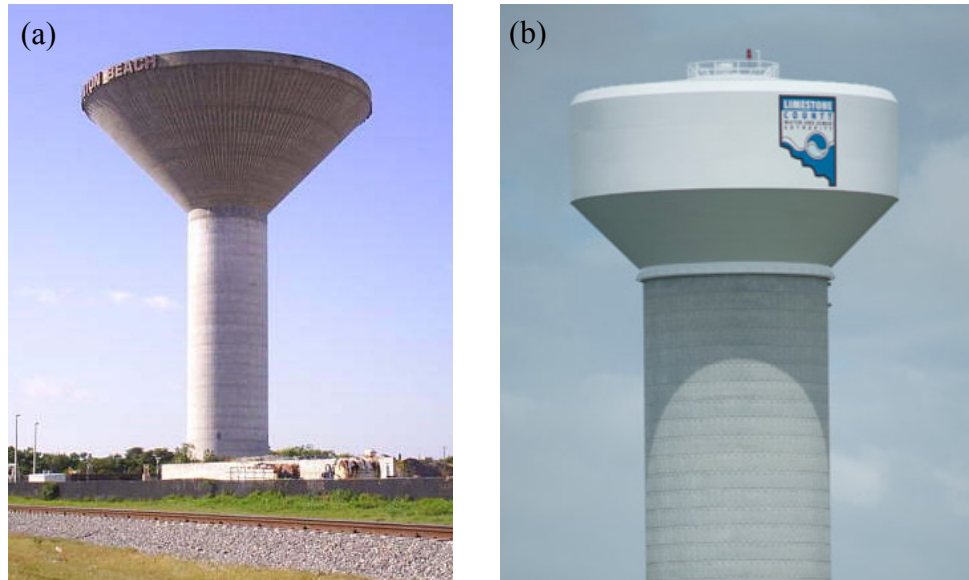
Fig. 1-1 (a) Pure conical tank[1], (b) Combined conical tank[2]

A conical tank in static conditions has to support its own weight in addition to the applied hydrostatic pressure acting on the tank walls and base. For steel conical tanks, the hydrostatic pressure will be more critical than the weight of the tank due to the relatively light weight of steel structures. For the case of liquid-storage conical tanks under dynamic loads, the behaviour is more complicated than other ordinary structures. This is due to the presence of the contained liquid, which vibrates with different dynamic (vibration) characteristics than those of the tank walls.

For a liquid-filled conical tank subjected to an earthquake excitation, the walls, the floor, and the contained liquid are subjected to acceleration. As a result, the walls are affected by the inertial forces of the wall in addition to the hydrodynamic pressure of the contained liquid. The contained liquid can be divided into two parts: the first part is mainly the lower

---

[1] http://forums.auran.com/trainz/showthread.php?17876-FEC-Key-West-extension-modern-day/page7

[2] http://www.caldwellwatertanks.com

amount of liquid, which moves with the walls of the tank and is called the impulsive liquid mass. The second part is mainly the upper amount of liquid and is called the convective liquid mass, which undergoes sloshing due to vibration. The ratio of the convective mass to the impulsive one increases as the tank becomes shallower. Also, the frequency of the impulsive vibration modes is much higher than those of the convective vibration mode.

1.2 Background

Dynamic behaviour of Liquid storage tanks is so important to understand as any failure to such structures might have a serious consequences in addition to the structure damage; for example, losing water supply or release of combustible materials stored inside. In 1964, Alaska earthquake caused damage to a lot of liquid storage tanks highlighting the need for revising the design guidelines found by that time. A lot of studies have been performed regarding the behaviour of liquid tanks, especially cylindrically-shaped, when subjected to earthquake excitations. One of the main findings was the importance of including the tank walls' flexibility when analyzing a liquid tank under seismic action, especially for the case of steel tanks due to the relatively small wall thickness, instead of assuming rigid walls. The vertical component for an earthquake excitation was also found to be important to include when analyzing a liquid tank as vertical acceleration is transmitted to a horizontal hydrodynamic loading acting on a tank wall. As a result, tensile hoop stresses are amplified and might lead to inelastic buckling of the shell.

The equivalent mechanical model was then introduced as a simplified approach to analyze liquid tanks subjected to earthquake excitations. The idea was to replace the contained fluid with a set of lumped masses and linear springs that mimic the total base forces obtained from dynamic analysis. The base forces are the base shear and overturning moment for the case of horizontal excitation and total vertical force for the case of vertical excitation.

Although steel liquid tanks in the form of truncated cones are widely used for the purpose of liquid storage in an industrial facility or for water supply and fire protection and despite the fact that some of these tanks have failed during the last decades, most of the seismic design specifications and guidelines focus on the design of steel cylindrical tanks. The only

seismic design guidelines for conical tanks found in some specifications are based on using an equivalent cylinder.

The state of stresses under hydrostatic pressure for the case of cylindrical tanks is not similar to the case of conical tanks due to the inclination of the tank walls resulting in high compressive meridional stresses near the tank base in addition to tensile hoop stresses. For the case of horizontal seismic excitation, the induced hydrodynamic pressure will amplify both meridional and hoop stresses at one side of the tank and reduce them at the other side based on the direction of the ground acceleration, while the induced hydrodynamic pressure due to vertical excitation will amplify or reduce the induced stresses in an axisymmetric manner based on the direction of the ground acceleration, i.e., upwards or downwards.

A set of experimental and numerical studies have been carried out on steel conical tanks under both hydrostatic and hydrodynamic pressure in order to investigate the effect of wall inclination on the tank behaviour and state of stresses. For the seismic-related studies, the majority of them focused on calculating the base forces that are transmitted to the supporting structure due to a seismic event using equivalent mechanical models, while none of them addressed the conical tank's resistance when subjected to either horizontal or vertical ground excitation. This tank resistance is required to assess the vessel wall thickness to insure its adequacy to resist the applied hydrodynamic pressure due to a seismic event.

In the previous studies for steel conical tanks under horizontal ground excitations, the supporting structure in the form of steel framing system or reinforced concrete shaft was assumed to be rigid regarding rotational motions, i.e., no tank base rocking is allowed. For the case of a flexible supporting system, the rocking base motion is expected to change the vibration characteristics of the tank-support system and, consequently, the induced hydrodynamic forces.

Based on the previous background for research conducted on steel conical tanks, the research conducted in the current Ph.D. thesis will try to build on and extend the previous studies found in literature by obtaining the steel conical tank capacities to avoid yielding and buckling of the vessel when subjected to horizontal and vertical ground excitations.

These capacities are then used to provide a simplified design procedure to design steel conical tanks subjected to earthquake excitations. The effect of allowing base rocking motion on seismic behaviour of steel conical tanks is also studied and a mechanical model is provided for such case.

1.3 Literature Review

1.3.1 Conical Tanks under Hydrostatic Pressure

As for most building structures, the motivations for performing detailed investigations are usually related to total or partial failures. The first study related to steel conical tanks was conducted by Vandepitte et al. (1982) after the collapse of a conical steel water tower in Belgium. In this study, a large number of small-scale conical tank models were tested experimentally under hydrostatic pressure. The models were gradually filled with water till buckling occurred. The test results were used to develop a set of design curves for different base restraining conditions. The effect of geometric imperfections on the safety factor of the conical tanks was also studied. In 1990, a steel conical water tower collapsed in Fredericton, Canada when it was filled with water for the first time. Vandepitte (1999) concluded that the main cause of failure was related to the inadequate thickness of the tank walls at the base. This was due to the designer's underestimation of the amplitude of the geometric imperfections as their design was based on results obtained from the field of aerospace where a superior quality control takes place.

El Damatty et al. (1997a) and El Damatty et al. (1998) considered a number of steel conical tanks with practical dimensions in order to assess their buckling capacity under hydrostatic pressure. The effect of geometric imperfections and residual stresses due to circumferential and longitudinal welding on the buckling capacity of the tanks were assessed. Based on the results of the study, it was concluded that the inelastic behavior has to be considered as most of the tanks yielded before buckling instability took place. Also it was concluded that the critical geometric imperfection shape that led to the minimum buckling capacity is the axisymmetric one. Finally, the hoop residual stresses due to circumferential welding are more critical than residual meridional stresses.

Hafeez et al. (2010) investigated the buckling behavior of combined conical tanks under the effect of hydrostatic pressure. The study was conducted numerically using a three-dimensional finite element model. The effects of geometric imperfection and residual stresses as well as the variation of the geometric and material parameters on the buckling capacity of combined conical tanks were also investigated. Finally, a comparison between the buckling capacities of combined and equivalent pure conical tanks was conducted. It was concluded that the concept of equivalent pure cones underestimate the buckling capacity and the yield load of the combined cones.

Several attempts have been made to provide a simplified design procedure for steel conical tanks under hydrostatic pressure suitable for everyday use by practicing engineers. El Damatty et al. (1999) developed a simple design approach for steel conical tanks with a load factor value of 1.4 taking into account geometric imperfections, snow and roof loads, and the existence of an upper cylindrical cap. The idea was to avoid the yielding state of tanks, which was shown to always precedes buckling for the tank at any point. An economic design approach was also proposed by reducing the tank wall thickness as height increases. This study was limited to conical tanks with vertical inclination angle of 45°. Sweedan and El Damatty (2009) extended the latter study of combined conical tanks under hydrostatic loading using regression analysis based on the results of large number of analyzed tanks. This large database included a variation of tank dimensions, angle of inclination of the wall, cylindrical cap ratio, yield strength values, and geometric imperfection level.

El Ansary et al. (2010) provided a powerful numerical tool that couples a non-linear finite element model and a genetic algorithm optimization technique for the analysis and design of steel conical tanks under hydrostatic pressure. This numerical tool is capable of selecting the set of design variables which satisfies the structure safety requirements while achieving a minimum structure weight and cost.

As the compressive stresses are concentrated at the base of the conical tanks and the buckling is expected at this location, El Damatty et al. (2001) studied the effect of adding longitudinal steel stiffeners at the base. Two types of stiffeners were used; the first is free

at the tank base simulating the case of retrofitting an existing tank, while the second is pinned to the base representing the case of a newly designed tank. It was concluded that, the addition of extra free stiffeners increases the limit loads of the tanks by 35% to 64%, while for the case of pinned stiffeners this increase varies between 71% and 136%.

1.3.2   Liquid Tanks under Seismic Loading

1.3.2.1   Horizontal Excitation

The first studies regarding seismic behaviour of cylindrical liquid tanks were based on the assumption that the tank walls are rigid, i.e., the flexibility of the tank walls has no effect on the contained fluid vibrations (Jacobsen (1949), Housner (1957), and Housner (1963)). This notion was considered valid until the earthquake in Alaska in the year 1964 where considerable damage occurred to a large number of cylindrical liquid storage tanks in the form of roof damage, wall buckling, and total collapse (Hanson (1968)).

More studies were carried out after earthquake in Alaska in an attempt to accurately interpret the vibration characteristics, taking into consideration the effect of the wall flexibility where the tank deformations affect the hydrodynamic pressure, i.e., fluid-structure interaction takes place. It was concluded that the flexibility of cylindrical tank walls amplifies the tank's response. Therefore, it has to be accounted for (Veletsos (1974), and Haroun and Housner (1981,1982)).

Many studies in the literature were found to be related to the buckling capacity of cylindrical liquid tanks under seismic loading. Virella et al. (2006) investigated the dynamic buckling of aboveground anchored cylindrical steel tanks subjected to horizontal components of real earthquake records numerically using the finite element method. The objective was to estimate the critical horizontal peak ground acceleration (PGA) causing either elastic or plastic buckling for the cylindrical shell. Three tank-liquid systems with different slenderness ratios were considered subjected to two natural excitation records. Dynamic buckling computations including material and geometric non-linearity were carried out. It was concluded that buckling at the top of the shell was caused by a negative net pressure at the zone in the tank where the impulsive hydrodynamic pressure induced by the earthquake excitation exceeds the hydrostatic pressure. This negative net pressure

induces membrane compressive circumferential stresses causing buckling to the tank shell. The elastic buckling at the top represented the critical state for the medium and tall models, while plasticity was reached at the shell before buckling for the shallow tank. The slenderness ratio was found to have some influence on the critical PGA with no clear trend.

Virella et al. (2008) proposed a nonlinear static procedure based on the capacity spectrum method found in ATC-40 in order to evaluate the elastic buckling of above-ground anchored steel tanks due to horizontal seismic excitations. The objective was to obtain the minimum peak ground acceleration (PGA) value that produces buckling in the tank shell. The obtained critical PGA estimates were then compared with those calculated using the dynamic buckling analyses performed in the latter study. The following was concluded: (a) the nonlinear static procedure resulted in slightly smaller, i.e., conservative, values for the critical PGA compared to the dynamic buckling results, (b) similar first buckling modes were observed by using both static and dynamic buckling analyses, (c) the critical PGA decreases with the slenderness ratio.

Djermane et al. (2014) attempted to evaluate the current design guidelines related to dynamic instability provided by AWWA-D100 and EC8 provisions for cylindrical steel tanks using a numerical shell finite element model. The idea was to evaluate the critical PGA values that cause the tank instability and then compare with their counterparts obtained by the codes' provisions. The authors concluded the following: (a) comparison for broad tanks showed a good agreement between numerical and EC8 results, (b) standards need some revisions in order to provide improved consideration of the imperfections and geometric nonlinearities for the case of tall tanks, (c) simple stress limitation found in the standards is very conservative.

Buratti and Tavano (2014) discussed different buckling modes for liquid-containing circular cylindrical steel tanks that are fully anchored at the base with a special focus on the secondary buckling occurring in the top part of the tank. A case study for a broad cylindrical tank was used in order to investigate various aspects of dynamic buckling using a finite element model where the fluid was modelled in the form of unvarying added masses, i.e., assuming rigid tank. The following was concluded: (a) hoop stresses due to

the hydrostatic pressure reduces the periods for shell-type vibration modes, but it does not affect cantilever-type vibration modes, (b) the secondary buckling is an elastic buckling mode, but it is strongly influenced by the occurrence of plasticity in other parts of the structure.

El Damatty et al. (1997b,c) conducted the first study to assess the behavior of conical tanks under seismic loading where a coupled shell element-boundary element formulation was developed to simulate the fluid-structure interaction. A fluid added mass matrix was derived and added to the mass matrix of the structure to be incorporated into a nonlinear dynamic analysis routine. The results showed that some of the tanks suffered dynamic instability although they were designed with factor of safety of about 2.5 under hydrostatic pressure. This in turn reflects the importance of the seismic loading compared to the hydrostatic one.

As the finite element dynamic analysis for the tank-fluid system is considered computationally expensive, researchers tried to find a simpler procedure to estimate the total forces acting on the liquid tank structure when subjected to an earthquake event. A practical alternative was to model the contained liquid as lumped masses attached to the tank wall rigidly or through linear springs instead of modelling the contained fluid as a continuum, which in turn reduce the computation cost for the tank-fluid dynamic analysis. The masses-springs system is called equivalent mechanical model whose main objective is to match the resulting forces and moments obtained using dynamic analysis.

Haroun and Housner (1981) introduced a three masses mechanical model for cylindrical steel tanks. The three masses are the impulsive fluid mass, the convective fluid mass, and the mass reflecting the effect of the flexibility of the tank's wall. The impulsive mass represents the mass of the fluid vibrating in synchronism with the ground and rigidly connected to the tank's wall, while the convective one represents the mass of the fluid undergoing sloshing motion at the free surface. El Damatty and Sweedan (2006) developed a similar mechanical model for conical tanks in order to predict the base shear and overturning moment acting on the tanks when subjected to earthquake events.

Moslemi et al. (2011) analyzed an elevated steel conical tank twice when subjected to El-Centro ground motion; once using finite element analysis where the fluid was modeled using displacement-based elements and once using the ACI procedure which is based on Housner's mechanical model for equivalent cylindrical tank. The difference between the two methods in terms of base shear and base moment was around 6%.

1.3.2.2 Vertical Excitation

Regarding the vertical component, Marchaj (1979) attributed the failure of metallic tanks during past earthquakes to the lack of consideration of vertical acceleration in their design. Veletsos and Kumar (1984) studied the effect of wall flexibility on the response of cylindrical tanks when subjected to vertical component of ground shaking. It was concluded that the hydrodynamic effects for a flexible tank might be substantially larger than those induced in a rigid tank of the same dimensions, and for an intense excitation, they might be of the same order of magnitude as the hydrostatic effects.

The latter study considered only the radial motion of the tank walls and neglected the effect of axial deformations. This assumption was validated by Haroun and Tayel (1985a) who provided an analytical method for the computation of the dynamic characteristics in terms of natural frequencies, corresponding mode shapes and stress distributions for partly filled cylindrical tanks subjected to vertical excitations. Results were compared to numerical solution where the liquid region was treated analytically and the elastic shell was modeled by finite elements (Haroun and Tayel (1985b)) and both methods showed excellent agreement.

Veletsos and Tang (1986) provided a practical procedure to evaluate the dynamic response of rigid and flexible steel and concrete cylindrical tanks with different base conditions when subjected to vertical excitations including soil-structure interaction. The main conclusion was that soil-structure interaction reduces the maximum hydrodynamic effects and might be approximated by a change in the fundamental natural frequency of the tank-liquid system or an increase in damping

Haroun and Tayel (1985) analyzed some cylindrical liquid storage tanks under simultaneous horizontal and vertical excitations numerically using finite element method. The goal of the study was to assess the relative importance of inclusion of the vertical component of the earthquake in the behaviour of the cylindrical tanks. The axial stresses resulting from the vertical component was found to be much lower compared to those induced due to the horizontal component of the earthquake due to overturning moment. However, the hoop stresses due to vertical component was higher than those due to horizontal component which might lead to the yielding of the steel shell increasing the probability of buckling of the tank walls near the base of the tank.

Haroun and Abou-Izzeddine (1992) performed a parametric study in order to evaluate the effects of different factors that influence the seismic response of an elastic cylindrical tank supported on a rigid base when subjected to a vertical excitation by considering shell-liquid-soil interaction. It was concluded that foundation soil-tank interaction reduces the tank response in general, and this reduction is a function of the soil shear-wave velocity as well as tank geometric properties.

El Damatty et al. (1997b,c) derived a fluid-added mass matrix for both horizontal and vertical ground motions to be incorporated in time history analysis and it was shown how the contribution of vertical excitation to the dynamic instability is important. This coupled shell element-boundary element model was verified experimentally using shaking table testing for scaled conical shell aluminum models (Sweedan and El Damatty (2002), El Damatty et al. (2005), and El Damatty et al. (2005)).

Jolie et al. (2014) assessed the importance of considering the vertical component of ground excitations when designing steel conical tanks using an equivalent mechanical model that estimates the acting normal forces due to vertical excitations. In addition, a three-dimensional finite element model has been developed using shell elements in order to predict maximum membrane and overall meridional stresses due to both hydrodynamic and hydrostatic pressures. The results showed that the vertical ground acceleration has a considerable effect on the increase of the meridional wall stresses compared to those resulting from hydrostatic pressure, especially for high seismic hazard regions emphasizing

the importance of vertical excitation consideration. Also, meridional wall stresses at the extreme inner fibre at the tank base are shown to be higher than those developing at the mid-surface due to bending effects associated with the boundary conditions at the tank base.

1.4   Objectives of Thesis

The major objectives of the thesis can be summarized in the following:

1- Estimate the capacity of steel conical tanks under hydrodynamic pressure due to horizontal ground excitations using nonlinear static analysis for both perfect and imperfect conical tanks.

2- Estimate the capacity of steel conical tanks under hydrodynamic pressure due to vertical ground excitations using nonlinear static analysis for both perfect and imperfect conical tanks.

3- Provide a simplified seismic design procedure for steel conical tanks when subjected to both horizontal and vertical ground excitations and validating this procedure using dynamic analysis.

4- Study the effect of the base rocking motion on the seismic behaviour of steel conical tanks

5- Develop an equivalent mechanical model for steel conical tanks taking the base rocking motion into consideration.

1.5   Scope of Thesis

The thesis has been prepared in 'Integrated-Article' format. In the present chapter, a review of the studies related to steel conical tanks under seismic loading and the objectives and thesis's scope are provided. The following four chapters address collectively the thesis objectives. Chapter 6 presents the conclusion of the study together with suggestions for further research work. A description of scope of each chapter is provided below.

1.5.1 Chapter 2 – Capacity of Liquid Steel Conical Tanks under Hydrodynamic Pressure Due To Horizontal Ground Excitation

In this chapter, the capacity of liquid steel conical tanks when subjected to hydrodynamic pressure resulting from horizontal ground excitation is obtained. In order to achieve that, a numerical finite element model is used based on static pushover analysis. The capacity is expressed in terms of the resulting total base shear at failure for the two components of the hydrodynamic pressure; impulsive and sloshing. As the impulsive and sloshing vibration modes are well-separated regarding their natural frequencies, the analyses are done separately for each pressure component. Base shear capacities for perfect steel conical tanks are presented in the form of charts for different dimensions, walls' thicknesses, and angles of inclination. As geometric imperfections play an important role in defining the capacity of shell structures, the effect of the geometric imperfections on the capacity of steel conical tanks is then studied and similar charts are provided for the case of imperfect tanks. On the other side, the seismic demands in the form of total base shear are obtained using equivalent mechanical model found in the literature for both impulsive and sloshing vibration modes and compared to the obtained capacities in order to assess the design of the steel conical tanks. Three seismic zones are considered in this comparison representing moderate to high seismic zones in Canada.

1.5.2 Chapter 3 – Capacity of Liquid-Filled Steel Conical Tanks under Vertical Excitation

In this chapter, the capacity of liquid steel conical tanks when subjected to hydrodynamic pressure resulting from vertical ground excitation is obtained using static pushover analysis. The capacity is expressed in terms of the resulting total vertical force at failure Vertical force capacities for perfect steel conical tanks are presented in the form of charts for different dimensions, walls' thicknesses, and angles of inclination. The effect of the geometric imperfections on the capacity of steel conical tanks is then studied and similar charts are provided for the case of imperfect tanks. The vertical force capacities of the conical tanks are then compared with the seismic demands in the form of total vertical force obtained using equivalent mechanical model found in the literature in order to assess the initial design for the steel conical tanks. A procedure based on artificial ground excitations

is used to convert the horizontal response spectra for the same three seismic zones considered in the previous chapter to vertical spectra.

1.5.3 Chapter 4 – Design Procedure for Liquid Storage Steel Conical Tanks under Seismic Loading

In this chapter, a simplified design procedure is proposed to design steel conical liquid tanks subjected to horizontal and vertical components of ground excitations. The approach is based on satisfying a design equation which is function of the steel conical tank capacities and seismic demands. The steel conical tank capacities are those obtained in the previous two chapters using non-linear static analyses for both horizontal and vertical excitations, while the seismic demands are obtained using equivalent mechanical models found in the literature. This design approach takes into consideration the effect of geometric imperfections and the effect of sloshing hydrodynamic pressure. In order to validate this design procedure, non-linear time history analyses are conducted and their outcomes are compared with those of the proposed design procedure in terms of the minimum wall thickness. The time history analyses are conducted based on 11 natural earthquake records scaled to different seismic zones in Canada. The selection of the ground motions is based on a procedure where the seismic hazard is deaggregated in terms of the distance and magnitude of the ground motion for different spectral acceleration values.

1.5.4 Chapter 5 – Effect of Base Rocking Motion on the Seismic Behaviour of Conical Shaped Steel Liquid Storage Tanks

In this chapter, the effect of base rocking motion for steel conical tanks during a horizontal ground excitation is studied. First, the effect of this rocking motion on the change of the vibration properties of steel conical tanks is studied. This is achieved using free-vibration analysis for the tank-fluid system and comparing the results with the case of no rocking motion. Secondly, the effect of this rocking motion on the hydrodynamic pressure acting on the tank walls and base due to the existing fluid-structure interaction is studied. This is achieved through non-linear time history analysis under artificial earthquake records matching three seismic zones in Canada. Finally, a mechanical model that includes the effect of base rocking motion is developed in the second part of this chapter using a frequency analysis approach. The proposed model takes into consideration the impulsive

component of the hydrodynamic pressure, deformability of the tank walls, and the hydrodynamic pressure acting on the tank base. The model is then validated through comparison with a mechanical model taking the rocking motion under consideration for cylindrical tanks found in literature. The parameters of the mechanical model are presented in the form of charts for different geometries of steel conical tanks. The proposed mechanical model can be used for either ground or elevated steel conical tanks undergoing horizontal translation and/or base rotation.

1.6 References

(API), A.P.I., 2005. Welded Storage Tanks for Oil Storage. Washington D.C, USA: American Petroleum Institute Standard.

(AWWA), A.W.W.A., 2005. Welded Steel Tanks for Water Storage. Denver, CO, USA.

(ECS), E.C.f.S., 1998. Design provisions for earthquake resistance of structures. Eurocode 8.

ACI 371, 2008. Guide for the Analysis, Design, and Construction of Elevated Concrete and Composite Steel-Concrete Water Storage Tanks. American Concrete Institute.

Buratti, and Tavano, M., 2014. Dynamic buckling and seismic fragility of anchored steel tanks by the added mass method. Earthquake Engng. Struct. Dyn., 43, pp.1-21.

Djermane, M. et al., 2014. Dynamic buckling of steel tanks under seismic excitation: Numerical evaluation of code provisions. Engineering Structures, 70, pp.181-96.

El Ansary, A.M. et al., 2010. A coupled finite element genetic algorithm technique for optimum design of steel conical tanks. Thin-Walled Structures, 48, pp.260-73.

El Damatty, A.A. et al., 1998. Inelastic stability of conical tanks. Thin-Walled Structures, 31, pp.343-59.

El Damatty, A.A. et al., 1997a. Stability of Imperfect Conical Tanks under Hydrostatic Loading. Journal of Structural Engineering, 123(6), pp.703-12.

El Damatty, A.A. et al., 1997d. Large displacement extension of consistent shell element for static and dynamic analysis. Computers and Structures, 62(6), pp.943-60.

El Damatty, A.A. et al., 1999. Simple design procedure for liquid-filled steel conical tanks" Journal of structural engineering. Journal of structural engineering, 125(8), pp.879-90.

El Damatty, A.A. et al., 2001. Behavior of stiffened liquid-filled conical tanks. Thin-Walled Structures, 39, pp.353-73.

El Damatty, A.A. et al., 1997c. Stability of elevated liquid-filled conical tanks under seismic loading, Part II-Applications. Earthquake Engng. Struct. Dyn., 26, pp.1209-29.

El Damatty, A.A. et al., 1997b. Stability of elevated liquid-filled conical tanks under seismic loading, Part I-Theory. Earthquake Engng. Struct. Dyn., 26, pp.1191-208.

El Damatty, A.A. et al., 2005. Dynamic characteristics of combined conical-cylindrical shells. Thin-Walled Structures, 43, pp.1380-97.

El Damatty, A.A. et al., 2005. Experimental study conducted on a liquid-filled combined conical tank model. Thin-Walled Structures, 43, pp.1398-417.

El Damatty, A.A. and Sweedan, A.M., 2006. Equivalent mechanical analog for dynamic analysis of pure conical tanks. Thin-Walled structures, 44, pp.429-40.

Hafeez, G. et al., 2010. Stability of combined imperfect conical tanks under hydrostatic loading. Journal of Constructional Steel Research, 66, pp.1387-97.

Hanson, R.D., 1968. Behavior of liquid storage tanks, the great Alaska earthquake of 1964. Washington, D.C.: National Research Council.

Haroun, M.A. and Abou-Izzeddine, W., 1992. Parametric Study of Seismic Soil-Tank Interaction. ii: Vertical Excitation. Journal of Structural Engineering, 118(3), pp.798-812.

Haroun, M.A. and Housner, G.W., 1981. Seismic design of liquid storage tanks. Journal of the Technical Councils, 107(TC1), pp.191-207.

Haroun, M.A. and Housner, G.W., 1982. Dynamic characteristics of liquid storage tanks. Journal of the Engineering Mechanics Division, 108(5), pp.783-800.

Haroun, M.A. and Tayel, M.A., 1985a. Axisymmetrical vibrations of tanks—Numerical. J. Eng. Mech., 111(3), pp.329-45.

Haroun, M.A. and Tayel, M.A., 1985b. Axisymmetrical vibrations of tanks—Analytical. J. Eng. Mech., 111(3), pp.346-58.

Haroun, M.A. and Tayel, M., 1985. Response of tanks to vertical seismic excitation. Earthquake Engng. Struct. Dyn., 13, pp.583-95.

Housner, G.W., 1957. Dynamic pressures on accelerated fluid containers. Bulletin Seism. Soc. America, 47(1), pp.15-35.

Housner, G.W., 1963. The Dynamic Behavior of Water Tanks. Bulletin Seism. Soc. America, 53(1), pp.381-87.

Jacobsen, L.S., 1949. Impulsive hydrodynamics of fluid inside a cylindrical tank and of a fluid surrounding a cylindrical pier. Bulletin Seism. Soc. America, 39, pp.189-204.

Jolie, M. et al., 2014. Seismic analysis of elevated pure conical tanks under vertical excitation. Can. J. Civ. Eng., 41, pp.909-17.

Jolie, M. et al., 2013. Assessment of current design procedures for conical tanks under seismic loading. Can. J. Civ. Eng., 40, pp.1151-63.

Koizey, B. and Mirza, F.A., 1997. Consistent thick shell element. Computer & Structures, 65(12), pp.531-41.

Marchaj, T.J., 1979. Importance of vertical acceleration in the design of liquid containing tanks. In 2nd U.S. National Conference on Earthquake Engineering. Stanford, CA, 1979.

Moslemi, M. et al., 2011. Seismic response of liquid-filled elevated tanks. Engineering Structures, 33, pp.2074-84.

Sweedan, A.M., 2009. Equivalent mechanical model for seismic forces in combined tanks subjected to vertical earthquake excitation. Thin-Walled structures, 47, pp.942-52.

Sweedan, A.M.I. and El Damatty, A.A., 2002. Experimental and analytical evaluation of the dynamic characteristics of conical shells. Thin-Walled Structures, 40, pp.465-86.

Sweedan, A.M. and El Damatty, A.A., 2005. Equivalent models of pure conical tanks under vertical ground excitation. Journal of Structural Engineering, ASCE, 131(5), pp.725-33.

Sweedan, A.M. and El Damatty, A.A., 2009. Simplified procedure for design of liquid-storage combined conical tanks. Thin-Walled structures, 47, pp.750-59.

Vandepitte, D., 1999. Confrontation of shell buckling research results with the collapse of a steel water tower. Journal of Constructional Steel Research, 49, pp.303-14.

Vandepitte, D. et al., 1982. Experimental investigation of hydrostatically loaded conical shells and practical evaluation of the buckling load. In Proc. State of the Art Colloquium. Universitat Stuttgart, Germany, 1982.

Veletsos, A.S., 1974. Seismic effects in flexible liquid storage tanks. In International Association for Earthquake Engineering. Fifth World Conference. Rome, Italy, 1974.

Veletsos, A.S. and Kumar, A., 1984. Dynamic response of vertically excited liquid storage tanks. In 8th World Conf. on Earthquake Engineering. San Francisco, CA, 1984.

Veletsos, A.S. and Tang, Y., 1986. Dynamics of vertically excited liquid storage tanks. J. Struct. Eng., 112(6), pp.1228-46.

Virella, J.C. et al., 2006. Dynamic buckling of anchored steel tanks subjected to horizontal earthquake excitation. Journal of Constructional Steel Research, 62, pp.521-31.

Virella, J.C. et al., 2008. A static nonlinear procedure for the evaluation of the elastic buckling of anchored steel tanks due to earthquakes. Journal of Earthquake Engineering, 12, pp.999-1022.

Chapter 2

2 Capacity of Liquid Steel Conical Tanks under Hydrodynamic Pressure Due To Horizontal Ground Excitation

Steel conical tanks are widely used for liquid storage around the world and especially in North America. A number of those tanks collapsed in the last decades at different places as a result of instability of the steel shells. Despite being widely used, no specific design procedure is available for conical tanks under dynamic conditions. Most of the previous studies related to steel conical tanks focused on calculating the acting forces due to a seismic event. This study however, focuses on evaluating the capacity of conical tanks under hydrodynamic pressure resulting from horizontal ground excitation using non-linear static pushover analysis. The capacity is then compared to the seismic demand obtained using a previously developed mechanical model found in the literature for different seismic zones. This paper is a part of a larger study aiming to provide a simplified design procedure for steel conical tanks when subjected to earthquakes. The study is conducted numerically using a non-linear finite element model that accounts for the effects of large deformations and geometric imperfections on the stability of steel conical tanks.

2.1 Introduction

Steel conical-shaped liquid storage tanks are commonly used for the purpose of storing different kinds of liquids. The contained liquid can either be water used for both drinking as well as fire protection or a chemical used in a specific industry. Steel vessels are advantageous in comparison to their concrete counterparts as they are composed of prefabricated steel panels, which simplify the erection procedure and reduce construction costs. A conical tank consists solely of a pure truncated cone, as shown in Fig. 2-1a or might be capped with a cylindrical part and is referred to as combined conical tank as shown in Fig. 2-1b. Although such tanks whether pure or combined are commonly constructed, no specific design procedure is found for conical tanks in most liquid-tanks specifications. The only guidelines, found in some design provisions (AWWA (2005), API

(2005), ECS (1998), and ACI 371 (2008)) are based on treating a conical-shaped tank as a cylindrical tank with equivalent height, radius, and thickness.
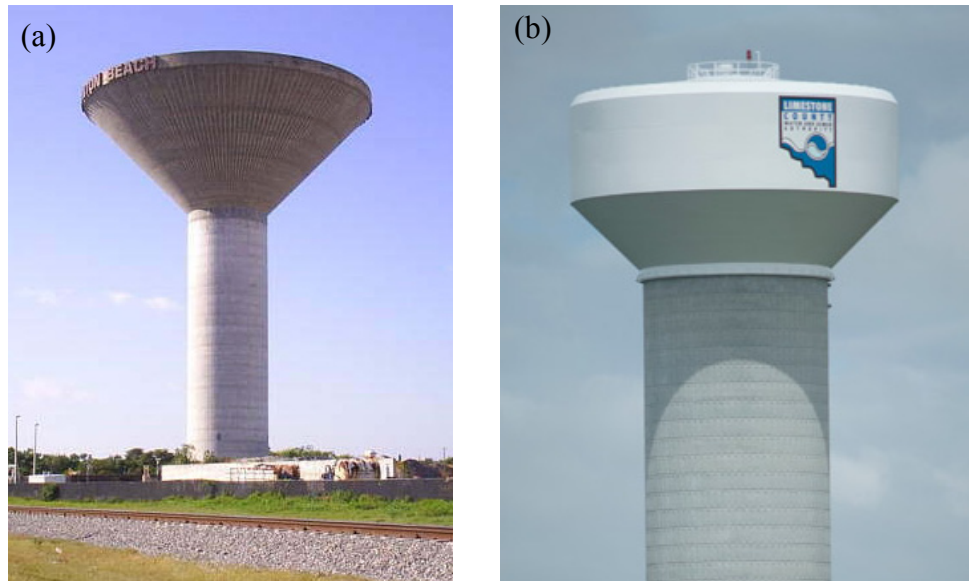
Fig. 2-1 (a) Pure conical tank[3], (b) Combined conical tank[4]

The main difference between conical and cylindrical tanks in the structural behaviour is due to the inclination of the conical tank wall. For the case of hydrostatic pressure, the volume of the contained liquid can be divided into two portions: vol. 1 and vol.2 as shown in Fig. 2-2. The latter volume increases as the base of the tank is approached and is associated with a decrease in the vessel radius. This leads to the development of high compressive meridional stresses σ_m in this region. Tensile hoop stresses σ_h are also induced circumferentially through the tank shells. The hydrodynamic pressure due to horizontal seismic excitation will amplify both σ_m and σ_h at one side of the tank and reduces them at the other side based on the direction of the ground acceleration.

---

[3] http://forums.auran.com/trainz/showthread.php?17876-FEC-Key-West-extension-modern-day/page7

[4] http://www.caldwellwatertanks.com
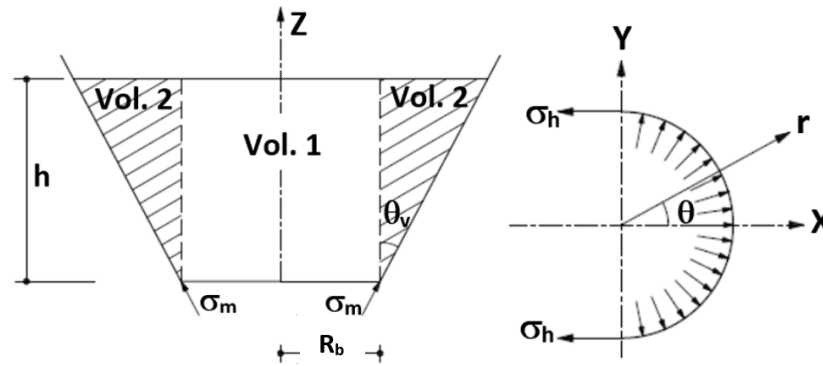
Fig. 2-2 Stresses induced due to inclination of the wall

The equivalent cylinder proposed by AWWA (2005) and API (2005) is based on the average conical tank radius and a total height equals to the inclined wetted surface height of the conical tank. On the other side, ECS (1998) and ACI 371 (2008) recommend using an equivalent cylindrical tank that has the same free surface diameter as the conical tank and a depth that results in the same volume as the conical tank. Jolie et al. (2013) assessed the equivalent cylinder concept proposed by different specifications in terms of the resulting base shear and overturning moments. The study showed that while the base shear is overly-estimated by the AWWA and API, it remains well-predicted by the Eurocode. All the design codes are found to under estimate the overturning moment, which was related to not including the effect of the vertical hydrodynamic pressure component when assuming the tank walls to be vertical not inclined.

A conical tank in static conditions has to support its own weight in addition to the applied hydrostatic pressure acting on the tank walls and base. For steel conical tanks, the hydrostatic pressure will be more critical than the weight of the tank due to the relatively light weight of steel structures. For the case of liquid-storage conical tanks under dynamic loads, the behaviour is more complicated than other ordinary structures. This is due to the presence of the contained liquid, which vibrates with different dynamic (vibration) characteristics than those of the tank walls.

For a liquid-filled conical tank subjected to an earthquake excitation, the walls, the floor, and the contained liquid are subjected to acceleration. As a result, the walls are affected by

the inertial forces of the wall in addition to the hydrodynamic pressure of the contained liquid. The contained liquid can be divided into two parts: the first part is mainly the lower amount of liquid, which moves with the walls of the tank and is called the impulsive liquid mass. The second part is mainly the upper amount of liquid and is called the convective liquid mass, which undergoes sloshing due to vibration. The ratio of the convective mass to the impulsive one increases as the tank becomes shallower. Also, the frequency of the impulsive vibration modes is much higher than those of the convective vibration mode.

The first study related to steel conical tanks was conducted by Vandepitte et al. (1982) after the collapse of a conical steel water tower in Belgium. In this study, a large number of small-scale conical tank models were tested experimentally under hydrostatic pressure. The models were gradually filled with water till buckling occurred. The test results were used to develop a set of design curves for different base restraining conditions. The effect of geometric imperfections on the safety factor of the conical tanks was also studied. In 1990, a steel conical water tower collapsed in Fredericton, Canada when it was filled with water for the first time. Vandepitte (1999) concluded that the main cause of failure was related to the inadequate thickness of the tank walls at the base. This was due to the designer's underestimation of the amplitude of the geometric imperfections as their design was based on results obtained from the field of aerospace where a superior quality control takes place.

Several attempts have been made to provide a simplified design procedure for steel conical tanks under hydrostatic pressure suitable for everyday use by practicing engineers. El Damatty et al. (1999) developed a simple design approach for steel conical tanks with a load factor value of 1.4 taking into account geometric imperfections, snow and roof weights, and the existence of an upper cylindrical cap. The idea was to avoid the yielding state of tanks, which was shown to always precedes buckling for the tank at any point. An economic design approach was also proposed by reducing the tank wall thickness as height increases. This study was limited to conical tanks with vertical inclination angle of 45°. Sweedan and El Damatty (2009) extended the latter study of combined conical tanks under hydrostatic loading using regression analysis based on the results of large number of analyzed tanks. This large database included a variation of tank dimensions, angle of

inclination of the wall, cylindrical cap ratio, yield strength values, and geometric imperfection level.

The first studies regarding seismic behaviour of cylindrical liquid tanks were based on the assumption that the tank walls are rigid, i.e., the flexibility of the tank walls has no effect on the contained fluid vibrations (Jacobsen (1949), Housner (1957), and Housner (1963)). This notion was considered valid until the earthquake in Alaska in the year 1964 where considerable damage occurred to a large number of cylindrical liquid storage tanks in the form of roof damage, wall buckling, and total collapse (Hanson (1968)).

More studies were carried out after earthquake in Alaska in an attempt to accurately interpret the vibration characteristics, taking into consideration the effect of the wall flexibility where the tank deformations affect the hydrodynamic pressure, i.e., fluid-structure interaction takes place. It was concluded that the flexibility of cylindrical tank walls amplifies the tank's response. Therefore, it has to be accounted for (Veletsos (1974), and Haroun and Housner (1981, 1982)).

Many studies in the literature were found to be related to the buckling capacity of cylindrical liquid tanks under seismic loading. Virella et al. (2006) investigated the dynamic buckling of aboveground anchored cylindrical steel tanks subjected to horizontal components of real earthquake records numerically using the finite element method. The objective was to estimate the critical horizontal peak ground acceleration (PGA) causing either elastic or plastic buckling for the cylindrical shell. Three tank-liquid systems with different slenderness ratios were considered subjected to two natural excitation records. Dynamic buckling computations including material and geometric non-linearity were carried out. It was concluded that buckling at the top of the shell was caused by a negative net pressure at the zone in the tank where the impulsive hydrodynamic pressure induced by the earthquake excitation exceeds the hydrostatic pressure. This negative net pressure induces membrane compressive circumferential stresses causing buckling to the tank shell. The elastic buckling at the top represented the critical state for the medium and tall models, while plasticity was reached at the shell before buckling for the shallow tank. The slenderness ratio was found to have some influence on the critical PGA with no clear trend.

Virella et al. (2008) proposed a nonlinear static procedure based on the capacity spectrum method found in ATC-40 in order to evaluate the elastic buckling of above-ground anchored steel tanks due to horizontal seismic excitations. The objective was to obtain the minimum peak ground acceleration (PGA) value that produces buckling in the tank shell. The obtained critical PGA estimates were then compared with those calculated using the dynamic buckling analyses performed in the latter study. The following was concluded: (a) the nonlinear static procedure resulted in slightly smaller, i.e., conservative, values for the critical PGA compared to the dynamic buckling results, (b) similar first buckling modes were observed by using both static and dynamic buckling analyses, (c) the critical PGA decreases with the slenderness ratio.

Djermane et al. (2014) attempted to evaluate the current design guidelines related to dynamic instability provided by AWWA-D100 and EC8 provisions for cylindrical steel tanks using a numerical shell finite element model. The idea was to evaluate the critical PGA values that cause the tank instability and then compare with their counterparts obtained by the codes' provisions. The authors concluded the following: (a) comparison for broad tanks showed a good agreement between numerical and EC8 results, (b) standards need some revisions in order to provide improved consideration of the imperfections and geometric nonlinearities for the case of tall tanks, (c) simple stress limitation found in the standards is very conservative.

Buratti and Tavano (2014) discussed different buckling modes for liquid-containing circular cylindrical steel tanks that are fully anchored at the base with a special focus on the secondary buckling occurring in the top part of the tank. A case study for a broad cylindrical tank was used in order to investigate various aspects of dynamic buckling using a finite element model where the fluid was modelled in the form of unvarying added masses, i.e., assuming rigid tank. The following was concluded: (a) hoop stresses due to the hydrostatic pressure reduces the periods for shell-type vibration modes, but it does not affect cantilever-type vibration modes, (b) the secondary buckling is an elastic buckling mode, but it is strongly influenced by the occurrence of plasticity in other parts of the structure.

El Damatty et al. (1997b,c) conducted the first study to assess the behavior of conical tanks under seismic loading where a coupled shell element-boundary element formulation was developed to simulate the fluid-structure interaction. A fluid added mass matrix was derived and added to the mass matrix of the structure to be incorporated into a nonlinear dynamic analysis routine. The formulation was conducted for both horizontal and vertical excitations and the results showed that some of the tanks suffered dynamic instability although they were designed with factor of safety of about 2.5 under hydrostatic pressure. This in turn reflects the importance of the seismic loading compared to the hydrostatic one. Also, it was concluded that the contribution of vertical excitation to the dynamic instability has to be included.

As the finite element dynamic analysis for the tank-fluid system is considered computationally expensive, researchers tried to find a simpler procedure to estimate the total forces acting on the liquid tank structure when subjected to an earthquake event. A practical alternative was to model the contained liquid as lumped masses attached to the tank wall rigidly or through linear springs instead of modelling the contained fluid as a continuum, which in turn reduces the computation cost for the tank-fluid dynamic analysis. The masses-springs system is called equivalent mechanical model whose main objective is to match the resulting forces and moments obtained using dynamic analysis.

Haroun and Housner (1981) introduced a three masses mechanical model for cylindrical steel tanks. The three masses are the impulsive fluid mass, the convective fluid mass, and the mass reflecting the effect of the flexibility of the tank's wall. The impulsive mass represents the mass of the fluid vibrating in synchronism with the ground and rigidly connected to the tank's wall, while the convective one represents the mass of the fluid undergoing sloshing motion at the free surface. El Damatty and Sweedan (2006) developed a similar mechanical model for conical tanks in order to predict the base shear and overturning moment acting on the tanks when subjected to earthquake events.

Moslemi et al. (2011) analyzed an elevated steel conical tank twice when subjected to El-Centro ground motion; once using finite element analysis where the fluid was modeled using displacement-based elements and once using the ACI procedure which is based on

Housner's mechanical model for equivalent cylindrical tank. The difference between the two methods in terms of base shear and base moment was around 6%.

The aim of this study is to determine the capacity of steel conical tanks under hydrodynamic pressure due to horizontal ground excitation. The capacity, expressed in terms of base shear, is obtained using a finite element model through non-linear static pushover analysis. Two base shear capacities corresponding to impulsive and sloshing hydrodynamic pressure are obtained. Geometric imperfections are incorporated in the finite element model in order to study their effect on the capacity of the steel conical tanks. The base shear capacities for different levels of geometric imperfections are represented in the form of charts for different tank dimensions. Finally, the tank capacities are compared to the seismic demand for different seismic zones in Canada obtained using previously developed mechanical model found in literature in order to assess the design of the steel conical tanks.

2.2 Hydrodynamic Pressure

Hydrodynamic pressure is induced on the tank walls and floor during seismic excitation acting on a conical tank. The total hydrodynamic pressure can be divided into two components: impulsive pressure P_I and convective pressure due to sloshing of the water surface P_S. The sloshing component is a long period component relative to the impulsive one and hence the two components can be decoupled in the analysis.

The impulsive component associated with the hydrodynamic pressure for a conical tank containing an ideal fluid and prevented from rocking is governed with the following set of equations and boundary conditions (El Damatty et al. 1997b):

$$\nabla^2 P_I(r,\theta,z,t) = 0 \qquad\qquad \text{inside the fluid volume} \qquad [2\text{-}1]$$

$$\partial P_I(r,\theta,z,t)/\partial n = -\rho_F \ddot{u}\,(r,\theta,z,t).n \qquad\qquad \text{at the surface } S_1 \qquad [2\text{-}2]$$

$$P_I = 0 \qquad\qquad \text{at the surface } S_3 \qquad [2\text{-}3]$$

$$\partial P_I(t)/\partial n = 0 \qquad\qquad \text{at the surface } S_2 \qquad [2\text{-}4]$$

where $\ddot{u}\,(r,\theta,z,t)$ is the acceleration vector at any point of the tank's wall, n is the unit vector normal to the surface of the tank, and ρ_F is the fluid density. Surfaces S_1, S_2 and S_3;

coordinates r, θ, and z are shown in Fig. 2-3 and t is the time. The condition in Eq. 2-3 reflects the assumption of no sloshing effect as it can be decoupled from the impulsive one, while Eq. 2-4 reflects the assumption of no base rocking motion.
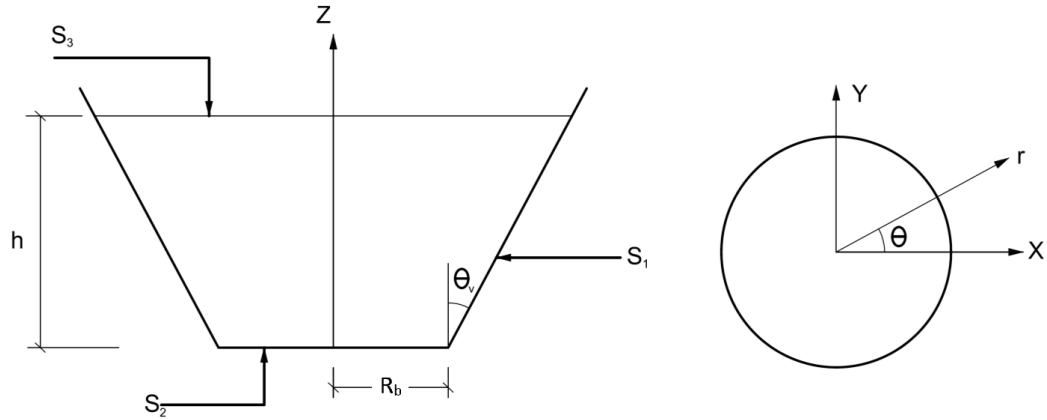
Fig. 2-3 Co-ordinate system for the steel conical tank and dimensional parameters

The solution of the above differential equation was done using the boundary element method by (Haroun, 1980) for cylindrical tanks and the same approach was followed by (El Damatty et al. 1997b) for conical tanks. The basic idea is to interpolate the dynamic pressure using different shape functions satisfying the partial differential equation. The impulsive component of the hydrodynamic pressure can be interpolated as follows:

$$P_I(r,\theta,z,t) = \sum_{n=1}^{N_2} \sum_{i=1}^{N_1} A_{in}(t)\, I_n(\alpha_i r)\, \cos(\alpha_i z)\, \cos(n\theta) \qquad [2\text{-}5]$$

$$\alpha_i = (2i\text{-}1)\,\pi/2h \qquad [2\text{-}6]$$

where $A_{in}(t)$ is an amplitude function of time, I_n are the modified Bessel's functions of the first kind. The term $\cos(\alpha_i z)$ represents the variation of the hydrodynamic pressure for mode i in the vertical Z direction, while the term $\cos(n\theta)$ represents the variation of the hydrodynamic pressure for mode n in the circumferential direction where n is the wave number. The distribution of the first three pressure modes is shown in Fig. 2-4(a-c).
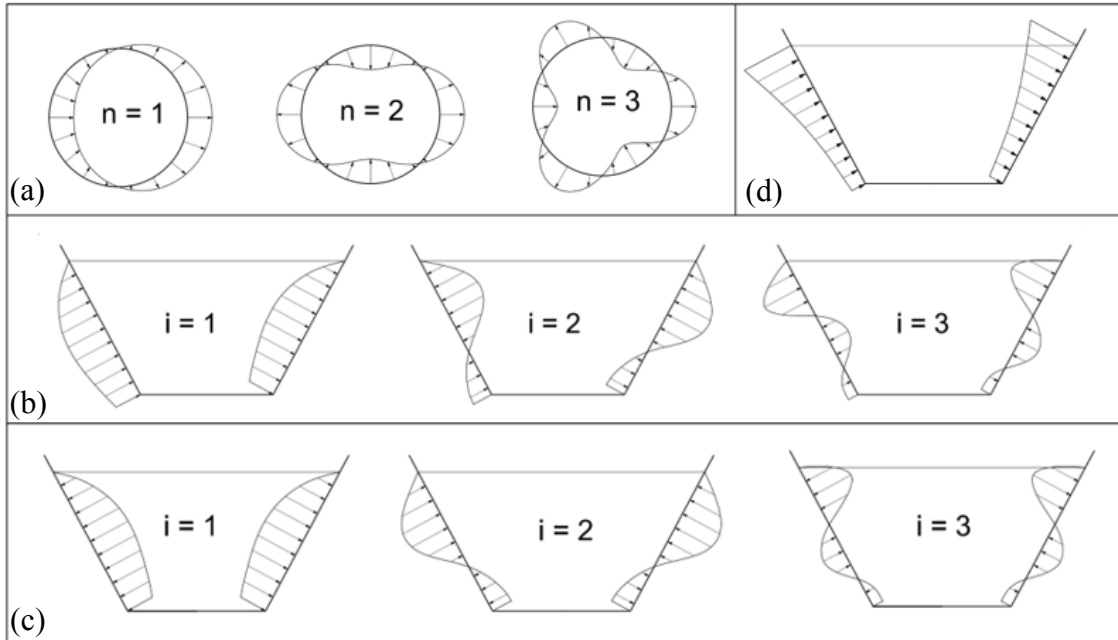
Fig. 2-4 Distribution of different pressure modes: (a) Circumferential distribution, (b) Vertical distribution for impulsive pressure modes n=1, 3, 5, .. , (c) Vertical distribution for impulsive pressure modes n=2, 4, 6, .., (d) Vertical distribution for fundamental sloshing pressure mode

As a result of the decoupling between liquid sloshing modes and shell vibration modes, the sloshing component $P_S(r,\theta,z,t)$ can be evaluated assuming the tank walls are rigid. Based on this assumption, El Damatty et al. (2000) derived an expression for the fundamental sloshing component of the hydrodynamic pressure as follows

$$P_S(r,\theta,z,t) = B(t)\, \rho_F\, J_1(k_1 r)\, \cosh(k_1 z)\cos(\theta) \qquad\qquad [2\text{-}7]$$

where $J_1(k_1 r)$ is the Bessel's function of the first kind of order one, $B(t)$ is arbitrary function of time, and ρ_F is the fluid density. A procedure to evaluate the constant k_1 was discussed in detail by El Damatty et al. (2000). The vertical distribution for the fundamental sloshing pressure mode is shown in Fig. 2-4d. Details of the impulsive and sloshing pressure derivations are found in Appendix D.

2.3 Finite Element Model

In this study, three-dimensional numerical models are developed for steel conical tanks using the finite element method. The numerical model is based on a consistent 13 noded subparametric triangular shell element shown in Fig. 2-5a, which was developed by Koizey and Mirza (1997). This element has the advantages of being free of the spurious shear modes, i.e., locking phenomenon observed in isoparametric shell elements when used in modeling thin shell structures. El Damatty et al. (1997d) extended the formulation of this shell element to include geometric and material non-linearities. Accordingly, this model can be used to predict both elastic and inelastic buckling. Due to symmetry about the horizontal axis in both loading and geometry, only half of the cone is modelled and used in the analysis. A mesh sensitivity analysis was performed in order to determine the mesh size that is able to capture the expected buckling accurately. It is found that a mesh of 512 triangular elements as shown in Fig. 2-5b is sufficient to accurately capture the buckling waves near the tank base.

The length of the elements is not uniform as the mesh is chosen to be finer near the base of the tank due to the stress concentration at this location where buckling is expected to occur. The tanks are assumed to be hinged at the base along the circumference and free at the top.
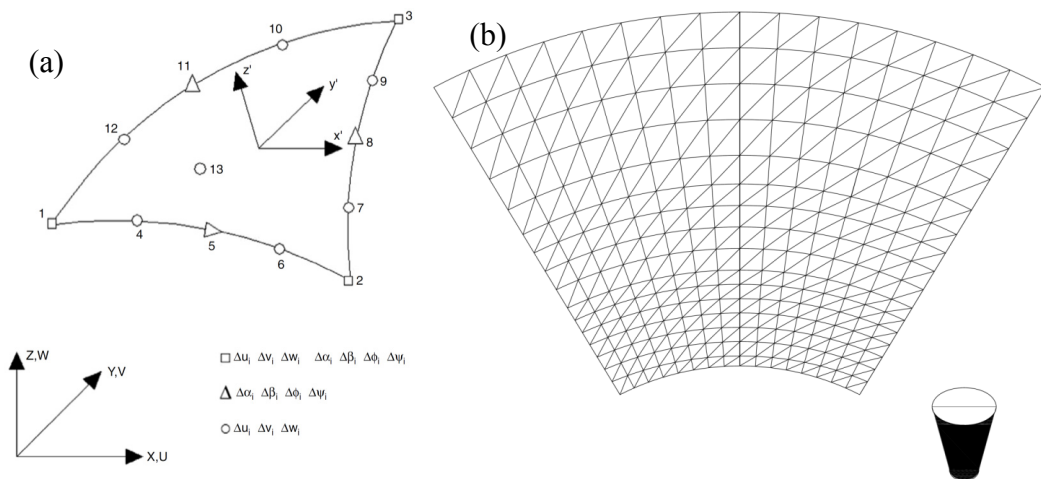
Fig. 2-5 (a) Coordinates and degrees of freedom for a consistent shell element, (b) Finite element mesh for half cone

2.4 Method of Analysis

In this study, non-linear static analysis, commonly known as pushover analysis, is used to obtain the load-carrying capacity of the conical tanks. The non-linear static analysis is carried out by increasing the load value incrementally till reaching failure, which is in the form of buckling of the steel vessel. The load increase is achieved using an increasing load factor, which is multiplied by the applied hydrodynamic pressure load pattern. The non-linearity in the analysis comes from the inclusion of both geometric and material non-linearity in the finite element model previously discussed. To include both the hydrostatic and hydrodynamic pressure in the analysis, two load factors are used. The first is P_{HS}, which corresponds to the hydrostatic pressure while the second is P_{HD}, which corresponds to the hydrodynamic pressure. The analysis starts with a value of the load factor P_{HD} equals to zero and then the load factor P_{HS} is increased incrementally until it reaches the actual value of the hydrostatic pressure acting on the tank. After this stage, the value of P_{HS} is kept constant and the value of P_{HD} begins at zero and increases until failure occurs. At the end of the analysis, the value of P_{HD} at failure is recorded along with the deformations, forces, and stresses corresponding to the failure value. It should be noted that the load increments near the failure are reduced in order to better capture the failure load factor. This is achieved by doing more than one trial for each analysis.

A group of 75 tanks of practical dimensions are chosen for this study with R_b ranging from 4.0m to 6.0m, h from 5.0m to 9.0m, and $\theta_v = 30^o$, 45°, 60° with steel yield stress of 300 MPa. The tanks are preliminary designed under hydrostatic pressure based on the simplified method proposed by Sweedan and El Damatty (2009) assuming good tanks regarding the level of geometric imperfection. As yielding of the tank usually precedes buckling, i.e., inelastic buckling is expected, the main idea of this simplified design procedure was to prevent the tank shell from reaching the yielding state at any point under hydrostatic pressure. The concept was based on developing a stress magnification factor that relates the maximum stresses that occur in the walls of the tanks resulting from membrane, bending and geometric imperfection effects, to the theoretical values obtained from membrane behaviour.

Based on the distribution of different pressure modes shown in Fig. 2-4, it is clear that the total base shear will result from cos θ mode only, i.e., n=1. Regarding the vertical distribution of the pressure modes, only the first vertical mode, i.e., i=1, is included in the analysis of calculating the conical tank capacities.

The analysis starts with applying the axi-symmetric hydrostatic pressure on the tank walls. A typical plot for the radial deformations of the tank walls at different angles θ is shown in Fig. 2-6. As it is expected due to the inclination of the walls, a buckling wave is noticed near the base of the tank due to the high compressive stresses at that location. It is worth mentioning that although this buckling wave occurred, the tank is still able to resist more loads due to hydrodynamic pressure. This is the case since the tanks are designed to sustain a value of P_{HS} exceeding the actual hydrostatic pressure. After reaching this stage, the hydrodynamic pressure with the cos θ pattern is applied on the walls of the tank and increased incrementally while the hydrostatic pressure is kept constant.

By comparing the radial deformations of the tank walls at failure shown in Fig. 2-6 to those just after the hydrostatic pressure phase, it is noticed that along the line $\theta = 0^o$ the radial displacement peak location is shifted up and the buckling wave near the base of the tank becomes more clear. At $\theta=90^o$, the distribution and the values of the radial displacement are nearly the same. Finally at $\theta=180^o$, the radial displacements at failure are with negative sign, i.e., inwards the tank and the buckling wave is reduced. A typical circumferential distribution of the tank deformations is shown in Fig. 2-7.
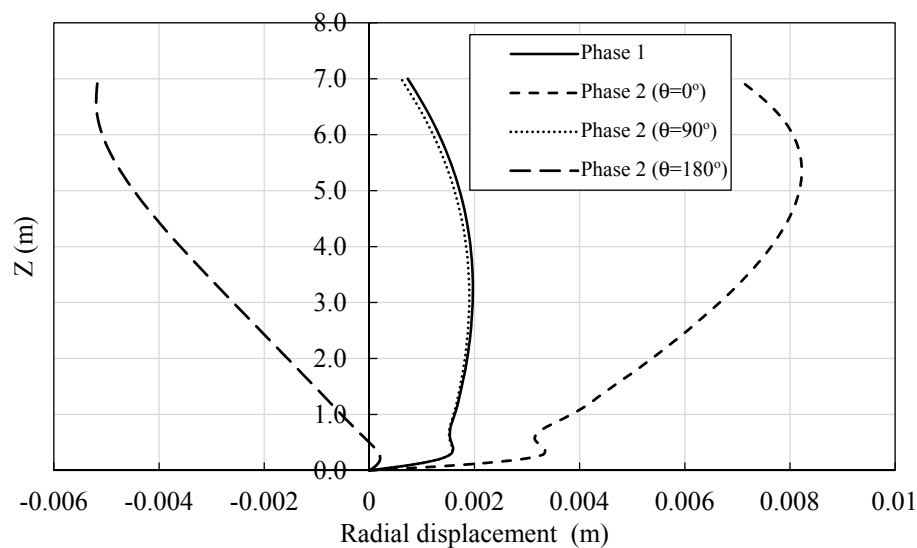
Fig. 2-6 Radial deformations of the tank walls at the end of each phase
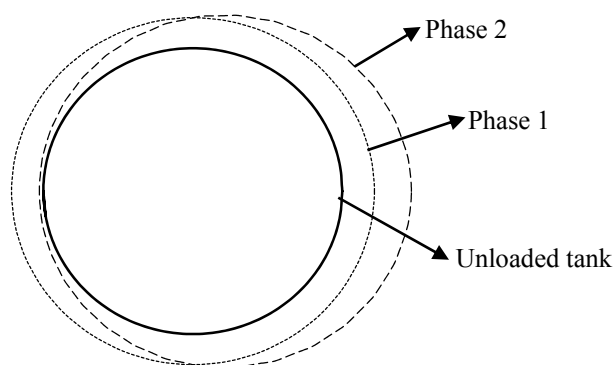
Fig. 2-7 Deformed shape at the end of each phase of loading

In order to check the assumption of excluding the base rocking motion effects on the hydrodynamic pressure when obtaining the capacities of steel conical tanks, two sets of time history analyses were performed; one with allowing the tank base to undergo rocking motion while the other preventing such motion. The results of the analyses showed that the difference between the base shear values recorded at buckling for the two cases to be less than 5% for different tank configurations, i.e., inclination angle and level of imperfections. As such, the curves developed in this study for estimating the seismic capacity of steel conical tanks can be applied to both ground and elevated tanks.

2.5   Impulsive Base Shear Capacity

2.5.1   Perfect Tanks

The capacity of the tanks can be expressed using the value of the load factor P_{HD} at failure, but a more relevant quantity especially for seismic related problems is the value of the base shear at failure. The purpose of this part of the study is to assess the base shear capacity of steel conical tanks under the effect of hydrodynamic pressure in addition to the existing hydrostatic pressure. For conical tanks, the value of the base shear reflects the overturning moment acting on the tank, which could be very critical. In addition, the base shear combined with the overturning moment is required for the design of the supporting shaft as well as the foundations. In this study, a steel conical steel tank is considered a failed one whenever one of the following two failure criteria takes place: (1) Yielding failure where the tank shell yields before buckling instability takes place (2) Buckling failure where the tank shell suffers instability before yielding, i.e., elastic buckling. As a result, the base shear capacity of a steel conical tank in the current study represents the base shear value just before yielding or buckling for the tank vessel.

In order to understand how the base shear value at failure varies with changing the tank geometric parameters, a parametric study is performed. The base shear V_I is normalized to the total weight of the fluid contained in the tank W in the form of the base shear ratio V_I/W. For the 75 steel conical tanks discussed earlier, Figs. 2-8, 2-9, and 2-10 shows the variation of the ratio V_I/W with the parameters h, R_b, and θ_v, respectively for different wall thicknesses t_w. For each chart, the geometric parameter under consideration is changed in addition to the wall thickness while keeping all the other parameters unchanged. The default values for different parameters are h=7.0m, R_b=5.0m, and θ_v=45°. It is concluded from the charts that the value of V_I/W decreases as the height of the tank or the bottom radius or the angle θ_v increase. Finally, the ratio V_I/W increase with increasing the thickness of the tank walls.
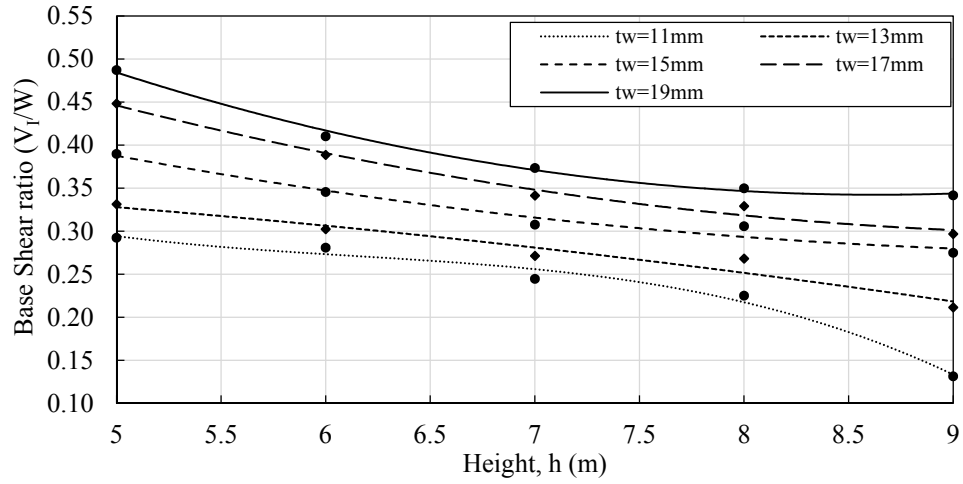
Fig. 2-8 Variation of impulsive base shear ratio with the tank height and thickness
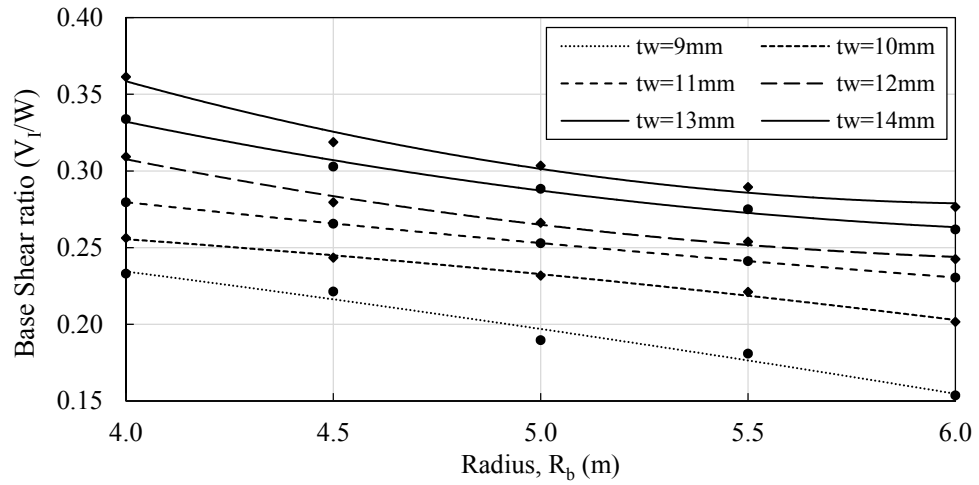
Fig. 2-9 Variation of impulsive base shear ratio with the tank radius and thickness
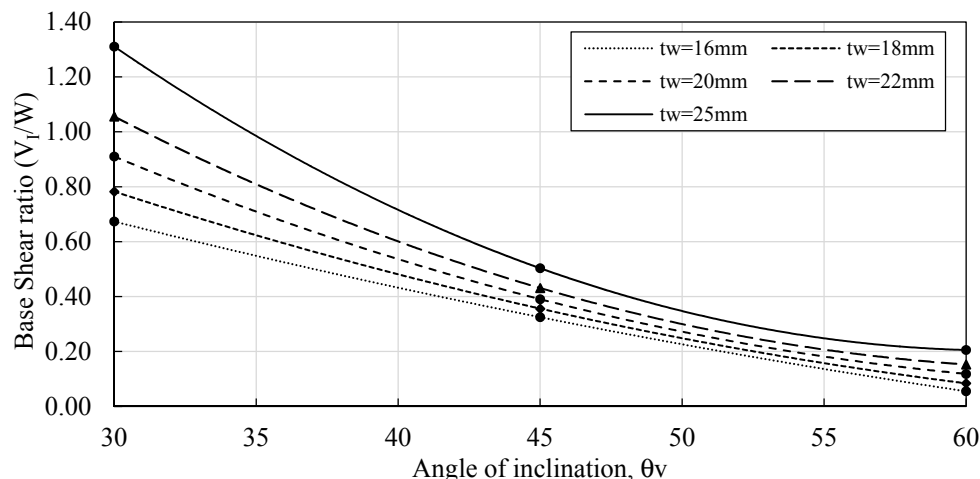
Fig. 2-10 Variation of impulsive base shear ratio with the tank angle of inclination and thickness

As mentioned earlier, this study represents part of a larger investigation that aims to provide a simplified design procedure for steel conical tanks when subjected to ground excitations. Although the latter charts related the impulsive base shear capacity to the tank dimensions, they cannot be used for other combinations of conical tank dimensions. As a result, a more generalized form is required to express the impulsive base shear capacity for steel conical tanks with random dimensions to assess the tank design. In order to achieve that, several forms of the relation between the base shear ratio V_I/W and the tank dimensions are studied and it is found that the two dimensionless parameters h/R_b and V_IR_b/Wh can represent such relation.

The variation of the parameters h/R_b and V_IR_b/Wh is presented in Figs. 2-22 to 2-24 in Appendix A for different values of the angle θ_v. The effect of wall thickness is shown through a family of curves represented in the form of multiplier of t_s which is the thickness obtained by the simplified hydrostatic design method proposed by Sweedan and El Damatty (2009). Using these charts, the base shear capacity V_I for a perfect i.e., no geometric imperfections, pure steel conical tank with specific geometric parameters under impulsive hydrodynamic pressure can be obtained. Regarding the governing failure mode for the considered group of steel conical tanks, the general trend is that the probability for yielding failure to occur is higher when the angle θ_v is increased. In addition, the increase

in the tank wall thickness is found to make the elastic buckling failure criterion more probable.

2.5.2   Imperfect Tanks

In the previous section, the capacity of perfect steel conical tanks was evaluated based on the tank dimensions. In fact, it requires a superior quality control to get perfect straight thin steel plates, which can be almost impossible. As a result, geometric imperfections of the conical tank walls will exist and their amplitude will be dependent on the quality control applied by the builder. Geometric imperfections play an important role in defining the buckling capacity of shell structures in general. Although geometric imperfections are randomly distributed in a shell, a conservative used model for simulating the geometric imperfections is shown in Fig. 2-11 and described by the following expression:

$$W(s) = w_0 \sin(2\pi s/L_I) \cos(n\theta) \qquad\qquad [2\text{-}8]$$

where w_0 is the imperfection amplitude, L_I is the imperfection wavelength, s is a coordinate measured along the generator of the vessel, and n is an integer defining the circumferential wavelength of the imperfection shape. According to Vandepitte et al. (1982), a conical tank with the ratio (w_0/L_I) less than 0.004 is considered a good cone while a conical tank with the ratio (w_0/L_I) greater than 0.004 but less than 0.01 is considered a poor cone.
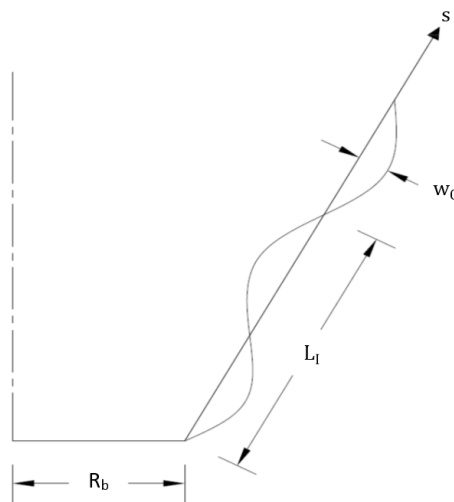
Fig. 2-11 Assumed imperfection shape along the generator of tank

In this section, the effect of geometric imperfections on the capacity of the steel conical tanks when subjected to both hydrodynamic and hydrostatic pressure is studied. The geometric imperfection is incorporated in the finite element model discussed in Section 2.3 in the form of initial strains prior to load application. Firstly, the critical imperfection shape i.e., L_I and n, leading to minimum buckling capacity of the steel conical tank has to be determined. Under the effect of hydrostatic pressure only, Vandepitte et al. (1982) used experimental results to get an expression for the critical buckling wave length L_{CR} which turned out to be independent of the height of the tank. Regarding the circumferential distribution of the imperfections along the surface of the vessel, El Damatty et al. (1997a) have shown that an axisymmetric distribution, i.e., n=0, leads to minimum buckling capacity of pure conical tanks. This is due to the presence of hydrostatic pressure, which tends to force the structure to buckle in an axisymmetric mode; consequently an imperfection shape matching this mode is the critical one.

Following the same analogy and knowing that hydrostatic pressure has an axisymmetric distribution, and hydrodynamic pressure is in the form of cosθ mode, a distribution of geometric imperfections corresponding to n=0 or n=1 will lead to the minimum buckling capacity of the steel conical tanks when subjected to both hydrodynamic and hydrostatic pressure. In order to determine which imperfections' distribution is critical, a group of 60 steel conical tanks of practical dimensions are used. The same two-phase loading procedure discussed in Section 2.4 is repeated for each tank twice; one with inclusion of axisymmetric imperfections tanks and the other with antisymmetric distribution i.e., n=1 with the same buckling wave length L_I recommended by Vandepitte et al. (1982). It is found that a value of n=0 will always lead to a lower buckling capacity for the steel conical tanks. This means that the hydrostatic pressure loading governs the buckling capacity of the conical tanks due to the initiation of the buckling waves during the hydrostatic pressure only loading phase as discussed earlier.

In order to understand how the impulsive hydrodynamic pressure in the form of cosθ mode affects the buckling capacity of the conical tanks, a hypothetical analysis is performed where the conical tanks are subjected to only hydrodynamic pressure in the form of cosθ mode with no hydrostatic pressure till failure. A typical deformed shape at failure for one

of the cases is shown in Figs. 2-12, 2-13. In these figures, no clear buckling wave occurred along the meridian of the tank similar to the case of the hydrostatic pressure ,while the failure happened due to buckling in the circumferential direction near θ =180°. Comparing the deformed shape for the two cases, it is concluded that hydrostatic pressure tends to force a conical tank to buckle along the meridian, which matches the assumed imperfection shape shown in Fig. 2-11. The hydrodynamic pressure on the other hand tends to force a conical tank to buckle in the circumferential direction making an axisymmetric imperfections' distribution more critical.

It has to be mentioned that the inclusion of the axisymmetric geometric imperfections in the non-linear static analyses results in the increase of the buckling capacity in some of the studied cases, especially with θ_v=30, in comparison to the case of perfect tanks. This is due to the fact that the hydrodynamic pressure in the form of $\cos\theta$ mode acts in the same direction of hydrostatic pressure in one half of the tank and in opposite direction in the other half. This might delay the failure due to the buckling of the conical tank. This occurs since the distribution of the geometric imperfections is axisymmetric i.e., similar to the hydrostatic pressure. In order to make the geometric imperfections more critical and avoid increasing the buckling capacity of the tanks, a geometric imperfection pattern with n=0 is used but only in the side where the hydrodynamic pressure is acting in the same direction of the hydrostatic pressure i.e., θ = 0 to 90.
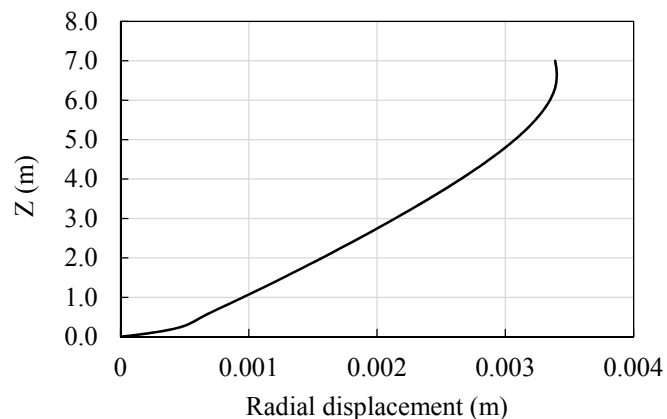
Fig. 2-12 Variation of radial displacements with height for the case of hydrodynamic pressure only
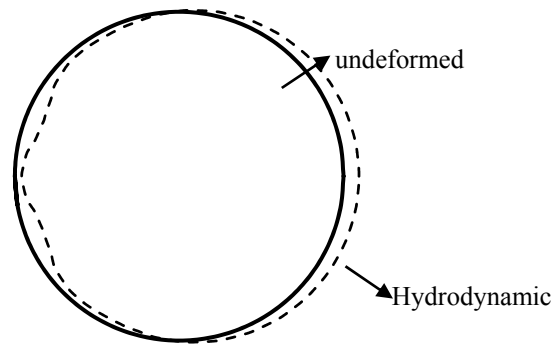
Fig. 2-13 Deformed shape at failure for the case of hydrodynamic pressure only

In order to determine the critical imperfection wave length L_{CR}, several analyses are performed for each of the 60 conical tanks with different imperfection wave lengths, and that which leads to a minimum buckling capacity is considered the critical imperfection wave length L_{CR}. A similar expression to that proposed by Vandepitte et al. (1982) is assumed. Using regression analysis as shown in Fig. 2-14, the final expression is

$$L_{cr} = 4.03\sqrt{R_b t_w / \cos\theta_v} \qquad\qquad\qquad [2\text{-}9]$$

where R_b is the tank bottom radius, t_w is the wall thickness and θ_v is the angle of inclination with the vertical. The effect of variation of the tank height on the critical imperfection wave length is found to be insignificant as noticed by Vandepitte et al. (1982).
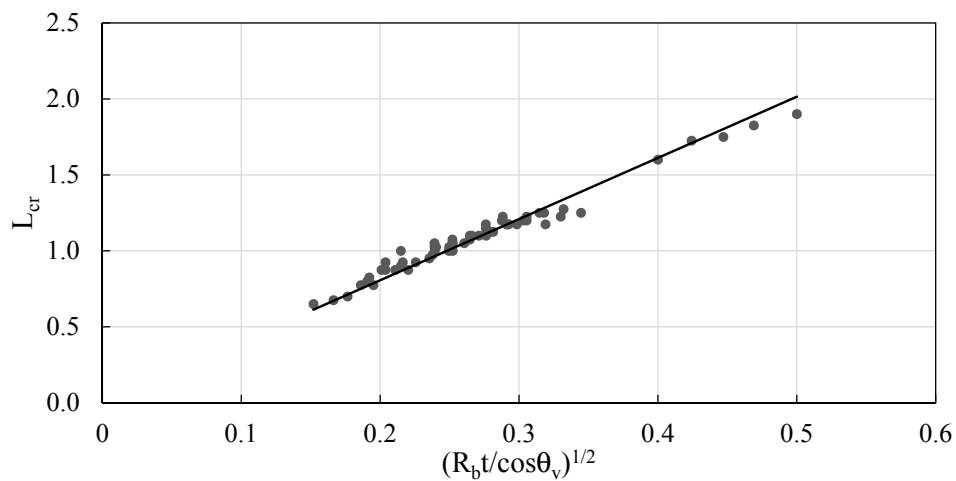
Fig. 2-14 Relation between critical imperfection wave length and $(R_b t_w / \cos\theta_v)^{0.5}$

After deriving an expression for the critical imperfection wave length L_{CR}, an axisymmetric imperfection pattern based on Eq. 2-8 is applied to the tanks. Two levels of imperfections are studied: the first with $w_0 = 0.004L_{cr}$ to represents good tanks and the second with $w_0 = 0.01L_{cr}$ represents poor tanks. Figs. 2-15 to 2-17 show the reduction in the base shear capacity of the 75 steel conical tanks for the two levels of imperfections, where t_s is the thickness obtained by the simplified hydrostatic design method.
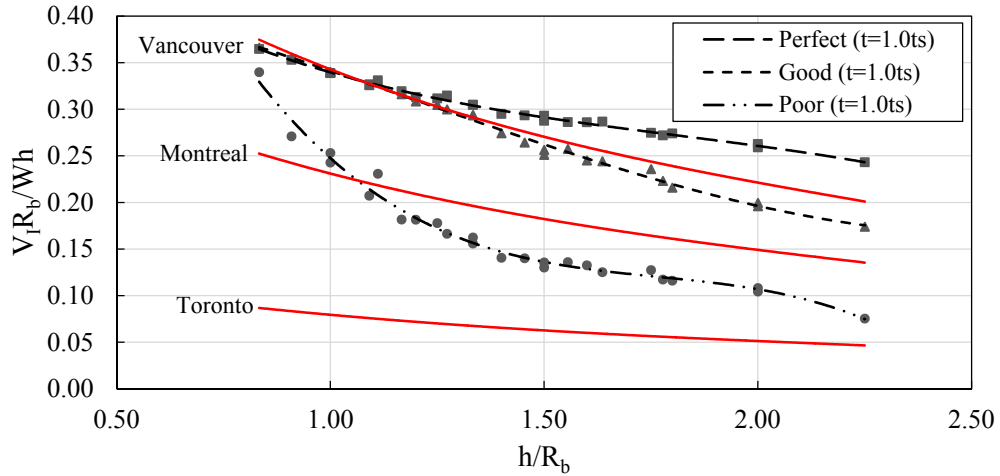
Fig. 2-15 Comparison of impulsive base shear capacity for different imperfection levels and actual base shear values for the three seismic zones (θ_v=30)
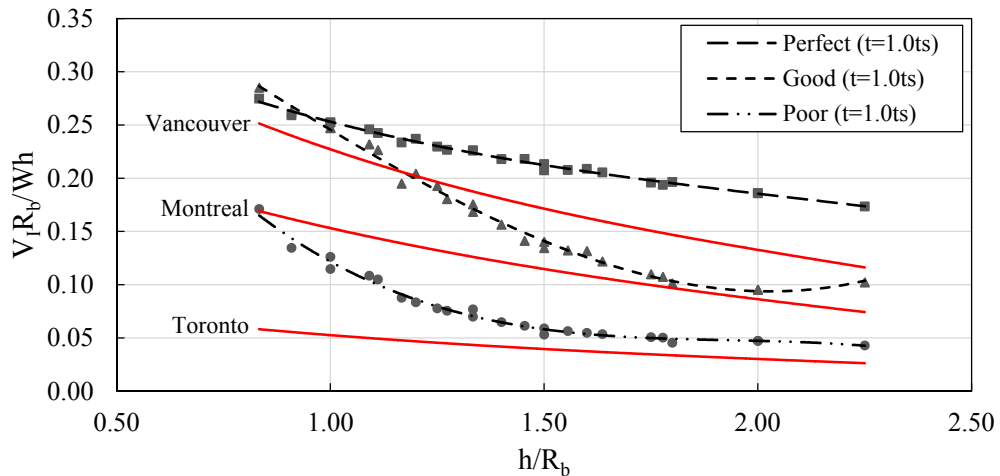
Fig. 2-16 Comparison of impulsive base shear capacity for different imperfection levels and actual base shear values for the three seismic zones (θ_v=45)
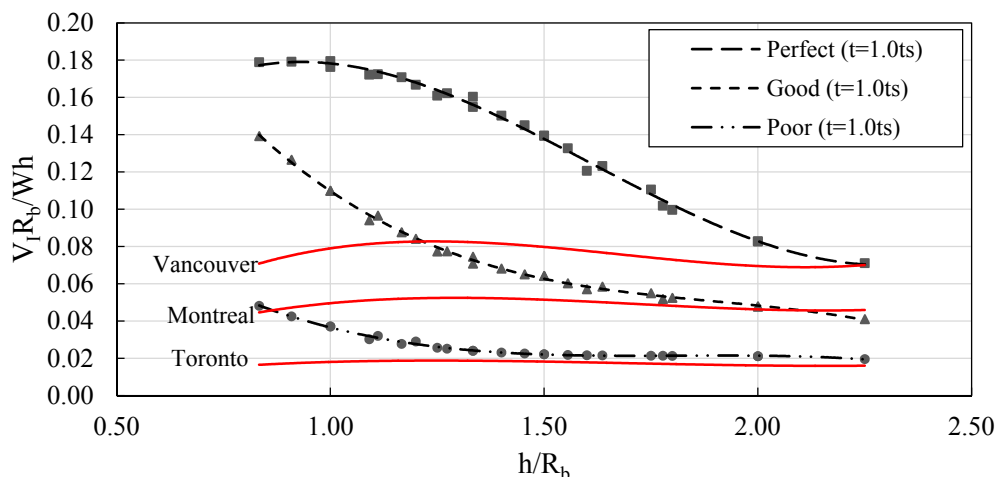
**Fig. 2-17 Comparison of impulsive base shear capacity for different imperfection
levels and actual base shear values for the three seismic zones (θ_v=60)**

In the case of θ_v=30, it is observed that an imperfection with amplitude of 0.004L or less has no remarkable effect on the normalized base shear capacity for the tanks with h/R_b less than 1.1. In the case of an imperfection amplitude equals to 0.01L, the reduction in the normalized base shear capacity increases with higher h/R_b. For θ_v=45, it is found that an imperfection with an amplitude of 0.004L or less does not have a remarkable effect on the normalized base shear capacity for tanks with h/R_b less than 1.0 while for an imperfection amplitude of 0.01L, the reduction in the normalized base shear capacity is almost the same regardless of the value h/R_b. Finally for θ_v=60, the reduction in the normalized base shear capacity decreases for higher h/R_b values, and this is valid for the two level of imperfections studied.

The variation of the impulsive base shear capacity ratio $V_I R_b/Wh$, with the ratio of h/R_b, for imperfect steel conical tanks is shown in Figs. 2-25 to 2-30 found in Appendix A for different values of the angle θ_v. In these figures, t_s is the thickness obtained by the simplified hydrostatic design method. With regards to the governing failure mode in the case of imperfect steel conical tanks, the general trend is that the probability for inelastic buckling to take place increases with higher geometric imperfections' amplitude.

2.6 Sloshing Base Shear Capacity

In the previous sections, only the impulsive component of the hydrodynamic pressure was included in the analysis. As discussed in Section 2.2, another component of the hydrodynamic pressure that acts on the tank walls when subjected to a horizontal excitation is the convective pressure, which results from the sloshing of the water surface. Since the natural frequencies of the impulsive and sloshing vibration modes are well separated from one another, the analysis for each component can be performed separately and then combined using appropriate combination rule.

The goal of this section is to evaluate the sloshing base shear capacity for a steel conical tank. A similar set of non-linear static analyses to those performed for the impulsive component of the hydrodynamic pressure discussed in Section 2.4 are repeated for the sloshing component using the sloshing hydrodynamic pressure pattern corresponding to Eq. 2-7. The sloshing coefficient K_1 is obtained as described by El Damatty et al. (2000).

The output of each analysis is the base shear value at failure V_S which is normalized in the form of $V_S R_b / Wh$. The variation of the base shear ratio $V_S R_b / Wh$ with the parameter h/R_b for different angles of inclination with the vertical θ_v is shown in Figs. 2-31 to 2-33 found in Appendix A. The effect of wall thickness is included through a family of curves represented in the form of multipliers t_s which represents the thickness obtained by the simplified hydrostatic design method. Using these charts, the sloshing base shear capacity V_S for a perfect pure steel conical tank with specific geometric parameters under impulsive hydrodynamic pressure can be obtained. As for the governing failure mode for the considered group of steel conical tanks, the same observations as those in the case of impulsive pressure are valid for the case of sloshing pressure.

Since the impulsive and connective hydrodynamic pressures act simultaneously, the effect of geometric imperfection on the sloshing base shear capacity of the steel conical tanks is studied using the same imperfection pattern discussed earlier for the impulsive case. An axisymmetric geometric imperfection distribution with a wave length following Eq. 2-9 is incorporated in the finite element model in the form of initial strains. Two levels of imperfections are studied: the first with $w_0 = 0.004 L_{cr}$ representing good tanks and the

second with $w_0 = 0.01L_{cr}$ representing poor tanks. The variation of the normalized sloshing base shear capacity V_SR_b/Wh with the ratio h/R_b, for the two levels of imperfection as well as the case of perfect tanks for the purpose of comparison is shown in Figs. 2-18 to 2-20 for different angles θ_v.
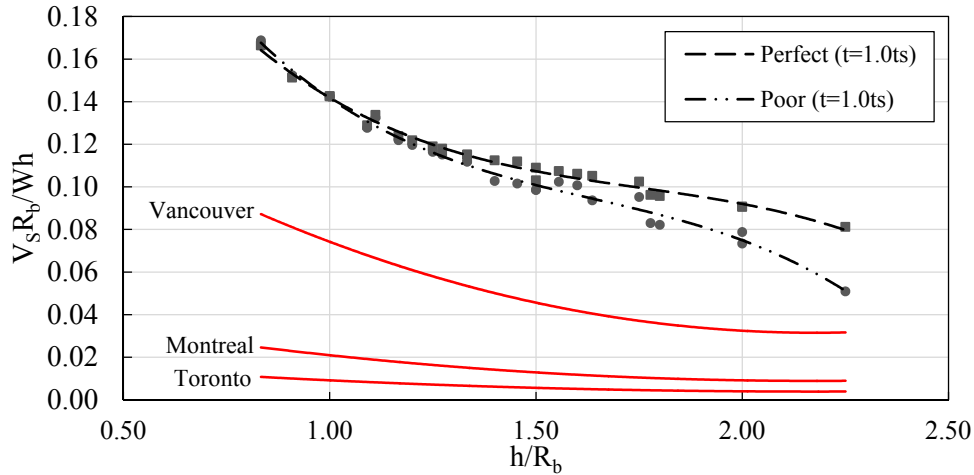
Fig. 2-18 Comparison of sloshing base shear capacity for different imperfection levels and actual base shear values for the three seismic zones (θ_v=30)
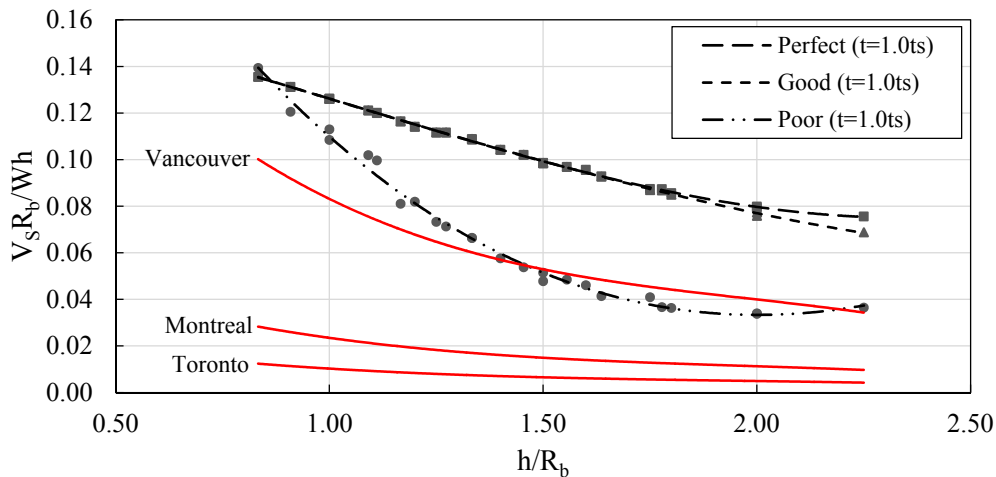
Fig. 2-19 Comparison of sloshing base shear capacity for different imperfection levels and actual base shear values for the three seismic zones (θ_v=45)
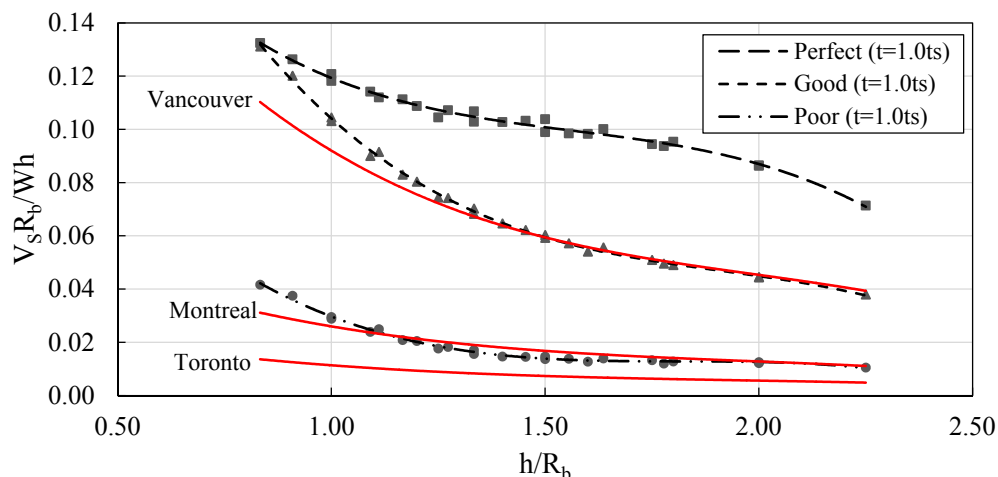
Fig. 2-20 Comparison of sloshing base shear capacity for different imperfection levels and actual base shear values for the three seismic zones (θ_v=60)

For the case of θ_v=30, an imperfection with amplitude 0.004L or less has no effect on the normalized base shear capacity. On the other hand for the case of imperfection amplitude equals to 0.01L, the reduction in the normalized base shear capacity increases with higher h/R_b. For θ_v=45, it is found that an imperfection with amplitude 0.004L or less has no remarkable effect on the normalized base shear capacity for tanks with h/R_b less than 1.8, while for imperfection amplitude of 0.01L, the reduction in the normalized base shear capacity is higher for larger h/R_b until a value of 2. Finally for θ_v=60 with imperfection amplitude of 0.004L, the reduction in the normalized base shear capacity is higher with larger h/R_b until a value of 2. Significant reduction in the normalized base shear capacity is observed with the case of 0.01L imperfection amplitude.

The variation of sloshing base shear capacity in the form of V_SR_b/Wh with the ratio h/R_b for imperfect steel conical tanks with different wall thicknesses are shown in Figs. 2-34 to 2-39 found in Appendix A for different values of the angle θ_v.

2.7   Base Shear Seismic Demand

In the previous sections, the base shear capacity of a steel conical tank subjected to both hydrostatic and hydrodynamic pressures was obtained based on the geometry of the tank and the level of geometric imperfections using non-linear static analysis. In this section,

the previously obtained impulsive and sloshing base shear capacities are compared to seismic demands for the seismic zone in which the conical tank will be located in order to assess the initial design of the steel conical tanks under hydrostatic pressure only. Seismic demands are represented in the form of actual base shear acting on the steel conical tank when subjected to a horizontal ground excitation.

The idea of the mechanical model is to represent the conical tank as a set of lumped masses and springs in order to achieve the same resulting base shear and overturning moment obtained by dynamic analysis when subjected to the earthquake event. The mechanical model derived by El Damatty and Sweedan (2006) shown in Fig. 2-21 is used in this study to obtain the seismic demand. The masses m_r, m_f, and m_s represent the impulsive mass component, the mass reflecting the effect of walls' flexibility, and the convective mass component, respectively. The total base shear is given by

$$Q_{max} = \sqrt{Q_{Ir}^2 + Q_{If}^2 + Q_S^2}$$ [2-10]

$$Q_{Ir} = [(m_r - m_f) + m_{o\text{-}sh}]\ddot{G}_{max}$$ [2-11]

$$Q_{If} = [m_f + m_{e\text{-}sh}]S_{a\text{-}sys}$$ [2-12]

$$Q_S = m_s\, S_{a\text{-}s}$$ [2-13]

where Q_{Ir} and Q_{If} reflect the contribution of the rigid and flexible components of the impulsive pressure and Q_S reflects the sloshing contribution. The masses m_{o-sh} and m_{e-sh} represent the portion of the walls' mass associated with the rigid and flexible vibration modes, respectively. The acceleration $\ddot{G}_{max}$ is the maximum ground acceleration for the earthquake excitation also known as the peak ground acceleration PGA while S_{a-sys} and S_{a-s} represent the spectral accelerations corresponding to the natural frequencies of the liquid-shell system and the first sloshing mode, respectively.
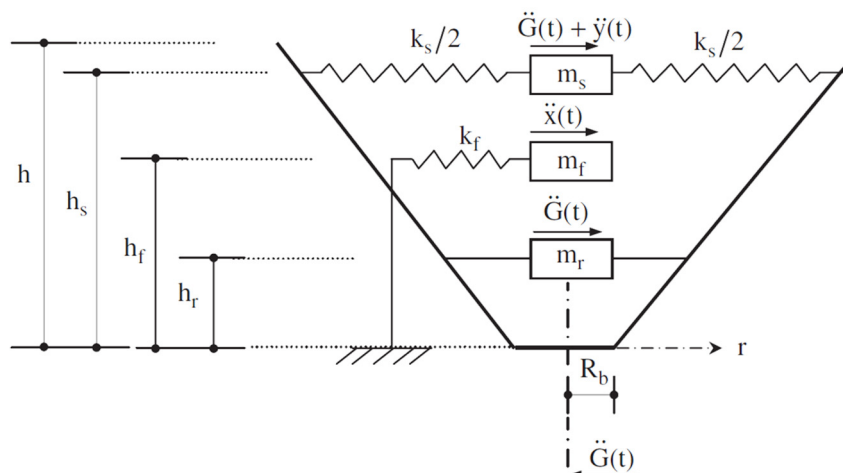
Fig. 2-21 Schematic presentation of the equivalent mechanical analog (El Damatty and Sweedan 2006)

Regarding the damping, a value of 0.5% damping is recommended regarding the sloshing vibration mode, while a value of 2% for steel tanks is recommended with regards to the impulsive mode. Three Canadian seismic zones are considered, which are Toronto, Montreal, and Vancouver seismic zones. Toronto is chosen to represent a moderate seismically active region while Montreal and Vancouver are chosen to represent zones with high activity. The NBCC (2010) 5% damping horizontal hazard design values for the three areas are summarized in Table 1.

Table 2-1 Seismic hazard design values for selected locations in terms of (g)

Location	PGA	Sa(0.2)	Sa(0.5)	Sa(1.0)	Sa(2.0)	Sa(4.0)
Toronto	0.12	0.22	0.13	0.067	0.021	0.0105
Montreal	0.33	0.64	0.31	0.14	0.048	0.024
Vancouver	0.47	0.95	0.65	0.34	0.17	0.085

In order to obtain the response spectrum corresponding to damping ratios different than 5%, a technique based on artificial acceleration time histories compatible with the NBCC 2010 spectra is used. Preliminary, a set of acceleration time histories with different durations compatible with the 5% NBCC 2010 spectra are obtained. Secondly, the response spectra for other values of damping ratio are evaluated and compared to the 5% response

spectrum. Finally, an average value of the increase ratio required for the damping conversion is calculated. This technique is applied separately for impulsive and convective vibration modes each with their corresponding range of frequencies for the set of tanks used in this study. It is found that the 5% response spectrum should be increased with an average factor of 1.44 and 1.2 in order to obtain the 2% damping spectrum and the 0.5% damping spectrum, respectively.

For the impulsive mode, the base shear demand values for impulsive pressure $Q_I = \sqrt{Q_{Ir}^2 + Q_{If}^2}$ are normalized in the form of Q_IR_b/Wh for the sake of comparison with the impulsive base shear capacity obtained in Section 2.5. The variation of the normalized impulsive base shear demand Q_IR_b/Wh with the ratio h/R_b for the three seismic zones is shown in Figs. 2-15 to 2-17 for different angles θ_v represented as solid lines. Also demonstrated on the same charts are the normalized base shear capacity V_IR_b/Wh values for perfect, good, and poor tanks.

With reference to conical tanks with $\theta_v=30$, the initial design under hydrostatic pressure only is considered satisfactory regarding the impulsive hydrodynamic pressure for the following cases: Toronto seismic zone for all levels of imperfections, perfect and good tanks corresponding to Montreal seismic zone, poor tanks corresponding to Montreal seismic zone with h/R_b less than 1.1, and perfect tanks corresponding to Vancouver seismic zone with h/R_b higher than 1.1. In all other cases, the initial design is considered unsatisfactory.

With regards to conical tanks with $\theta_v=45$, the initial design under hydrostatic pressure only is considered satisfactory regarding the impulsive hydrodynamic pressure for the following cases: Toronto seismic zone for all levels of imperfections, perfect tanks corresponding to Montreal seismic, perfect tanks corresponding to Vancouver seismic zone with h/R_b less than 1.2. For all other cases, the initial design is considered unsatisfactory.

Regarding conical tanks with $\theta_v=60$, the initial design under hydrostatic pressure only is considered satisfactory regarding the impulsive hydrodynamic pressure for the following cases: Toronto seismic zone for all levels of imperfections, perfect tanks corresponding to

Montreal seismic zone, perfect tanks corresponding to Vancouver seismic zone with h/R_b less than 1.25. For all other cases, the initial design is considered unsatisfactory.

The same procedure is repeated for the sloshing component. The sloshing base shear demand Q_s values are normalized in the form of Q_sR_b /Wh for the sake of comparison with the sloshing base shear capacity obtained in Section 2.6. The variation of the normalized sloshing base shear Q_sR_b /Wh with the ratio h/R_b for the three seismic zones is shown in Figs. 2-18 to 2-20 represented as solid lines. Presented on the same charts are the normalized sloshing base shear capacity values V_sR_b /Wh for each of the cases of perfect, good, and poor tanks.

For conical tanks with θ_v=30, the initial design under hydrostatic pressure only is considered satisfactory regarding the sloshing hydrodynamic pressure. This is valid for the three seismic zones regardless the level of imperfection. For conical tanks with θ_v=45, the initial design under hydrostatic pressure only is considered satisfactory regarding the sloshing hydrodynamic pressure for the three seismic zones, with the exception of poor tanks with h/R_b greater than 1.5 corresponding to Vancouver seismic zone. As for conical tanks with θ_v=60, the initial design under hydrostatic pressure only is considered satisfactory for perfect and good tanks corresponding to the three seismic zones. Finally, for poor tanks, initial design is inadequate for Vancouver seismic zone and Montreal seismic zone with h/R_b greater than 1.1.

It has to be mentioned that the overturning moment capacity corresponding to the base shear capacity provided in Sections 2.5 and 2.6 for impulsive and sloshing hydrodynamic pressure components, respectively, can be obtained by equating the ratio between the overturning moment demand to the base shear demand to the ratio between the overturning moment capacity to the base shear capacity. In other words, the ratio between the overturning moment capacity to the base shear capacity will be equal to the height h_r and h_s for the impulsive and sloshing hydrodynamic pressure components, respectively, which can be obtained using El Damatty and Sweedan (2006) mechanical model shown in Fig. 2-21.

2.8   Conclusions

This study represents the first attempt to estimate the capacity of liquid steel conical tanks when subjected to hydrodynamic pressure resulting from horizontal ground excitation. In order to achieve this, a numerical finite element model is used based on static pushover analysis.

The capacity is expressed in terms of the resulting total base shear at failure for the two components of the hydrodynamic pressure, which are impulsive and sloshing. As the impulsive and sloshing vibration modes are well-separated regarding their natural frequencies, the analyses are performed separately for each pressure component. The failure criterion considered in this study for a steel conical tank subjected to both hydrostatic and hydrodynamic pressure due to horizontal excitation, is the first which takes place of the following two criteria: (1) Yielding failure where the tank shell yields before buckling instability takes place (2) Buckling failure where the tank shell suffers instability before yielding, i.e., elastic buckling.

Base shear capacities for perfect steel conical tanks are presented in the form of charts for different dimensions, walls' thicknesses, and angles of inclination. Regarding the governing failure mode for both impulsive and sloshing components, the general trend is that the probability for yielding failure to take place is higher when the angle θ_v is increased, while the increase in the tank wall thickness is found to push the failure criterion to elastic buckling.

Since geometric imperfections play an important role in defining the capacity of shell structures, the effect of the geometric imperfections on the capacity of steel conical tanks is studied. It has been found that an axisymmetric distribution of the geometric imperfections will lead to the lowest buckling capacity for steel conical tanks. This means that the hydrostatic pressure loading phase governs the buckling capacity of the conical tanks, as the buckling waves initiate during this loading phase. In order to completely define the critical imperfections' distribution, an expression for the critical imperfection wave length is obtained based on regression analysis. The effect of variation of the tank height on the critical imperfection wave length is found to be insignificant. Finally, similar

charts to those corresponding to perfect conical tanks are provided for the case of imperfect tanks where two levels of imperfections' amplitude are considered and referred to as good and poor conical tanks. The probability for yielding failure is found to increase for higher geometric imperfections' amplitude.

After evaluating the base shear capacities of the conical tanks, the seismic demands in the form of total base shear are obtained using equivalent mechanical model found in the literature for both impulsive and sloshing vibration modes and compared to the obtained capacities in order to assess the initial design for the steel conical tanks. Three seismic zones are considered in this Section representing moderate to high seismic zones in Canada. Based on the comparison between the conical tank capacities and seismic demands, it is concluded that for the impulsive hydrodynamic pressure component, the initial design under hydrostatic pressure is found to be adequate for the majority of perfect and good tanks corresponding to Toronto and Montreal seismic zones. However, it is not adequate for poor tanks corresponding to the two seismic zones. With regards to Vancouver seismic zone, the initial design under hydrostatic pressure has been found to be adequate only for the case of perfect tanks. For sloshing hydrodynamic pressure component, the initial design under hydrostatic pressure only is considered satisfactory for most of the cases, with the exception of some good and poor imperfect conical tanks.

2.9   References

(API), A.P.I., 2005. Welded Storage Tanks for Oil Storage. Washington D.C, USA: American Petroleum Institute Standard.

(AWWA), A.W.W.A., 2005. Welded Steel Tanks for Water Storage. Denver, CO, USA.

(ECS), E.C.f.S., 1998. Design provisions for earthquake resistance of structures. Eurocode 8.

ACI 371, 2008. Guide for the Analysis, Design, and Construction of Elevated Concrete and Composite Steel-Concrete Water Storage Tanks. American Concrete Institute.

Buratti, & Tavano, M., 2014. Dynamic buckling and seismic fragility of anchored steel tanks by the added mass method. Earthquake Engng. Struct. Dyn., 43, pp.1-21.

Djermane, M., Zaoui, & Hammadi, F., 2014. Dynamic buckling of steel tanks under seismic excitation: Numerical evaluation of code provisions. Engineering Structures, 70, pp.181-96.

El Damatty, A.A., Korol, R. M, R.M. & Mirza, F., 1997a. Stability of Imperfect Conical Tanks under Hydrostatic Loading. Journal of Structural Engineering, 123(6), pp.703-12.

El Damatty, A.A., Korol, R.M. & Mirza, F.A., 1997d. Large displacement extension of consistent shell element for static and dynamic analysis. Computers and Structures, 62(6), pp.943-60.

El Damatty, A.A., El-Attar, M. & Korol, R.M., 1999. Simple Design Procedure For Liquid-Filled Steel Conical Tanks" Journal of structural engineering. Journal of structural engineering, 125(8), pp.879-90.

El Damatty, A.A., Korol, R.M. & Tang, L.M., 2000. The sloshing response of conical tanks. In World Conference of Earthquake Engineering. New Zealand, 2000.

El Damatty, A.A., Mirza, F.A. & Korol, R., 1997c. Stability of elevated liquid-filled conical tanks under seismic loading, Part II-Applications. Earthquake Engng. Struct. Dyn., 26, pp.1209-29.

El Damatty, A.A., Mirza, F.A. & Korol, R.M., 1997b. Stability of elevated liquid-filled conical tanks under seismic loading, Part I-Theory. Earthquake Engng. Struct. Dyn., 26, pp.1191-208.

El Damatty, A.A. & Sweedan, A.M., 2006. Equivalent mechanical analog for dynamic analysis of pure conical tanks. Thin-Walled structures, 44, pp.429-40.

Hanson, R.D., 1968. Behavior of Liquid Storage Tanks, The Great Alaska Earthquake of 1964. Washington, D.C.: National Research Council.

Haroun, M.A., 1980. Dynamic analyses of liquid storage tanks. Pasadena, CA: California Institute of Technology.

Haroun, M.A. & Housner, G.W., 1981. Seismic design of liquid storage tanks. Journal of the Technical Councils, 107(TC1), pp.191-207.

Haroun, M.A. & Housner, G.W., 1982. Dynamic Characteristics of Liquid Storage Tanks. Journal of the Engineering Mechanics Division, 108(5), pp.783-800.

Housner, G.W., 1957. Dynamic Pressures on Accelerated Fluid Containers. Bulletin Seism. Soc. America, 47(1), pp.15-35.

Housner, G.W., 1963. The Dynamic Behavior of Water Tanks. Bulletin Seism. Soc. America, 53(1), pp.381-87.

Jacobsen, L.S., 1949. Impulsive Hydrodynamics of Fluid inside a Cylindrical Tank and of a Fluid Surrounding a Cylindrical Pier. Bulletin Seism. Soc. America, 39, pp.189-204.

Jolie, M., Hassan, M.M. & El Damatty, A.A., 2013. Assessment of current design procedures for conical tanks under seismic loading. Can. J. Civ. Eng., 40, pp.1151-63.

Koizey, B. & Mirza, F.A., 1997. Consistent thick shell element. Computer & Structures, 65(12), pp.531-41.

Moslemi, M., Kianoush, M.R. & Pogorzelski, W., 2011. Seismic response of liquid-filled elevated tanks. Engineering Structures, 33, pp.2074-84.

NBCC, 2010. National Building Code of Canada. Ottawa, ON, Canada: National Research Council of Canada.

Sweedan, A.M. & El Damatty, A.A., 2009. Simplified procedure for design of liquid-storage combined conical tanks. Thin-Walled structures, 47, pp.750-59.

Vandepitte, D., 1999. Confrontation of shell buckling research results with the collapse of a steel water tower. Journal of Constructional Steel Research, 49, pp.303-14.

Vandepitte, D. et al., 1982. Experimental investigation of hydrostatically loaded conical shells and practical evaluation of the buckling load. In Proc. State of the Art Colloquium. Universitat Stuttgart, Germany, 1982.

Veletsos, A.S., 1974. Seismic Effects in Flexible Liquid Storage Tanks. In International Association for Earthquake Engineering. Fifth World Conference. Rome, Italy, 1974.

Virella, J.C., Godoy, L.A. & Suarez, L.E., 2006. Dynamic buckling of anchored steel tanks subjected to horizontal earthquake excitation. Journal of Constructional Steel Research, 62, pp.521-31.

Virella, J.C., Suárez, L.E. & Godoy, L.A., 2008. A Static Nonlinear Procedure for the Evaluation of the Elastic Buckling of Anchored Steel Tanks Due to Earthquakes. Journal of Earthquake Engineering, 12, pp.999-1022.

Appendix A
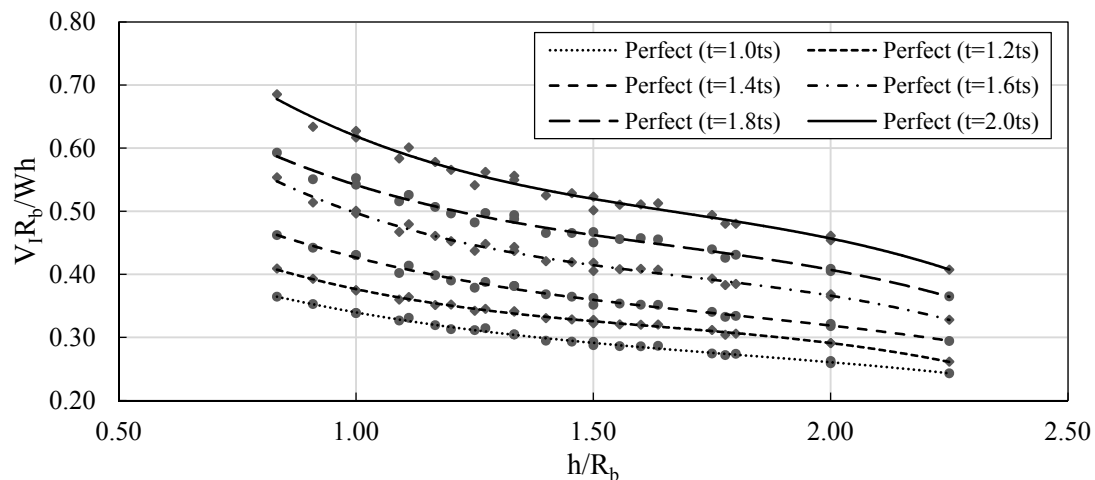
Fig. 2-22 Variation of ratio V_IR_b/Wh with h/R_b for perfect tanks (θ_v =30)
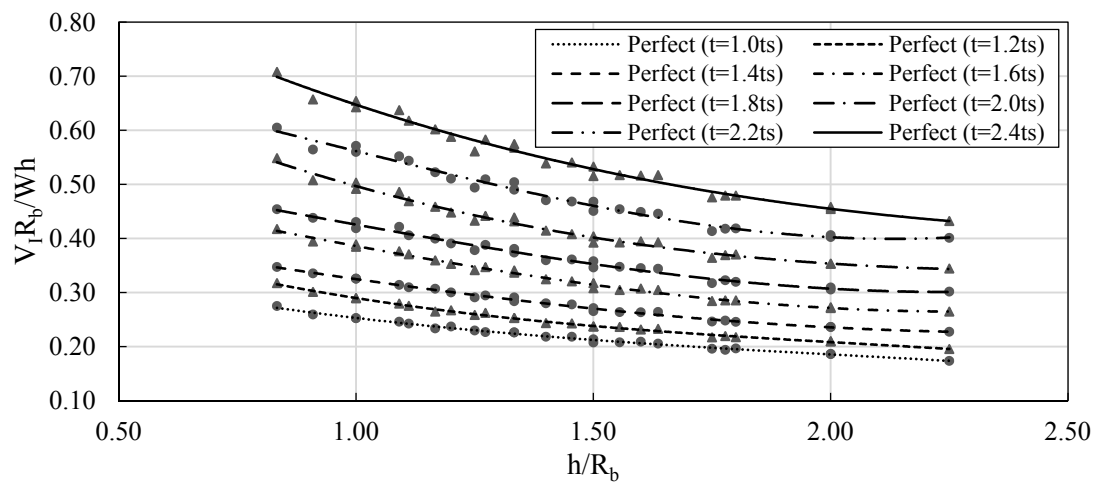
Fig. 2-23 Variation of ratio V_IR_b/Wh with h/R_b for perfect tanks (θ_v=45)
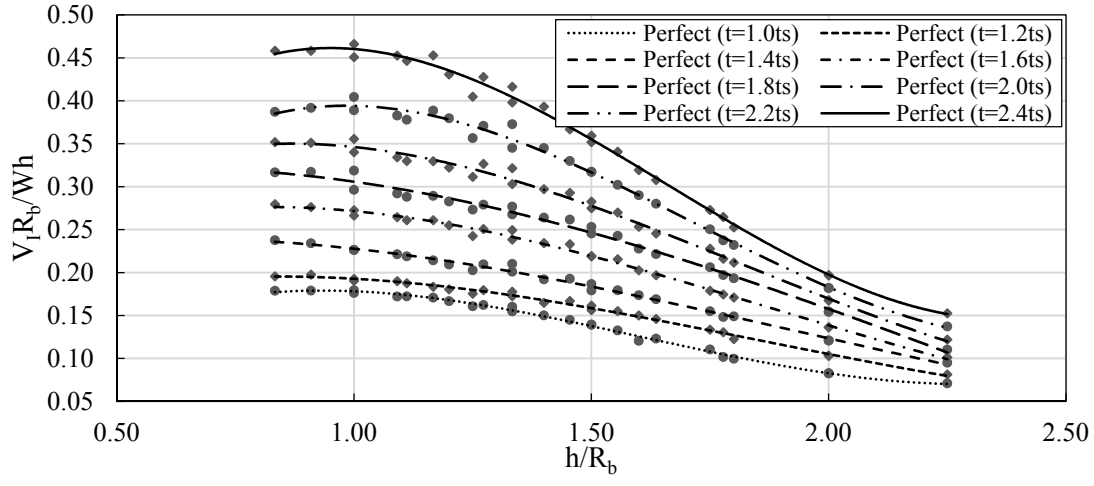
Fig. 2-24 Variation of ratio $V_I R_b/Wh$ with h/R_b for perfect tanks (θ_v=60)
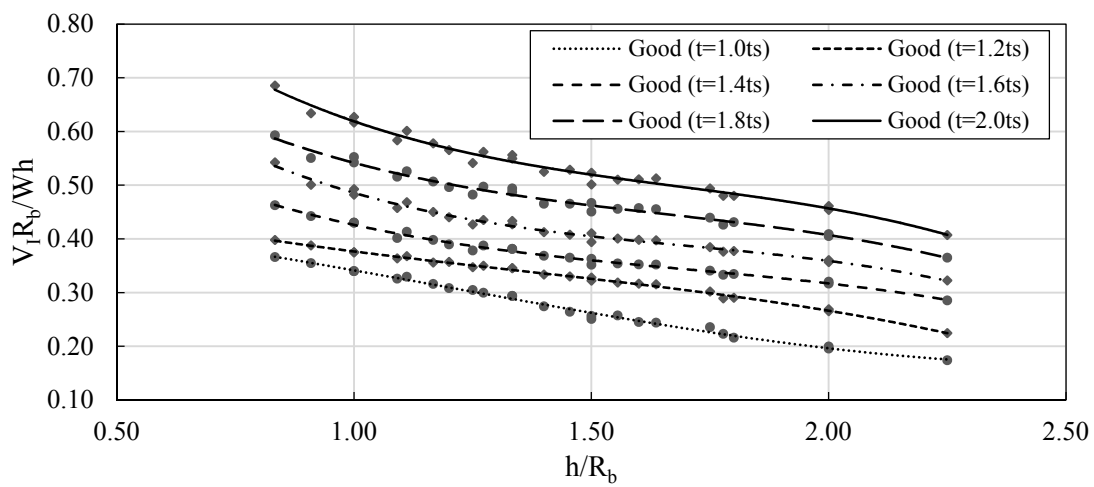
Fig. 2-25 Variation of ratio $V_I R_b/Wh$ with h/R_b for good tanks (θ_v=30)
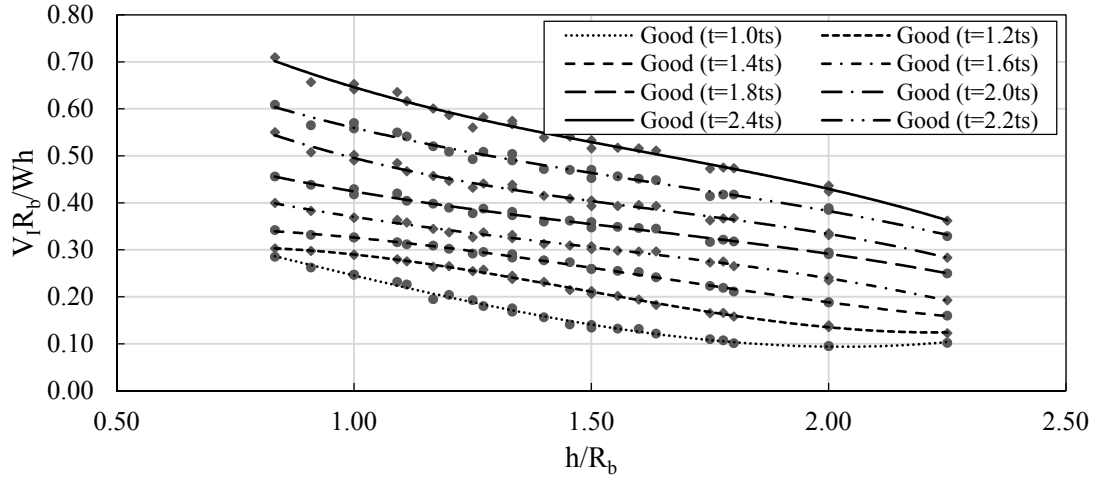
Fig. 2-26 Variation of ratio V_IR_b/Wh with h/R_b for good tanks (θ_v=45)
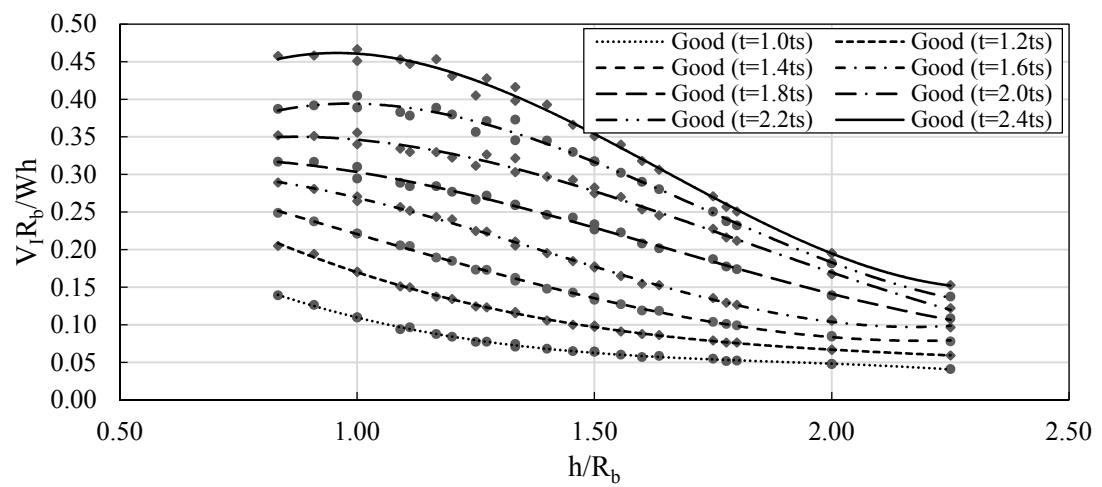
Fig. 2-27 Variation of ratio V_IR_b/Wh with h/R_b for good tanks (θ_v=60)
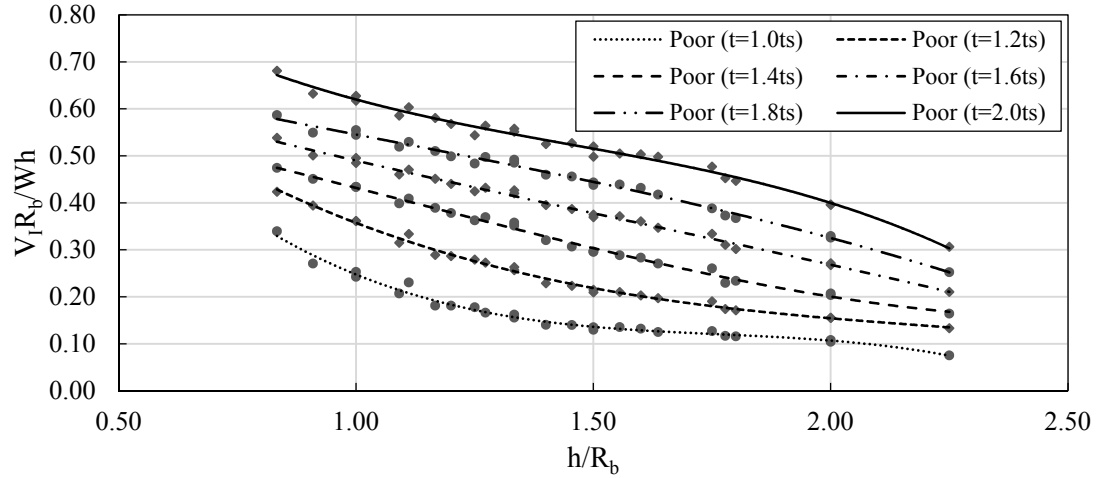
Fig. 2-28 Variation of ratio V_IR_b/Wh with h/R_b for poor tanks (θ_v=30)
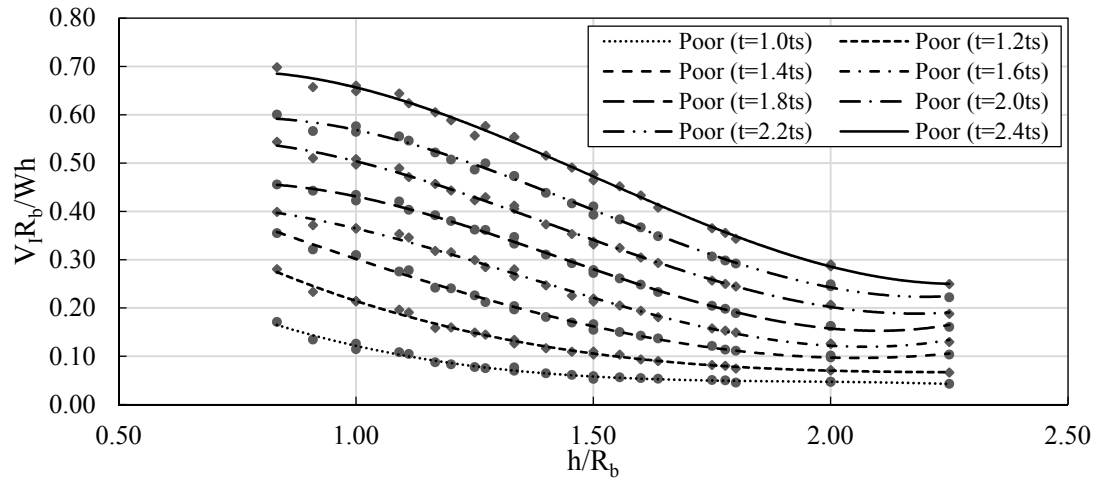
Fig. 2-29 Variation of ratio V_IR_b/Wh with h/R_b for poor tanks (θ_v=45)
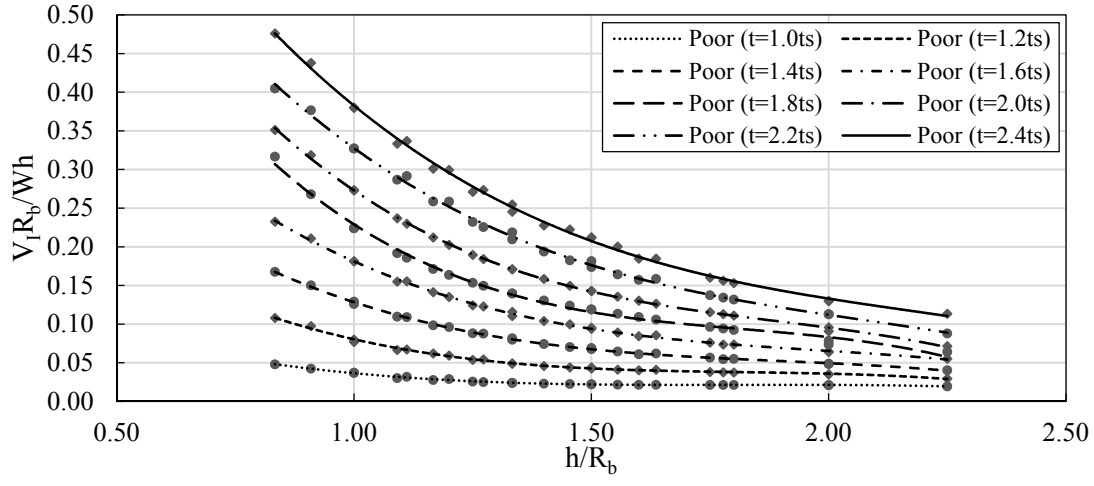
Fig. 2-30 Variation of ratio V_IR_b/Wh with h/R_b for poor tanks (θ_v=60)
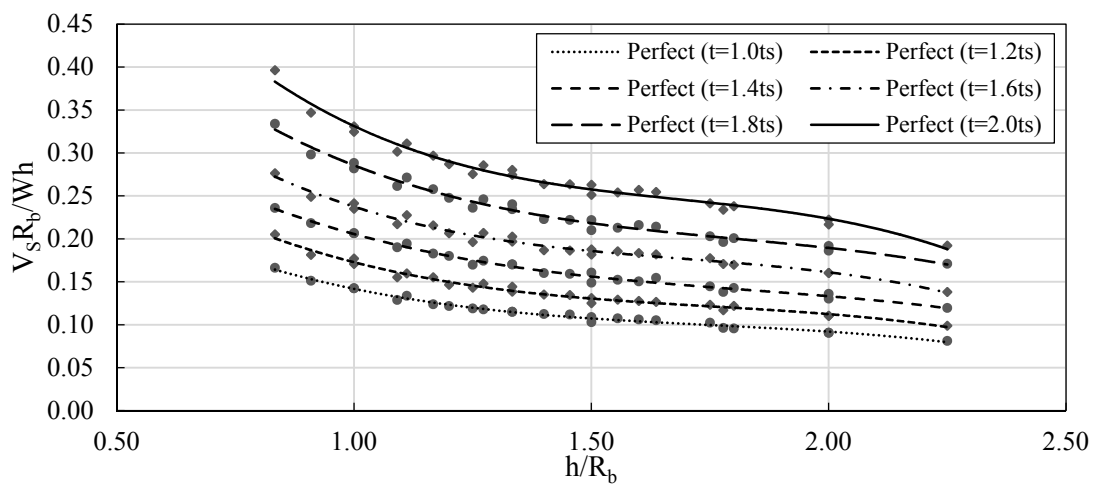
Fig. 2-31 Variation of ratio V_SR_b/Wh with h/R_b for perfect tanks (θ_v=30)
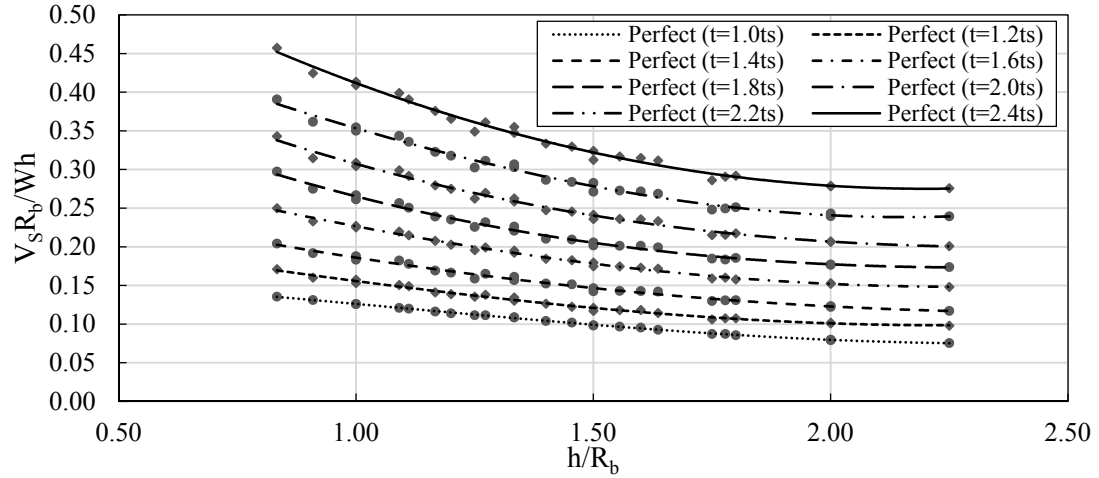
Fig. 2-32 Variation of ratio V_SR_b/Wh with h/R_b for perfect tanks (θ_v=45)
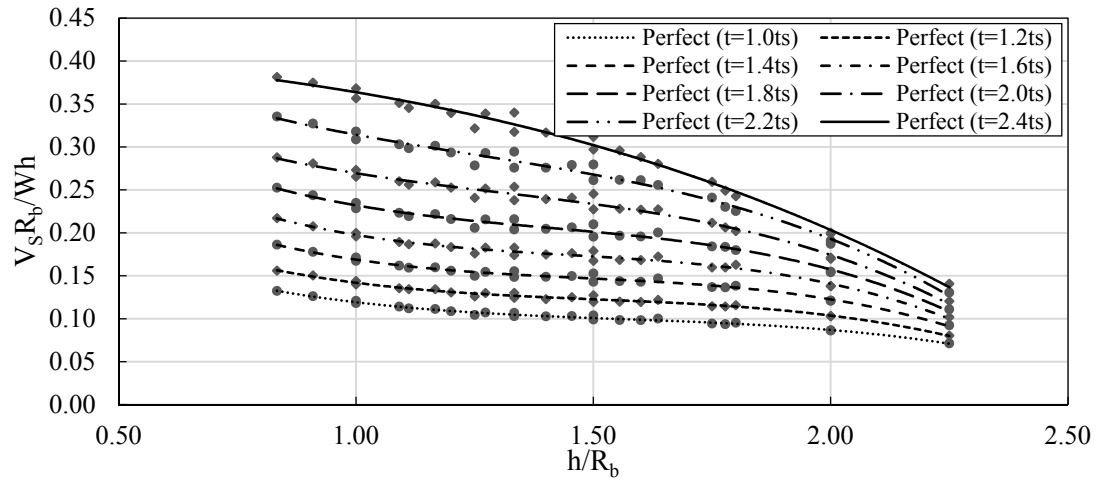
Fig. 2-33 Variation of ratio V_SR_b/Wh with h/R_b for perfect tanks (θ_v=60)
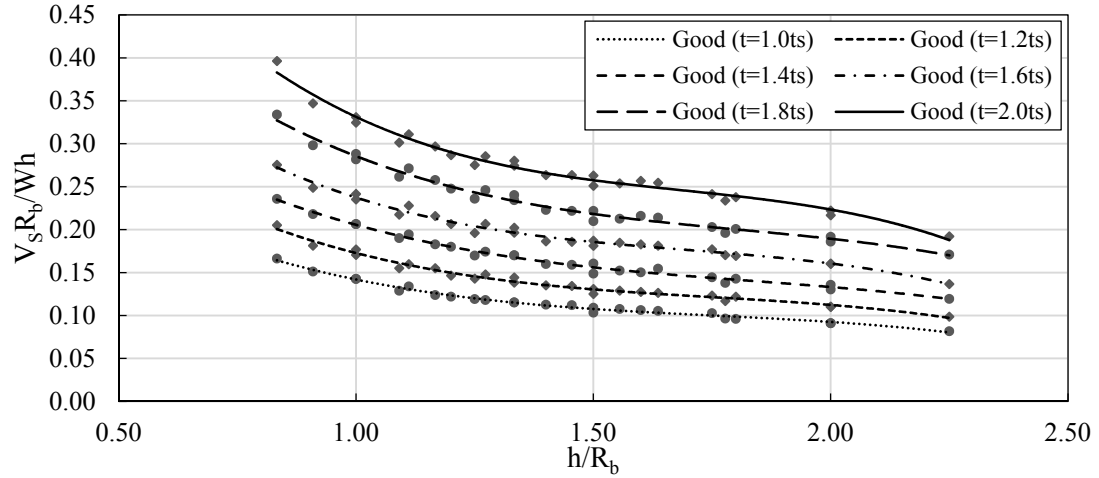
Fig. 2-34 Variation of ratio $V_S R_b/Wh$ with h/R_b for good tanks (θ_v=30)
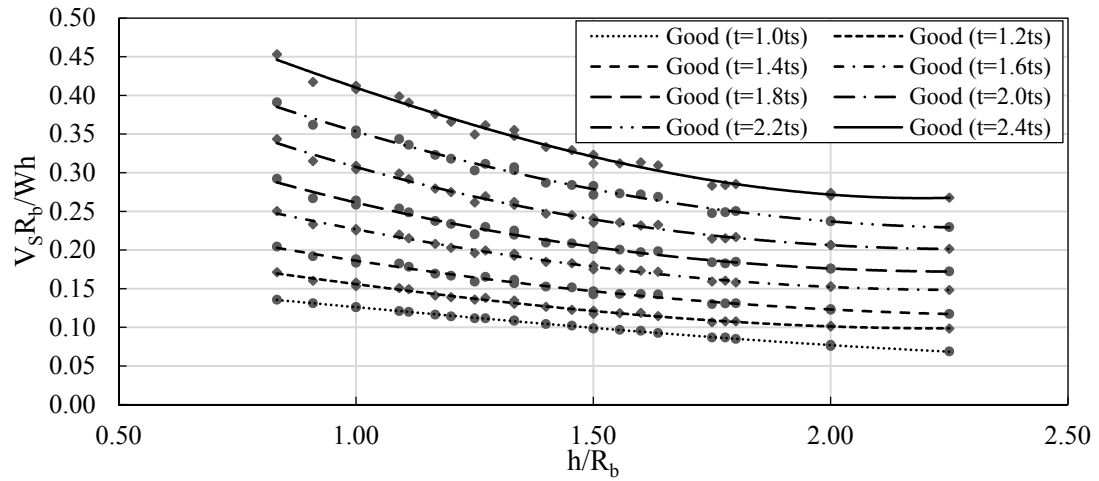
Fig. 2-35 Variation of ratio $V_S R_b/Wh$ with h/R_b for good tanks (θ_v=45)
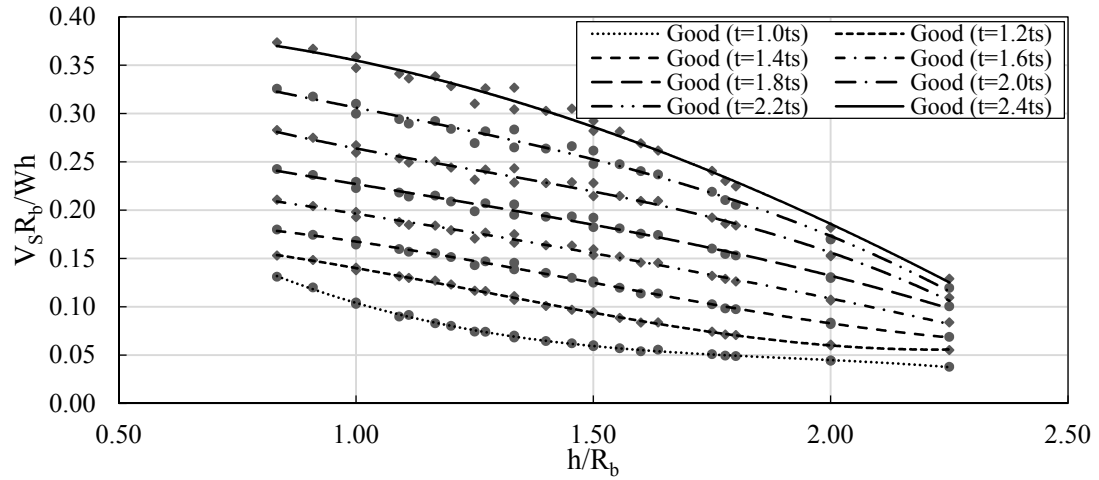
Fig. 2-36 Variation of ratio V_SR_b/Wh with h/R_b for good tanks (θ_v=60)
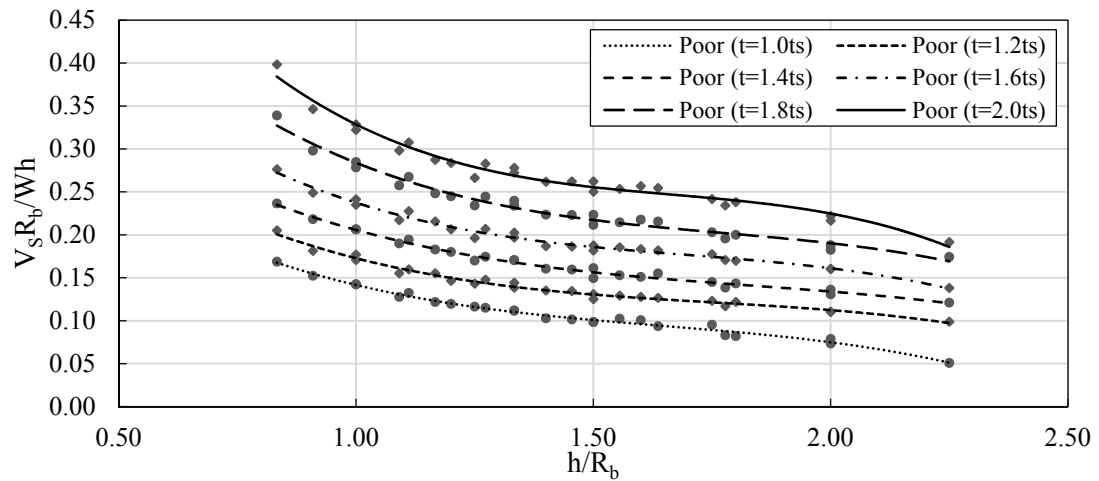
Fig. 2-37 Variation of ratio V_SR_b/Wh with h/R_b for poor tanks (θ_v=30)
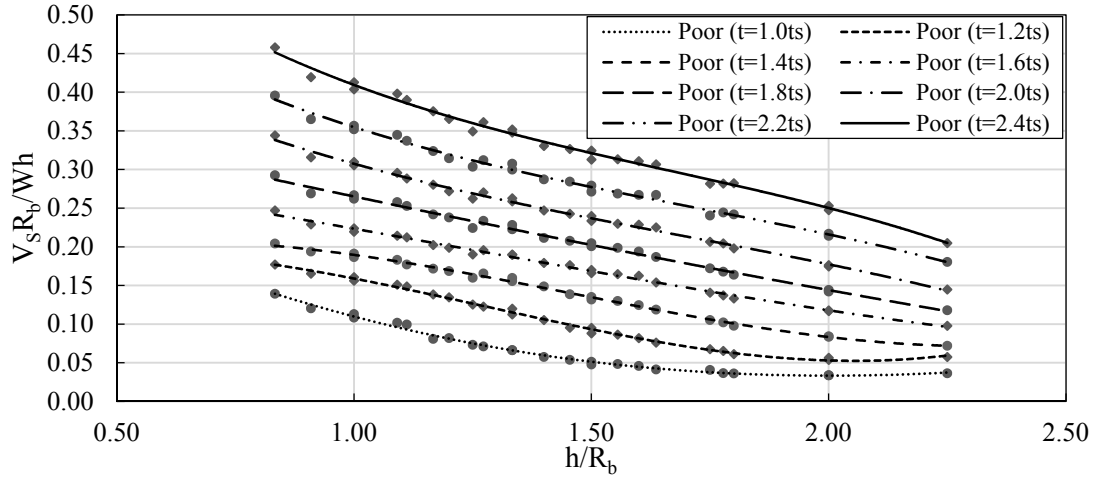
Fig. 2-38 Variation of ratio V_SR_b/Wh with h/R_b for poor tanks (θ_v=45)
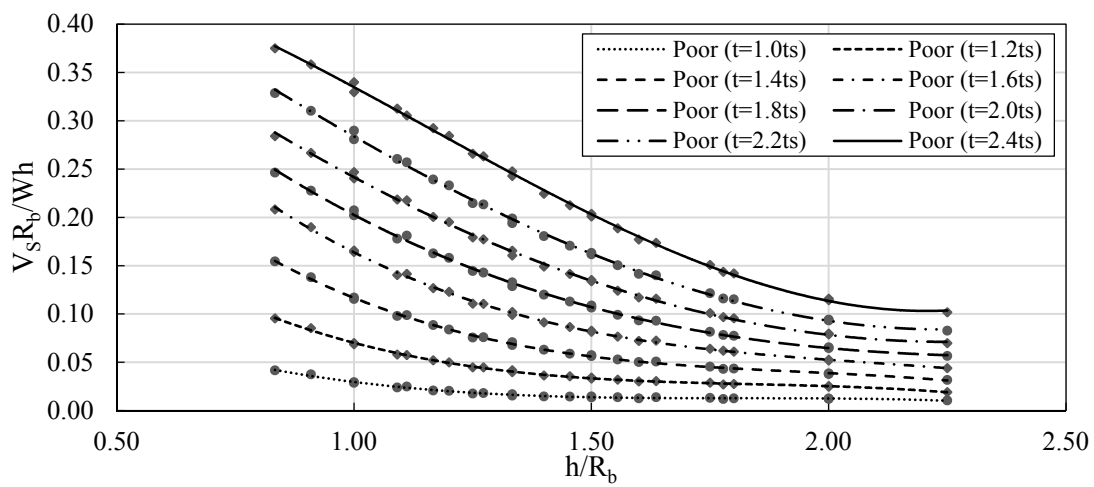
Fig. 2-39 Variation of ratio V_SR_b/Wh with h/R_b for poor tanks (θ_v=60)

Chapter 3

3 Capacity of Liquid-Filled Steel Conical Tanks under Vertical Excitation

Liquid tanks in the form of truncated cones are commonly used for liquid storage in North America and in other locations. This chapter is a part of an extensive research program aimed to develop a comprehensive design procedure for liquid-filled steel conical tanks under seismic loading. Because of the inclination of the walls of conical tanks, the vertical component of the ground motion excitation has a significant effect on conical tanks compared to the case of cylindrical tanks. To the best of the authors' knowledge, the current study is the first to focus on the assessment of the capacity of steel conical tanks under the vertical component of a seismic excitation. The study is carried out numerically using an in-house finite element model by conducting nonlinear static pushover analysis under a load distribution simulating hydrodynamic pressure associated with vertical ground excitations. The numerical model accounts for the effects of geometric and material nonlinearities as well as initial geometric imperfections. Charts are developed to estimate the capacity of steel conical tanks to resist vertical ground excitations based on yielding and buckling criteria for different imperfection levels. The developed charts are used to estimate the capacities of a number of steel conical tanks which are then compared to the hydrodynamic loading associated with various seismic zones.

3.1 Introduction

Steel conical tanks are commonly used as liquid-containments. They consist of vessels made up of welded steel panels having pure truncated conical shapes or combined conical-cylindrical shapes as shown in Fig. 3-1. To the best of the authors' knowledge, no design specifications for water structures worldwide provides a clear and rational procedure for the seismic design of such structures. The AWWA (2005), API (2005), and ECS (1998) recommend converting conical tanks into equivalent cylinders with equivalent height, radius, and thickness. This equivalent cylinder approach can be questionable under horizontal ground motion, but it is definitely far from reality under vertical ground motion as will be discussed later in this section.

Fig. 3-1 Combined steel conical tank

Researchers realized the importance of studying the effect of ground motions on the behaviour of liquid tanks long time ago specially after the Alaska earthquake 1964 where considerable damage occurred to a large number of liquid storage tanks. Earlier studies were based on assuming the tank walls to be rigid when evaluating the hydrodynamic pressure resulting from ground motions (Jacobsen (1949), Housner (1957), and Housner (1963)). It was then realized that the flexibility of the tank walls and the interaction that happens between the vibration of the walls and the contained fluid affect significantly the hydrodynamic pressure and consequently the structural response (Veletsos, (1974), and Haroun and Housner (1981,1982)).

In order to reduce the computation time for analyzing liquid-tank systems, a practical alternative is to model the contained liquid as lumped masses attached to the tank wall rigidly or through linear springs instead of modelling the contained fluid as a continuum. The masses-springs system is called equivalent mechanical model whose main objective is to match the resulting forces and moments obtained using dynamic analysis for the continuum liquid-tank system subjected to the same horizontal ground excitation. Haroun and Housner (1981) introduced a three masses mechanical model for cylindrical steel tanks

subjected to horizontal excitations. The three masses are the impulsive fluid mass, the convective fluid mass, and the mass reflecting the effect of the flexibility of the tank's wall. The impulsive mass represents the mass of the fluid vibrating in synchronism with the ground and rigidly connected to the tank's wall, while the convective one represents the mass of the fluid undergoing sloshing motion at the free surface.

On the resistance side, a number of studies related to the buckling capacity of cylindrical liquid tanks under horizontal ground excitations are found in the literature. Virella et al. (2006) investigated the dynamic buckling of anchored cylindrical steel tanks with different slenderness ratio subjected to real earthquake records numerically using the finite element method in order to estimate the critical horizontal peak ground acceleration (PGA) at which elastic or plastic buckling for the cylindrical shell will take place.

Virella et al. (2008) proposed a nonlinear static procedure based on the capacity spectrum method found in ATC-40 in order to assess the elastic buckling of above-ground anchored steel tanks due to horizontal seismic excitations. The objective was to obtain the minimum peak ground acceleration (PGA) value that produces buckling in the tank shell. The obtained critical PGA estimates were then compared with those calculated using the dynamic buckling analyses performed in the latter study.

Djermane et al. (2014) attempted to evaluate the current design guidelines related to dynamic instability provided by AWWA-D100 and EC8 provisions for cylindrical steel tanks using a numerical shell finite element model. The idea was to evaluate the critical PGA values that cause the tank instability and then compare with their counterparts obtained by the codes' provisions.

Buratti and Tavano (2014) discussed different buckling modes for liquid-containing circular cylindrical steel tanks that are fully anchored at the base with a special focus on the secondary buckling occurring in the top part of the tank. A case study for a broad cylindrical tank was used in order to investigate various aspects of dynamic buckling using a finite element model where the fluid was modelled in the form of lumped added masses.

The previous studies focused on the horizontal component of the ground excitation. Regarding the vertical component, vertical accelerations are transmitted to a horizontal hydrodynamic loading acting on the tank wall amplifying the hydrostatic induced pressures that might lead to inelastic buckling of the steel shell. As a result, it is important to include the effect of vertical ground excitations when it comes to analyzing liquid storage tanks. Marchaj (1979) attributed the failure of metallic tanks during past earthquakes to the lack of consideration of vertical acceleration in their design. Veletsos and Kumar (1984) studied the effect of wall flexibility on the response of cylindrical tanks when subjected to vertical component of ground shaking. It was concluded that the hydrodynamic effects for a flexible tank might be substantially larger than those induced in a rigid tank of the same dimensions, and for an intense excitation, they might be of the same order of magnitude as the hydrostatic effects.

The latter study considered only the radial motion of the tank walls and neglected the effect of axial deformations. This assumption was validated by Haroun and Tayel (1985a) who provided an analytical method for the computation of the dynamic characteristics in terms of natural frequencies, corresponding mode shapes and stress distributions for partly filled cylindrical tanks subjected to vertical excitations. Results were compared to numerical solution where the liquid region was treated analytically and the elastic shell was modeled by finite elements Haroun and Tayel (1985b) and both methods showed excellent agreement.

Veletsos and Tang (1986) provided a practical procedure to evaluate the dynamic response of rigid and flexible steel and concrete cylindrical tanks with different base conditions when subjected to vertical excitations including soil-structure interaction. The main conclusion was that soil-structure interaction reduces the maximum hydrodynamic effects and might be approximated by a change in the fundamental natural frequency of the tank-liquid system or an increase in damping

Haroun and Tayel (1985) analyzed some cylindrical liquid storage tanks under simultaneous horizontal and vertical excitations numerically using finite element method. The goal of the study was to assess the relative importance of inclusion of the vertical

component of the earthquake in the behaviour of the cylindrical tanks. The axial stresses resulting from the vertical component was found to be much lower compared to those induced due to the horizontal component of the earthquake due to overturning moment. However, the hoop stresses due to vertical component was higher than those due to horizontal component which might lead to the yielding of the steel shell increasing the probability of buckling of the tank walls near the base of the tank.

Haroun and Abou-Izzeddine (1992) performed a parametric study in order to evaluate the effects of different factors that influence the seismic response of an elastic cylindrical tank supported on a rigid base when subjected to a vertical excitation by considering shell-liquid-soil interaction. It was concluded that foundation soil-tank interaction reduces the tank response in general, and this reduction is a function of the soil shear-wave velocity as well as tank geometric properties.

A number of studies have been done related to conical tanks under hydrostatic pressure. Motivated with the collapse of a conical steel water tower in Belgium, Vandepitte et al., (1982) tested a large number of small-scale conical tank models experimentally under hydrostatic pressure by gradually filling the model till buckling occur. Design charts for different base restraining conditions were developed based on this experimental program. In 1990, a steel conical water tower collapsed in Fredericton, Canada due to underestimation of the effect of geometric imperfections according to Vandepitte (1999) in addition to analyzing the conical tank as a pressurized vessel which is not always a conservative assumption. El Damatty et al. (1997a), El Damatty et al. (1998), and Hafeez et al. (2010) assessed the inelastic stability of pure and combined liquid-filled steel conical tanks including the effect of geometric imperfections and residual stresses due to welding of the steel panels forming the conical shell.

El Damatty et al. (1999) and Sweedan and El Damatty (2009) provided a simplified design procedure for steel conical tanks under hydrostatic pressure for steel conical tanks taking into account geometric imperfections. The idea was to avoid the yielding state of tanks which was shown to always precedes buckling for the case of hydrostatic pressure.

El Damatty et al. (1997b,c) derived a fluid-added mass matrix for both horizontal and vertical ground motions to be incorporated in time history analysis using coupled shell element-boundary element formulation to simulate the fluid-structure interaction. By analyzing some steel conical tanks using this approach, it was shown how serious could be the dynamic loading compared to the static one and how the contribution of vertical excitation to the dynamic instability is important. This coupled shell element-boundary element model was verified experimentally using shaking table testing for scaled conical shell aluminum models (Sweedan and El Damatty (2002) and El Damatty et al. (2005)).

Comparing cylindrical to conical tanks regarding the state of stresses, a vertical ground acceleration will lead to an axisymmetric hydrodynamic pressure, in addition to the existing hydrostatic pressure, resulting in meridional axial stresses that do not exist for the case of cylindrical tanks due to the inclination of the conical tank walls. As both hydrostatic pressure and hydrodynamic pressure due to vertical excitation are axisymmetric, the state of stresses for both of them is similar and is shown in Fig. 3-2, where the contained liquid can be divided into two zones: Z_1 which is resting on the tank base and Z_2 resting on the inclined wall. As the pressure due to the liquid in Z_2 increases with a reduction in the vessel radius closer to the tank base, high compressive meridional stresses σ_m are developed in this region compared to the case of a cylindrical tank. In addition to the compressive meridional stresses, tensile hoop stresses σ_h are also induced circumferentially through the tank shells. Hydrodynamic pressure due to vertical excitation will magnify or reduce the hydrostatic pressure induced stresses based on the direction of the ground acceleration, i.e., upwards or downwards.
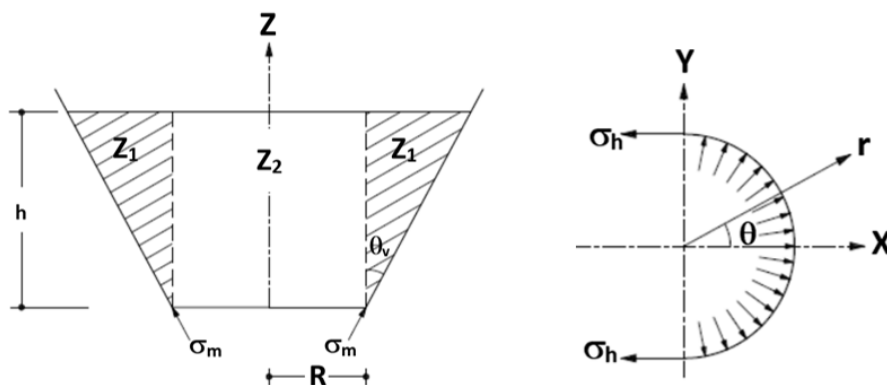
Fig. 3-2 Stresses induced due to inclination of the wall

Jolie et al. (2014) assessed the importance of considering the vertical component of ground excitations when designing steel conical tanks using an equivalent mechanical model that estimates the acting normal forces due to vertical excitations. In addition, a three-dimensional finite element model has been developed using shell elements in order to predict maximum membrane and overall meridional stresses due to both hydrodynamic and hydrostatic pressures. The results showed that the vertical ground acceleration has a considerable effect on the increase of the meridional wall stresses compared to those resulting from hydrostatic pressure, especially for high seismic hazard regions emphasizing the importance of vertical excitation consideration. Also, meridional wall stresses at the extreme inner fibre at the tank base are shown to be higher than those developing at the mid-surface due to bending effects associated with the boundary conditions at the tank base.

Similar to the case of liquid filled steel conical tanks subjected to horizontal ground excitations, equivalent mechanical model was used in order to obtain the loads acting on steel conical tanks subjected to vertical excitations. The model's parameters are obtained such that the model yields the same total vertical force obtained through dynamic analysis for the continuum liquid-tank system. Sweedan and El Damatty (2005) proposed a two-mass mechanical model for pure conical tanks. The two masses are the rigid fluid mass, and the mass reflecting the effect of the flexibility of the tank's wall. This model is described in more details in Section 3.7 as it will be used in this study. Sweedan (2009)

introduced a similar mechanical model that can be used for combined conical-cylindrical tanks subjected to vertical excitations.

As mentioned earlier, most of the previous studies focused on studying the behaviour of steel conical tanks when subjected to vertical ground excitations and how acting loads can be obtained in order to design such structures. The other side of the design inequality which is the tank resistance has not been studied before to the best of the author's knowledge. As a result, this study focuses on obtaining the capacity of steel conical tanks when subjected to vertical ground excitations. Nonlinear static pushover analysis is used to determine this capacity using finite element modeling for the steel conical tanks. In addition, the effect of geometric imperfections on the evaluated buckling capacity is studied. After obtaining the capacity for the steel conical tanks, it is then compared to the acting loads corresponding to different seismic zones obtained through a previously developed mechanical model for vertical ground excitations in order to assess the design of the tanks.

3.2 Hydrodynamic Pressure

When a conical tank is subjected to a vertical ground excitation, the tank is subjected to accelerations resulting in hydrodynamic pressure acting on the tank walls and base in addition to the existing hydrostatic pressure. The hydrodynamic pressure due to vertical excitation acting on a conical tank containing an ideal fluid is governed with the following set of equations and boundary conditions El Damatty et al. (1997b):

$$\nabla^2 P_I(r,\theta,z,t) = 0 \qquad\qquad \text{inside the fluid volume} \qquad\qquad [3\text{-}1]$$

$$\frac{\partial P_I(r,\theta,z,t)}{\partial n} = -\rho_F \ddot{u}\,(r,\theta,z,t).n \qquad\qquad \text{at the surface } S_1 \qquad\qquad [3\text{-}2]$$

$$P_I = 0 \qquad\qquad \text{at the surface } S_3 \qquad\qquad [3\text{-}3]$$

$$\frac{\partial P_I(t)}{\partial n} = -\rho_F \ddot{G}_v(t).n \qquad\qquad \text{at the surface } S_2 \qquad\qquad [3\text{-}4]$$

where $\ddot{u}\,(r,\theta,z,t)$ is the acceleration vector at any point of the tank's wall, n is the unit vector normal to the surface of the tank, $\ddot{G}_v(t)$ is the vertical acceleration acting on the tank base, and ρ_F is the fluid density. Surfaces S_1, S_2 and S_3 are as shown in Fig. 3-3.
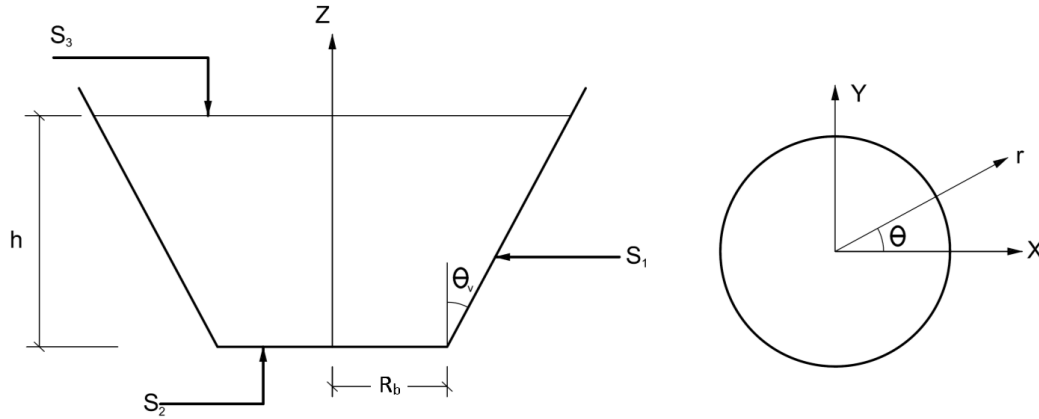
Fig. 3-3 Co-ordinate system for the steel conical tank and dimensional parameters

The solution of the above differential equation was done by interpolating the dynamic pressure using different shape functions that satisfy the boundary conditions on the tank surfaces El Damatty et al. (1997b). The hydrodyanmic pressure P_D associated with an axisymmetric excitation can be then expressed as

$$P_D(r,\theta,z,t) = \sum_{i=1}^{N_1} A_{io}(t)\, I_0(\alpha_i r)\, \cos(\alpha_i z) + \ddot{G}_v(t)(1 - \frac{z}{h})$$ [3-5]

where $A_{io}(t)$ are the amplitude functions of time, I_0 are the modified Bessel's functions of the first kind and α_i depend on the height, h, of the fluid in the tank as

$\alpha_i = (2i-1)\,\pi/2h$ [3-6]

The time varying parameters $A_{io}(t)$ were obtained using coupled finite element-boundary element method by El Damatty et al. (1997b) for steel conical tanks, where the tank walls are modeled using a shell element while the boundary element method is used to simulate the hydrodynamic pressure resulting from the acting vertical ground excitation $\ddot{G}_v(t)$.

In the hydrodynamic pressure expression, the term $\cos(\alpha_i z)$ represents the variation of the hydrodynamic pressure for mode i in the vertical Z direction. A typical plot of the first three vertical pressure modes is shown in Fig. 3-4.
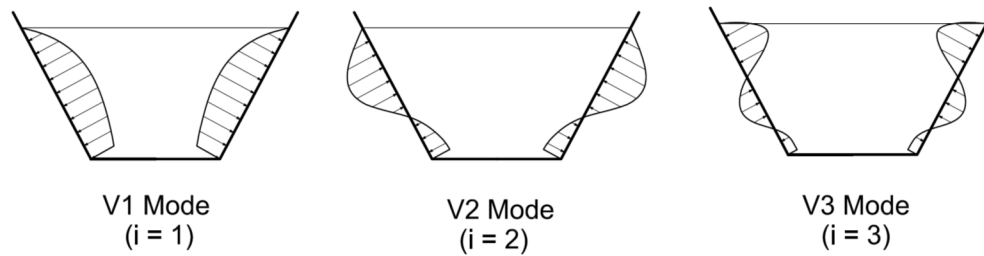
Fig. 3-4 Different vertical axisymmetric pressure modes

3.3 Finite Element Model

As mentioned earlier, the current study aims at evaluating the buckling capacity of steel conical tanks subjected to vertical ground excitations. In order to achieve that, 3D numerical models are developed for steel conical tanks using the finite element method. The finite element used is the 13 noded subparametric triangular shell element developed by Koizey and Mirza (1997) as shown in Fig. 3-5a. This subparametric element is advantageous in terms of being free of the spurious shear modes and the locking phenomenon observed in isoparametric shell elements counterparts when used in modeling thin shell structures such as steel conical tanks. In addition, this finite element model can be used to predict both elastic buckling and inelastic buckling of the tank shell as the used shell element was extended to include both geometric and material non-linearities (El Damatty et al. (1997d)).

For the finite element mesh used, modelling half of the conical tank is sufficient due to symmetry about the horizontal axis in both loading and geometry. The used mesh is shown in Fig. 3-5b which consists of 512 triangular finite elements. Due to the expected stress concentration near the tank base as result of the inclination of the walls, the finite element mesh is chosen to be finer near the base of the tank. The tanks are assumed to be hinged at the base along the circumference and free at the top.
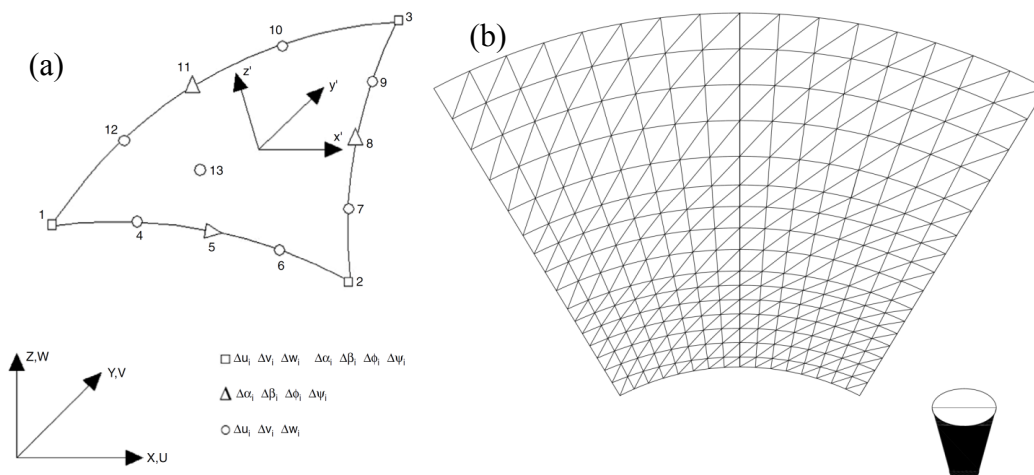
Fig. 3-5 Coordinates and degrees of freedom for a consistent shell element, (b) Finite element mesh for half cone

3.4 Method of Analysis

Nonlinear static pushover analysis is used in this study to evaluate the buckling capacity of steel conical tanks subjected to vertical ground excitations. This is done by increasing the acting water pressure incrementally till instability occurs. The incremental load increase is achieved using a load factor. As hydrostatic pressure on the tank walls is always present, two load factors are used: the first is P_{HS} which corresponds to the hydrostatic pressure and the second is P_{HD} which corresponds to the hydrodynamic pressure.

The analysis is divided into two phases: For phase 1, which represents the stage of hydrostatic pressure only, P_{HS} is increased incrementally till the value corresponding to the actual hydrostatic pressure while P_{HD} is kept at zero value. For phase 2, which represents the stage where both hydrostatic and hydrodynamic pressure act simultaneously, P_{HS} is kept constant at the value corresponding to the actual hydrostatic pressure while P_{HD} is increased incrementally till instability occurs.

The group of steel conical tanks considered in this study have the following practical dimensions, bottom radius R_b ranging from 4.0m to 6.0m, cone height h ranging from 5.0m to 9.0m, and angle of inclination with the vertical $\theta_v = 30°$, $45°$, $60°$ with steel yield stress of 300 MPa yielding a total of 75 tanks. In order to obtain the wall thickness, the tanks are

designed under hydrostatic pressure only based on the simplified method proposed by Sweedan and El Damatty (2009) assuming good tanks regarding the level of geometric imperfection according to the classification proposed by Vandepitte et al., (1982).

Similar to the case of hydrostatic pressure, all the pressure modes associated with vertical excitation are axisymmetric and consequently no base shear force is expected due to this excitation. However, because of the inclination of the walls, a net vertical force will act at the bottom section of the walls. This vertical force will be used to express the buckling capacity of the steel conical tanks as will be shown in the coming sections. Regarding the vertical distribution of the pressure modes, only the first vertical mode, i.e., i=1, is included in the analysis in calculating the buckling capacity for the conical tanks.

3.5   Results of Analysis

3.5.1   Deformed Shape

Figure 6 shows a typical distribution for the axisymmetric radial deformations of the tank walls along the height. The distribution is shown at the end of each stage of the discussed two-phase loading scheme. At the end of the hydrostatic pressure only loading, i.e., phase1, buckling wave is noticed near the tank base due to the compressive stress concentration at this location. As the steel conical tanks considered in the current study are designed under hydrostatic pressure with a load factor greater than unity, the tanks are still able to resist more loads in the second phase of loading which incorporate both hydrostatic pressure and hydrodynamic pressure corresponding to vertical ground excitations. During this second phase, radial deformations are increased as the hydrodynamic pressure load factor is increased especially near the mid-height of tank. This is due to the hydrodynamic pressure distribution which have the peak value at this location. The amplitude of the buckling wave is amplified during this second stage till instability happens indicating the end of the analysis. A schematic for the circumferential distribution of the tank deformations is shown in Fig. 3-7
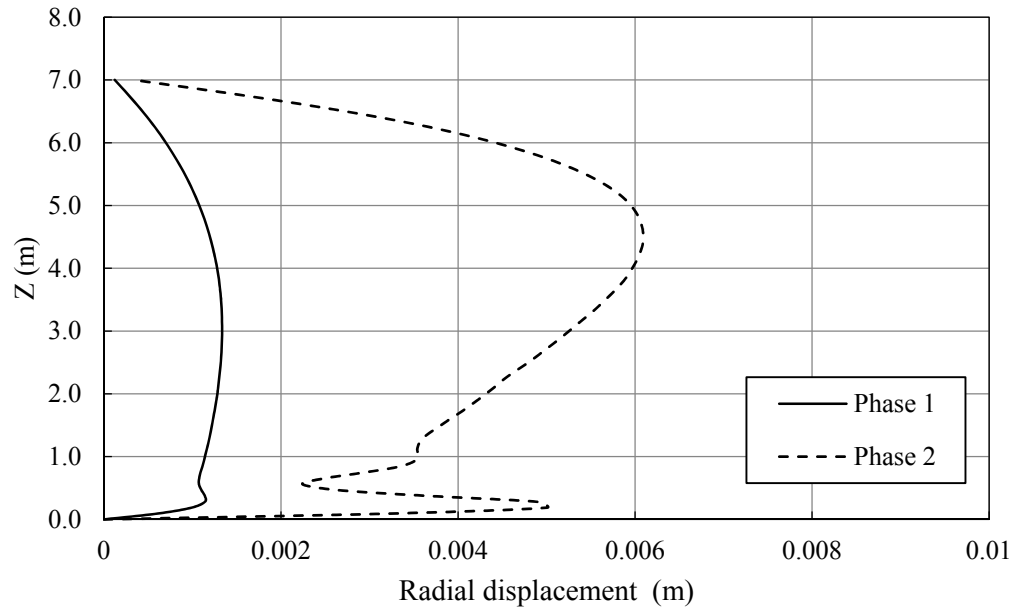
Fig. 3-6 Radial deformations of the tank walls at the end of each phase of loading (R=4.0m, h=7.0m, θ_v=45°)
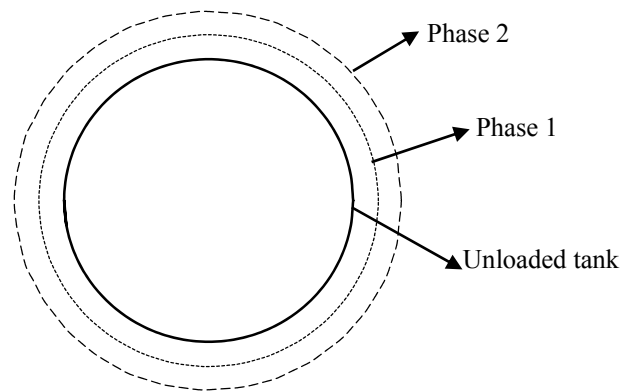
Fig. 3-7 Deformed shape at the end of each phase of loading

3.5.2 Vertical Force Capacity

In this section, the resistance capacity for steel conical tanks subjected to vertical ground excitations is evaluated using the nonlinear static pushover procedure described in the previous section. The capacity is expressed in the form of the total vertical force N at failure. Two possible failure criteria are defined for a steel conical tank subjected to both

hydrostatic and hydrodynamic pressure: (1) Yielding failure criterion where the tank shell yields before instability takes place, (2) Buckling failure criterion where the tank shell suffers elastic instability before yielding.

For the group of steel conical tanks considered in this study, the tank shell was found to yield before instability takes place which means that the yielding criterion is the governing for failure. The same observation was noted by El Damatty et al. (1997a) for the case of steel conical tanks under hydrostatic pressure which has an axisymmetric distribution similar to the case of the hydrodynamic pressure due to vertical excitations. As a result, the steel conical tank resistance in this study will be expressed in terms of the total vertical force corresponding to the first yielding of the tank vessel.

As a first step to understand how the vertical force resistance varies with the tank dimensions, a parametric study is performed where a datum steel conical tank is used with h=7.0m, R_b=5.0m, and θ_v=45°. One parameter is studied at a time in order to assess the effect of this parameter on the vertical force resistance. The vertical force N is normalized to the total weight of the fluid contained in the tank W in the form of the vertical force ratio N/W. For the steel conical considered in this study, Figs. 3-8 to 3-10 show how the ratio N/W values change with the parameters R_b, H, and θ_v, respectively. For each chart, a family of curves exists to reflect the effect of increasing the tank wall thickness t_w on the vertical force resistance. It is concluded from the charts that the value of N/W decreases with increasing the height of the tank or the bottom radius or the angle θ_v. Finally, the ratio N/W is higher for thicker steel conical tanks.
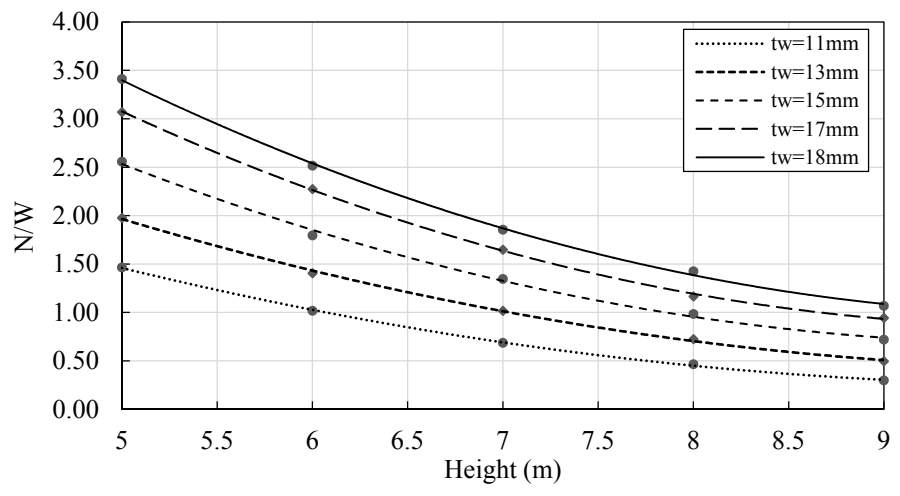
Fig. 3-8 Variation of total vertical force ratio with the tank height and thickness

(R_b=5.0m, θ_v=45º)
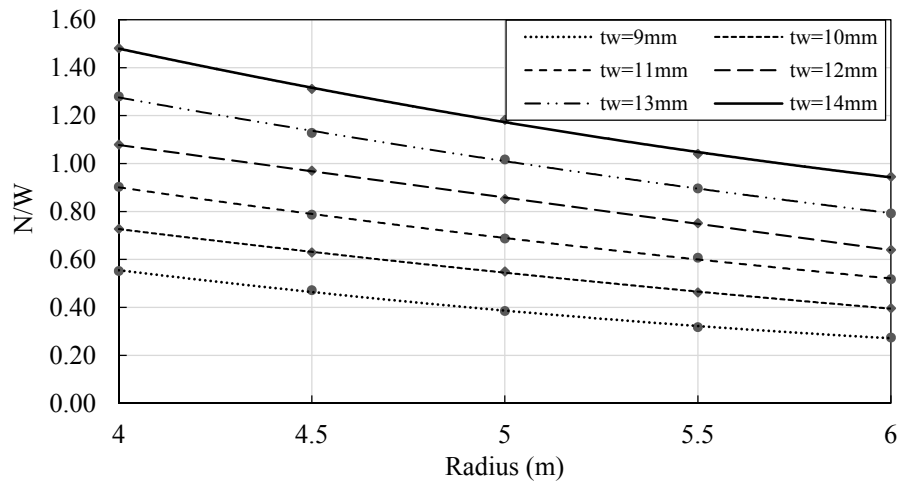
Fig. 3-9 Variation of total vertical force ratio with the tank radius and thickness

(h=7.0m, θ_v=45º)
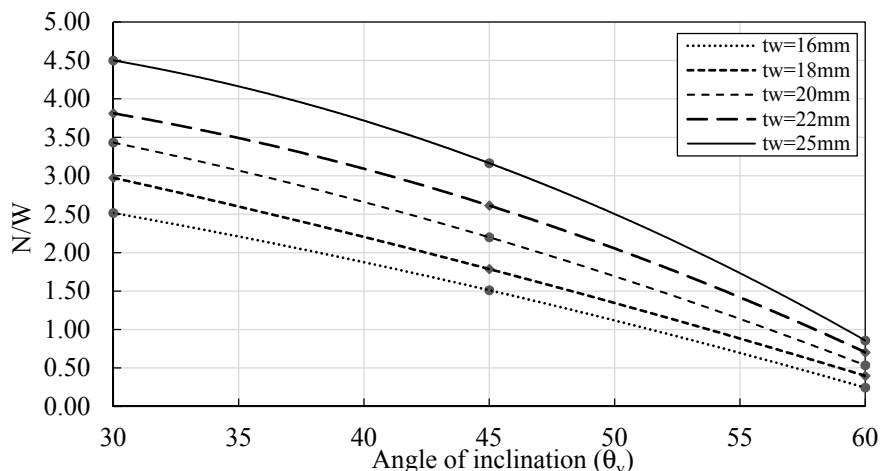
Fig. 3-10 Variation of total vertical force ratio with the tank angle of inclination and thickness (R_b=5.0m, h=7.0m)

The previous charts showed how the vertical force resistance for a steel conical tanks subjected to hydrodynamic pressure due to a vertical ground excitation changes with the steel conical tank dimensions each at a time. In order to express the vertical force resistance for a steel conical tank with random dimensions, different geometric parameters should be combined together. The variation of the vertical force resistance with tank geometric parameters is expressed in the form of the relation between the dimensionless parameters h/R_b and Nh/W_cR_b in the form of charts, where W_c is the cylindrical part weight of the contained fluid. These two dimensionless parameters are validated by making sure that for different tanks with the same ratio h/R_b the value of the parameter Nh/W_cR_b have the same value. The charts are shown in Figs. 3-20 to 3-22 found in Appendix B for different values of the angle θ_v. The effect of wall thickness is included through a family of curves represented as multipliers of t_s which is the thickness obtained by the simplified hydrostatic design method proposed by Sweedan and El Damatty (2009).

As mentioned earlier, this chapter represents a part of a larger study aiming to provide a simplified design procedure for steel conical tanks when subjected to ground excitations. By providing these charts, the vertical force resistance N for a pure steel conical tank can be obtained and then compared with the acting loads in order to assess the design of conical

tanks to resist the hydrodynamic pressure due to vertical ground excitations. This design assessment will be done in the coming sections.

3.6 Effect of Geometric Imperfection

As steel conical tanks are constructed of steel panels welded together in both longitudinal and circumferential directions, geometric imperfections will exist and their amplitude is dependent on the quality control applied during construction. For steel thin walled structures as for the case of steel conical tanks, geometric imperfections are very critical when it comes to buckling instability. In this section, the vertical force resistance for steel conical tanks subjected to hydrodynamic pressure due to vertical ground excitations is evaluated for the case of imperfect tanks following the same procedure used in the previous section.

Despite geometric imperfections are randomly distributed by nature, a conservative model for simulating the geometric imperfections is shown in Fig. 3-11 and is described by the following expression:

$$W(s)=w_0\sin\left(\frac{2\pi s}{L_I}\right)\cos(n\theta)$$ [3-7]

where w_0 is the imperfection amplitude, L_I is the imperfection wavelength, s is a coordinate measured along the generator of the vessel, and n is an integer defining the circumferential wavelength of the imperfection shape. Two categories of imperfect steel conical tanks according to Vandepitte et al. (1982) are considered in the current study: good conical tank with w_0/L_I less than 0.004, poor conical tank with w_0/L_I greater than 0.004 but less than 0.01.
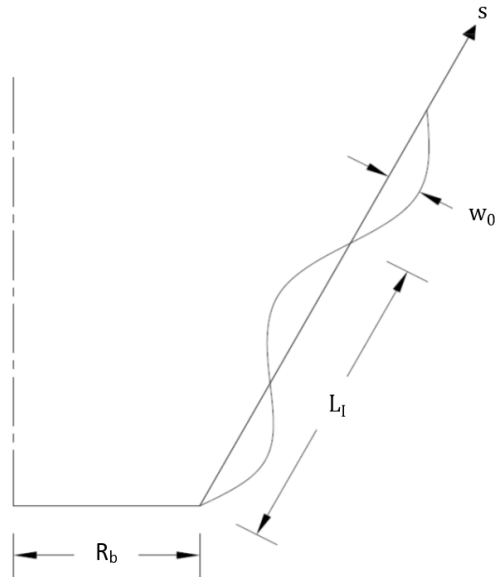
Fig. 3-11 Assumed imperfection shape along the generator of tank

Using this model, geometric imperfections are incorporated in the finite element model discussed in Section 3.3 in the form of initial strains prior to load application. Previous studies (Vandepitte et al. (1982), El Damatty et al. (1997a)) related to the effect of geometric imperfections on the capacity of conical tanks under hydrostatic pressure have shown that the critical buckling wave length L_{CR} is not a function of the height of the conical tank and that an axisymmetric distribution, i.e., n=0, leads to minimum buckling capacity due to the axisymmetric distribution of the hydrostatic pressure.

For the case of combined hydrostatic pressure and hydrodynamic pressure due to vertical ground excitations, an axisymmetric geometric imperfections' distribution will be the most critical as both hydrostatic and hydrodynamic pressures have axisymmetric distributions and consequently force the tank walls to buckle in an axisymmetric manner. In order to determine the critical imperfection wave length, several values for the imperfection wave length are assumed for each tank and the one leading to the minimum tank capacity is considered the critical wave length L_{cr}. An expression for L_{cr} is then obtained using regression analysis in the form of

$$L_{cr} = 4.03\sqrt{R\,t\,/\cos\theta_v} \qquad\qquad [3\text{-}8]$$

The effect of variation of the tank height on the critical imperfection wave length was found to be insignificant as noticed by Vandepitte et al. (1982) for the case of hydrostatic pressure only. The L_{cr} expression in Eq. 3-8 is similar to the one obtained by Vandepitte et al., (1982) for the case of hydrostatic pressure with a different constant value of 3.6. This relatively small difference implies that the hydrostatic pressure loading phase governs the capacity of imperfect conical tanks as the buckling waves initiate during this loading phase.

Using the above critical wave length with an axisymmetric distribution, geometric imperfections are incorporated in the finite element model and applied to the steel conical tanks using the same nonlinear pushover two-phase loading scheme discussed before. Two levels of imperfections' amplitude are studied: $w_0 = 0.004L_{cr}$ to represent good tanks, $w_0 = 0.01L_{cr}$ to represent poor tanks. Figures 3-12 to 3-14 show for different angles θ_v the variation of the normalized total vertical force resistance Nh/W_cR with the ratio h/R_b for the two levels of imperfections in addition to the case of perfect tanks for comparison. Similar to the case of perfect conical tanks, yielding of the tank walls is found to occur prior to shell instability for tanks with geometric imperfections included.

The reduction in the normalized total vertical force capacity Nh/W_cR_b is found to increase as the tank walls become more inclined. The average percentage of the reduction for good tanks is found to be 40%, 53%, and 63% for θ_v=30, 45, and 60, respectively. For poor tanks, the average percentage of the reduction is found to be 69%, 83%, and 95% for θ_v=30, 45, and 60, respectively.
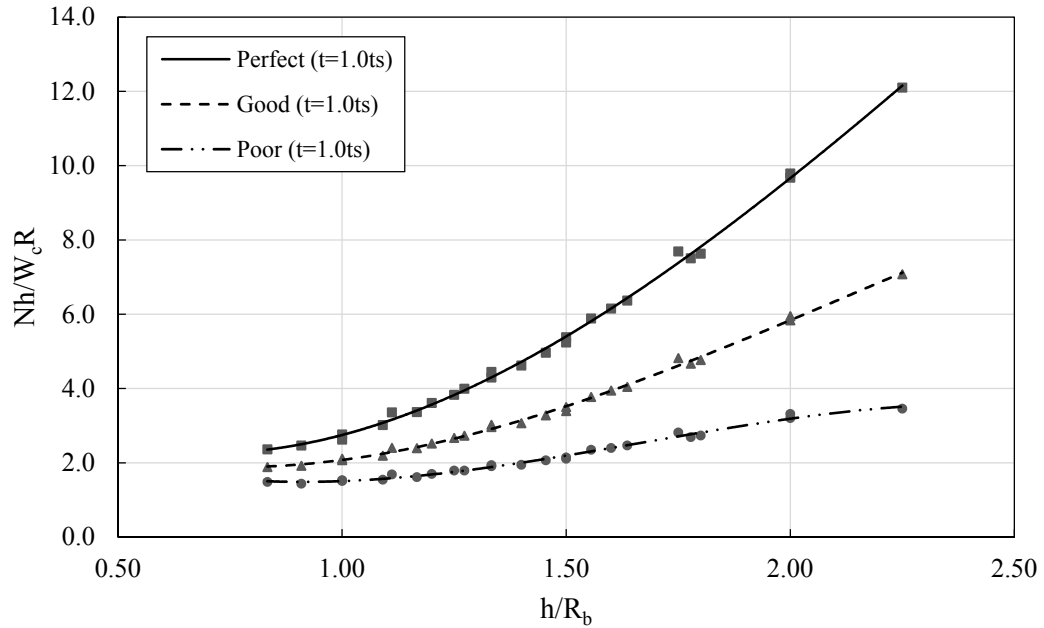
Fig. 3-12Effect of level of geometric imperfection on the total vertical force capacity

(θ_v=30)
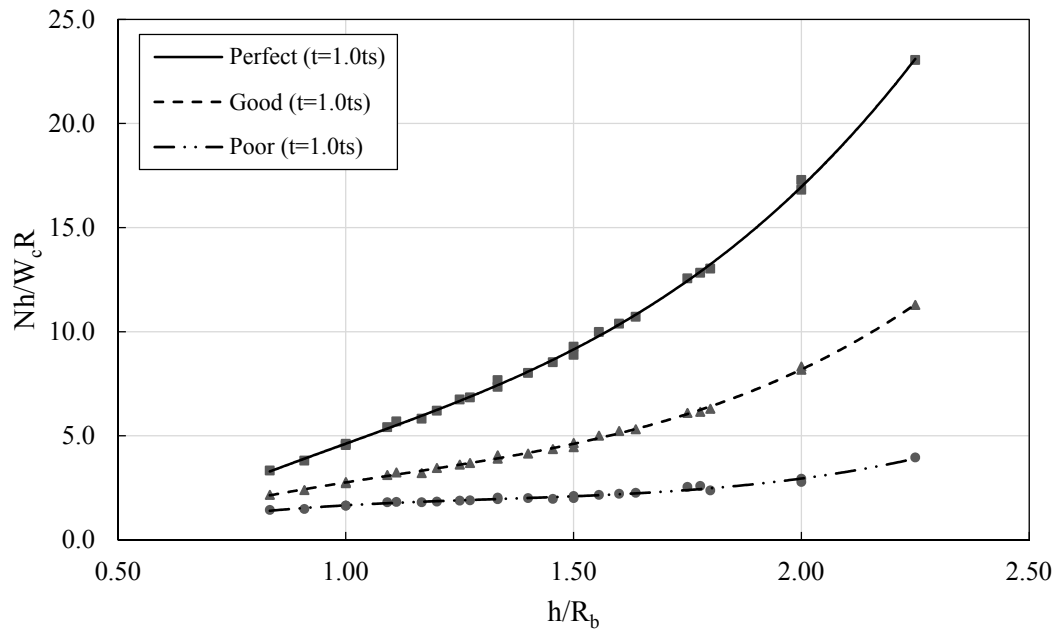
Fig. 3-13 Effect of level of geometric imperfection on the total vertical force capacity

(θ_v=45)
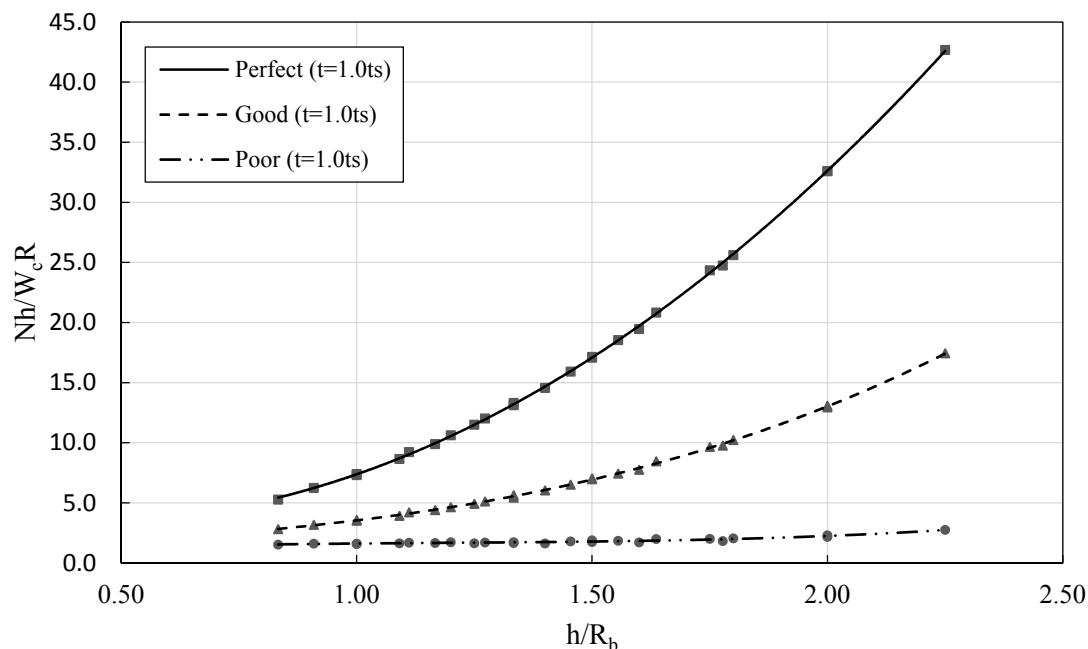
Fig. 3-14 Effect of level of geometric imperfection on the total vertical force capacity
(θ_v=60)

3.7 Equivalent Mechanical Model

The purpose of the previous part of this study was to be able to obtain the total vertical force capacity for perfect and imperfect steel conical tanks subjected to both hydrostatic and hydrodynamic pressure due to vertical ground excitations. In order to design the tanks, the obtained capacity should be compared with the acting loads, also known as seismic demand, corresponding to the seismic zone where the conical tank will be located. Seismic demand for the case of vertical ground excitations is represented in the form of total vertical force acting just above the steel conical tank base. This total vertical force demand can be obtained using an equivalent mechanical model simulating the steel conical tanks with the contained fluid.

Sweedan and El Damatty (2005) introduced a two masses mechanical model for steel conical tanks subjected to vertical ground excitation as shown in Fig. 3-15. The two masses are the rigid fluid mass, and the mass reflecting the effect of the flexibility of the tank's wall. The mass m_{o-w} is rigidly attached to the supporting tower and vibrates with the ground

acceleration, while the mass $m_{f\text{-}w}$ is a flexible mass that vibrates with the fundamental frequency of the tank-liquid system. The masses, and natural frequencies were presented in charts based on the tank dimensions. The total vertical force N_v is given by

$$N_v=\sqrt{N_1^2+N_2^2} \tag{3-9}$$

$$N_1=(m_{o\text{-}w}-m_{o\text{-}s})\ddot{G}_{vmax} \tag{3-10}$$

$$N_2=(m_{f\text{-}w}+m_{f\text{-}s})S_{a\text{-}sys} \tag{3-11}$$

where N_1 and N_2 reflect the contribution of the rigid and flexible components of the hydrodyanmic pressure, respectively. The masses $m_{o\text{-}s}$ and $m_{f\text{-}s}$ represent the portion of the tank walls' mass associated with the rigid and flexible vibration modes, respectively. The acceleration $\ddot{G}_{vmax}$ is the maximum vertical ground acceleration for the earthquake excitation also known as the peak ground acceleration PGA while $S_{a\text{-}sys}$ is the spectral acceleration corresponding to the natural frequency of the liquid-shell system.
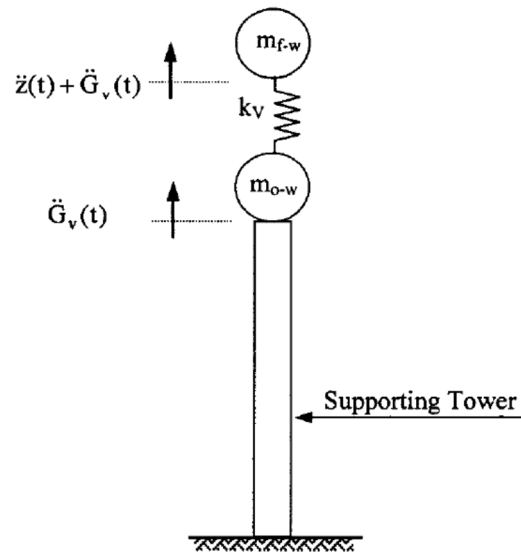
Fig. 3-15 Schematic presentation of the equivalent mechanical model, (Sweedan and El Damatty (2005))

As case studies, three seismic zones in Canada are considered which are Toronto, Montreal, and Vancouver. Toronto is chosen to represent a moderate seismically active region while Montreal and Vancouver are chosen to represent zones with high activity. The 5% damping

NBCC (2010) horizontal response spectra corresponding to the three seismic zones are summarized in Table 1.

Table 3-1 Seismic hazard design values for selected locations in terms of (g)

Location	PGA	Sa(0.2)	Sa(0.5)	Sa(1.0)	Sa(2.0)	Sa(4.0)
Toronto	0.12	0.22	0.13	0.067	0.021	0.0105
Montreal	0.33	0.64	0.31	0.14	0.048	0.024
Vancouver	0.47	0.95	0.65	0.34	0.17	0.085

As a value of 2% damping is recommended for hydrodynamic vibration mode, a technique based on artificial acceleration time histories compatible with the NBCC 2010 spectra is used to obtain spectra for damping values different than the 5% ones. In this proposed technique, the first step is to obtain a set of acceleration time histories with different durations compatible with the 5% NBCC 2010 spectra. Secondly, the 2% damping response spectra are evaluated and then compared to the 5% damping ones. Finally, an average value for the increase in the spectrum values is calculated. Following this technique, it is found that the 5% response spectrum should be increased with an average factor of 1.44 in order to obtain the 2% damping spectrum. Another point of importance is that the NBCC 2010 spectra are to be used for horizontal not vertical ground excitations. In order to get the vertical response spectra, the vertical-to-horizontal response spectral ratio V/H has to be determined. The ratio V/H is very sensitive to the spectral period and the distance from the fault and is higher at short periods and might exceed unity as noted by Bozorgnia et al. (1995) and Bozorgnia et al. (1996). Bozorgnia and Campbell (2004) performed an extensive study using 443 earthquake records in order to come up with a simplified model, as shown in Fig. 3-16, for the ratio V/H based on the natural period, soil conditions, and distance from the fault.

As the natural period for the first vertical vibration mode for the set of steel conical tanks used in this study ranges from 0.08 sec to 1.18sec, the commonly used value of 2/3 for the ratio V/H is found to be conservative assuming an earthquake with distance more than 60 km based on the model proposed by Bozorgnia and Campbell (2004). Based on that, a V/H

value of 2/3 is used to reduce the 2% damping horizontal response spectra in order to obtain the vertical spectra for different seismic zones.

Firm soils

Firm rock, soft rock, very firm soil
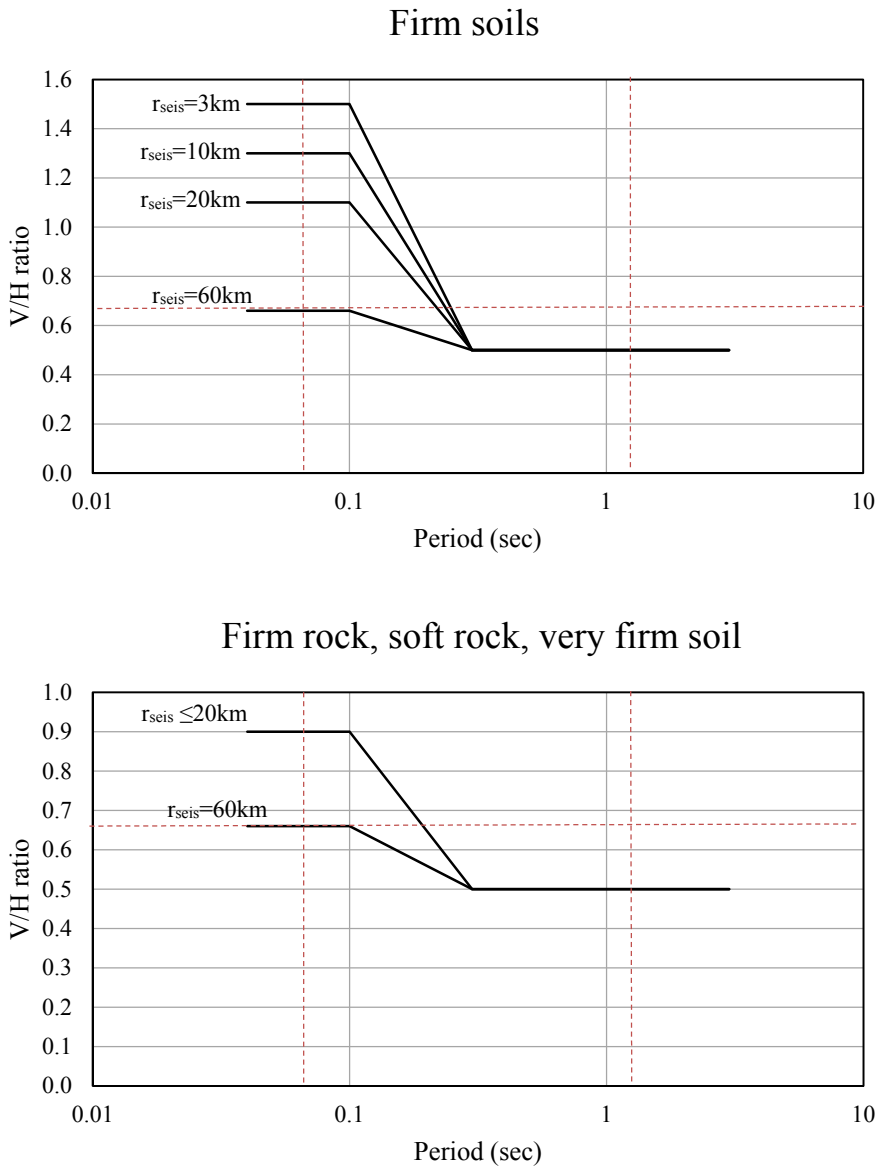
Fig. 3-16 Simplified V/H response spectral ratio, (Bozorgnia and Campbell (2004))

After obtaining the vertical response spectra for different seismic zones, the equivalent mechanical model for steel conical tanks is used in order to obtain the values of the total vertical force for the set of steel conical tanks described in Section 3.4. The values of the total vertical forces are expressed in the form of the ratio $N_v h / W_c R_b$ for the sake of

comparison with the total vertical force capacities obtained in Section 3.5 using the non-linear static analysis. The variation of the normalized total vertical force N_vh/W_cR_b with the ratio h/R_b for the three seismic zones is shown in Figs. 3-17 to 3-19 represented by the solid lines. On the same charts, the normalized total vertical force capacity values are shown for the cases of perfect, good, and poor tanks.
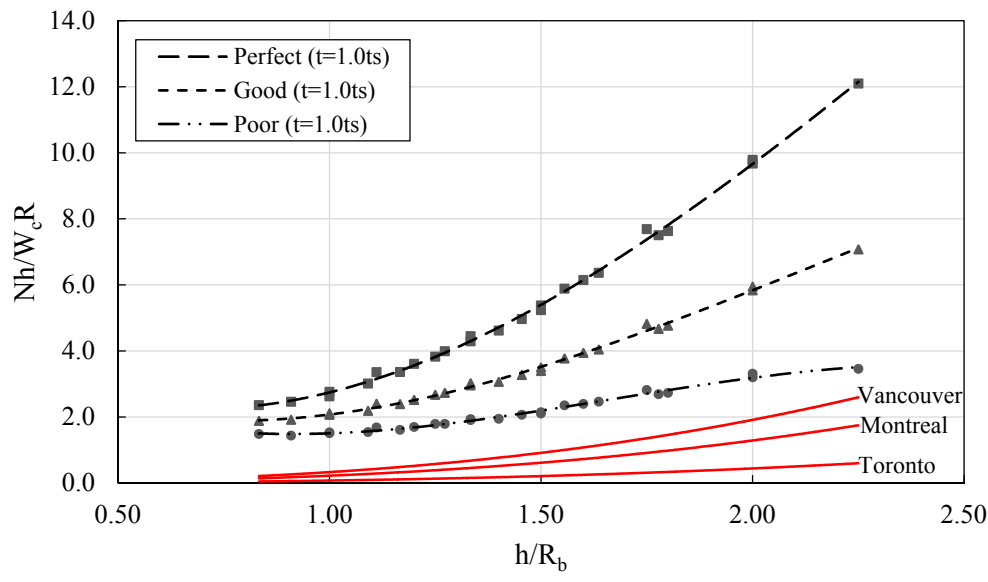
Fig. 3-17 Comparison of total vertical force capacity to the vertical force demand for the three seismic zones ($\theta_v=30$)
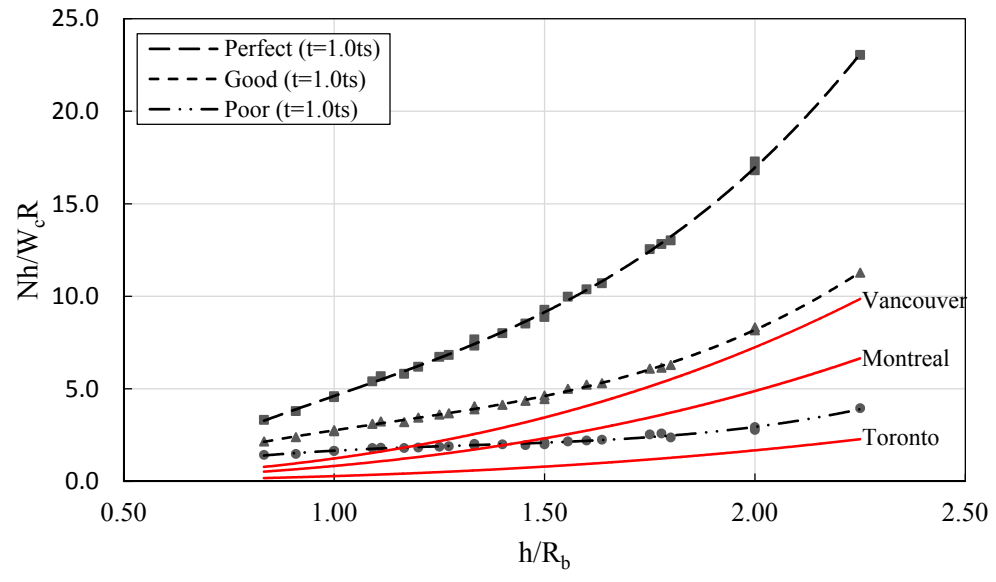
Fig. 3-18 Comparison of total vertical force capacity to the vertical force demand for the three seismic zones (θ_v=45)
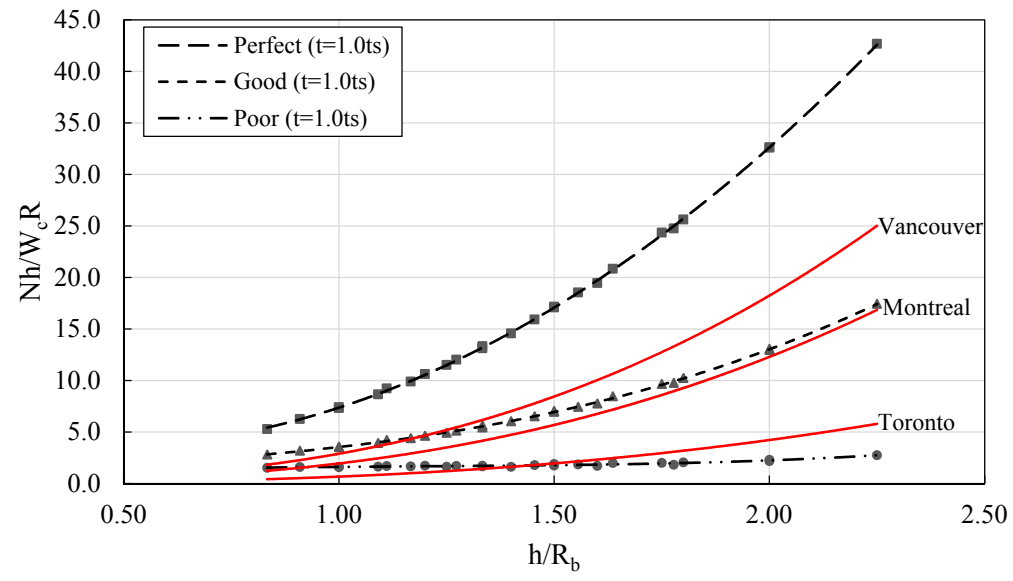
Fig. 3-19 Comparison of total vertical force capacity to the vertical force demand for the three seismic zones (θ_v=60)

For conical tanks with θ_v=30, the initial design under hydrostatic pressure only is found to be satisfactory to resist the total vertical forces corresponding to the three seismic zones regardless the level of geometric imperfections. As θ_v reaches a value of 45, the initial

design is found to be satisfactory except for the following cases: poor tanks corresponding to Montreal seismic zone with h/R_b more than 1.5, and poor tanks corresponding to Vancouver seismic zone with h/R_b more than 1.2. Finally for conical tanks with θ_v=60, the initial design is found to be satisfactory except for the following cases: good tanks corresponding to Vancouver seismic zone with h/R_b more than 1.2, poor tanks corresponding to Toronto seismic zone with h/R_b more than 1.4, and poor tanks corresponding to Montreal and Vancouver seismic zones.

3.8 Conclusions

As most of the studies found in literature related to seismic behaviour of steel conical tanks focused on evaluating the acting loads on the tank walls due to the resulting hydrodynamic pressure, this study represents the first attempt to evaluate the capacity of steel conical tanks subjected to hydrodynamic pressure due to vertical ground excitations. The capacity is obtained using nonlinear finite element model through nonlinear static pushover analysis. The conical tank capacity is expressed in terms of the total vertical force acting just above the tank base at failure. The governing failure criteria for the case of steel conical tanks subjected to both hydrostatic and hydrodynamic pressure due to vertical ground excitation is found to be the yielding of the tank walls.

The vertical force resistance for a series of steel conical tanks with practical dimensions is obtained and normalized in the form of the dimensionless parameter Nh/W_cR_b. The normalized vertical force resistance for the group of tanks is then plotted with the height to bottom radius ratio. The charts are provided for different wall inclination angles and thicknesses to study their effects on conical tanks' resistance.

The aforementioned charts are obtained assuming the tank walls to be free of any geometric imperfections which is almost impossible to occur as the tank vessel is constructed of welded steel panels. As a result, the effect of these unavoidable geometric imperfections on the vertical force resistance is studied. The geometric imperfections are incorporated in the finite element model in the form of initial strains. An axisymmetric imperfections distribution is assumed to be the most critical being similar to the distribution of both hydrostatic and hydrodynamic pressure for the case of vertical excitations. An expression

for the critical imperfection wave length that leads to the minimum tank capacity is obtained using regression analysis as a function of the tank dimensions.

Two levels of geometric imperfections are considered which are good and poor based on the amplitude of imperfections. Finally, similar charts to those in the first part are provided in order to know how much the total vertical force resistance is reduced with the inclusion of the imperfections in the analyses. The reduction in the normalized total vertical force capacity Nh/W_cR_b is found to increase with the angle θ_v. The average percentage of the reduction for good tanks is found to be 40%, 53%, and 63% for θ_v=30, 45, and 60, respectively, while for poor tanks, the average percentage of the reduction is found to be 69%, 83%, and 95% for θ_v=30, 45, and 60, respectively.

In order to assess the design of steel conical tanks under hydrostatic pressure only, the obtained vertical force resistance has to be compared with the loads acting on the tank walls due to the vertical ground excitation. The acting loads are also referred to as the vertical force demand corresponding to a specific ground excitation. This total vertical force demand is obtained based on equivalent mechanical model found in the literature for the case of vertical excitations where the contained fluid is modelled in the form of lumped masses connected to the tank walls through linear springs.

The total vertical force demand is obtained for three different seismic zones representing moderate and highly active zones in Canada. The NBCC 2010 5% damping horizontal response spectra are first converted to the 2% damping vertical response spectra using 2 conversion factors. The first factor is the damping factor which is obtained through a technique based on NBCC 2010-corresponding artificial ground excitation records, while the second factor is the horizontal to vertical conversion factor which is obtained from models found in the literature based on the natural frequencies of the steel conical tanks considered in the current study. The obtained vertical force demand values are compared to the vertical force resistance values obtained previously in the current study and it is found that the design of the steel conical tanks under hydrostatic pressure only is considered enough to resist the total vertical forces induced by the vertical excitation for the three seismic zones except for poor tanks with θ_v=45° corresponding to Montreal

seismic zone with h/R_b more than 1.5 and Vancouver seismic zone with h/R_b more than 1.2; good tanks with $\theta_v=60^o$ corresponding to Vancouver seismic zone with h/R_b more than 1.2, poor tanks with $\theta_v=60^o$ corresponding to Toronto seismic zone with h/R_b more than 1.4 and Montreal and Vancouver seismic zones.

3.9 References

(API), A.P.I., 2005. *Welded Storage Tanks for Oil Storage*. Washington D.C, USA: American Petroleum Institute Standard.

(AWWA), A.W.W.A., 2005. *Welded Steel Tanks for Water Storage*. Denver, CO, USA.

(ECS), E.C.f.S., 1998. Design provisions for earthquake resistance of structures. *Eurocode 8*.

Bozorgnia, Y. and Campbell, K.W., 2004. The vertical-to-horizontal response spectral ratio and tentative procedures for developing simplified V/H and vertical design spectra. *Earthquake Engineering*, 8(2), pp.175-207.

Bozorgnia, Y. et al., 1995. Characteristics of free-field vertical ground motion during the Northridge earthquake. *Earthquake Spectra*, 11, pp.515-25.

Bozorgnia, Y. et al., 1996. Relationship between vertical and horizontal ground motion for the Northridge earthquake. In *11th World Conference on Earthquake Engineering*. Acapulco, Mexico, 1996.

Buratti, and Tavano, M., 2014. Dynamic buckling and seismic fragility of anchored steel tanks by the added mass method. *Earthquake Engng. Struct. Dyn.*, 43, pp.1-21.

Djermane, M. et al., 2014. Dynamic buckling of steel tanks under seismic excitation: Numerical evaluation of code provisions. *Engineering Structures*, 70, pp.181-96.

El Damatty, A.A. et al., 1998. Inelastic stability of conical tanks. *Thin-Walled Structures*, 31, pp.343-59.

El Damatty, A.A. et al., 1997a. Stability of Imperfect Conical Tanks under Hydrostatic Loading. *Journal of Structural Engineering*, 123(6), pp.703-12.

El Damatty, A.A. et al., 1997d. Large displacement extension of consistent shell element for static and dynamic analysis. *Computers and Structures*, 62(6), pp.943-60.

El Damatty, A.A. et al., 1999. Simple Design Procedure For Liquid-Filled Steel Conical Tanks" Journal of structural engineering. *Journal of structural engineering*, 125(8), pp.879-90.

El Damatty, A.A. et al., 1997c. Stability of elevated liquid-filled conical tanks under seismic loading, Part II-Applications. *Earthquake Engng. Struct. Dyn.*, 26, pp.1209-29.

El Damatty, A.A. et al., 1997b. Stability of elevated liquid-filled conical tanks under seismic loading, Part I-Theory. *Earthquake Engng. Struct. Dyn.*, 26, pp.1191-208.

El Damatty, A.A. et al., 2005. Dynamic characteristics of combined conical-cylindrical shells. *Thin-Walled Structures*, 43, pp.1380-97.

El Damatty, A.A. et al., 2005. Experimental study conducted on a liquid-filled combined conical tank model. *Thin-Walled Structures*, 43, pp.1398-417.

Hafeez, G. et al., 2010. Stability of combined imperfect conical tanks under hydrostatic loading. *Journal of Constructional Steel Research*, 66, pp.1387-97.

Haroun, M.A. and Abou-Izzeddine, W., 1992. Parametric Study Of Seismic Soil-Tank Interaction. ii: Vertical Excitation. *Journal of Structural Engineering*, 118(3), pp.798-812.

Haroun, M.A. and Housner, G.W., 1981. Seismic design of liquid storage tanks. *Journal of the Technical Councils*, 107(TC1), pp.191-207.

Haroun, M.A. and Housner, G.W., 1982. Dynamic Characteristics of Liquid Storage Tanks. *Journal of the Engineering Mechanics Division*, 108(5), pp.783-800.

Haroun, M.A. and Tayel, M.A., 1985a. Axisymmetrical vibrations of tanks—Numerical. *J. Eng. Mech.*, 111(3), pp.329-45.

Haroun, M.A. and Tayel, M.A., 1985b. Axisymmetrical vibrations of tanks—Analytical. *J. Eng. Mech.*, 111(3), pp.346-58.

Haroun, M.A. and Tayel, M., 1985. Response of tanks to vertical seismic excitation. *Earthquake Engng. Struct. Dyn.*, 13, pp.583-95.

Housner, G.W., 1957. Dynamic Pressures on Accelerated Fluid Containers. *Bulletin Seism. Soc. America*, 47(1), pp.15-35.

Housner, G.W., 1963. The Dynamic Behavior of Water Tanks. *Bulletin Seism. Soc. America*, 53(1), pp.381-87.

Jacobsen, L.S., 1949. Impulsive Hydrodynamics of Fluid Inside a Cylindrical Tank and of a Fluid Surrounding a Cylindrical Pier. *Bulletin Seism. Soc. America*, 39, pp.189-204.

Jolie, M. et al., 2014. Seismic analysis of elevated pure conical tanks under vertical excitation. *Can. J. Civ. Eng.*, 41, pp.909-17.

Koizey, B. and Mirza, F.A., 1997. Consistent thick shell element. *Computer & Structures*, 65(12), pp.531-41.

Marchaj, T.J., 1979. Importance of Vertical Acceleration in the Design of Liquid Containing Tanks. In *2nd U.S. National Conference on Earthquake Engineering*. Stanford, CA, 1979.

NBCC, 2010. *National Building Code of Canada*. Ottawa, ON, Canada: National Research Council of Canada.

Sweedan, A.M., 2009. Equivalent mechanical model for seismic forces in combined tanks subjected to vertical earthquake excitation. *Thin-Walled structures*, 47, pp.942-52.

Sweedan, A.M.I. and El Damatty, A.A., 2002. Experimental and analytical evaluation of the dynamic characteristics of conical shells. *Thin-Walled Structures*, 40, pp.465-86.

Sweedan, A.M. and El Damatty, A.A., 2005. Equivalent Models of Pure Conical Tanks under Vertical Ground Excitation. *Journal of Structural Engineering, ASCE*, 131(5), pp.725-33.

Sweedan, A.M. and El Damatty, A.A., 2009. Simplified procedure for design of liquid-storage combined conical tanks. *Thin-Walled structures*, 47, pp.750-59.

Vandepitte, D., 1999. Confrontation of shell buckling research results with the collapse of a steel water tower. *Journal of Constructional Steel Research*, 49, pp.303-14.

Vandepitte, D. et al., 1982. Experimental investigation of hydrostatically loaded conical shells and practical evaluation of the buckling load. In *Proc. State of the Art Colloquium*. Universitat Stuttgart, Germany, 1982.

Veletsos, A.S., 1974. Seismic Effects in Flexible Liquid Storage Tanks. In *International Association for Earthquake Engineering. Fifth World Conference*. Rome, Italy, 1974.

Veletsos, A.S. and Kumar, A., 1984. Dynamic response of vertically excited liquid storage tanks. In *8th World Conf. on Earthquake Engineering*. San Francisco, CA, 1984.

Veletsos, A.S. and Tang, Y., 1986. Dynamics of vertically excited liquid storage tanks. *J. Struct. Eng.*, 112(6), pp.1228-46.

Virella, J.C. et al., 2006. Dynamic buckling of anchored steel tanks subjected to horizontal earthquake excitation. *Journal of Constructional Steel Research*, 62, pp.521-31.

Virella, J.C. et al., 2008. A Static Nonlinear Procedure for the Evaluation of the Elastic Buckling of Anchored Steel Tanks Due to Earthquakes. *Journal of Earthquake Engineering*, 12, pp.999-1022.

Appendix B

Fig. 3-20 Variation of ratio Nh/W$_c$R$_b$ with h/R$_b$ for perfect tanks (θ_v=30)
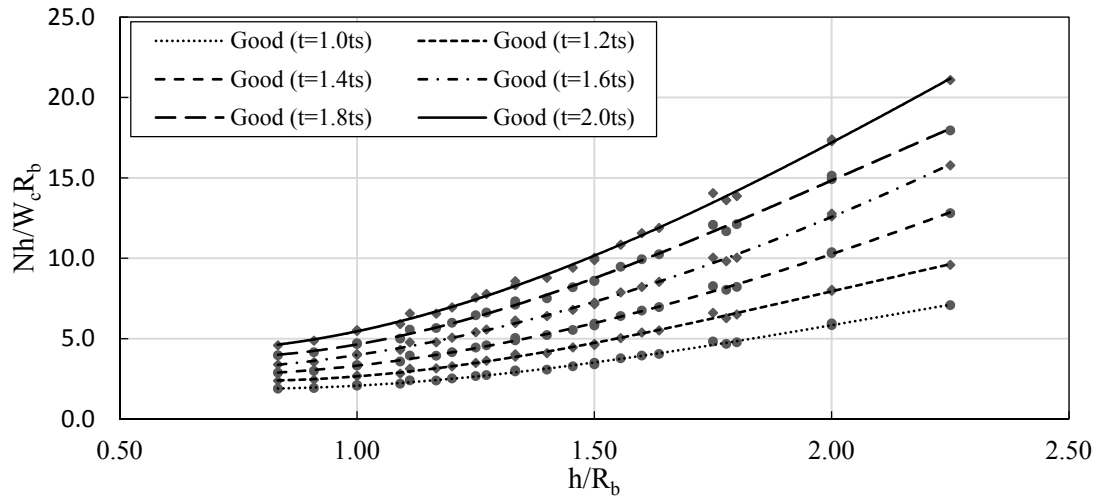
Fig. 3-21 Variation of ratio Nh/W$_c$R$_b$ with h/R$_b$ for good tanks (θ_v=30)
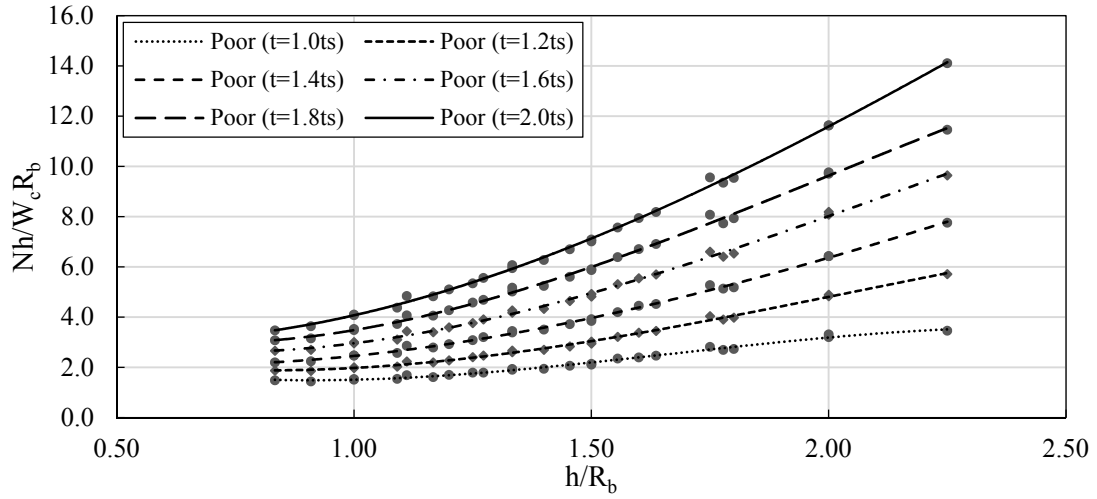
Fig. 3-22 Variation of ratio Nh/W_cR_b with h/R_b for poor tanks (θ_v=30)
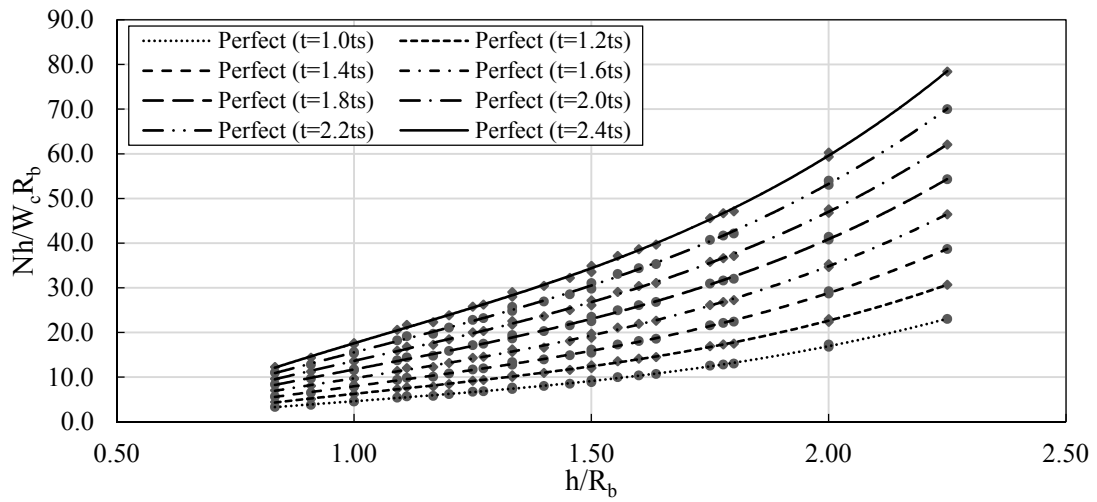
Fig. 3-23 Variation of ratio Nh/W_cR_b with h/R_b for perfect tanks (θ_v=45)
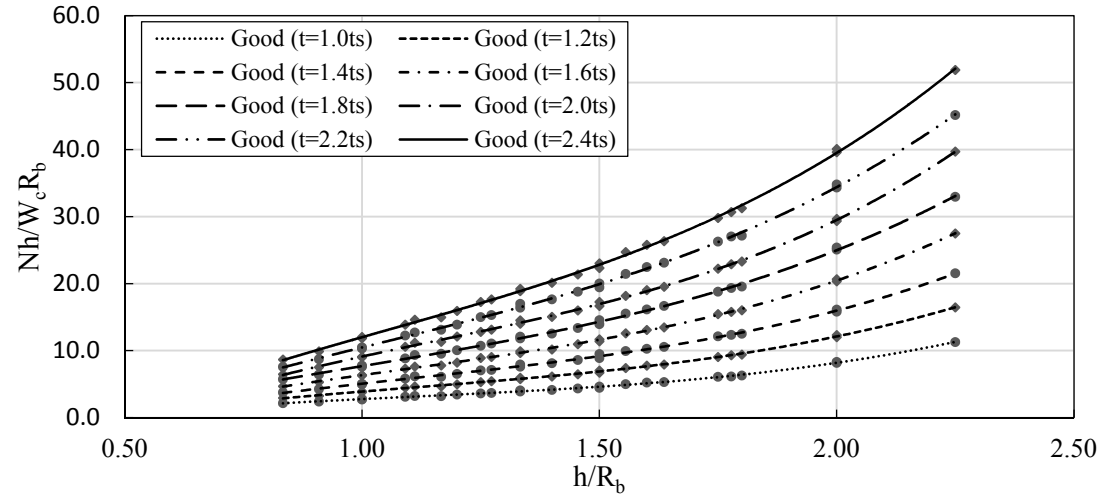
Fig. 3-24 Variation of ratio Nh/W_cR_b with h/R_b for good tanks (θ_v=45)
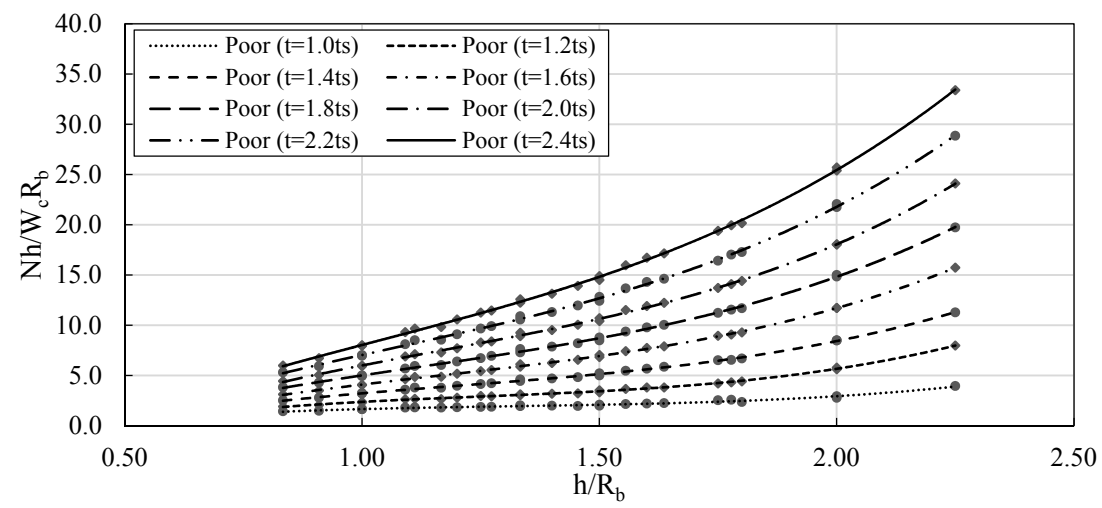
Fig. 3-25 Variation of ratio Nh/W_cR_b with h/R_b for poor tanks (θ_v=45)
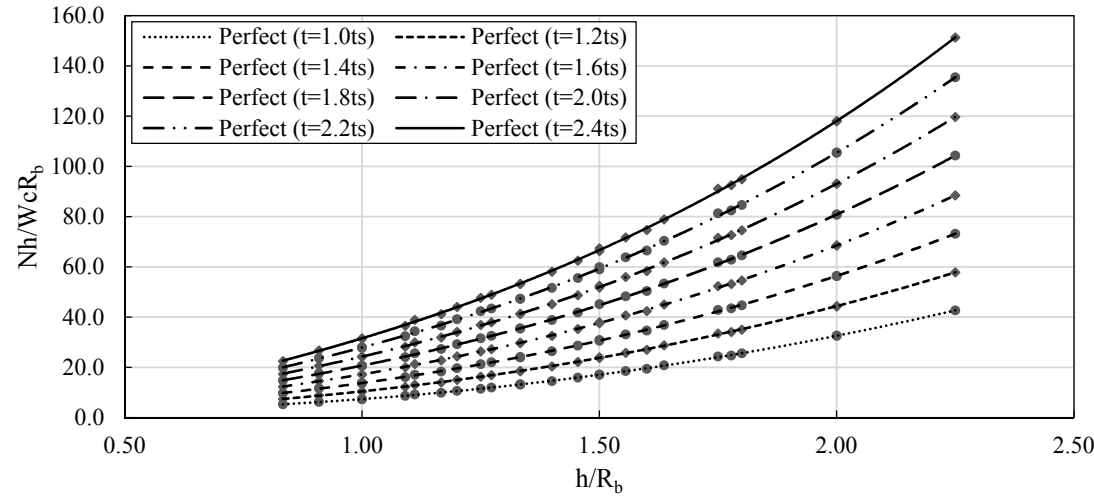
Fig. 3-26 Variation of ratio Nh/W_cR_b with h/R_b for perfect tanks (θ_v=60)
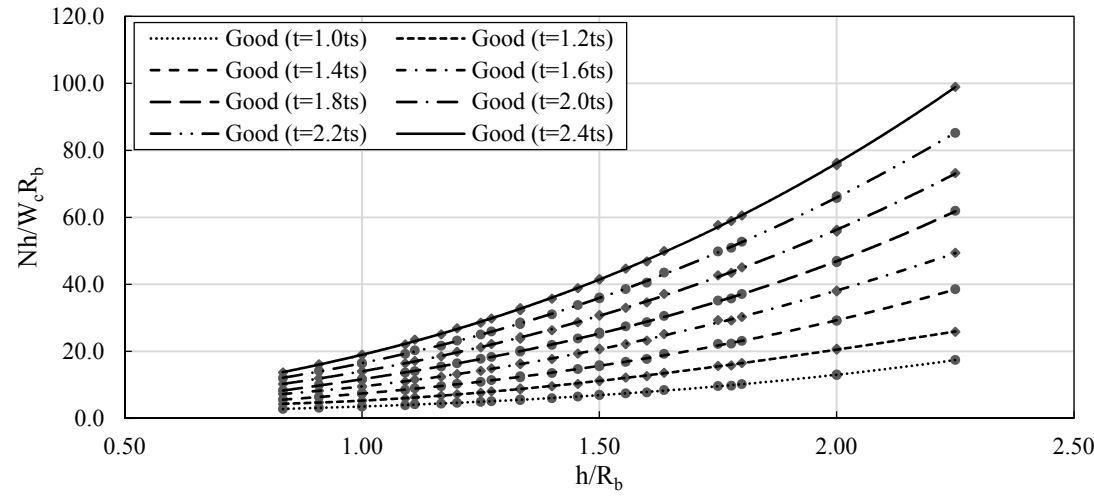
Fig. 3-27 Variation of ratio Nh/W_cR_b with h/R_b for good tanks (θ_v=60)
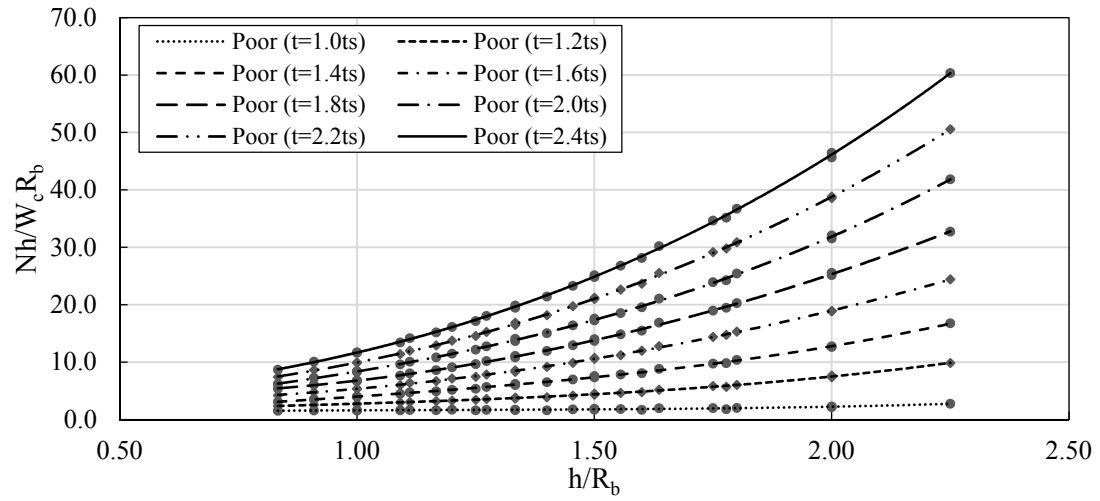
Fig. 3-28 Variation of ratio Nh/W$_c$R$_b$ with h/R$_b$ for poor tanks (θ_v=60)

Chapter 4

4 Design Procedure for Liquid Storage Steel Conical Tanks under Seismic Loading

Steel liquid tanks in the form of truncated cones are widely used for the purpose of liquid storage in an industrial facility or for water supply and fire protection. Despite the fact that some of these tanks have failed during the last decades, most of the seismic design specifications and guidelines focus on the design of steel cylindrical tanks with the only design guidelines for conical tanks, found in some specifications, are based on using an equivalent cylinder approach. This approach is not based on any theoretical or experimental basis highlighting the need for more realistic seismic design procedure for this shape of liquid tanks. In this study, a simplified procedure that avoids both yielding and buckling of the steel tank vessel is proposed to design liquid filled steel conical tanks subjected to horizontal and vertical earthquake excitations. The proposed design procedure is based on satisfying a design formula that combines the ratio of seismic demand to the tank resistance when subjected to hydrodynamic pressure due to horizontal and vertical excitations. The design procedure is then validated by comparing its outcomes with those obtained using non-linear time history analysis as a reference. The design approach accounts for the initially-existing geometric imperfections. The study is carried out numerically using an in-house finite element model that accounts for the effects of geometric and material nonlinearities.

4.1 Introduction

Steel conical-shaped liquid tanks are used as fluid containment in an industrial facility or for water supply and fire protection. A conical tank consists of a steel vessel resting on a supporting structure. The conical vessel is constructed of prefabricated steel panels welded together circumferentially and longitudinally. Based on the required pressure head, a conical tank vessel might be elevated above ground through a reinforced concrete shaft. Two common configurations for steel conical tanks exist: (1) Pure truncated cone as shown in Fig. 4-1a, (2) Combined conical tank with a cylindrical cap as shown in Fig. 4-1b.
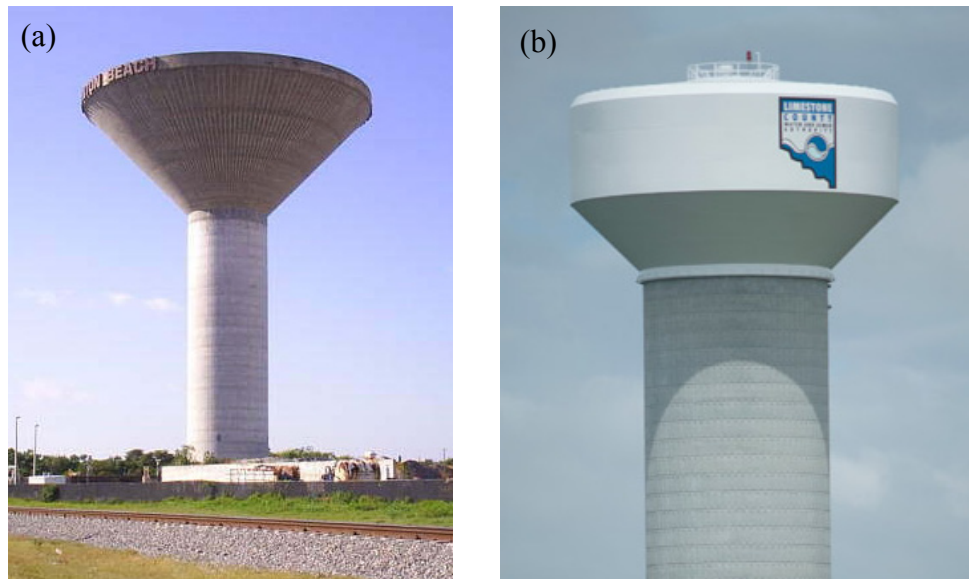
Fig. 4-1 (a) Pure conical tank[5], (b) Combined conical tank[6]

Despite the fact that some of these tanks have failed during the last decades, most of the previous studies and, consequently, seismic design specifications focused on the design of steel cylindrical tanks. The most common failure mode for steel conical tanks is in the form of shell instability due to the relatively small wall thickness. The only seismic design guidelines for conical tanks found in some specifications (AWWA (2005), API (2005), and ECS (1998)) are based on using equivalent cylinder approach which is not based on any theoretical or experimental basis.

The state of stresses under hydrostatic pressure for the case of cylindrical tanks is not similar to the case of conical tanks due to the inclination of the tank walls. To better understand the resulting stresses for the case of conical tanks, the volume of the contained liquid is divided into vol. 1 and vol.2 as shown in Fig. 4-2. The first one is transferred directly to the tank base, while the second one is resting on the tank inclined walls. Due to

---

[5] http://forums.auran.com/trainz/showthread.php?17876-FEC-Key-West-extension-modern-day/page7

[6] http://www.caldwellwatertanks.com

the inclination of the walls, compressive meridional stresses σ_m are developed in addition to tensile hoop stresses σ_h meridionally and circumferentially, respectively, through the tank shells. Compressive stresses σ_m are maximum near the tank base due to the reduction in the tank radius in addition to the increase of the fluid volume resting on the tank walls, i.e., vol.2. These compressive stresses are very critical for the case of steel tanks as they might lead to shell instability.
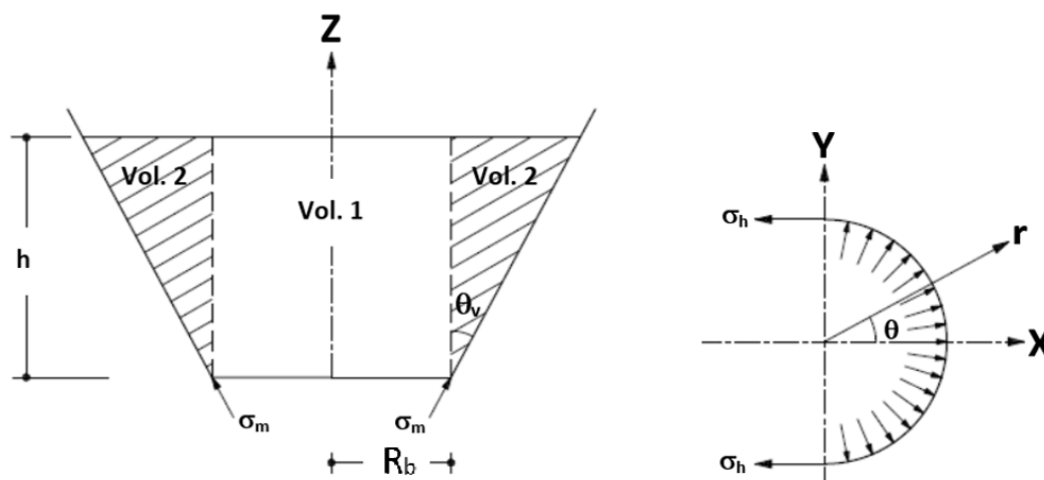
Fig. 4-2 Stresses induced due to inclination of the wall

Motivated by the collapse of a conical steel water tower in Belgium, Vandepitte et al. (1982) tested a large number of small-scale conical tank models experimentally under hydrostatic pressure. The objective was to develop a set of design charts for different base restraining conditions and geometric imperfections' levels. In 1990, a steel conical water tower collapsed in Fredericton, Canada when it was filled with water for the first time. The tank failed as the amplitude of the geometric imperfections was underestimated (Vandepitte (1999)). For the design of steel conical tanks under hydrostatic pressure, El Damatty et al. (1999) and Sweedan and El Damatty (2009) provided simplified design approach that takes into account geometric imperfections and the existence of an upper cylindrical cap.

Seismic behaviour of Liquid storage tanks is important to understand as any failure to such structures might have a serious consequences in addition to the structure damage; for

example, losing water supply or release of combustible materials stored inside. A lot of studies were carried out in order to understand the seismic behaviour of cylindrical steel either assuming the tank walls to be rigid (Jacobsen (1949), Housner (1957), and Housner (1963)) or taking into consideration the effect of wall flexibility in the form of fluid-structure interaction (Veletsos (1974), Haroun and Housner (1981,1982)). It was concluded that the flexibility of cylindrical tank walls amplifies the tank response and has to be accounted for.

The induced hydrodynamic pressure on a liquid storage tank walls due to a horizontal ground excitation is divided into two components known as impulsive and sloshing components. The impulsive component corresponds to the lower amount of liquid which moves with the walls of the tank. As a result, it has a maximum value near the tank base. The long period sloshing component corresponds to the upper amount of liquid undergoing sloshing. In general, the impulsive pressure is the most critical unless the liquid tank is extremely shallow.

When a steel conical tank is subjected to earthquake excitation, hydrodynamic pressure is induced on the tank walls. For the case of horizontal excitation, the induced hydrodynamic pressure will amplify both σ_m and σ_h at one side of the tank and reduce them at the other side based on the direction of the ground acceleration, while the induced hydrodynamic pressure due to vertical excitation will amplify or reduce both σ_m and σ_h in an axisymmetric manner based on the direction of the ground acceleration, i.e., upwards or downwards.

Jolie et al. (2013) assessed using the equivalent cylinder approach found in AWWA (2005), API (2005), and ECS (1998) when analyzing conical tanks subjected to horizontal ground excitations. This was done by comparing the base shear and overturning moment obtained using equivalent mechanical model for conical tanks to those obtained using the equivalent cylinder approach. It was shown that the base shear is well-predicted by the Eurocode, while it is overly-estimated by the AWWA and API. On the other side, the three design codes under-estimated overturning moment due to ignoring the effect of the vertical component of the hydrodynamic forces due to horizontal excitation when assuming the tank walls to be vertical not inclined.

El Damatty et al. (1997b,c) conducted the first study to assess the behavior of conical tanks under seismic loading where a coupled shell element-boundary element formulation was developed to simulate the fluid-structure interaction for both horizontal and vertical excitations. A fluid added mass matrix that can be incorporated into a nonlinear dynamic analysis routine was derived.

Early studies about seismic behaviour of cylindrical liquid tanks often ignored the effect of the vertical excitations as most of the structures are relatively stiff in the vertical direction. However, it has been observed that the maximum amplitude of the vertical excitation component can exceed peak horizontal amplitude especially near the center of the earthquake. Vertical acceleration is transmitted to a horizontal hydrodynamic loading acting on the tank walls. As a result, tensile hoop stresses are amplified and might lead to inelastic buckling of the shell. Marchaj (1979) attributed the failure of metallic tanks during past earthquakes to the lack of consideration of vertical acceleration in their design. Veletsos and Kumar (1984) and Haroun and Tayel (1985a) showed that the flexibility of cylindrical tank walls amplifies the tank response and has to be accounted for the case of vertical excitations as well.

Veletsos and Tang (1986) provided a practical procedure to evaluate the dynamic response of rigid and flexible steel and concrete cylindrical tanks with different base conditions when subjected to vertical excitations including soil-structure interaction. The main conclusion was that soil-structure interaction reduces the maximum hydrodynamic effects and might be approximated by a change in the fundamental natural frequency of the tank-liquid system or an increase in damping. Haroun and Abou-Izzeddine (1992) performed a parametric study in order to evaluate the effects of different factors that influence the seismic response of an elastic cylindrical tank supported on a rigid base when subjected to a vertical excitation by considering shell-liquid-soil interaction. It was concluded that foundation soil-tank interaction reduces the tank response in general, and this reduction is a function of the soil shear-wave velocity as well as tank geometric properties.

The analysis of steel liquid tanks when subjected to ground excitations is considered relatively complicated due to the existence of the contained liquid that results in fluid-

structure interaction. As a result, researchers introduced the concept of equivalent mechanical models where the contained liquid is simulated as lumped masses attached to the tank wall rigidly or through linear springs. By doing that, the complicated tank-liquid system is replaced with a set of masses and springs that can be incorporated in dynamic analysis reducing the computation time extensively. The main objective of an equivalent mechanical model is to match the resulting base forces and moments obtained using dynamic analysis for the original tank-liquid system.

For horizontal ground excitations, Haroun and Housner (1981) introduced a three masses mechanical model for cylindrical steel tanks. The three masses are the impulsive fluid mass, the sloshing fluid mass, and the mass reflecting the effect of the flexibility of the tank walls. El Damatty and Sweedan (2006) developed a similar mechanical model for conical tanks in order to predict the base shear and overturning moment acting on a conical tank base.

For vertical ground excitations, Sweedan and El Damatty (2005) proposed a two-mass mechanical model for pure conical tanks in order to get the same values of the total vertical forces acting on the tank walls. The two masses are the rigid fluid mass, and the mass reflecting the effect of the flexibility of the tank's wall. Sweedan (2009) introduced a similar mechanical model that can be used for combined conical-cylindrical tanks subjected to vertical excitations.

To the best of the authors' knowledge, this study will be the first attempt to provide a design procedure for liquid steel conical tanks subjected to ground excitations including both horizontal and vertical components. The proposed design approach is based on satisfying a design interaction formula that combines the effect of hydrodynamic forces acting on conical tanks due to both horizontal and vertical components of a ground excitation. The proposed formula is a function of the conical tank capacity with respect to both yielding and buckling of the tank vessel in addition to the seismic demand which represents the actual forces acting on a structure when subjected to an earthquake. The capacity for different pressure components is obtained in the previous two chapters using non-linear static analysis, while the corresponding demand for each pressure component is obtained

based on previously developed equivalent mechanical models found in the literature. In order to validate the proposed design formula, non-linear time history analyses are used and their results are compared to those based on the proposed formula.

4.2 Hydrodynamic Forces

4.2.1 Horizontal Excitation

For a conical tank subjected to a horizontal excitation, a resulting base shear Q and a corresponding overturning moment M will act just above the tank base as shown in Fig. 4-3a. Based on the distributions of different circumferential hydrodynamic pressure modes, the total base shear will result from the $\cos \theta$ pressure mode only shown in Fig. 4-3b where θ is the circumferential angle.
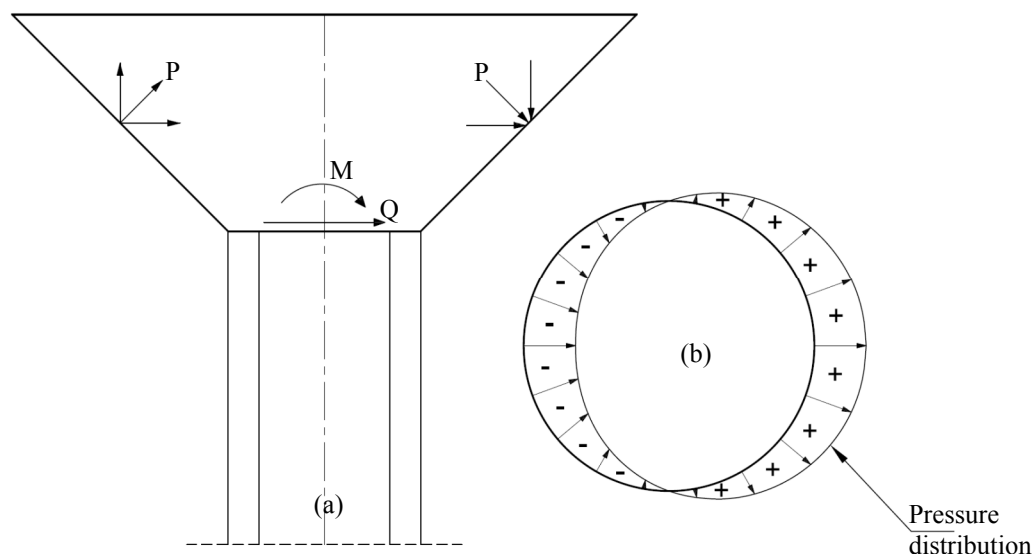
Fig. 4-3 Effect of horizontal acceleration on a conical tank

As discussed earlier, the idea of a mechanical model is to represent the contained fluid inside a conical tank as a set of lumped masses and springs in order to obtain the same resulting base shear and overturning moment obtained by dynamic analysis when subjected to the same earthquake event. The mechanical model derived by El Damatty and Sweedan (2006) shown in Fig. 4-4 is used in this study to obtain the seismic demand. The masses m_r, m_f, and m_s represent the impulsive mass component, the mass reflecting the effect of

walls' flexibility, and the convective mass component, respectively. The total maximum base shear Q_{max} is given by

$$Q_{max}=\sqrt{Q_{Ir}^2+Q_{If}^2+Q_S^2} \qquad\qquad [4\text{-}1]$$

$$Q_{Ir}=[(m_r-m_f)+m_{o\text{-}sh}]\ddot{G}_{max} \qquad\qquad [4\text{-}2]$$

$$Q_{If}=[m_f+m_{e\text{-}sh}]S_{a\text{-}sys} \qquad\qquad [4\text{-}3]$$

$$Q_S=m_s\,S_{a\text{-}s} \qquad\qquad [4\text{-}4]$$

where Q_{Ir} and Q_{If} reflect the contribution of the rigid and flexible components of the impulsive pressure and Q_S reflects the sloshing contribution. The masses m_{o-sh} and m_{e-sh} represent the portion of the walls' mass associated with the rigid and flexible vibration modes, respectively. The acceleration $\ddot{G}_{max}$ is the maximum ground acceleration for the earthquake excitation also known as the peak ground acceleration PGA while S_{a-sys} and S_{a-s} represent the spectral accelerations corresponding to the natural frequencies of the liquid-shell system and the first sloshing mode, respectively.
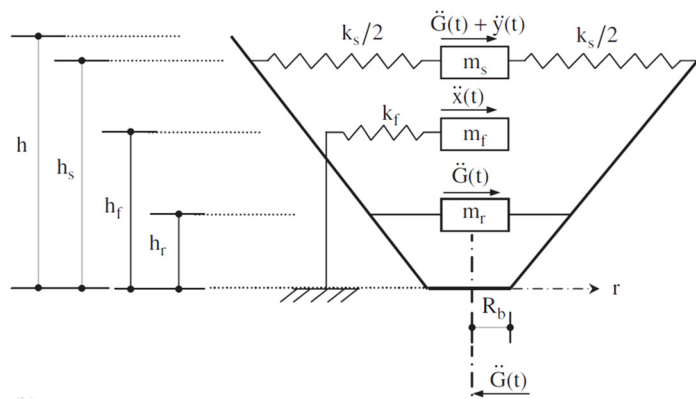
Fig. 4-4 Equivalent mechanical model for conical tanks subjected to horizontal excitation, (El Damatty and Sweedan (2006))

4.2.2   Vertical Excitation

For conical tanks subjected to a vertical excitation, a resulting total normal force N will act just above the tank base as shown in Fig. 4-5a. Due to the axisymmetric distribution of the

resulting hydrodynamic pressure as shown in Fig. 4-5b, neither a total base shear nor an overturning moment will result due to the vertical excitation.
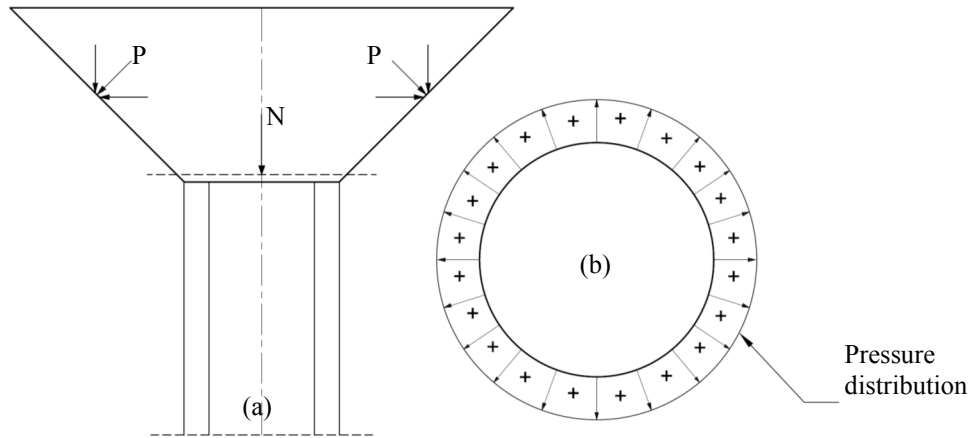
Fig. 4-5 Effect of vertical acceleration on a conical tank

Sweedan and El Damatty (2005) introduced a two masses mechanical model for steel conical tanks subjected to vertical ground excitation as shown in Fig. 4-6. The two masses are the rigid fluid mass, and the mass reflecting the effect of the flexibility of the tank's wall. The mass $m_{o\text{-}w}$ is rigidly attached to the supporting tower and vibrates with the ground acceleration, while the mass $m_{f\text{-}w}$ is a flexible mass that vibrates with the fundamental frequency of the tank-liquid system. The masses, and natural frequencies were presented in charts based on the tank dimensions. The total vertical force N_v is given by

$$N_v=\sqrt{N_1^2+N_2^2}$$ [4-5]

$$N_1=(m_{o\text{-}w}-m_{o\text{-}s})\ddot{G}_{vmax}$$ [4-6]

$$N_2=(m_{f\text{-}w}+m_{f\text{-}s})S_{a\text{-}sys}$$ [4-7]

where N_1 and N_2 reflect the contribution of the rigid and flexible components of the hydrodyanmic pressure, respectively. The masses $m_{o\text{-}s}$ and $m_{f\text{-}s}$ represent the portion of the tank walls' mass associated with the rigid and flexible vibration modes, respectively. The acceleration $\ddot{G}_{vmax}$ is the maximum vertical ground acceleration for the earthquake excitation i.e., PGA while $S_{a\text{-}sys}$ is the spectral acceleration corresponding to the natural frequency of the liquid-shell system.
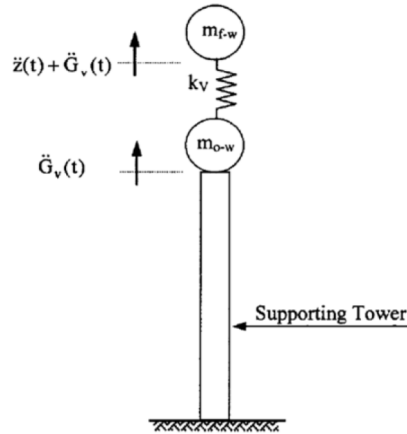
Fig. 4-6 Equivalent mechanical model for conical tanks subjected to vertical excitation Sweedan and El Damatty (2005)

4.3 Geometric Imperfections

The steel vessels of conical tanks are normally constructed from curved panels welded together along circumferential and longitudinal directions. As a result, geometric imperfections will exist and play an important role in defining the capacity of steel liquid conical tanks and might lead to failure if not estimated correctly as for the case of the collapsed steel conical water tower in Fredericton (Vandepitte (1999)). A commonly used model for simulating the geometric imperfections $W(s)$, Fig. 4-7, is described as:

$$W(s) = w_0 \sin\left(\frac{2\pi s}{L_I}\right) \cos(n\theta) \qquad\qquad [4\text{-}8]$$

where w_0 is the imperfection amplitude, L_I is the imperfection wavelength, s is a coordinate measured along the generator of the vessel, and n is an integer defining the circumferential wavelength of the imperfection shape. According to Vandepitte et al. (1982), a conical tank with the ratio w_0/L_I less than 0.004 is considered a good cone while a conical tank with the ratio w_0/L_I ranging from 0.004 to 0.01 is considered a poor cone.

For the case of steel conical tanks under the effect of hydrostatic pressure only, (Vandepitte et al., 1982) used experimental results to get an expression for the critical buckling wave length L_{CR} which was found to be independent on the height of the conical tank, while El Damatty et al. (1997a) have shown that an axisymmetric distribution, i.e., n=0, leads to

minimum buckling capacity due to the axisymettric nature of hydrostatic pressure. An expression for the critical buckling wave length was derived in Chapter 2. This critical buckling wave length leads to the minimum tank capacity for the case of combined hydrostatic and hydrodynamic pressure due to horizontal excitation using non-linear static analysis. The critical buckling wave length was given by

$$L_{cr} = 4.03 \sqrt{R_b\, t_w\, / \cos \theta_v} \qquad\qquad\qquad\qquad [4\text{-}9]$$

where R_b is the tank bottom radius, t is the wall thickness, and θ_v is the angle of inclination of the tank walls with the vertical.
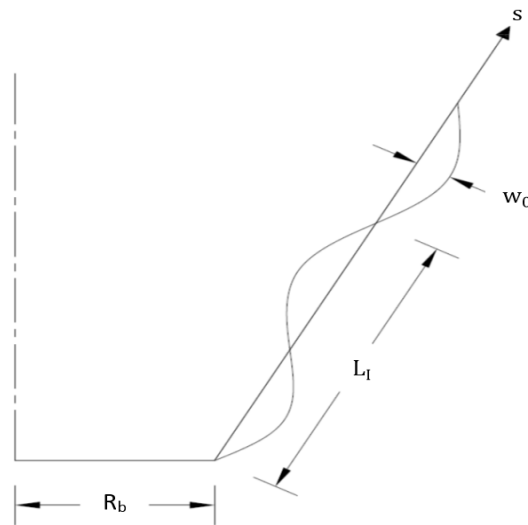
Fig. 4-7 Assumed imperfection shape along the generator of tank

The effect of variation of the tank height on the critical imperfection wave length was found to be insignificant as noticed by Vandepitte et al. (1982). Similar procedure was followed in order to estimate the critical imperfection wave length for the case of combined hydrostatic and hydrodynamic pressure due to vertical excitation. It was found that the same expression, i.e., Eq. 4-9, will lead to the minimum buckling capacity for this case as the buckling waves initiate during the initial hydrostatic pressure phase similar to the case of horizontal excitation. Two levels of geometric imperfections will be considered in this study: (1) $w_0 = 0.004 L_{cr}$ to represent the limit for good tank, (2) $w_0 = 0.01 L_{cr}$ to represent the limit for poor tanks.

4.4 Steel Conical Tank Capacities

4.4.1   Horizontal Excitation

The capacity for steel conical tanks with practical dimensions using non-linear static analysis when subjected to hydrodynamic pressure due to horizontal excitation was estimated in Chapter 2. A linear pressure pattern corresponding to the hydrostatic pressure was applied and increased incrementally till its actual value and then a pressure pattern corresponding to the hydrodynamic pressure distribution was increased incrementally, while maintaining the hydrostatic pressure constant, till failure occurs. The capacity of a steel conical tank was represented by the base shear value just before yielding or buckling for the tank vessel. Regarding the governing failure mode, the general trend was that the probability for yielding failure to occur is higher when the angle θ_v is increased. In addition, the increase in the tank wall thickness was found to make the elastic buckling failure, i.e., tank shell suffers instability before yielding, more probable.

A group of 75 tanks of practical dimensions were chosen with bottom radius R_b ranging from 4.0m to 6.0m, tank height h from 5.0m to 9.0m, and $\theta_v = 30^o$, 45°, 60°. The tanks were preliminary designed under hydrostatic pressure only based on the simplified method proposed by Sweedan and El Damatty (2009) assuming good tanks regarding the level of geometric imperfections. The tanks were analyzed with three levels of geometric imperfections; perfect, i.e., no imperfections, good, i.e., $w_0/L_I=0.004$, and poor, i.e., $w_0/L_I=0.01$. The same procedure was done for both impulsive and sloshing components of the hydrodynamic pressure. The base shear capacity for impulsive component V_I and sloshing component V_S were represented in the form of the unit-less parameter VR_b/Wh where W is the weight of the contained fluid. The effect of wall thickness was included through a family of curves represented in the form of multiplier of t_s which is the thickness obtained by the simplified hydrostatic design method. The variation of the normalized base shear V_IR_b/Wh and V_SR_b/Wh with the ratio h/R_b for different levels of imperfection and θ_v were presented in the form of charts (Appendix A).

4.4.2   Vertical Excitation

The total normal force capacity using non-linear static analyses was estimated in Chapter 3 following the same procedure described for the horizontal component. The same group of tanks described for the case of horizontal excitation were used for this study. The tanks were analyzed with three levels of geometric imperfections; perfect, good, and poor. The steel conical tank capacity was expressed in terms of the total vertical force N corresponding to the first yielding of the tank vessel. The total normal force capacity for impulsive component N was represented in the form of the unit-less parameter Nh/W_cR_b where W_c is the weight of the cylindrical volume of the contained fluid.

For the group of steel conical tanks considered, the tank shell was found to yield before instability takes place similar to what was noted by El Damatty et al. (1997a) for the case of steel conical tanks under hydrostatic pressure which has an axisymmetric distribution similar to the case of the hydrodynamic pressure due to vertical excitations. The effect of thickness change was included through a family of curves for different thicknesses. The variation of the normalized total vertical force Nh/W_cR_b with the ratio h/R_b for different levels of imperfection and θ_v were represented in the form of charts (Appendix B).

4.5   Proposed Design Procedure

The main goal of the current study is to propose a design procedure for steel liquid conical tanks subjected to both horizontal and vertical components of ground excitations taking into account the effect of geometric imperfections. The idea is to use an interaction formula which if satisfied means a conical tank is considered safe against both yielding and buckling of the tank shell when subjected to the ground excitation under consideration. The interaction formula is a function of the conical tank capacities and the seismic demands.

The proposed interaction formula is in the form of

$$\left(\frac{V_{ID}}{V_{IC}}\right)^n + \left(\frac{V_{SD}}{V_{SC}}\right)^n + \left(\frac{N_D}{N_C}\right)^n \leq 1.0 \qquad [4\text{-}10]$$

where V_{IC} and V_{SC} are the base shear capacities for a steel conical tank subjected to a horizontal excitation corresponding to impulsive and sloshing hydrodynamic pressure

components, respectively. They can be obtained as per Section 4.4.1. N_D is the total vertical force capacity for a steel conical tank subjected to a vertical excitation which can be obtained as per Section 4.4.2. V_{ID} and V_{SD} represent the base shear demands for a steel conical tank subjected to a horizontal excitation corresponding to the impulsive and sloshing hydrodynamic pressure components, respectively. They can be obtained using the equivalent mechanical model for horizontal excitations developed by El Damatty and Sweedan (2006). N_D is the total vertical force demand for a steel conical tank subjected to a vertical excitation which can be obtained from the equivalent mechanical model developed by Sweedan and El Damatty (2005). Finally, n is the power order of the combination which will be determined in the following section based on time history analysis.

4.6   Time-History Analysis

Although time history analysis is the most realistic and accurate when it comes to simulating structures undergoing ground excitations, it is computationally expensive and therefore not practical to be used by design engineers on a daily basis. Moreover, for the case of liquid storage tanks, time history analysis is more complicated due to the presence of the contained fluid where fluid-structure interaction has to be accounted for in order to capture the actual behaviour for such kind of structures. In this section, non-linear time history analyses are carried out for the same set of 75 steel conical tanks discussed in Section 4.4 with three levels of geometric imperfections i.e., perfect, good, and poor in order to evaluate the best estimate for the power n found in Eq. 4-10 and validate the proposed design approach.

A coupled shell element-boundary element formulation is used where a fluid-added mass matrix is obtained corresponding to the tank vessel degrees of freedom (El Damatty et al. (1997c)). This fluid-added matrix is added to the structure mass matrix and then incorporated in dynamic or free vibration analysis. This technique is considered computationally efficient compared to modelling the contained fluid using finite elements as the total number of degrees of freedom are considerably reduced.

The long-period sloshing component of the hydrodynamic pressure is included in the analysis assuming the tank walls to be rigid i.e., ignoring the fluid-structure interaction (El Damatty et al., (2000)). This assumption was found to be acceptable as noted by Haroun (1980) for cylindrical tanks and also due to the fact of relatively small sloshing hydrodynamic pressure compared to the impulsive pressure. During the time-history analysis, hydrostatic pressure is applied prior to the application of the ground accelerations at each time increment.

The time history analyses are conducted based on 11 natural earthquake records scaled to different seismic zones in Canada. The selection of the used ground motions is based on the deaggregation of seismic hazard procedure proposed by Halchuk and Adams (2004) for different locations in Canada where the seismic hazard is deaggregated in terms of the focal depth and the magnitude of the ground motion for different spectral acceleration values. Three Canadian seismic zones are considered in the current study which are Toronto, Montreal, and Vancouver. Using the deaggregation parameters for the three seismic zones considered, a search process is conducted using the PEER strong ground motions database in order to select the natural ground motion records. The selected records corresponding to different seismic zones are summarized in table 4-1.

After the selection of the ground motion records, they are scaled in order to match the target seismic zone. The scaling procedure is based on matching the spectral acceleration of the record under consideration with the spectral acceleration of the response spectrum obtained from NBCC (2010) at the natural frequency of the first impulsive vibration mode. This scaling is applied separately for each of the horizontal and vertical components of the ground motion record and is done for each tank separately as each conical tank has its own natural frequency. A schematic for the scaling procedure is shown in Fig. 4-8.

Table 4-1 Selected ground excitation records corresponding to different seismic zones

Seismic Zone	Record ID*	Record Name	Date	Duration (sec)
Toronto	557	Chalfant Valley-02	1986	20
	703	Whittier Narrows-01	1987	20
	1680	Northridge-04	1994	20
	2227	Chi-Chi, Taiwan-02	1999	30
Montreal	935	Big Bear-01	1992	25
	3510	Chi-Chi, Taiwan-06	1999	35
	947	Northridge-01	1994	20
	81	San Fernando	1971	20
Vancouver	323	Big Bear-01	1983	25
	927	Chi-Chi, Taiwan-05	1992	20
	3032	Coalinga-01	1999	30

* Record ID from http://peer.berkeley.edu/peer_ground_motion_database

In order to determine the natural frequencies for the impulsive vibration modes for both horizontal and vertical vibrations, free vibration analyses are performed using the coupled finite-boundary element code developed by El Damatty et al. (1997b). The derived fluid-added matrix is incorporated in the Eigen-value problem which results in the vibration mode shapes and natural frequencies. The damping was incorporated in the time history analyses based on the Rayleigh damping where it is represented as a linear combination of the mass and stiffness of the structure. A value of 2% damping is used for the impulsive hydrodynamic pressure component, while a value of 0.5% is used for the sloshing component.
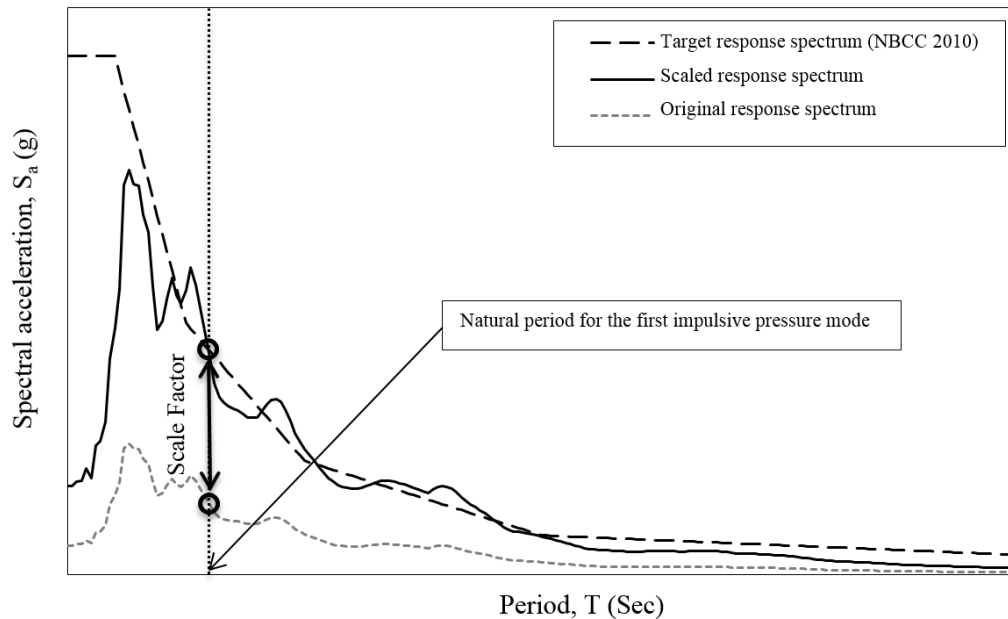
Fig. 4-8 Schematic for the scaling of the ground motion spectrum to match the NBCC 2010 spectrum

Three-dimensional numerical models are developed in this study for the steel conical tanks using the finite element method to carry on the time history analysis. The numerical models are based on a consistent subparametric triangular shell element shown in Fig. 4-9a that was developed by Koizey and Mirza (1997). Such a consistent subparametric formulation eliminated the spurious shear modes and locking phenomenon observed in isoparametric shell elements when used in modeling thin shell structures. El Damatty et al. (1997d) extended the formulation of this shell element to include both the large deformation geometric nonlinear effect in addition to material nonlinearity for steel. The geometric imperfection is incorporated in the finite element model in the form of initial strains prior to load application at each time step.
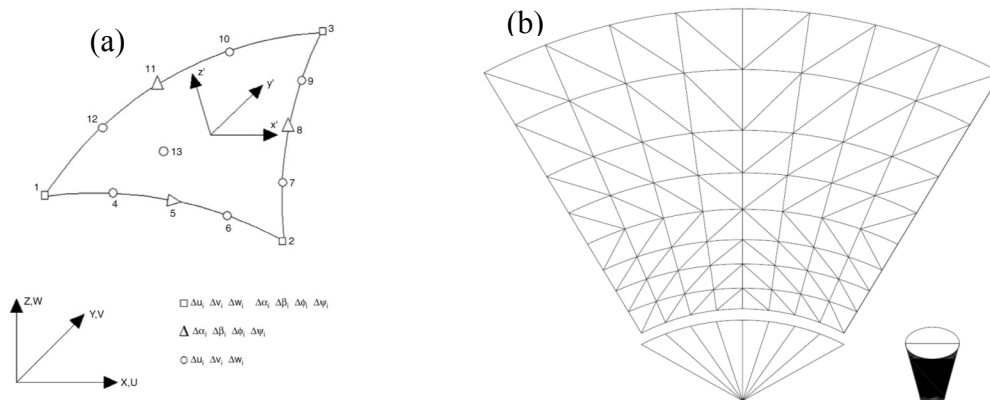
Fig. 4-9 (a) Coordinates and degrees of freedom for the consistent shell element (Koizey and Mirza (1997)), (b) Finite element mesh for half cone

Due to symmetry about the horizontal axis in both loading and geometry, only half of the cone is modelled and used in the analysis. A mesh of 128 triangular elements is used for the model and is shown in Fig. 4-9b. The length of the elements is not uniform as the mesh is chosen to be finer near the base of the tank due to the stress concentration at this location where buckling is expected to occur. The tanks are assumed to be hinged at the base along the circumference. Finally, the horizontal and vertical degrees of freedom at the tank base level are constrained in order to have the same deformations in order to simulate the rigid concrete slab underneath the tank.

4.7 Results of Time History Analysis

As mentioned in the last section, the set of the steel conical tanks chosen for this study are subjected to the eleven ground motion records summarized in table 1 in the form of horizontal and vertical ground accelerations. For the horizontal component, the output forces acting on the tank base will be in the form of total base shear V and a corresponding overturning moment M as shown in Fig. 4-3, while the vertical component of the ground motion will lead to a total vertical force N as shown in Fig. 4-5. It is worth mentioning that both M and N are calculated at a level just above the tank base as the base itself is not included in the finite element mesh discussed earlier.

The impulsive and sloshing base shear time histories are shown in Fig. 4-10 for one of the steel conical tanks subjected to Chalfant Valley-02 record. Comparing the base shear values for the two components, it can be concluded that the impulsive component is more critical compared to the sloshing one especially for the cases of $\theta_v=30^\circ, 45^\circ$. Contributions to the total base shear and overturning moment from sloshing mode is found to be negligible due to the small spectrum accelerations associated with such low frequency sloshing modes.
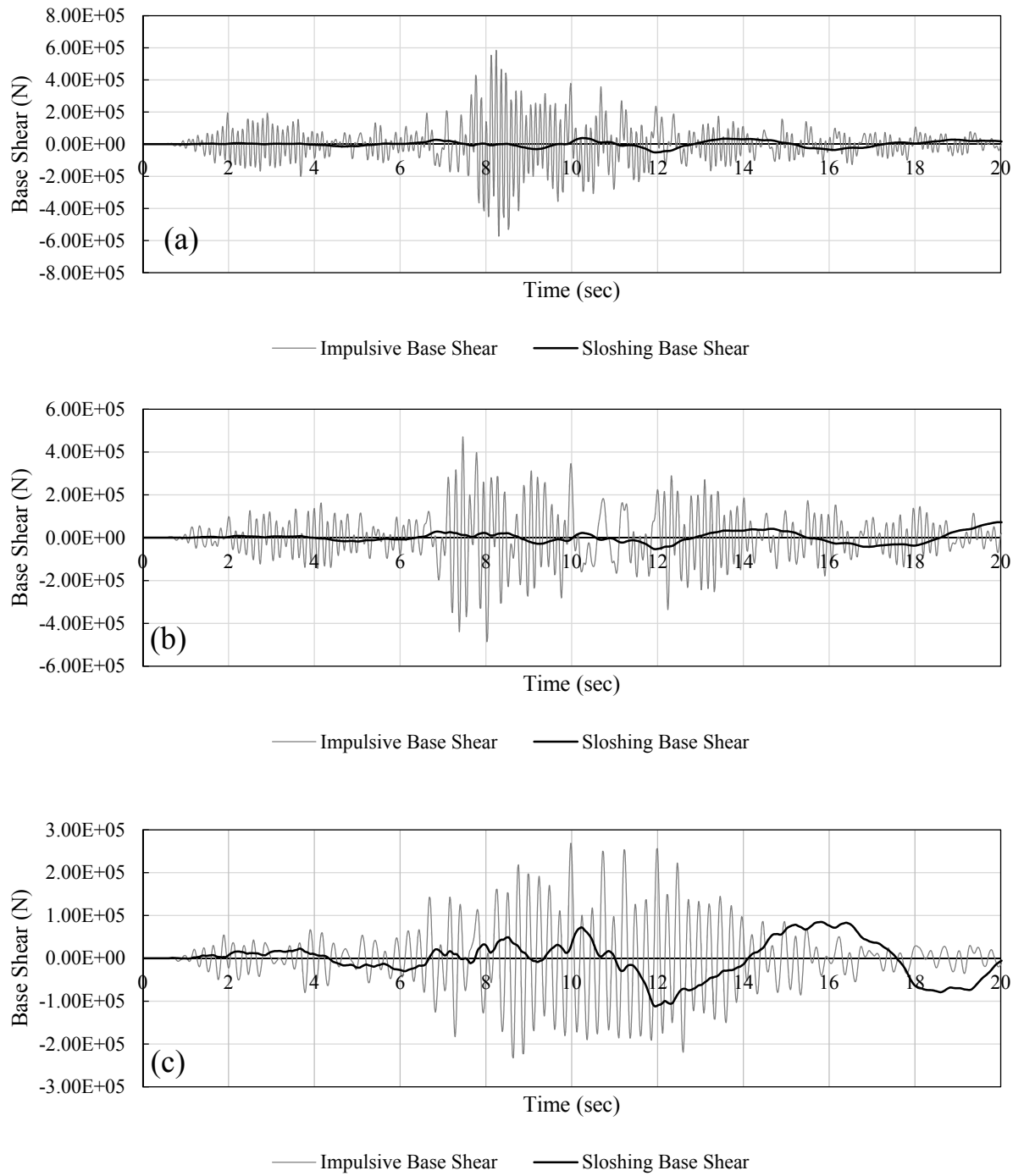
Fig. 4-10 Base shear time history for a steel conical tank (R_b=4m, h=5m) subjected to Chalfant Valley-02; (a) θ_v=30°, (b) θ_v=45°, (c) θ_v=60°

For the effect of the angle of inclination θ_v, the maximum impulsive base shear is reduced as the tank becomes more inclined, while the sloshing base shear is increased for higher θ_v values. This is due to the fact that as the conical tank becomes wider at top, the amount of fluid participating in the sloshing response is higher reducing the amount of fluid participating in the impulsive response. The overturning moment is found to be higher as θ_v is increased despite the lower fluid mass participating in the impulsive response for higher θ_v values. This is due to the longer moment arm for more inclined conical tanks. The same conclusion can be drawn for the total vertical force as conical tanks with higher θ_v values have larger horizontal projection for the inclined wetted surface leading to higher total vertical force.

The hydrodynamic pressure distribution along the height of one of the studied tanks subjected to Northridge-01 ground motion in terms of horizontal impulsive pressure, horizontal sloshing pressure, and vertical impulsive pressure is shown in Fig. 4-11. The plotted pressure distributions are the maximum throughout the excitation duration, i.e., do not occur at the same time. As the total output forces (Q, M, N) discussed earlier are obtained by integrating the pressure distribution over the wetted surface area, the same conclusions can be drawn for the corresponding pressure distribution. The maximum horizontal and vertical impulsive pressure is located in the lower half of the tank height and is shifted upward as the conical tank becomes more inclined, while the maximum sloshing pressure occurs at the liquid free surface. It has to be mentioned that the circumferential distribution of the horizontal impulsive and sloshing pressure has a $\cos\theta$ distribution, while the vertical impulsive pressure is axisymmetric.
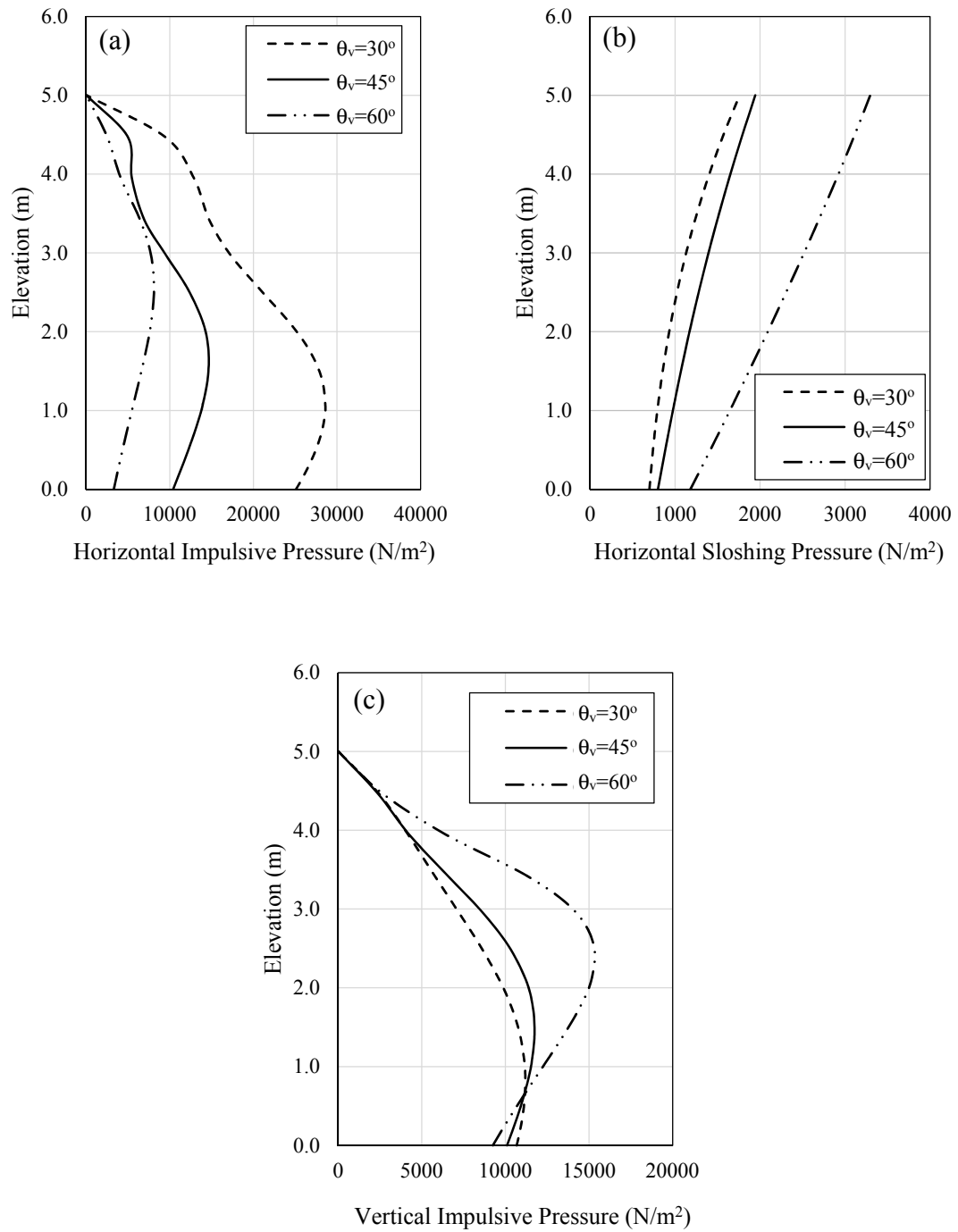
Fig. 4-11 Hydrodynamic pressure distribution for a steel conical tank (R_b=4m, h=5m) subjected to Northridge-01; (a) Horizontal Impulsive Pressure, (b) Horizontal Sloshing Pressure, and (c) Vertical Impulsive Pressure

Figure 4-12 shows the deformed shape for one of the conical tanks subjected to Northridge-01 ground motion at two stages: (1) Just after the application of the hydrostatic pressure, (2) At maximum displacement value throughout the duration of the ground motion. The deformed shape is plotted in terms of horizontal, vertical, and transversal displacement. Due to the stress concentration near the base of the steel conical tank, buckling waves starts to initiate just after the hydrostatic pressure stage and increase with the application of the hydrodynamic pressure. Such deformation pattern is commonly known as elephant-foot buckling and was noted in several liquid storage tanks after some earthquake events.
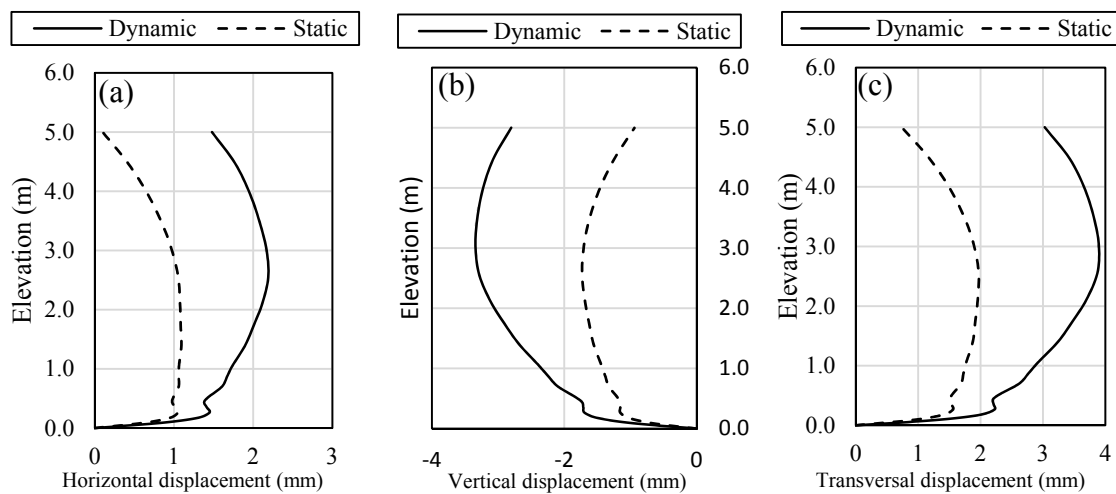
Fig. 4-12 Displaced shape for steel conical tank (R_b=4m, h=5m, θ_v=45°) subjected to Northridge-01; (a) Horizontal displacement, (b) Vertical displacement, and (c) Transversal displacement

As discussed in Section 4.4, the finite element model used in this study takes into consideration both geometric and material nonlinearities. As a result it is capable of capturing any localized buckling whether occurring prior to yielding of the tank shell i.e., elastic buckling or after yielding i.e., inelastic buckling. The conical tanks are preliminary designed under hydrostatic pressure only in order to obtain the wall thickness (t_s) based on the simplified method proposed by Sweedan and El Damatty (2009) assuming good tanks regarding the level of geometric imperfections.

For the set of steel conical tanks considered in this study, one of three final states can take place:

(1) *Safe Elastic*, if the tank survived the scaled ground excitation including horizontal and vertical components without yielding of the tank shell.

(2) *Safe Plastic*, if the tank survived the scaled ground excitation including horizontal and vertical components with yielding of the tank shell taking place.

(3) *Unsafe Plastic,* if the tank failed under the scaled ground excitation including horizontal and vertical components due to buckling instability which most probably will happen near the tank base due to the stress concentration resulting from inclination of the tank walls in addition to the confinement at the base supports.

Time history analyses for the perfect steel conical tanks i.e., no geometric imperfections, shows that all the tanks behaved elastically and survived ground motions corresponding to the three considered seismic zones. The same observation is found for the case of the steel conical tanks with good level of geometric imperfections corresponding to the seismic zones of Toronto and Montreal. For Vancouver seismic zone, the majority of the good conical tanks survived the three ground excitations either elastically or inelastically with a thickness factor ranging from 1.2-1.4. The thickness factor is the ratio between the thickness required for a steel conical tank to remain elastic and survive the ground excitation t_{req} under consideration to the initial thickness t_s.

Regarding tanks with poor level of imperfections, over 90% of the steel conical tanks designed to resist hydrostatic pressure with $\theta_v=30^o$, 45° survived the ground excitations corresponding to Toronto seismic zone elastically, while the remaining tanks survived inelastically with a thickness factor of 1.2. For tanks with $\theta_v=60^o$ corresponding to Toronto seismic zone, it is found that the majority of the tanks survived the ground excitations inelastically with some tanks failing due to buckling with a maximum thickness factor of 1.2.

For ground excitations corresponding to Montreal seismic zone, more than 90% of the poor conical tanks designed to resist hydrostatic pressure with $\theta_v=30^o$ did not survive the ground

excitations elastically, while none of the tanks with $\theta_v=45^o$, 60° survived the ground excitations elastically. The maximum thickness factor is 1.4, 1.4, and 1.6 for $\theta_v=30^o$, 45°, 60°, respectively. Finally for ground excitations corresponding to Vancouver seismic zone, all poor conical tanks designed to resist hydrostatic pressure only did not survive the ground excitations elastically with more than 90% of the tanks failing due to buckling with maximum thickness factor of 1.8.

4.8   Proposed Design Approach Validation

In this section, the proposed design approach which is expressed in the form of a design formula is validated by comparing the results obtained from Eq. 4-10 with the results of the non-linear time history analyses performed in the previous section. Starting with the hydrostatic wall thickness t_s, the tank capacities V_{IC}, V_{SC}, and N_C are obtained from the charts found in Appendices A and B based on the tank dimensions and level of geometric imperfections.

On the other hand, seismic demands V_{ID} , V_{SD}, and N_D are obtained using equivalent mechanical models based on the tank dimensions and the ground excitation characteristics. The left hand side of Eq. 4-10 is then computed and the minimum conical tank wall thickness required to satisfy the formula t_{req} is determined.

Regarding the validation using non-linear time history analysis, it is done as follows

1) The time history analysis is performed for the same conical tank including both horizontal and vertical components of the earthquake excitation corresponding to the same seismic zone starting with a tank wall thickness t_s.

2) The analysis is repeated for different wall thicknesses till the conical tank sustain the ground excitation without suffering any buckling or yielding and t_{req} is determined. As there is more than one ground motion corresponding to each seismic zone, the maximum t_{req} to sustain all the ground motions for the same zone is the one recorded.

3) The required thickness obtained based on the proposed design approach i.e., Eq. 4-10 should be greater than or equals to the one obtained from the non-linear time history analysis in order to consider the design approach validated.

The abovementioned procedure including the proposed design approach in addition to the non-linear time history analysis is repeated for each conical tank corresponding to different seismic zones and levels of geometric imperfections.

As mentioned earlier, the power order n of the design formula that is used to combine different pressure components is determined based on the time history analysis results. This is done for each tank by first assuming a value for the power order n and then check the design formula using the required thickness t_{req} obtained by nonlinear time history analysis. Finally, the lowest value for n satisfying the design formula is determined by trial and error and recorded.

In order to make the proposed design approach more practical, a single value for the power order n is chosen for all conical tanks corresponding to each level of geometric imperfections instead of using different values for each tank. By investigating the n values obtained for the steel conical tanks chosen in the current study, a value of n=2 is found to give a required wall thickness greater than or equals to the one obtained by time history analysis for all perfect and good steel conical tanks.

On the other side for poor tanks, the value n=2 is found to give lower values for the required wall thicknesses than those obtained by time history analysis meaning that the proposed formula is not applicable for poor conical tanks when using n=2. By trying different values for the power n, it is found that a value of n=1 is satisfactory for the case of poor steel conical tanks. As a result, a value of n=2 is proposed for perfect and good steel conical tanks, while a value of n=1 is proposed for the case of poor steel conical tanks.

The outcomes of the discussed validation procedure are summarized in Figs. 4-13 to 4-30 found in Appendix C where the ratio (t_{req}/t_s) obtained by the two methods, i.e., the proposed design approach and time history analysis, is plotted for the steel conical tanks located in different seismic zones with different levels of geometric imperfection. The conical tanks are described in the form of Rx-hy where x is the tank bottom radius, while y is the tank height, both in meters. Each plot corresponds to a certain seismic zone for a specific angle of inclination θ_v and level of geometric imperfections which are expressed in the form of (**Seismic zone-Level of imperfections-θ_v).** TOR, MON, and VAN represent Toronto,

Montreal, and Vancouver seismic zones, respectively. PE, GD, and PR represents perfect, good, and poor level of geometric imperfections, respectively. By inspecting the figures, it can be seen that the proposed design formula using n=2 for perfect and good tanks and n=1 for poor tanks will yield a tank wall thickness that is equals to or greater than the required thickness obtained by the time history analysis for all the conical tanks considered in the current study.

It has to be mentioned that the proposed design approach is general and not restricted to be used for steel conical tanks in Canada. The design approach can be used to design steel conical tanks located elsewhere by using the corresponding design spectrum for the seismic zone where the tank is to be located. Scaling the chosen earthquake records to match the Canadian seismic zones' spectra is done just to have a reference and due to the fact that the choice of the earthquake records is based on the deaggregation of seismic hazard procedure (Halchuk and Adams, 2004) for different locations in Canada.

4.9 Summary of the Design Approach

The steps of the proposed design approach for a steel conical tank subjected to horizontal and vertical ground excitations are as follows:

(1) Initially design the conical tank under hydrostatic pressure only assuming good level of geometric imperfection according to Sweedan and El Damatty (2009).

(2) Use the obtained thickness from step (1) t_s to obtain the conical tank capacity corresponding to:

(a) Horizontal impulsive component V_{IC} using charts in Appendix A

(b) Horizontal sloshing component V_{SC} using charts in Appendix A

(c) Vertical impulsive component N_C using charts in Appendix B

(3) For a specific ground excitation, the response spectra for both horizontal and vertical components are used to obtain the seismic demands for this excitation corresponding to:

(a) Horizontal impulsive component V_{ID} using the mechanical model developed by (El Damatty and Sweedan 2006)

(b) Horizontal sloshing component V_{SD} using the mechanical model developed by (El Damatty and Sweedan 2006)

(c) Vertical impulsive component N_D using the mechanical model developed by (Sweedan and El Damatty 2005)

(4) Calculate the left hand side of the formula in Eq. 4-10 with n=1 for poor conical tanks and n=2 for perfect and good conical tanks.

(5) If the left hand side is less than unity, then the used wall thickness is adequate to resist the stresses resulting from the ground motion excitation elastically. On the other hand, if the formula is not satisfied, then the wall thickness has to be increased and the steps (2) till (4) are repeated till Eq. 4-10 is satisfied.

4.10 Conclusions

In this study, a design approach for steel conical liquid tanks subjected to horizontal and vertical components of a ground excitation is proposed. The approach is based on satisfying a design formula which is a function of the steel conical tank capacities obtained by non-linear static analysis and seismic demands obtained using equivalent mechanical models. This design approach takes into consideration the effect of geometric imperfections and the effect of sloshing hydrodynamic pressure. Finally, the design approach is validated using non-linear time history analysis and the steps of the approach are summarized.

Regarding the time history analysis outputs, the total base shear, overturning moment, pressure distribution over the tank walls, and the deformed shape of the tank walls are investigated and the main conclusions were as follows: (1) Impulsive base shear is more critical compared to the sloshing base shear especially for tanks with $\theta_v=30^o$, 45°; (2) The maximum impulsive base shear is reduced as the tank becomes more inclined, while the sloshing base shear is increased for higher θ_v values; (3) The overturning moment is higher for more inclined tanks due to the longer moment arm; (4) The total vertical force is found to be higher for more inclined tanks due to the larger horizontal projection for the inclined wetted surface; (5) The maximum horizontal and vertical impulsive pressure is located in the lower half of the tank height and is shifted upward for more inclined tanks, while the maximum sloshing pressure occurs at the liquid free surface.

For the considered steel conical tanks designed under hydrostatic pressure, the following was noted regarding the final state at the end of the time history analysis: (1) Perfect tanks corresponding to the three seismic zones and good tanks corresponding to Toronto and Montreal seismic zones behaved elastically and survived the corresponding ground motions; (2) Majority of the good tanks corresponding to Vancouver seismic zone survived the ground motions either elastically or inelastically; (3) Over 90% of the poor tanks with $\theta_v=30^o$, 45° corresponding to Toronto seismic zone survived the ground motions elastically, while the remaining tanks survived inelastically; (4) Majority of the poor tanks with $\theta_v=60^o$ corresponding to Toronto seismic zone survived the ground motions inelastically with some tanks failing due to buckling; (5) Over 90% of the poor tanks with $\theta_v=30^o$ corresponding to Montreal seismic zone did not survive the ground motions elastically, while none of the tanks with $\theta_v=45^o$, 60° survived the ground motions elastically; (6) All poor tanks corresponding to Vancouver seismic zone did not survive the ground motions elastically with more than 90% of the tanks failing due to buckling.

4.11 References

(API), A.P.I., 2005. Welded Storage Tanks for Oil Storage. Washington D.C, USA: American Petroleum Institute Standard.

(AWWA), A.W.W.A., 2005. Welded Steel Tanks for Water Storage. Denver, CO, USA.

(ECS), E.C.f.S., 1998. Design provisions for earthquake resistance of structures. Eurocode 8.

El Damatty, A.A. et al., 1997d. Large displacement extension of consistent shell element for static and dynamic analysis. Computers and Structures, 62(6), pp.943-60.

El Damatty, A.A. et al., 1999. Simple Design Procedure For Liquid-Filled Steel Conical Tanks" Journal of structural engineering. Journal of structural engineering, 125(8), pp.879-90.

El Damatty, A.A. et al., 1997a. Stability of Imperfect Conical Tanks under Hydrostatic Loading. Journal of Structural Engineering, 123(6), pp.703-12.

El Damatty, A.A. et al., 1997a. Stability of Imperfect Conical Tanks under Hydrostatic Loading. Journal of Structural Engineering, 123(6), pp.703-12.

El Damatty, A.A. et al., 2000. The sloshing response of conical tanks. In World Conference of Earthquake Engineering. New Zealand, 2000.

El Damatty, A.A. et al., 1997c. Stability of elevated liquid-filled conical tanks under seismic loading, Part II-Applications. Earthquake Engng. Struct. Dyn., 26, pp.1209-29.

El Damatty, A.A. et al., 1997b. Stability of elevated liquid-filled conical tanks under seismic loading, Part I-Theory. Earthquake Engng. Struct. Dyn., 26, pp.1191-208.

El Damatty, A.A. and Sweedan, A.M., 2006. Equivalent mechanical analog for dynamic analysis of pure conical tanks. Thin-Walled structures, 44, pp.429-40.

Halchuk, K.S. and Adams, J., 2004. Deaggregation of Seismic Hazard for Selected Canadian Cities. In 13th World Conference on Earthquake Engineering. Vancouver, B.C., Canada, 2004.

Haroun, M.A., 1980. Dynamic analyses of liquid storage tanks. Pasadena, CA: California Institute of Technology.

Haroun, M.A. and Abou-Izzeddine, W., 1992. Parametric Study of Seismic Soil-Tank Interaction. ii: Vertical Excitation. Journal of Structural Engineering, 118(3), pp.798-812.

Haroun, M.A. and Housner, G.W., 1981. Seismic design of liquid storage tanks. Journal of the Technical Councils, 107(TC1), pp.191-207.

Haroun, M.A. and Housner, G.W., 1982. Dynamic Characteristics of Liquid Storage Tanks. Journal of the Engineering Mechanics Division, 108(5), pp.783-800.

Haroun, M.A. and Tayel, M.A., 1985a. Axisymmetrical vibrations of tanks—Numerical. J. Eng. Mech., 111(3), pp.329-45.

Housner, G.W., 1957. Dynamic Pressures on Accelerated Fluid Containers. Bulletin Seism. Soc. America, 47(1), pp.15-35.

Housner, G.W., 1963. The Dynamic Behavior of Water Tanks. Bulletin Seism. Soc. America, 53(1), pp.381-87.

Jacobsen, L.S., 1949. Impulsive Hydrodynamics of Fluid inside a Cylindrical Tank and of a Fluid Surrounding a Cylindrical Pier. Bulletin Seism. Soc. America, 39, pp.189-204.

Jolie, M. et al., 2013. Assessment of current design procedures for conical tanks under seismic loading. Can. J. Civ. Eng., 40, pp.1151-63.

Koizey, B. and Mirza, F.A., 1997. Consistent thick shell element. Computer & Structures, 65(12), pp.531-41.

Marchaj, T.J., 1979. Importance of Vertical Acceleration in the Design of Liquid Containing Tanks. In 2nd U.S. National Conference on Earthquake Engineering. Stanford, CA, 1979.

NBCC, 2010. National Building Code of Canada. Ottawa, ON, Canada: National Research Council of Canada.

Sweedan, A.M., 2009. Equivalent mechanical model for seismic forces in combined tanks subjected to vertical earthquake excitation. Thin-Walled structures, 47, pp.942-52.

Sweedan, A.M. and El Damatty, A.A., 2005. Equivalent Models of Pure Conical Tanks under Vertical Ground Excitation. Journal of Structural Engineering, ASCE, 131(5), pp.725-33.

Sweedan, A.M. and El Damatty, A.A., 2009. Simplified procedure for design of liquid-storage combined conical tanks. Thin-Walled structures, 47, pp.750-59.

Vandepitte, D., 1999. Confrontation of shell buckling research results with the collapse of a steel water tower. Journal of Constructional Steel Research, 49, pp.303-14.

Vandepitte, D. et al., 1982. Experimental investigation of hydrostatically loaded conical shells and practical evaluation of the buckling load. In Proc. State of the Art Colloquium. Universitat Stuttgart, Germany, 1982.

Veletsos, A.S., 1974. Seismic Effects in Flexible Liquid Storage Tanks. In International Association for Earthquake Engineering. Fifth World Conference. Rome, Italy, 1974.

Veletsos, A.S. and Kumar, A., 1984. Dynamic response of vertically excited liquid storage tanks. In 8th World Conf. on Earthquake Engineering. San Francisco, CA, 1984.

Veletsos, A.S. and Tang, Y., 1986. Dynamics of vertically excited liquid storage tanks. J. Struct. Eng., 112(6), pp.1228-46.

Virella, J.C. et al., 2006. Dynamic buckling of anchored steel tanks subjected to horizontal earthquake excitation. Journal of Constructional Steel Research, 62, pp.521-31.

Virella, J.C. et al., 2008. A Static Nonlinear Procedure for the Evaluation of the Elastic Buckling of Anchored Steel Tanks Due to Earthquakes. Journal of Earthquake Engineering, 12, pp.999-1022.

Appendix C

Fig. 4-13 Required thickness relative to t_s for the cases TOR-PE-30, TOR-PE-45, TOR-PE-60, TOR-GD-30, TOR-GD-45, TOR-GD-60, MON-PE-30, MON-PE-45, MON-PE-60, MON-GD-30
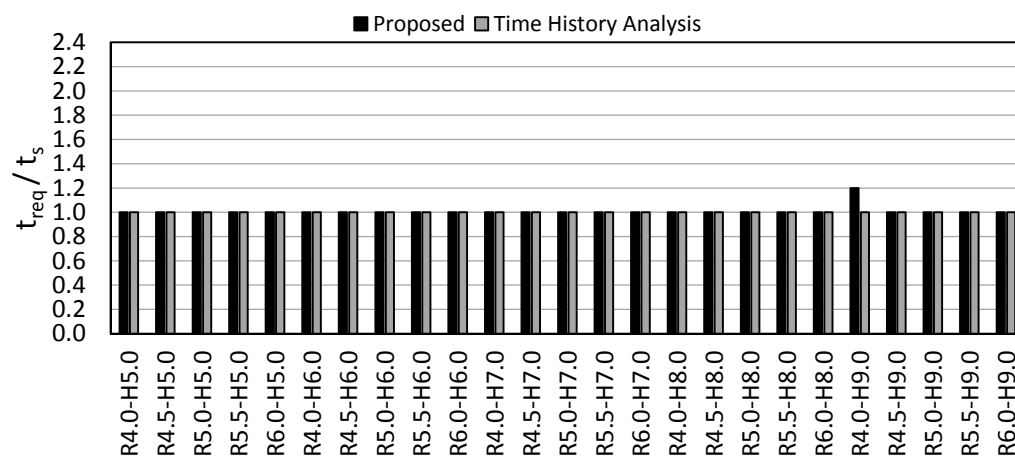
Fig. 4-14 Required thickness relative to t_s for the case TOR-PR-30
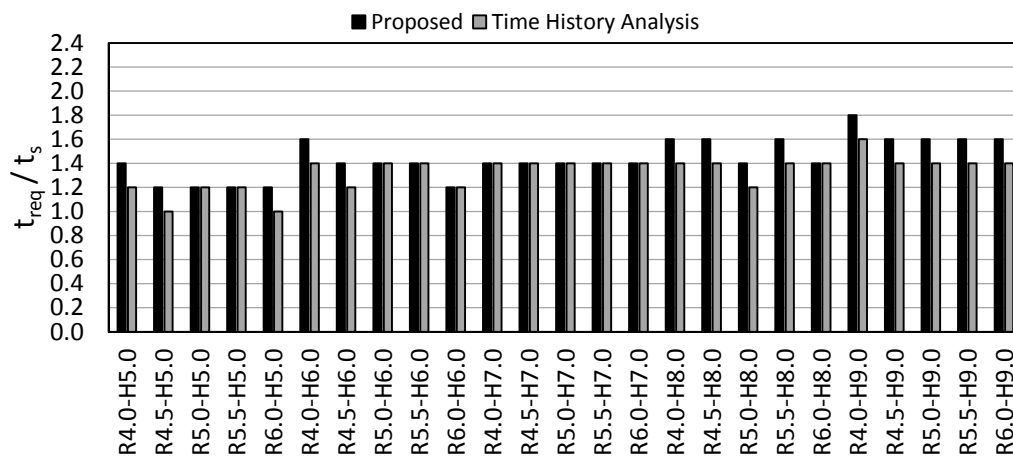
Fig. 4-15 Required thickness relative to t_s for the case MON-PR-30
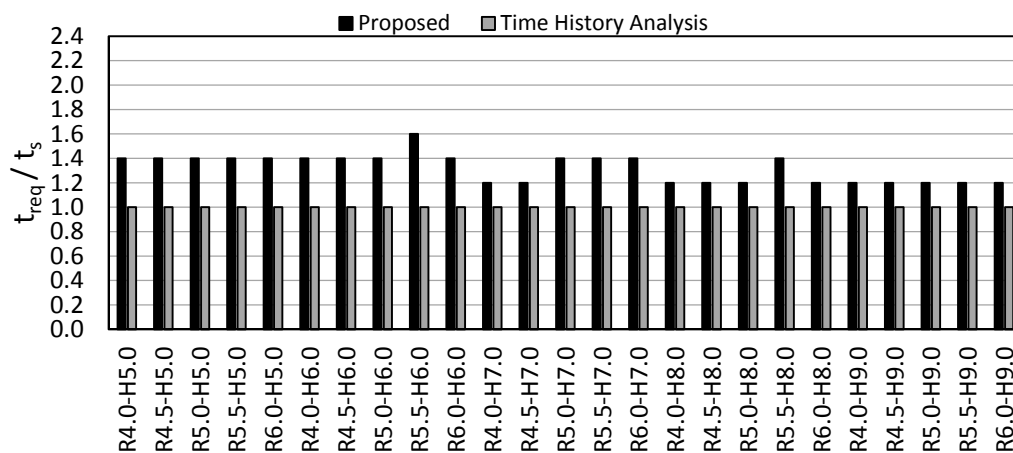
Fig. 4-16 Required thickness relative to t_s for the case VAN-PE-30
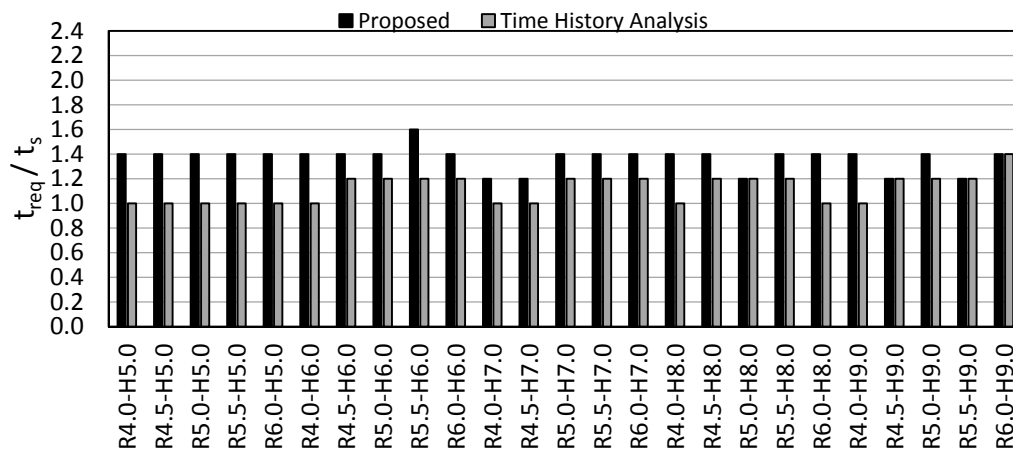
Fig. 4-17 Required thickness relative to t_s for the case VAN-GD-30
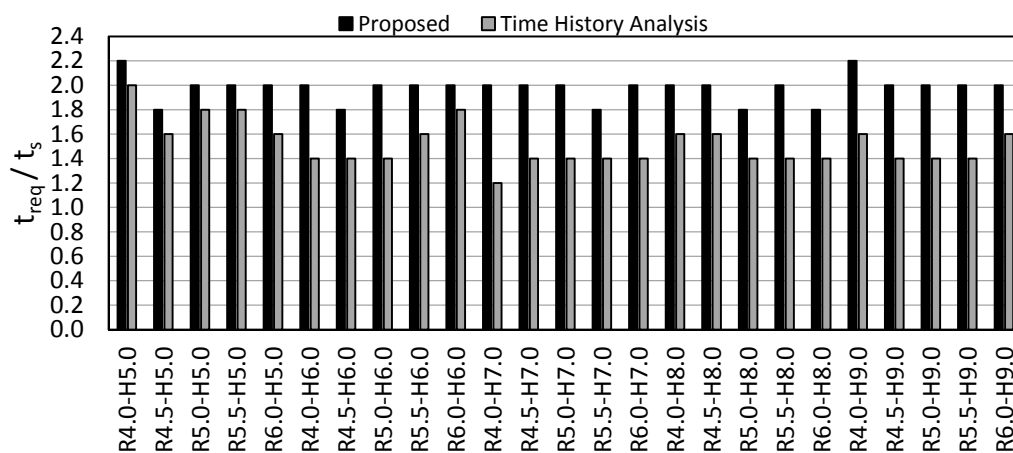
Fig. 4-18 Required thickness relative to t_s for the case VAN-PR-30
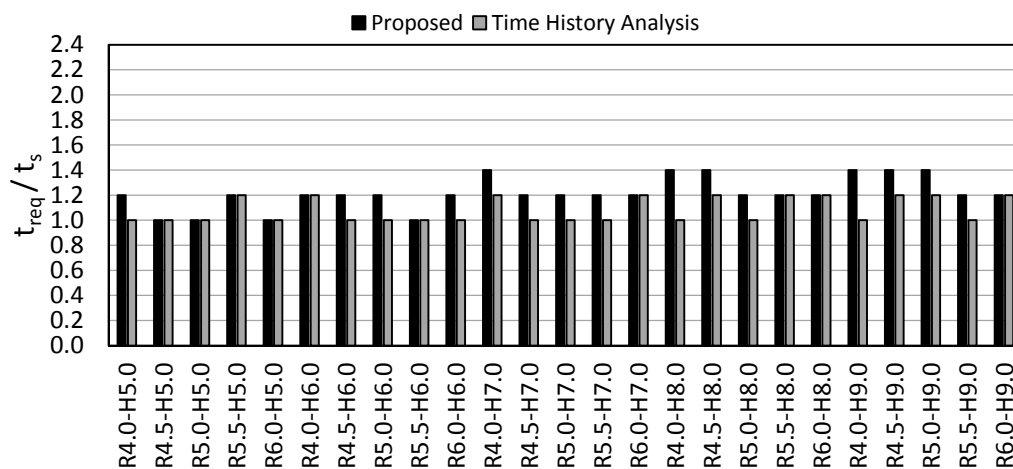
Fig. 4-19 Required thickness relative to t_s for the case TOR-PR-45
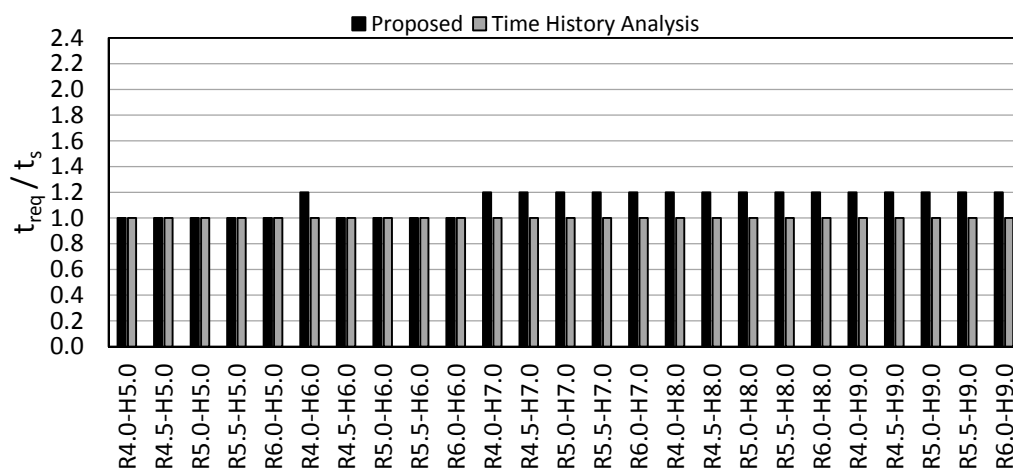
Fig. 4-20 Required thickness relative to t_s for the case MON-GD-45
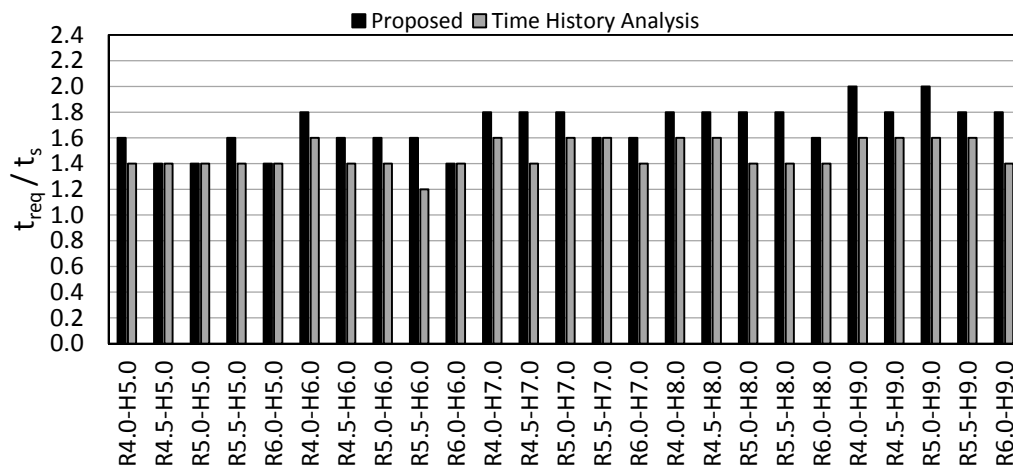
Fig. 4-21 Required thickness relative to t_s for the case MON-PR-45
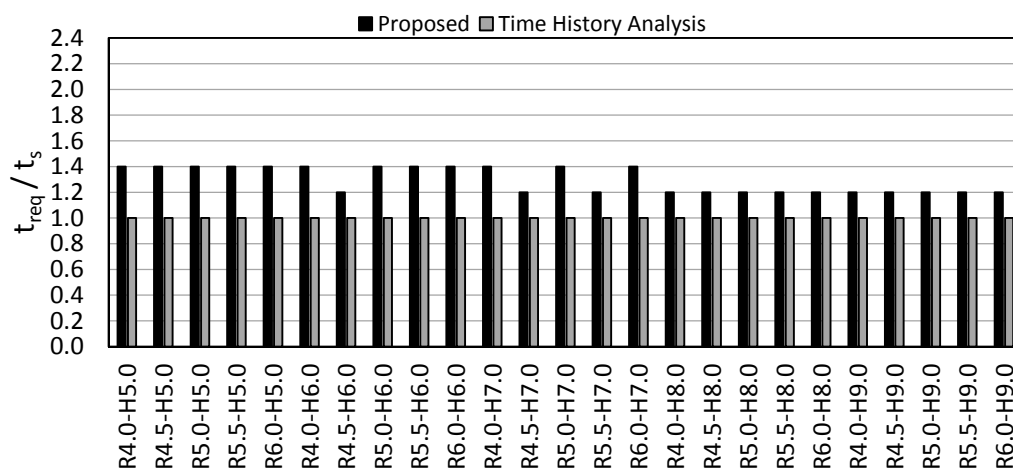
Fig. 4-22 Required thickness relative to t_s for the case VAN-PE-45

137
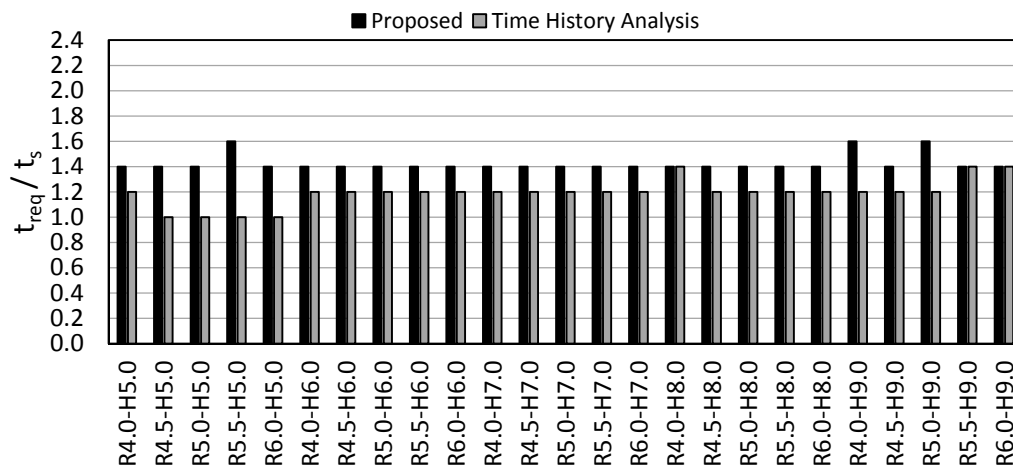
Fig. 4-23 Required thickness relative to t_s for the case VAN-GD-45
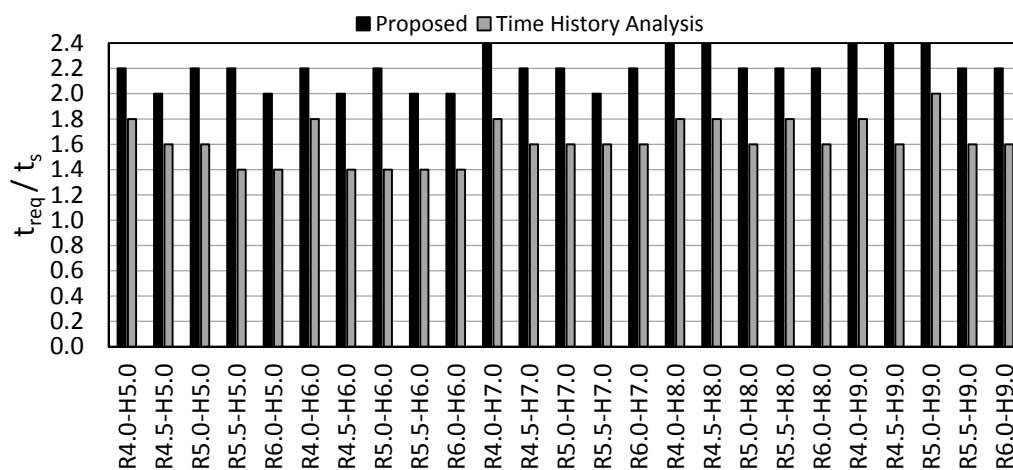
Fig. 4-24 Required thickness relative to t_s for the case VAN-PR-45
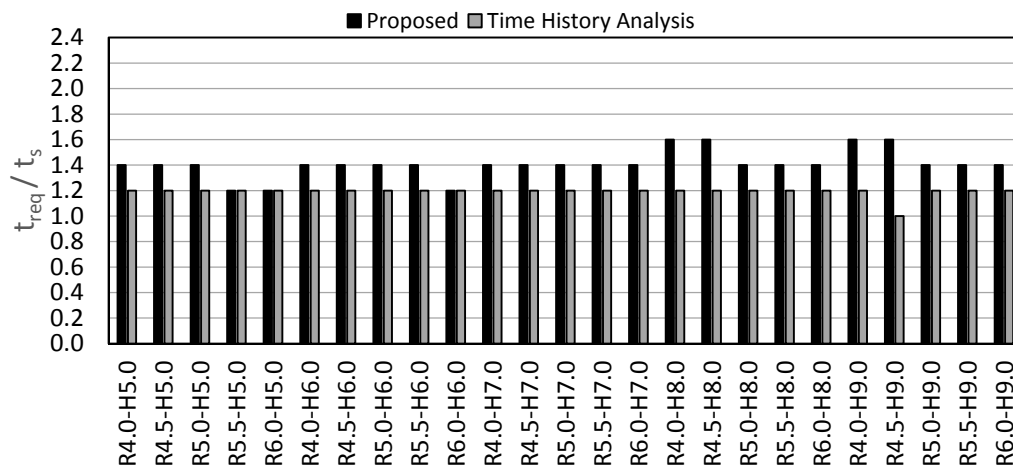
Fig. 4-25 Required thickness relative to t_s for the case TOR-PR-60
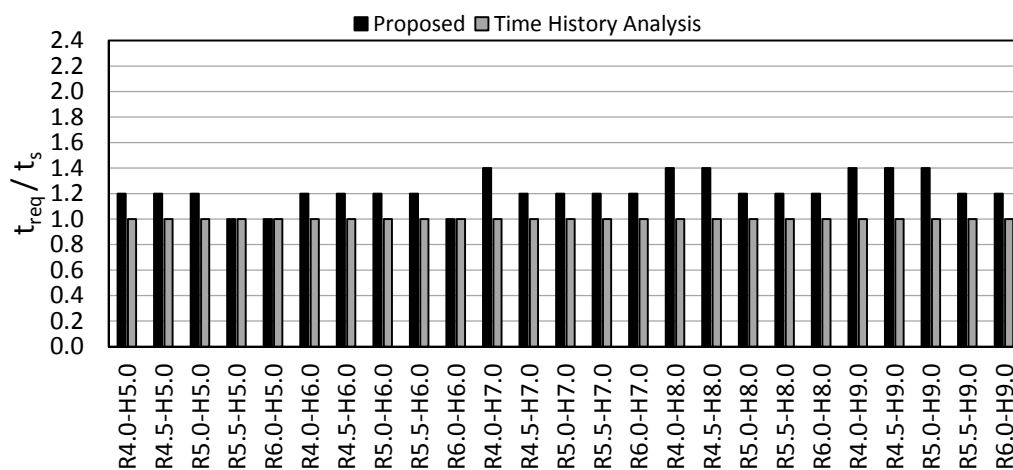
Fig. 4-26 Required thickness relative to t_s for the case MON-GD-60

139
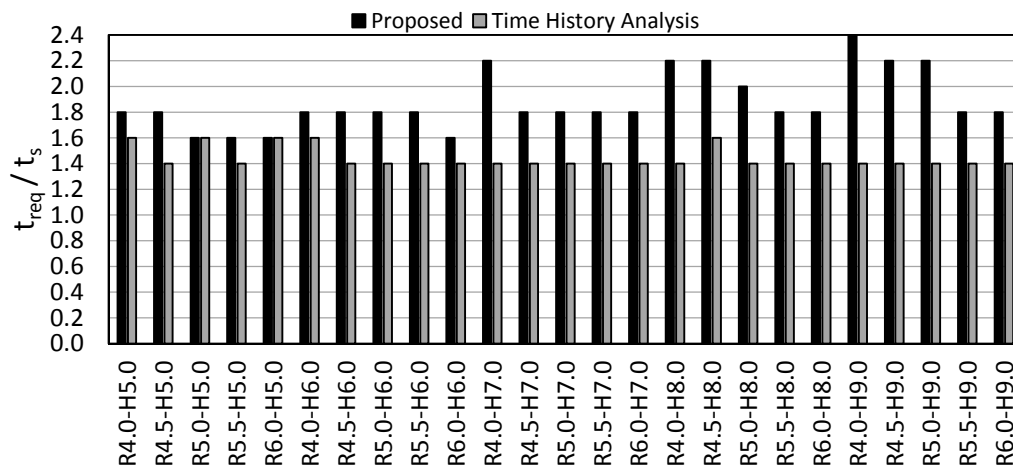
Fig. 4-27 Required thickness relative to t_s for the case MON-PR-60
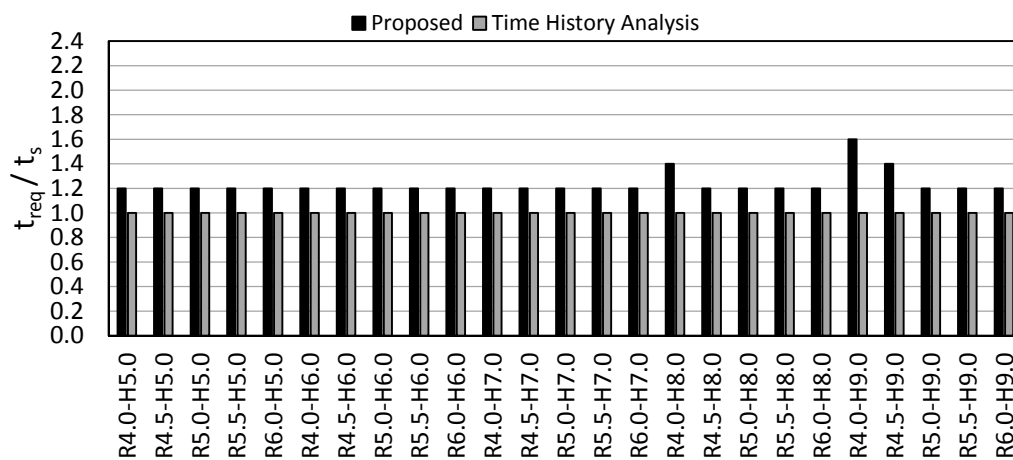
Fig. 4-28 Required thickness relative to t_s for the case VAN-PE-60
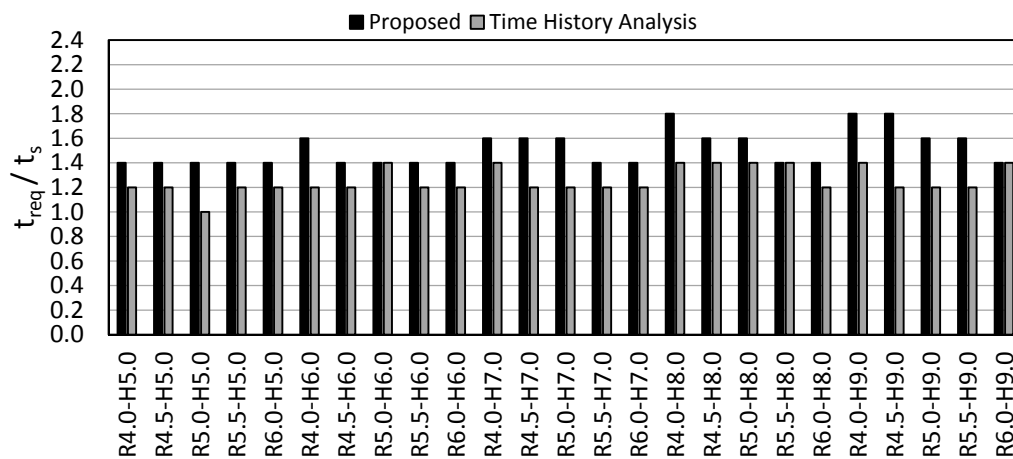
Fig. 4-29 Required thickness relative to t_s for the case VAN-GD-60
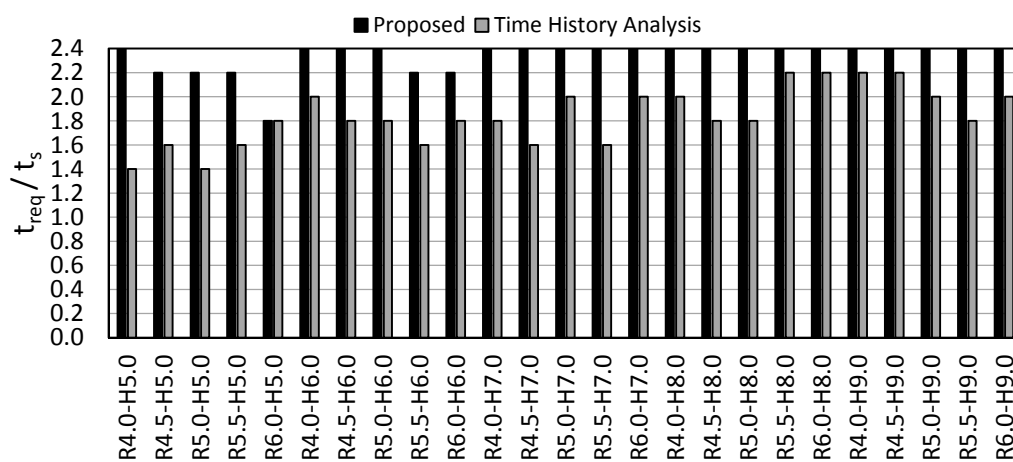
Fig. 4-30 Required thickness relative to t_s for the case VAN-PR-60

Chapter 5

5 Effect of Base Rocking Motion on the Seismic Behaviour of Conical Shaped Steel Liquid Storage Tanks

Liquid storage tanks in the form of truncated cone steel vessels are widely used in order to provide water supply and also to store other liquids that might be used for industrial purposes. For the case of elevated conical tanks, the effect of the tank base rocking motion has been assumed to be negligible in previous studies related to seismic behaviour of elevated steel conical tanks. In this study, the assumption of ignoring the base rocking motion is assessed by studying the effect of this motion on the seismic behaviour and the vibration characteristics of elevated steel conical tanks. A fluid-added mass matrix incorporating the rocking effect is derived and then incorporated in dynamic and free-vibration analyses. In addition, a mechanical analog that simulates the forces acting on an elevated conical tank subjected to a horizontal excitation including the effect of this rocking motion is developed. This mechanical model takes the flexibility of the tank walls into consideration as well the hydrodynamic pressure acting on the tank base and hence can be used to evaluate the maximum resulting forces for a rigid or a flexible conical tank subjected to a horizontal ground excitation. Different Parameters of the mechanical model are displayed in the form of charts for different tank dimensions. Finally, an example is provided to show how the developed mechanical model is applied to evaluate the response of steel conical tanks subjected to horizontal ground excitation taking base rotation into consideration.

5.1 Introduction

Conical vessels are commonly used as storage containments in elevated tanks. For such tanks, the vessels can consist solely from a truncated conical shell and they referred to as pure conical tank. If the truncated conical vessels have a superimposed top cylinder part, they are called combined conical tank. Photos of pure and combined conical tanks are shown in Fig. 5-1a and Fig. 5-1b, respectively. It is also quite common that the shafts of elevated conical tanks are made of reinforced concrete while the vessels are made of steel curved panels welded together. While few studies can be found in the literature regarding

the seismic behaviour of conical tanks, the guidelines for the design of liquid-filled structures do not provide rational procedure for designing such structures under seismic loading. The most comprehensive guidelines (AWWA (2005), API (2005)) consider the seismic analysis of conical tank by converting them to equivalent cylinders.
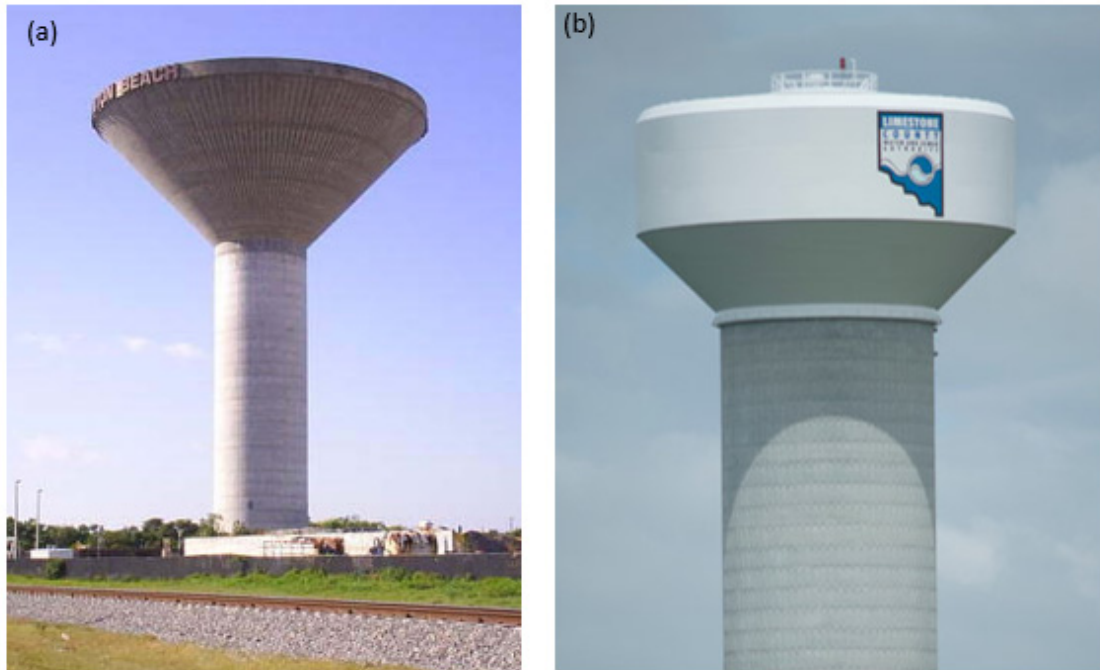
Fig. 5-1 (a) Pure conical tank[7], (b) Combined conical tank[8]

As a result of the inclination of the walls of conical tanks, the state of stresses in such structures, either under hydrostatic or hydrodynamic pressure (due to seismic excitation), are different from the state of stresses in cylindrical containers. Under hydrostatic pressure, a number of studies have been carried out for steel conical tanks focusing on elastic and inelastic stability and taking into account the effects of geometric imperfections and residual stresses (Vandepitte et al. (1982), Vandepitte (1999), El Damatty et al. (1997a), El Damatty et al. (1997b,c), El Damatty et al. (1998), El Damatty et al. (1999), and Hafeez et

---

[7] http://forums.auran.com/trainz/showthread.php?17876-FEC-Key-West-extension-modern-day/page7
[8] http://www.caldwellwatertanks.com

al. (2010)). Sweedan and El Damatty (2009) provided a simplified design procedure for steel conical tanks under hydrostatic pressure for steel conical tanks.

For the case of conical tanks subjected to horizontal excitations, hydrodynamic pressure is induced on the tank walls and base in addition to the acting hydrostatic pressure. This hydrodynamic pressure will magnify the hydrostatic-induced stresses at one side of the tank and reduce it on the other side leading to an acting overturning moment. The contained fluid is divided into impulsive and sloshing fluid masses. The impulsive liquid mass represents the lower amount of fluid that moves with the walls of the tank, while the sloshing fluid mass represents the surface amount of fluid undergoing sloshing.

It was noticed that seismic loadings can cause significant damages to liquid-filled storage tanks after the Alaska earthquake 1964. One of the challenges in analyzing liquid-filled containers under seismic loading is the estimation of the hydrodynamic pressure. Earlier studies were based on assuming the tank walls to be rigid when evaluating the hydrodynamic pressure (Jacobsen (1949), Housner (1957), and Housner (1963)). Later on, it was realized that the flexibility of the tank walls and the interaction that happens between wall vibrations and the contained liquid might significantly affect the impulsive hydrodynamic pressure distribution and consequently the structural response (Veletsos (1974), Haroun and Housner (1982), and Haroun and Housner (1981)). On the other side, the sloshing hydrodynamic pressure was found to be independent of wall vibrations and hence it can be obtained assuming rigid walls.

The first study conducted to assess the behavior of conical tanks under seismic loading was done by El Damatty et al. (1997b,c) where a coupled shell element-boundary element formulation was developed to simulate the fluid-structure interaction between the hydrodynamic pressure and the vibration of the tank walls during a seismic excitation including both horizontal and vertical components. A fluid added mass matrix was obtained from the above formulation and is added to the mass matrix of the structure to be incorporated into a nonlinear dynamic analysis routine. This coupled shell element-boundary element model was verified experimentally using shaking table testing of scaled

conical shell aluminum models (Sweedan and El Damatty (2002) and El Damatty et al. (2005)).

Using the numerical model, El Damatty and Sweedan (2006) developed an equivalent mechanical model that can be easily used in analyzing conical tanks under the horizontal component of a ground excitation. In this mechanical model, the contained fluid is represented using lumped masses attached to the tank walls through linear springs. The lumped masses represent both the impulsive and sloshing components. The properties of the mechanical model were developed such that the model mimics the base shear and overturning moment obtained using the sophisticated numerical model.

The aforementioned studies were all based on assuming that the tanks are not undergoing rocking movement, i.e., the tank base moves as a rigid body either vertically or horizontally. Depending on the pressure head required, a liquid tank might be elevated above the ground through a supporting structural system. The supporting system can be in the form of steel framing or a reinforced concrete shaft. Ignoring the base rocking motion might be valid for the case of ground tanks or elevated tanks with the supporting structure rigid enough to prevent such rocking motion. For cantilever type of supporting structure, the base of the liquid tank might undergo a significant rocking motion under the effect of horizontal earthquake excitation.

Haroun and Ellaithy (1985a) developed an analytical mechanical model for flexible cylindrical tanks taking into consideration the effect of rigid base rocking motion and lateral translation. Different model's parameters were presented in the form of analytical expressions and charts. Veletsos and Tang (1987) studied the dynamic response for rigid and flexible cylindrical tanks subjected to a rocking base motion and extended the mechanical model used for horizontal excitations to permit consideration of the effects of base rocking. Haroun and Ellaithy (1985b) analyzed two elevated cylindrical tanks; one supported by a X-braced frame and the second supported by a pedestal tower, in order to assess the effects of tank rotation, tank translation, and tank wall flexibility on the seismic response of the tanks. It was concluded that the effect of tank flexibility is measurable especially when coupled with tank rotation. In addition, including the tank rotation

increased the total base shear with 12% and 52% for X-braced and pedestal tanks, respectively.

To the best of the authors' knowledge, the current study represents the first attempt to investigate the effect of the tank base rocking motion on the seismic behaviour and vibration characteristics of steel conical tanks under the effect of horizontal excitations. The study starts with deriving a fluid-added mass matrix that simulates the induced hydrodynamic pressure including the effect of rocking motion using a coupled shell element-boundary element formulation. The finite element model for the steel conical tanks is then described. The derived fluid-added matrix is then incorporated in both dynamic and free-vibration analyses in order to assess the effect of including the base rocking motion on the seismic response and the vibration characteristics of the steel conical tanks. Finally, a mechanical model that takes into consideration the effect of the base rocking motion on the hydrodynamic pressure is developed using the derived mass-matrix for steel conical tanks subjected to horizontal excitations. The parameters of this mechanical model are presented in chart form showing their variations with the geometric parameters of conical tanks. Finally, a numerical example is presented to illustrate the application of the proposed mechanical analog in predicting the seismic forces acting on steel conical tanks subjected to horizontal excitations.

5.2 Hydrodynamic Pressure

Hydrodynamic pressure is induced on the tank walls and base during seismic excitation acting on a conical tank. The total hydrodynamic pressure can be divided into two components: impulsive pressure P_I and sloshing pressure P_S. The sloshing component is a long period component relative to the impulsive one and hence the two components can be decoupled in the analysis (Haroun (1980)).

The impulsive hydrodynamic pressure component for a conical tank filled with an ideal fluid is governed with the following set of equations and boundary conditions (El Damatty et al. (1997b)):

$\nabla^2 P_I(r,\theta,z,t) = 0$ inside the fluid volume   [5-1]

$\partial P_I(r,\theta,z,t)/\partial n = -\rho_F \ddot{u}(r,\theta,z,t).n$ at the surface S_1 [5-2]

$P_I = 0$ at the surface S_3 [5-3]

$\partial P_I(t)/\partial n = -\rho_F\, \ddot{u}_z\,(r,\theta,t)$ at the surface S_2 [5-4]

where $\ddot{u}\,(r,\theta,z,t)$ is the acceleration vector at any point of the tank's wall, n is the unit vector normal to the surface of the tank, and ρ_F is the fluid density. Surfaces S_1, S_2 and S_3; coordinates r, θ, and z are shown in Fig. 5-2 and t is the time. The sloshing component can be separately derived due to the well-seperation in natural periods between sloshing and impulsive pressure modes. This is reflected through the boundary condition at the fluid surface i.e., Eq. 5-3. The boundary condition at the tank base i.e., Eq. 5-4 allows the inclusion of the base rocking motion by relating the hydrodynamic pressure with the vertical movement of the tank base.
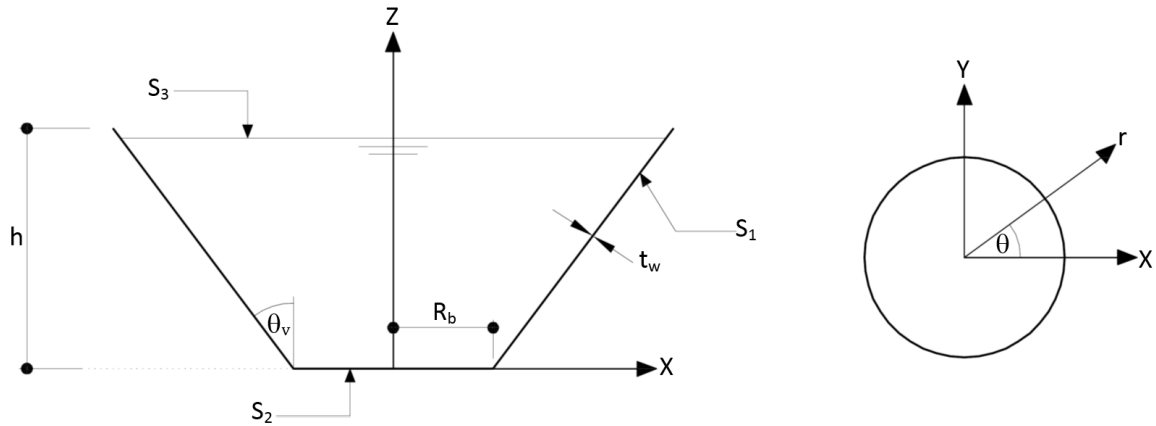
Fig. 5-2 Co-ordinate system for the steel conical tank and dimensional parameters

The solution of the above differential equation, Eq. 5-1, is done using the boundary element method by interpolating the dynamic pressure using different shape functions satisfying the boundary conditions described in Eqs. (2-4) as described by Haroun (1980) for cylindrical tanks and El Damatty et al. (1997b) for conical tanks. The obtained impulsive component of the hydrodynamic pressure is interpolated as follows:

$$P_I(r,\theta,z,t) = \left[\sum_{n=1}^{N_2}\sum_{i=1}^{N_1} A_{in}(t)\, H_{in}(r,\theta,z)\right] + B\,(t)\; H_{(N_1+1)}(r,\theta,z) \tag{5-5}$$

$$H_{i,n}(r,\theta,z) = I_n(\alpha_i r)\cos(\alpha_i z)\cos(n\theta) \tag{5-6}$$

$$H_{(N_1+1)} = (1-z/h)\, r\cos\theta \tag{5-7}$$

$$\alpha_i = (2i-1)\,\pi/2h \qquad\qquad\qquad\qquad\qquad\qquad\qquad\qquad\qquad [5\text{-}8]$$

where A_{in} (t), and $B(t)$ are the amplitude functions of time, I_n are the modified Bessel's functions of the first kind. The second term in Eq. 5-5 is included in order to satisfy the boundary condition at the base expressed in Eq. 5-4 which includes the effect of rocking base motion on the hydrodynamic pressure acting on the tank walls and base. Based on the distributions of different circumferential pressure modes $\cos(n\theta)$ shown in Fig. 5-3, the only mode that will yield a resulting base shear and corresponding overturning moment is the $\cos\theta$ mode, i.e., n=1.
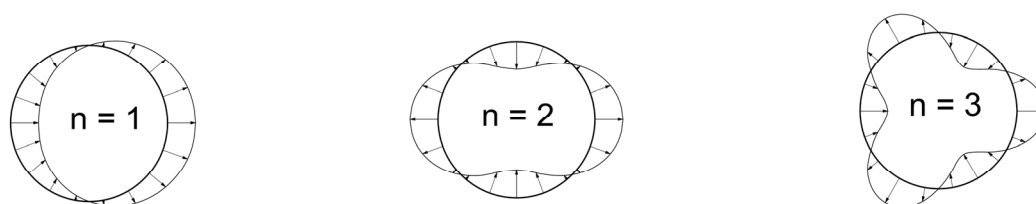
Fig. 5-3 Circumferential distribution of different pressure modes

As the boundary conditions along tank surfaces are functions of walls' acceleration which in turn depends on the hydrodynamic pressure value, fluid-structure interaction exists and should be accounted for in order to capture the real behaviour of a liquid tank subjected to a ground excitation. The fluid-structure interaction is more pronounced for the case of steel tanks as the flexibility of the tank vessel has a major contribution to the seismic response due to the relatively small thickness of the tank vessel.

A coupled shell element-boundary element formulation is carried out leading to the formulation of a fluid-added mass matrix which is added to the structure mass matrix and then incorporated in dynamic and free vibration analyses of the liquid-shell system. This technique is considered computationally efficient compared to modelling the contained fluid using finite elements as the total number of degrees of freedom are considerably reduced. The formulation is based on the consistent 13 noded subparametric triangular shell element shown in Fig. 5-4a that was developed by Koizey and Mirza (1997) and extended by (El Damatty et al. 1997d) to include nonlinear and dynamic behaviour. The formulation

is summarized in the following steps and more details can be found in El Damatty et al. (1997b).

The difference in the current formulation to the one found in El Damatty et al. (1997b) is due to the inclusion of the rocking term into the hydrodynamic pressure expression shown in Eq. 5-5 which corresponds to the subscript (N_1+1) in the following derivation described in Eqs. (5-9 to 5-20).

The variational functional J for the initial value problem, Eqs. (1-4) is given by

$$J= \int_{t_1}^{t_2} \left[\frac{1}{2} \int_{\Omega} (\nabla P_I . \nabla P_I)\, dv + \int_S \rho_F \ddot{u}.nP_I\, ds \right] dt \qquad [5\text{-}9]$$

Where ρ_F is the fluid mass density, Ω is the fluid volume and S is the sum of the wetted surfaces that are shown in Fig. 5-2. Green's theory is then applied to the first term to convert the volume integral into surface integral as

$$J= \int_{t_1}^{t_2} \left[\frac{1}{2} \left\{ \int_S P_I \frac{\partial P_I}{\partial n}\, ds - \int_{\Omega} P_I . \nabla^2 P_I\, dv \right\} + \int_S \rho_F \ddot{u}.nP_I\, ds \right] dt \qquad [5\text{-}10]$$

The term $\int_{\Omega} P_I . \nabla^2 P_I \, dv$ is equal to zero according to Eq. 5-1 to 5-4 reducing the variational functional to

$$J= \int_{t_1}^{t_2} \left[\frac{1}{2} \int_{S_1+S_2} P_I \frac{\partial P_I}{\partial n}\, ds + \int_{S_1+S_2} \rho_F \ddot{u}.nP_I\, ds \right] dt \qquad [5\text{-}11]$$

The impulsive hydrodynamic pressure can be then obtained by maximizing or minimizing the first variation of J satisfying the fluid wetted surfaces' boundary condition. In order to obtain the fluid added matrix [DM] that simulates the hydrodynamic pressure, virtual work concept is used where virtual displacements $\delta\{\Delta U\}$ are assumed and the virtual work done δW by the hydrodynamic pressure can be obtained as

$$\delta W = \delta\{\Delta U\}^T [DM]\{\ddot{u}^T\} \qquad [5\text{-}12]$$

The virtual displacements, wall and base accelerations $\{\ddot{u}\}$ are interpolated using the 13-noded shell element shape functions (Koizey and Mirza (1997)). The fluid mass matrix is obtained using the following procedure with including only the $\cos\theta$ mode, i.e., $N_2=1$:

The first term in the variational function J is expressed in matrix format as

$$\frac{1}{2}\int_{S_1+S_2} P_I \frac{\partial P_I}{\partial n} ds = \frac{1}{2}\{A_{i1}(t)\}^T_{1\times(N_1+1)} [C^*]_{(N_1+1)\times(N_1+1)} \{A_{i1}(t)\}_{1\times(N_1+1)} \qquad \text{[5-13]}$$

where

$$C^*_{ij}= \int_{S_1+S_2} H_{i1}\frac{\partial H_{j1}}{\partial n} ds \qquad \text{[5-14]}$$

$$\{A_{i1}(t)\}^T_{1\times(N_1+1)}=\{A_{11}(t) \quad A_{21}(t)\ldots\ldots\ldots A_{N_11}(t) \quad B(t)\} \qquad \text{[5-15]}$$

Using the chain rule as $\partial H_{j1}/\partial n=(\partial H_{j1}/\partial r)(\partial r/\partial n)+(\partial H_{j1}/\partial z)(\partial z/\partial n)$ leads to the following derivatives for the shape functions H with respect to the normal vector n
[5-16]   for tank walls

$$\frac{\partial H_{j1}}{\partial n}=\alpha_j I'_1(\alpha_j r) \cos(\alpha_j z) \cos(\theta) \cos(\theta_v) +\alpha_j I_1(\alpha_j r) \sin(\alpha_j z) \cos(\theta) \sin(\theta_v) \qquad j=1,\ldots,N_1$$

$$\frac{\partial H_{j1}}{\partial n}=\left(1-\frac{z}{h}\right) \cos(\theta) \cos(\theta_v) +\frac{r}{h} \cos(\theta) \sin(\theta_v) \qquad j=N_1+1$$

for tank base

$$\frac{\partial H_{j1}}{\partial n}=\alpha_j I_1(\alpha_j r) \sin(\alpha_j z) \cos(\theta) \qquad j=1,\ldots,N_1$$

$$\frac{\partial H_{j1}}{\partial n} =\frac{r}{h} \cos(\theta) \qquad j=N_1+1$$

The integration in Eq. 5-14 is performed numerically over the surfaces S_1 and S_2 which are discretized using shell elements. The second term in the variational function J can be expressed in the form of

$$\int_{S_1+S_2} \rho_F \ddot{u}.nP_I \, ds=\rho_F \sum_{i=1}^{N_1+1} A_{i1}(t) \sum_{N_{elem}} \int_{S_{elem}} H_{i1}\{G\}^T_{1\times 39}dS \{\ddot{u}^T\}_{39\times 1} \qquad \text{[5-17]}$$

where S_{elem} is the area of each shell element, N_{elem} is the total number of shell elements used to discretize the tank wall and base. The vector $\{G\}^T$ is a function of shell element shape functions and direction cosines that can be found in Koizey and Mirza (1997) and $\{\ddot{u}^T\}$ is the acceleration vector that includes the translational accelerations in the three directions at each of the 13-nodes for each shell element.

Taking the first derivative of the variational function J with respect to the amplitude function $A_{i1}(t)$ gives the following

$$\{A_{i1}(t)\}_{N_1 \times 1} = -\rho_F [C^*]^{-1}_{(N_1+1)\times(N_1+1)} \Sigma_{N_{elem}} [F]_{(N_1+1)\times 39} \{\ddot{u}^T\}_{39\times 1} \qquad [5\text{-}18]$$

where the matrix $[F]$ is function of shell element shape functions and direction cosines in addition to the pressure shape functions H_{i1}. Assembling the nodal acceleration vector $\{\ddot{u}\}$ and the matrix $[F]$, the impulsive hydrodynamic pressure can be expressed as follows where M is the total number of degrees of freedom.

$$P_I(r,\theta,z,t) = -\{H\}^T_{1\times(N_1+1)} \left[\rho_F [C^*]^{-1}_{(N_1+1)\times(N_1+1)} \sum_{N_{elem}} [F]_{(N_1+1)\times 39} \right]_{(N_1+1)\times M} \{\ddot{u}^t\}_{M\times 1} \qquad [5\text{-}19]$$

By obtaining the virtual work done by the hydrodynamic pressure assuming virtual displacements, the fluid added mass matrix [DM] can be obtained according to Eq. 5-12 and is given by

$$\sum_{N_{elem}} \int_{S_{elem}} \{G\}_{39\times 1} \{H\}^T_{1\times(N_1+1)} \left[\rho_F [C^*]^{-1}_{(N_1+1)\times(N_1+1)} \sum_{N_{elem}} [F]_{(N_1+1)\times 39} \right]_{(N_1+1)\times M} ds \qquad [5\text{-}20]$$

This fluid-added matrix can be added to the structure mass matrix and the total mass matrix can be then incorporated into nonlinear dynamic analysis or free vibration analysis for the steel conical tanks taking into consideration the base rocking motion in addition to the fluid-structure interaction. The sloshing component of the hydrodynamic pressure is not included assuming that the base rocking motion has negligible effects on the water sloshing as noticed experimentally by Chaduvula et al. (2013).

5.3   Finite Element Model

The numerical model used in the current study is based on the consistent 13 noded subparametric triangular shell element shown in Fig. 5-4a that was developed by Koizey and Mirza (1997). This element has the advantages of eliminating the spurious shear modes and locking phenomenon observed in isoparametric shell elements when used in modeling thin shell structures. El Damatty et al. (1997d) extended the formulation of this shell element to include geometric and material non-linearities as well as dynamic effect.

Three-dimensional numerical models are developed for steel conical tanks using the finite element method. Due to symmetry about the horizontal axis in both loading and geometry, only half of the cone is modelled and used in the analysis. A mesh of 136 triangular elements (128 for the tank walls and 8 for the tank base) is used for the model as shown in Fig. 5-4b. The length of the elements is not uniform as the mesh is chosen to be finer near the base of the tank due to the stress concentration at this location where buckling is expected to occur. The tanks are assumed to be free at the top.

In order to insure the sufficiency of the number of elements in the used mesh, a sensitivity analysis is performed where different mesh sizes, starting with a course one, are used to carry out the dynamic analysis till convergence in the output values takes place. Figure 5-5 shows the base shear force V time history for a steel conical tank subjected to a horizontal excitation using two different meshes: (1) using 52 elements (48 for the tank walls and 4 for the tank base), (2) using 136 elements (128 for the tank walls and 8 for the tank base). The two time histories are shown to yield almost the same base shear values over the excitation duration meaning that the used finite element mesh is sufficient.
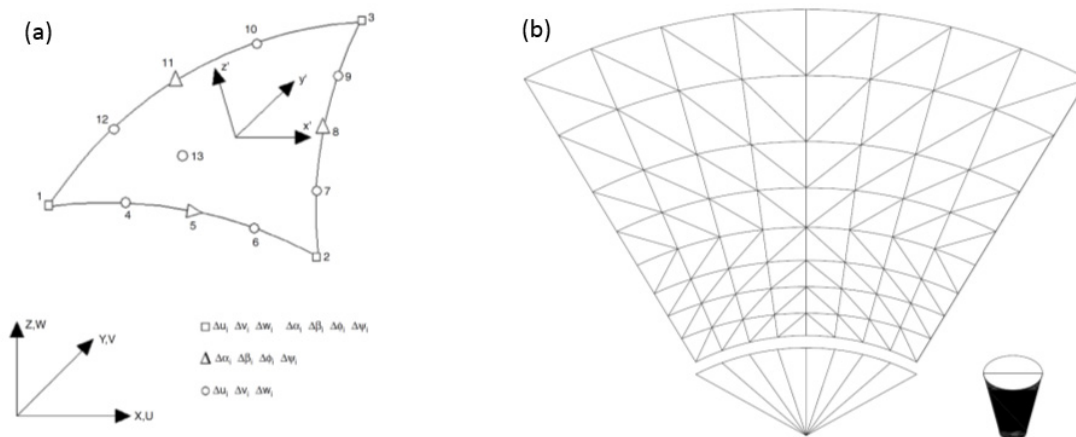
Fig. 5-4 (a) Coordinates and degrees of freedom for a consistent shell element, (b) Finite element mesh for half cone
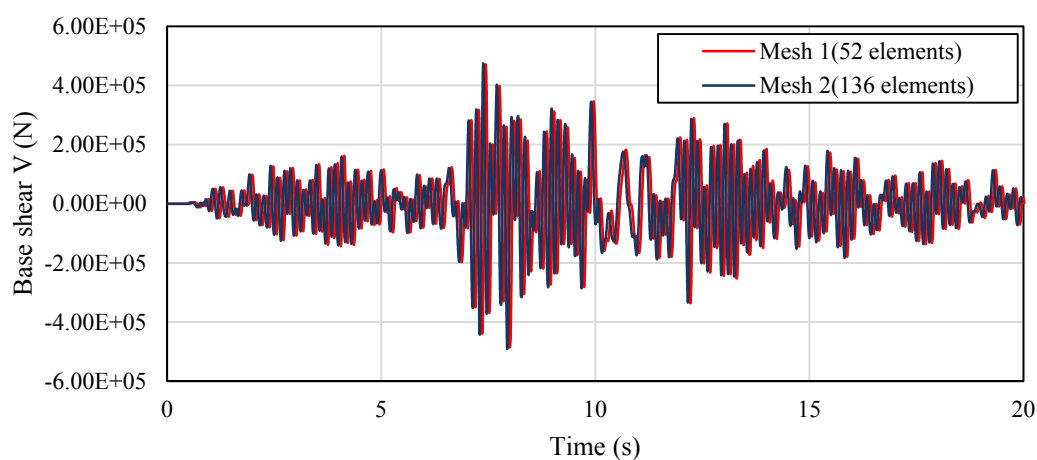
Fig. 5-5 Base shear force time history for a steel conical tank subjected to a horizontal excitation using two finite element meshes

5.4 Fluid-Added Matrix Validation

In order to validate the fluid-added matrix derivation, non-linear dynamic analyses are performed twice; the first one using the fluid-added matrix derived in the current study including the base rocking effect with a high rotational spring stiffness $K_{\alpha\alpha}$ value approaching infinity, while the second one using the fluid-added matrix derived by (El Damatty et al. 1997b) assuming no rocking base motion. A tank with R_b=4.0m , h=5.0m,

and $\theta_v=45^o$ is subjected to an artificial ground excitation corresponding to Montreal seismic zone for the two cases and the time history of both total base shear and overturning moment are compared as shown in Figs. 5-6, 5-7. The base shear V is normalized by the weight of the contained fluid W while the overturning moment M is normalized by the term $W.R_b$. The comparison indicated that the two cases yield the same base shear and overturning moments meaning validation of the derived fluid-added mass matrix.
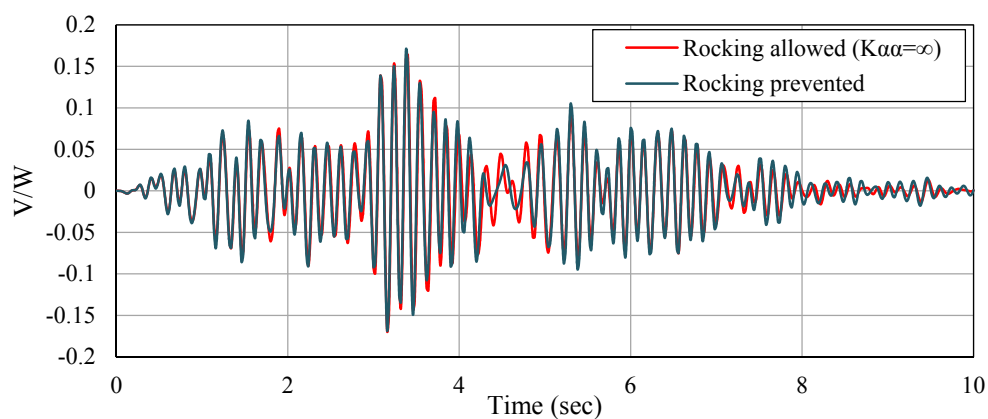
Fig. 5-6 Time history for V/W for cases of rocking allowed and prevented
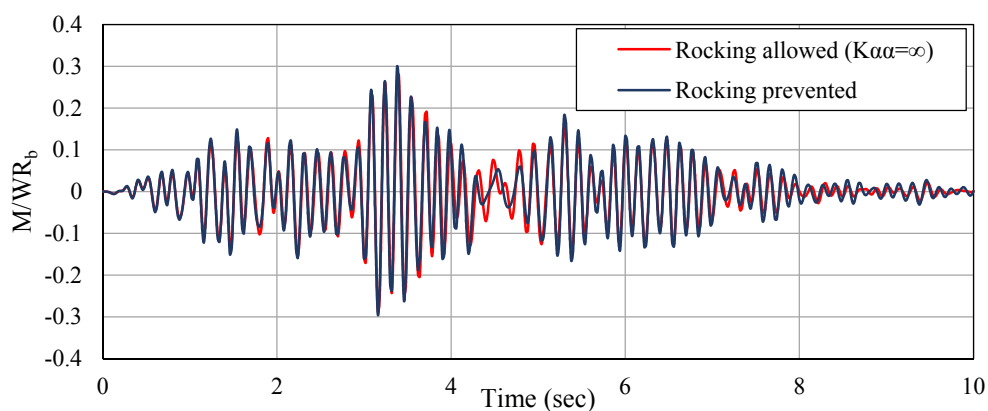
Fig. 5-7 Time history for M/WR$_b$ for cases of rocking allowed and prevented

5.5   Effect of Base Rocking Motion

The change in seismic behaviour of elevated steel conical tanks by allowing the tank base to undergo rocking motion is mainly attributed to two factors: (1) Allowing the tank base to undergo rocking motion, changes the vibration properties of the conical tank i.e., natural frequencies and mode shapes, (2) By undergoing rocking motion, the deformations and accelerations of the tank walls change consequently leading to a change in the hydrodynamic pressure acting on the tank walls and base due to the existing fluid-structure interaction. These two factors are discussed in details in the following sub-sections.

In order to study how the base rocking motion changes the natural frequencies of a steel conical tank, a group of 75 tanks of practical dimensions are chosen with cone bottom radius R_b ranging from 4.0m to 6.0m, cone height h from 5.0m to 9.0m, and angle of inclination with vertical $\theta_v = 30^o$, 45°, 60°. The conical tanks are assumed to be elevated above the ground through a hollow cylindrical reinforced concrete shaft with a concrete slab connecting the tank vessel to the shaft as shown in Fig. 5-8a,b. Assuming the RC shaft to behave elastically, it can be incorporated in the finite element analysis of the steel conical tanks through two translational springs with horizontal stiffness K_{xx}, vertical stiffness K_{zz} and a rotational spring with stiffness $K_{\alpha\alpha}$ as shown in Fig. 5-8c. Figure 5-8d shows the RC shaft stiffness matrix given by

$$K_{xx} = 12E_cI/L_{sh}^3 \qquad\qquad\qquad [5\text{-}21]$$

$$K_{zz} = E_cA/L_{sh} \qquad\qquad\qquad [5\text{-}22]$$

$$K_{\alpha\alpha} = 4E_cI/L_{sh} \qquad\qquad\qquad [5\text{-}23]$$

$$K_{x\alpha} = K_{x\alpha} = 6E_cI/L_{sh}^2 \qquad\qquad\qquad [5\text{-}24]$$

where E_c is the concrete modulus of elasticity, I and A are the RC shaft moment of inertia and cross sectional area, respectively. L_{sh} is the shaft length and $K_{x\alpha}$ is the coupling stiffness of the RC shaft. Table 1 gives the stiffness value $K_{\alpha\alpha}$ corresponding to four different RC shaft dimensions
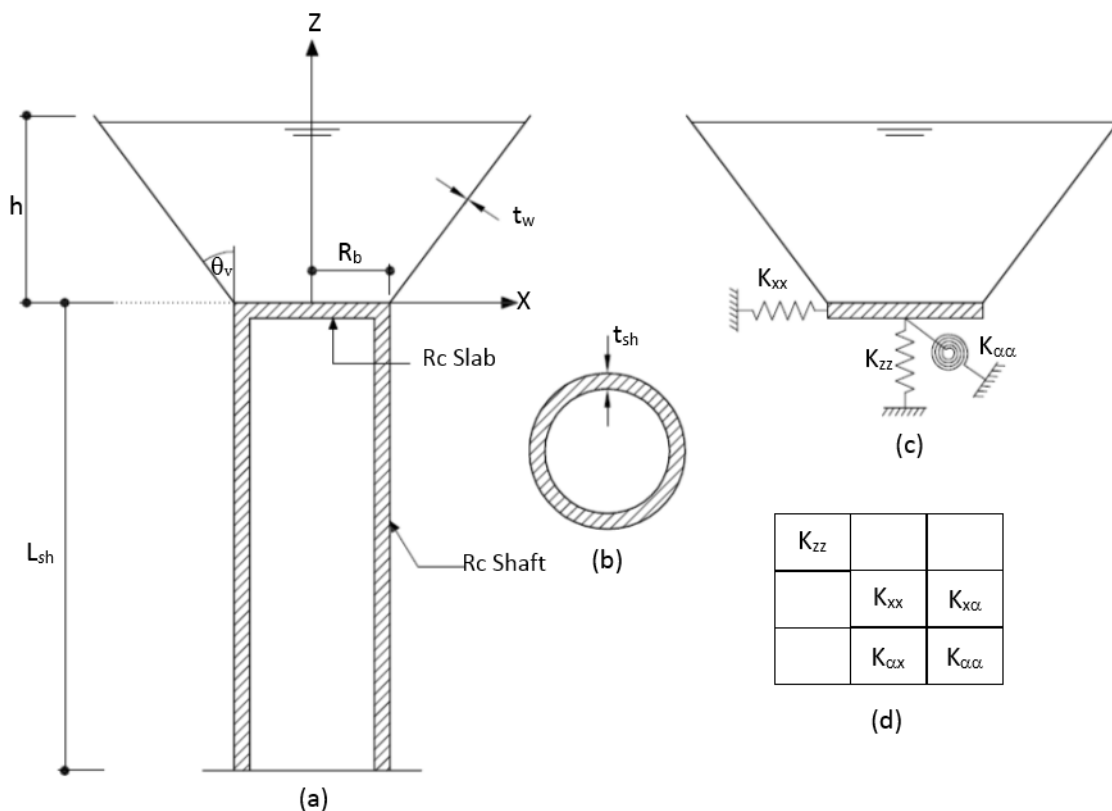
Fig. 5-8 (a) Elevated tank structure, (b) RC shaft cross-section, (c) Springs simulating the RC shaft, and (d) RC shaft stiffness matrix

Table 5-1 Practical RC shaft dimensions and corresponding rotational stiffness $K_{\alpha\alpha}$

Shaft	L_{sh} (m)	R_b (m)	t_{sh} (m)	$K_{\alpha\alpha}$ (N.m/rad)
1	10	3.0	0.2	1.53E+11
2	20	3.0	0.5	1.65E+11
3	10	6.0	0.2	1.29E+12
4	20	6.0	0.5	1.50E+12

5.5.1   Free Vibration Analysis

Free vibration analyses for the chosen group of steel conical tanks are performed using the coupled finite-boundary element routine discussed earlier. The natural frequencies ω and the corresponding mode shapes $\{\emptyset\}$ are obtained by solving the Eigen-value problem

$$([K]-\omega^2[M])\{\emptyset\}=\{0\} \tag{5-25}$$

where $[K]$ is the stiffness matrix of the conical tank vessel in addition to the RC shaft, $[M]$ is the fluid added mass matrix including the effect of rocking motion derived in Section 5.2. The shell mass is ignored in this part as it is relatively small compared to the fluid mass for the case of steel tanks. The tank base is assumed to behave rigidly either in translation or rotation due to the presence of the concrete slab at the tank base. This is reflected in the finite element model described in Section 5.3 by applying a constraint condition to the tank base horizontal degrees of freedom.

The analyses are repeated for the four RC shafts described in Table 5-1 in order to assess how changing the supporting shaft will affect the values of the natural impulsive frequency f_1. The natural frequency f_1 is represented in the form of the dimensionless parameter $(f_1 R_b \sqrt{\rho_s/E})$ where ρ_s is the mass density of the vessel material and E is the young's modulus of elasticity for the tank vessel. This dimensionless parameter is found to best represent the variation of f_1 with different parameters that affect its value when plotted against slenderness ratio h/R_b for a constant ratio t_w/R_b where t_w is the tank wall thickness.

The variation of the parameter $(f_1 R_b \sqrt{\rho_s/E})$ with the slenderness ratio h/R_b for the four RC shafts is shown in Fig. 5-9 for the case of allowing the rocking motion in addition to the case of ignoring such motion for the sake of comparison. The parameter $(f_1 R_b \sqrt{\rho_s/E})$ is found to be higher as the tank approach a cylindrical tank i.e., lower θ_v values and found to be lower for the case of including the rocking motion. The range of the percent reduction in the natural frequency f_1 due to including the rocking motion is summarized in Table 5-2 for different θ_v values. For example, the reduction in the natural frequency f_1 for the 25 elevated conical tanks supported by shaft 1 and inclined with $\theta_v=30°$ ranges from 6% to 19.2%.
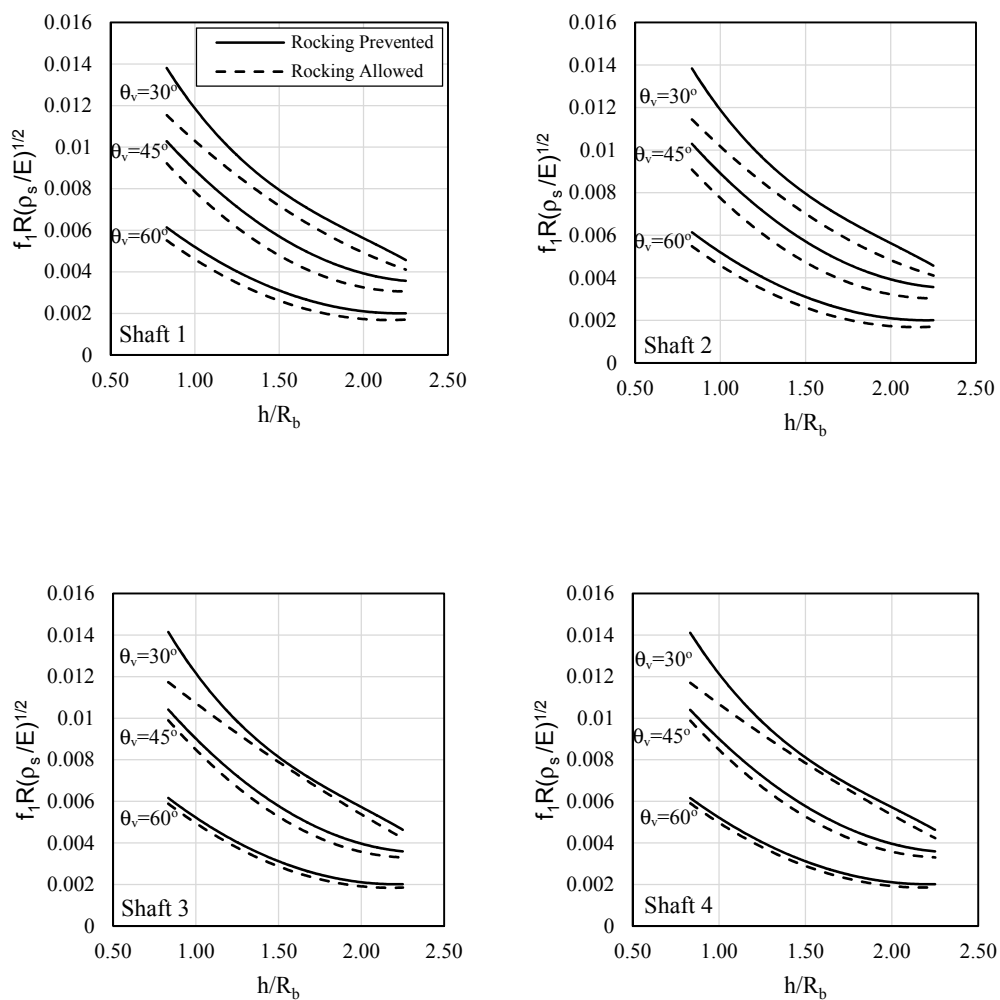
Fig. 5-9 Variation of the parameter $(f_1 R_b (\rho_s/E)^{0.5})$ with the slenderness ratio h/R_b

Table 5-2 % reduction range in the natural frequency (f_1) of the $\cos\theta$ impulsive mode

θ_v	Shaft 1	Shaft 2	Shaft 3	Shaft 4
30	6.0 ~ 19.2	7.2 ~ 19.6	4.0 ~ 21.2	4.3 ~ 21.0
45	9.4 ~ 21.0	10.1 ~ 22.5	4.8 ~ 10.5	4.8 ~ 10.0
60	8.2 ~ 22.1	8.3 ~ 22.5	4.50 ~ 10.3	4.2 ~ 9.1

As it can be seen from the previous table, allowing an elevated conical tank base to rock results in a reduction in the natural frequency that can reach up to 23% for the range of tanks considered in the current study. As a result, the seismic behaviour in addition to the base forces are expected to be different compared to the case of preventing the rocking motion as will be discussed in the subsequent section.

5.5.2   Non-Linear Dynamic Analysis

Allowing the tank base to undergo rocking motion will change the conical tank response and, consequently due to the existing fluid structure interaction, the hydrodynamic pressure distribution. In this sub-section, the overall seismic behaviour of steel conical tanks when they undergo rocking motion is assessed in terms of how the main seismic quantities such as total base shear and overturning moment are affected by such a rocking motion. The same group of steel conical tanks considered in the previous section are designed under hydrostatic pressure only based on the simplified method proposed by Sweedan and El Damatty (2009) in order to evaluate the wall thicknesses. The tanks are assumed to be good tanks regarding the level of geometric imperfection according to the classification proposed by Vandepitte et al. (1982).

In order to analyze the steel conical tanks subjected to ground excitation, non-linear time history analysis is used where the dynamic equations for the liquid-shell system which are given by

$$[M]\{\ddot{u}\} + [C]\{\dot{u}\} + [K]\{u\} = -[M]\{H\}\, a_h^t \qquad\qquad\qquad [5\text{-}26]$$

are solved numerically using Newmark's method at each time increment where $[M]$ is the summation of the shell mass matrix and the fluid-added matrix derived in Section 5.2, $[K]$ is the summation of the tangential stiffness matrix of the tank shell to the stiffness matrix of the RC shaft, $[C]$ is the damping matrix which is obtained as a linear combination of $[M]$ and $[K]$ according to the Rayleigh method (Chopra (2001)). $\{\ddot{u}\}$, $\{\dot{u}\}$, and $\{u\}$ are the tank wall or base acceleration, velocity, and displacement, respectively. The term $\{H\}\, a_h^t$ represents the ground horizontal excitation acting on the conical tank. More details on the solution technique for the nonlinear dynamic equations could be found in El Damatty et al.

(1997b). The damping ratio is assumed to be 2% which is the value for impulsive hydrodynamic pressure modes found in literature.

Three artificial earthquake excitations are generated in order to carry out the dynamic analysis for the steel conical tanks under consideration. These artificial excitations are designed to match the NBCC (2010) response spectrum for the seismic zones of Toronto, Montreal, and Vancouver. The artificial excitation for Toronto seismic zone with the corresponding response spectrum in addition to the NBCC (2010) spectrum are shown in Fig. 5-10.
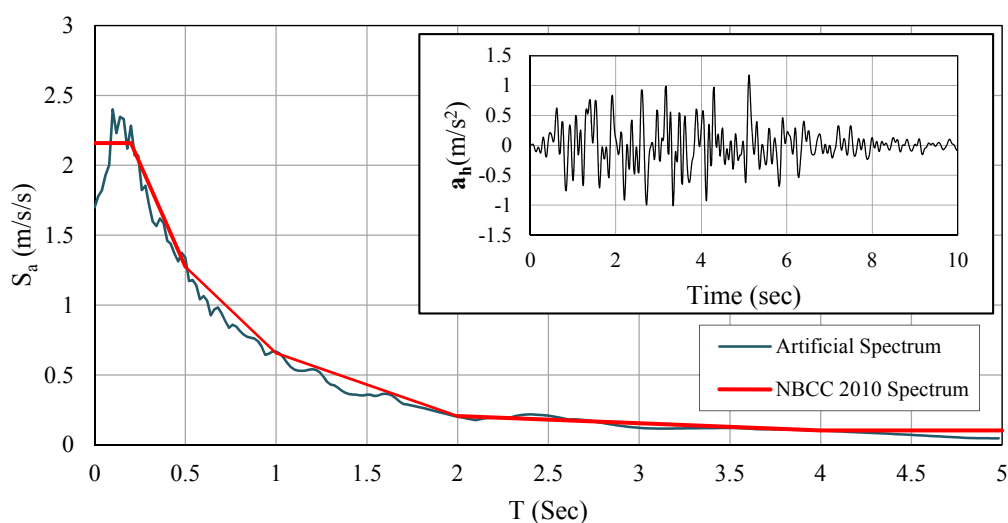
Fig. 5-10 Artificial ground excitation for Toronto seismic zone with the corresponding spectrum

Nonlinear time history analyses are performed for the 75 steel conical tanks under the effect of the three prescribed artificial ground excitation records for different RC shafts described in Table 5-1. The resulting total base shear V and overturning moment M due to the impulsive hydrodynamic pressure are obtained and the maximum value for both V and M is recorded for each case.

Comparing V_{max} and M_{max} obtained from the case of ignoring the rocking base motion to the corresponding case with allowing the tank base to undergo rocking motion, the

percentage increase or reduction in V_{max} and M_{max} is calculated for each seismic zone. The percentage increase or reduction in V_{max} and M_{max} for different RC shafts and angles θ_v is summarized in Tables 5-3, 5-4, respectively, in the form of *(maximum reduction ~ maximum increase)* where the reduction is represented with a negative sign. For example, the percentage change in V_{max} due to allowing the tank base to rock for the 25 tanks with $\theta_v=30^o$ supported with shaft 1 and subjected to artificial ground motion corresponding to Toronto seismic zone ranges from a reduction of 6.3% to an increase of 16.3%.

The percentage increase for the total base shear reaches 36.8%, 23%, 15.3% for $\theta_v=30^o,45^o,60^o$, respectively as shown in Table 4-3. On the other side, table 4 shows that the percentage increase for the overturning moment reaches 32.6%, 27.3%, 16.5% for $\theta_v=30^o,45^o,60^o$, respectively. As a result, allowing the tank base to rock might have a significant impact on the total seismic forces for elevated steel conical tanks.

Table 5-3 Upper and lower bounds for % change in V_{max} for different seismic zones

θ_v	Toronto				Montreal				Vancouver			
	Shaft 1	Shaft 2	Shaft 3	Shaft 4	Shaft 1	Shaft 2	Shaft 3	Shaft 4	Shaft 1	Shaft 2	Shaft 3	Shaft 4
30	-6.3	-5.8	-7.5	-10.9	-11.2	-7.5	-5.2	-13.5	-6.6	-9.0	-4.0	-13.0
	16.3	28.1	2.2	18.8	36.8	32.4	5.1	17.2	25.1	23.9	4.6	8.4
45	-14.6	-7.1	-16.6	-10.1	-23.6	-6.4	-17.6	-15.4	-20.2	-12.9	-17.3	-13.8
	9.1	23.0	5.8	2.1	5.2	22.2	3.4	6.9	5.8	13.6	6.1	0.1
60	-18.8	-42.6	-18.4	-10.7	-21.8	-25.3	-22.9	-15.7	-20.0	-24.2	-16.9	-17.5
	5.9	5.5	15.3	11.7	5.1	5.3	7.5	9.5	7.0	6.9	13.9	9.9

Table 5-4 Upper and lower bounds for % change in M_{max} for different seismic zones

θ_v	Toronto				Montreal				Vancouver			
	Shaft 1	Shaft 2	Shaft 3	Shaft 4	Shaft 1	Shaft 2	Shaft 3	Shaft 4	Shaft 1	Shaft 2	Shaft 3	Shaft 4
30	-9.1	-9.4	-8.7	-13.9	-13.0	-11.4	-9.1	-15.3	-8.9	-12.8	-7.9	-13.5
	17.0	22.7	0.8	12.8	31.8	32.6	3.1	14.6	23.6	18.0	2.5	7.7
45	-11.7	-6.3	-15.6	-10.1	-21.2	-7.7	-16.4	-16.8	-18.2	-12.6	-16.2	-13.7
	10.5	27.3	3.7	1.4	3.9	22.3	4.4	6.6	4.4	12.1	5.5	0.2
60	-20.6	-41.0	-18.2	-10.6	-25.3	-22.9	-15.7	-14.2	-21.4	-22.5	-15.6	-14.9
	4.2	6.8	16.5	11.6	5.3	7.5	9.5	4.6	7.9	6.1	12.6	9.4

5.6 Mechanical Model for Steel Conical Tanks Undergoing Rocking

According to the previous section, it was shown that including the base rocking motion might have a significant effect on the total output forces acting on steel conical tanks subjected to horizontal excitations. As discussed in Section 4.1, a mechanical model where the contained fluid is represented by lumped masses attached to the tank wall through linear springs can be used to simulate the fluid inside the tank. The main function of a mechanical model is to mimic the resulting total base shear and overturning moment obtained using dynamic analysis.

In this section, a mechanical model for steel conical tanks including the effect of base rocking motion is developed and charts are provided for the model's parameters. The proposed model is shown in Fig. 5-11b where the impulsive rigid mass m_r is located at a height h_{rb} while the mass m_f which is located at a height h_{fb} represents the portion of m_r which participates in the vibration of the flexible walls of the steel conical tank. Based on the mechanical model, the total shear force $Q(t)$ and the overturning moment $M(t)$ are given by

$$Q(t) = m_f \ddot{x}(t) + m_r \ddot{G}(t) + m_r h_{rb} \ddot{\alpha}(t) \qquad [5\text{-}27]$$

$$M(t) = m_f h_{fb} \ddot{x}(t) + m_r h_{rb} \ddot{G}(t) + I_{tb} \ddot{\alpha}(t) \qquad [5\text{-}28]$$

$$I_{tb} = (m_r h_{rb}^2 + I_{rb}) \qquad [5\text{-}29]$$

where I_{rb} is the central moment of inertia of the mass m_r. $\ddot{x}(t)$, $\ddot{G}(t)$, and $\ddot{\alpha}(t)$ represent the relative acceleration of the mass m_f, the base translational acceleration, and the base rotational acceleration, respectively. The first tem represents the flexible component of the base shear $Q_f(t)$ and overturning moment $M_f(t)$, while the summation of the last two terms represents the rigid components $Q_r(t)$ and $M_r(t)$. The subscript b is used to reflect the inclusion of the moment acting on the tank base. In order to obtain the moment just above the base, the terms h_{rb}, h_{fb}, and I_{tb} have to be replaced with h_r, h_f, and I_t respectively, in the first two terms in Eqs. 13 and 14.

It has to be mentioned that the forces due to the flexible mass m_f are corresponding to the relative acceleration $\ddot{x}(t)$. As a result, the mechanical model described in Fig. 5-11a has to be used when the steel conical tank is combined with other dynamic systems such as a supporting structure. The transformation between the two models is based on the following relations

$$m_0 = m_r - m_f \tag{5-30}$$

$$m_0 h_{0b} = m_r h_{rb} - m_f h_{fb} \tag{5-31}$$

$$m_0 h_{0b}^2 + I_0 = I_{tb} - m_f h_{fb}^2 \tag{5-32}$$
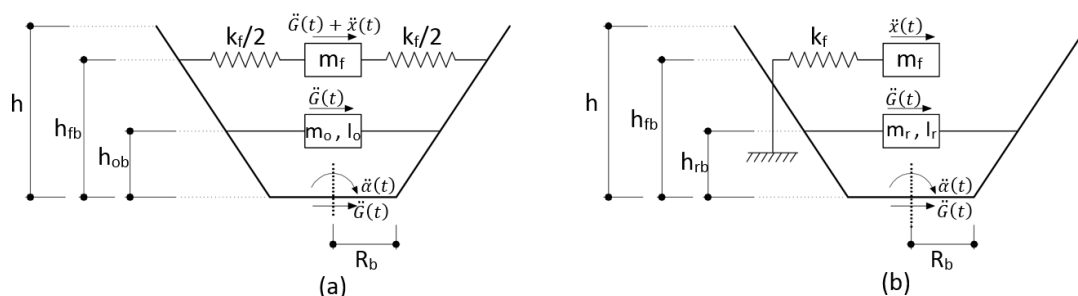
Fig. 5-11 Schematic presentation of the equivalent mechanical model

In order to completely define the proposed mechanical model, six parameters are needed to be determined which are the masses m_f, m_r and their effective heights h_{rb}, h_{fb} in addition to the central moment of inertia I_r and the spring stiffness k_f. The spring stiffness k_f is obtained through free vibration analyses using the fluid-added mass matrix derived in Section 5.2, where the natural frequency of the first impulsive $\cos\theta$ pressure mode f_1 is recorded. The frequency f_1 and the spring stiffness K_f are related through $f_1 = 1/2\pi \sqrt{k_f/m_f}$. The free vibration analysis is repeated for the set of 75 conical tanks described earlier with three different values of the ratio t_w/R_b where t_w is the tank wall thickness.

The variation of the parameter $(f_1 R_b \sqrt{\rho_s/E})$ with the slenderness ratio h/R_b for different t_w/R_b values is shown in Fig. 5-12. In order to validate the free vibration results, a similar set of analyses are carried out for the same set of tanks but with vertical walls representing the case of cylindrical tanks and compared to the results obtained by Haroun and Ellaithy (1985a) as shown in Fig. 5-12a where an excellent agreement is shown.

(a) $t_w/R_b=0.001$

(b) $t_w/R_b=0.005$

(c) $t_w/R_b=0.01$
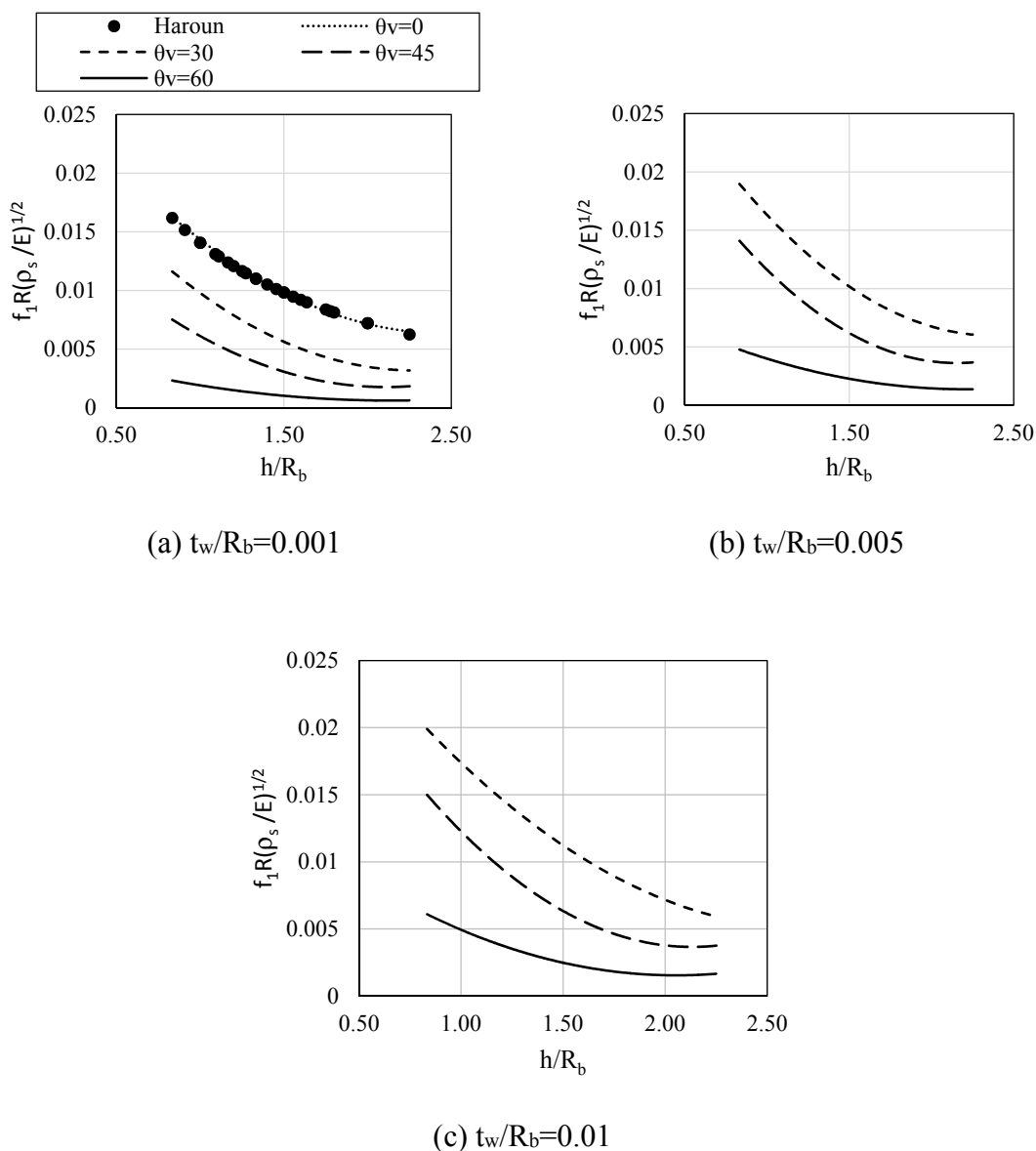
Fig. 5-12 Variation of ($f_1R_b(\rho_s/E)^{0.5}$) with slenderness ratio h/R_b for different θ_v

The remaining parameters of the proposed mechanical model are determined according to the following procedure for each steel conical tank:

1) The Conical tank is subjected to a horizontal ground excitation in the form of white noise covering the frequency range of the group of tanks being studied.

2) At first, the conical tank is assumed to be rigid i.e., the accelerations of the tank walls are the same as the ground acceleration $\ddot{G}(t)$, in order to obtain the rigid component of the resulting base shear $Q_r(t)$.

3) Being in phase with $\ddot{G}(t)$, the base shear $Q_r(t)$ is used to obtain the rigid mass m_r as the ratio between $Q_r(t)$ and $\ddot{G}(t)$

4) The effective height of the rigid mass h_{rb} is determined based on the rigid component of the overturning moment $M_r(t)$ as the ratio between $M_r(t)$ and $m_r\ddot{G}(t)$.

5) The same analysis in step (2) is repeated taking the wall flexibility into consideration in order to get the total base shear $Q(t)$ where the flexible component of the base shear $Q_f(t)$ can be obtained as $Q_f(t) = Q(t) - Q_r(t)$

6) A frequency analysis is performed to obtain the transfer function $\left|H_{Qf}(t)\right|$ between the flexible base shear $Q_f(t)$ and the excitation acceleration $\ddot{G}(t)$. The transfer function $\left|H_{Qf}(t)\right|$ is found to have the trend of the transfer function of a single oscillator with a peak value occurring at the resonant frequency of the $\cos\theta$ impulsive mode. As a result, $\left|H_{Qf}(t)\right|$ can be expressed as the product of the flexible mass m_f and the dynamic amplification factor DAF of the acceleration experienced by this mass where

$$\text{DAF} = \left(\frac{f_{ex}}{f_I}\right)^2 \frac{1}{\sqrt{[1-(f_{ex}/f_I)^2]^2 + [2\xi(f_{ex}/f_I)]^2}} \qquad \text{[5-33]}$$

where f_{ex} is the excitation frequency, ξ is the damping ratio and f_I is the natural frequency of the $\cos\theta$ impulsive mode.

7) A curve fitting process is conducted to assess the best estimates for the parameters m_f, f_I and ξ. The fitting process is based on the least square technique. The estimated values of f_I and ξ are found to match the $\cos\theta$ natural frequency obtained from the free vibration analysis and the damping ratio assumed in the time history analysis, respectively. A sample of the curve fitting process for a steel conical tank ($\theta_v=45°$, $R_b=4m$, $h=5m$) is shown in Fig. 5-13.

8) In order to obtain effective height of the flexible mass h_{fb}, steps 5 to 7 are repeated for the flexible component of the overturning moment $M_f(t)$. The transfer function $\left|H_{Mf}(t)\right|$ is found to have the trend of the transfer function of a single oscillator as well and is given by $\left|H_{Mf}(t)\right| = m_f\, h_{fb}*\text{DAF}$. The best estimate of the height h_{fb} is obtained from the curve fitting process.

9) Finally the term I_{tb} is obtained by subjecting the steel conical tank to a ground excitation in the form of rotational excitation $\ddot{\alpha}(t)$ and recording the rigid component of the overturning moment $M_r(t) = I_{tb}\ddot{\alpha}(t)$ from where I_{tb} is calculated.
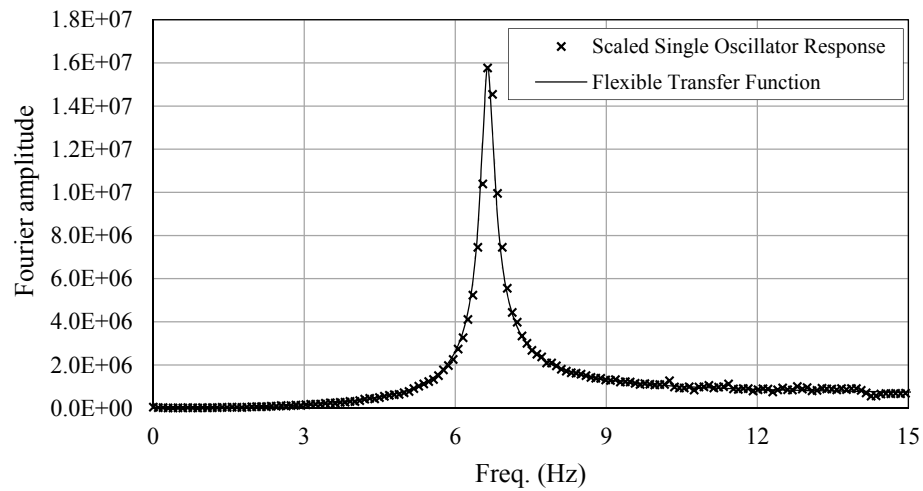
Fig. 5-13 Fitting the transfer function of the flexible component of the base shear to a scaled single oscillator response

In order to validate the proposed mechanical model, the same prescribed procedure is applied to a similar group of cylindrical tanks and the model's parameters are compared to those obtained according to the mechanical model developed by Haroun and Ellaithy (1985a) as shown in Fig. 5-14 where an excellent agreement can be noticed.
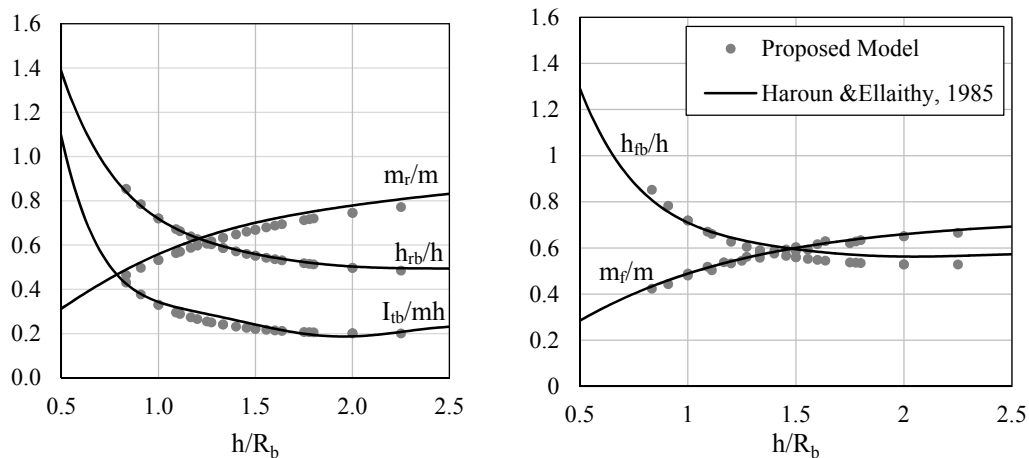
Fig. 5-14 Comparison between the proposed mechanical model parameters and the values provided by (Haroun and Ellaithy 1985a)

Being validated, the entire process (steps 1-9) involving finite element time history analysis, Fourier analysis and curve fitting is repeated for all conical tanks considered in this study. As a result, the variation of the mechanical model parameters m_r/m_t, m_f/m_t, h_{rb}/h, h_r/h, h_{fb}/h, h_f/h, $I_t/m_t h^2$ and $I_{tb}/m_t h^2$ with the parameters h/R_b and θ_v are determined where m_t is the total mass of the contained fluid. The analyses indicates that all parameters are independent of the wall thickness t_w. The variation of the mechanical model parameters with h/R_b and θ_v are shown in Figs. 5-15 to 5-19. It is worth mentioning that the difference between the total fluid mass m_t and the rigid mass m_r represents the mass contributing in the long period sloshing pressure modes.
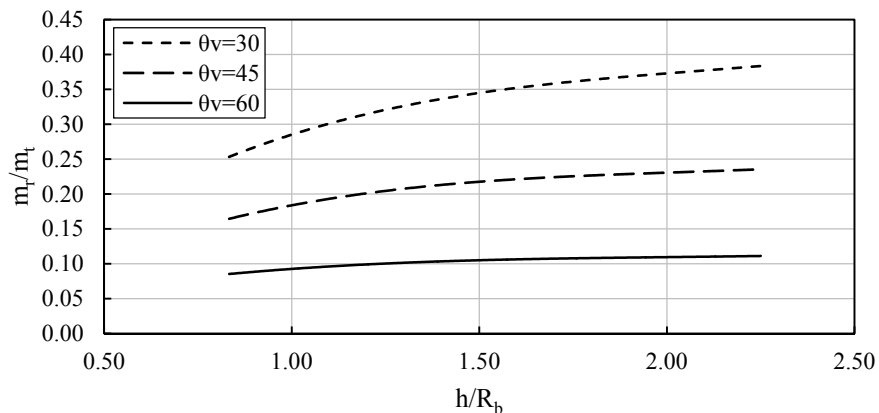
Fig. 5-15 Variation of the parameter m_r/m_t with ratio h/R_b
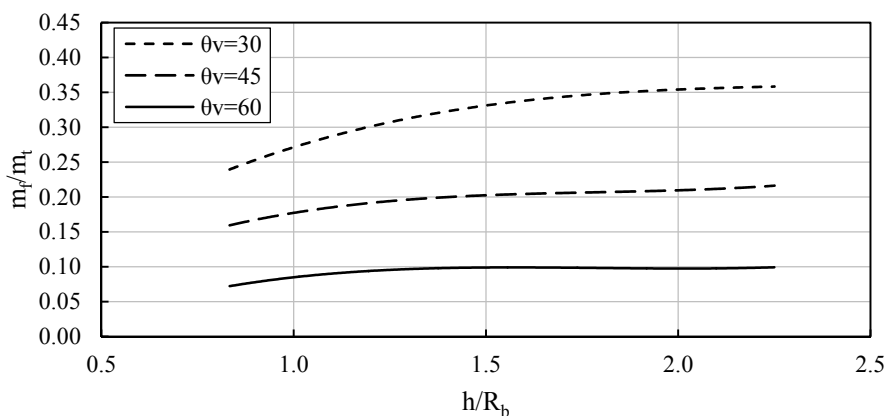
Fig. 5-16 Variation of the parameter m_f/m_t with the slenderness ratio h/R_b
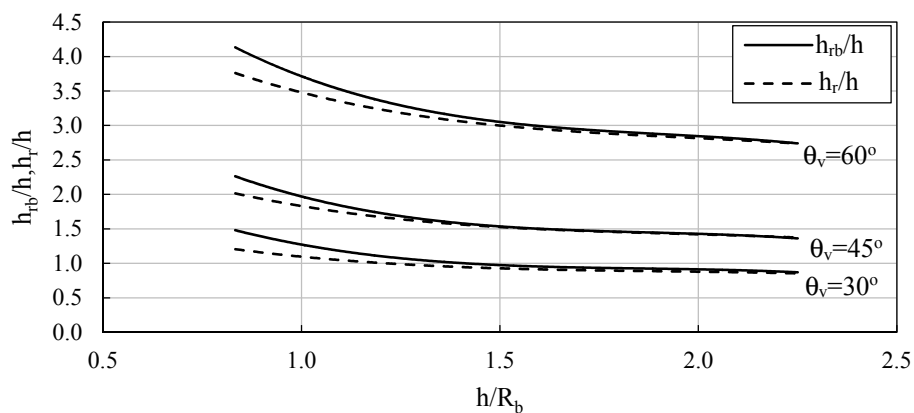
Fig. 5-17 Variation of the parameters h_{rb}/h and h_r/h with the slenderness ratio h/R_b
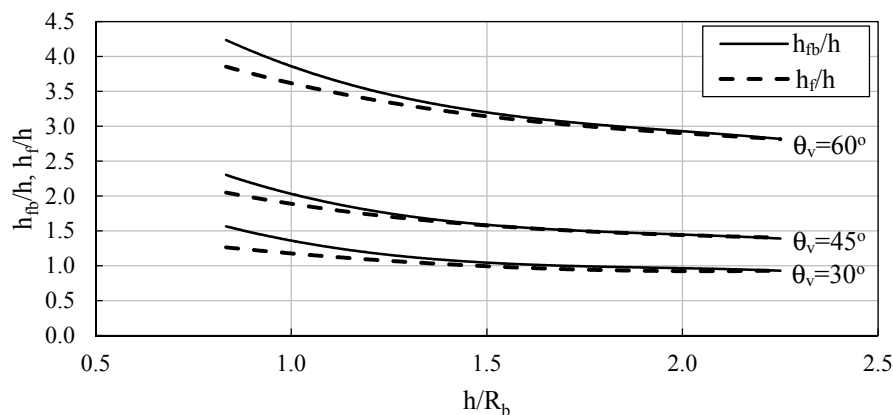
Fig. 5-18 Variation of the parameter h_{fb}/h and h_f/h with the slenderness ratio h/R_b
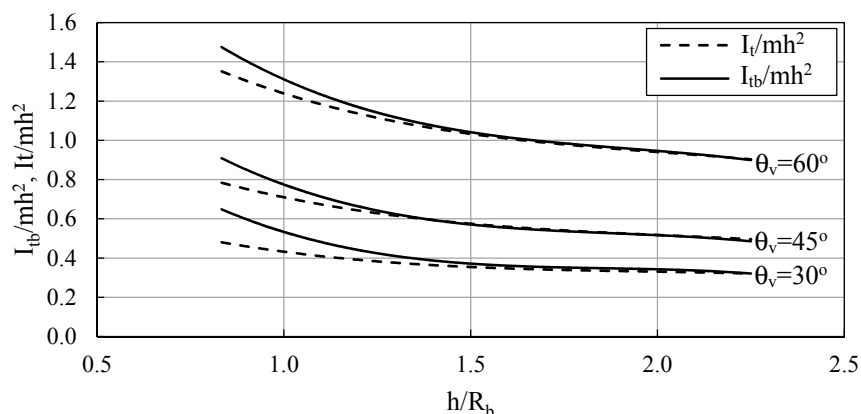
Fig. 5-19 Variation of the parameter I_{tb}/mh^2 and I_t/mh^2 with the slenderness ratio h/R_b

The rigid mass ratio m_r/m_t is found to have higher values as the inclination of the tank walls is reduced which means higher contribution of impulsive mass and less participation of sloshing mass for the same tank as the tank approach a cylindrical tank. This is related to the fact that conical tanks with higher θ_v can be observed as a broader cylindrical tank where the contribution of the sloshing response is increased compared to the impulsive one. On the contrary, the ratios h_{rb}/h, h_{fb}/h, and I_{tb}/mh^2 have higher values as the inclination of the tank walls is increased. This is related to the couple associated with the vertical component of the hydrodynamic pressure which significantly increases with the increase in θ_v.

5.7   Numerical Example

In this section, a numerical example is presented in order to illustrate how the mechanical model developed in the previous section can be used to predict the total seismic forces acting on steel conical tanks undergoing base rocking motion when subjected to a horizontal excitation.

The elevated steel conical tank under consideration has the following dimensions: R_b=4m, h=6m, t_w=10mm, θ_v=45°. The steel Modulus of elasticity is assumed to be 2×10^5 Mpa. The tank is elevated through a hollow circular RC shaft with an outer radius of 4m, L_{sh}=20m, t_{sh}=0.25m. The RC Modulus of elasticity is assumed to be 2×10^4 Mpa. The tank is subjected to the 1940 El-Centro earthquake that occurred in Southern California.

Based on the RC modulus of elasticity and the shaft dimensions, the corresponding stiffness values for the RC shaft are:

K_{xx}=1.37x10^9 N/m   (Eq. 5-21)

$K_{\alpha\alpha}$=8.83x10^{11}N.m/rad   (Eq. 5-23)

$K_{x\alpha}$=1.37x10^{10} N/rad   (Eq. 5-24)

Based on the ratios h/R_b=1.5 and t_w/R_b=0.0025, the following parameters for the mechanical model can be obtained:

f_l=5.9 Hz   (Fig. 5-12)

m_r/m=0.217   (Fig. 5-15)

m_f/m=0.201   (Fig. 5-16)

h_{rb}/h=1.545   (Fig. 5-17)

h_{fb}/h=1.596   (Fig. 5-18)

I_{tb}/mh^2=0.575 (Fig. 5-19)

Due to the existence of the RC shaft in addition to including the base rotation, the steel elevated conical tank can be represented by a 3-DOF system, Fig. 5-11a. The 3 degrees of freedom are: horizontal translation at the tank base y(t) which is different that the ground displacement G(t), base rotation α(t), and horizontal translation of the flexible fluid mass relative to the tank axis x(t).

The problem can be solved using the modal superposition technique where the eigenvalue problem represented by Eq. 5-25 is solved to obtain the eigenvalues, i.e., natural frequencies ω and eigenvectors, i.e., mode shapes ϕ. The mass matrix [M] and stiffness matrix [K] for the 3-DOF system with respect to the displacement vector $d^T=\{x(t) \quad y(t) \quad \alpha(t)\}$ are given by

$$[\mathbf{M}]=\begin{bmatrix} m_f & m_f & m_f h_{fb} \\ m_f & m_f+m_o & m_o h_o+m_f h_{fb} \\ m_f h_{fb} & m_o h_o+m_f h_{fb} & m_o h_o^2+m_f h_{fb}^2+I_o \end{bmatrix} \qquad [\mathbf{K}]=\begin{bmatrix} K_f & 0 & 0 \\ 0 & K_{xx} & K_{x\alpha} \\ 0 & K_{x\alpha} & K_{\alpha\alpha} \end{bmatrix}$$

The relation between the terms m_o, h_o, I_o and m_r, h_{rb}, I_t are given by Eqs. 5-30 to 5-32. The spring stiffness for the flexible mass can be obtained as $K_f=(2\pi f_1)^2 m_f$. Solving the eigenvalue problem for the steel conical tank considered, the natural periods $T_i=2\pi/\omega_i$ and the corresponding mode shapes, normalized to unit x displacement, are

$T_1=0.32$ s $\qquad\qquad\qquad$ $\{\emptyset_1\}^T=\{1 \quad 1.459 \quad 0.125\}$

$T_2=0.037$ s $\qquad\qquad\qquad$ $\{\emptyset_2\}^T=\{1 \quad -0.507 \quad -0.046\}$

$T_3=0.011$ s $\qquad\qquad\qquad$ $\{\emptyset_3\}^T=\{1 \quad -4.536 \quad 0.370\}$

After obtaining different mode shapes $\{\emptyset_i\}$, the modal participation factor Γ for vibration mode i can be obtained as

$$\Gamma_i=\frac{\{\emptyset_i\}[M]\{r\}}{\{\emptyset_i\}[M]\{\emptyset_i\}}$$

where $\{r\}^T=\{0\ 1\ 0\}$

The total base shear V_i and overturning moment M_i can be then obtained as

$V_i=\Gamma_i(\{\emptyset_i\}[M]\{r\})S_{a,i}$

$M_i=\Gamma_i(\{\emptyset_i\}[M]\{m\})S_{a,i}$

where $\{m\}^T=\{0\ 0\ 1\}$ and $S_{a,i}$ is the spectral acceleration for vibration mode i obtained from the 2% damping El-Centro acceleration response spectrum which are $S_{a,1}=0.986g$, $S_{a,2}=0.429g$, and $S_{a,3}=0.319g$ where g is the gravitational acceleration. Finally, the base shear V_i and overturning moment M_i can be obtained for each mode and then combined

using the SRSS combination rule leading to V_{SRSS}=2011 kN and M_{SRSS}=19478 kN. The contribution of higher vibration modes was found to be negligible for the case of the considered elevated steel conical tank.

It has to be mentioned that the mass and mass moment of inertia of the supporting RC shaft were ignored in this example. However, they can be included by adding them to the mass m_o and moment of inertia I_o in the diagonal elements for the mass matrix [M].

5.8 Conclusions

The effect of base rocking motion for steel conical tanks during a horizontal ground excitation is studied. The change in the tank behaviour compared to the case of no rocking motion is mainly attributed to the change of the vibration properties of the conical tank in addition to the variation in the hydrodynamic pressure acting on the tank walls and base due to the existing fluid-structure interaction.

In order to carry out the fluid-structure interaction, a coupled shell element-boundary element formulation is used where a fluid-added mass matrix is obtained corresponding to the tank vessel degrees of freedom including the effect of this base rocking motion. This fluid added matrix is added to the structure mass matrix and then can be incorporated in dynamic or free vibration analysis. For the effect of allowing the tank base to rock on the natural frequency of the $\cos\theta$ impulsive mode and it is found that the percent reduction in the natural frequency is higher for thicker tanks. The percent reduction in the natural frequency is almost constant for the cases of 30º and 45º, while it is lower for θ_v=60º.

The steel conical tanks are then subjected to artificial earthquake excitations corresponding to the NBCC (2010) spectra using non-linear dynamic analysis based on the derived fluid-added mass matrix. The resulting base shear and overturning moment acting on the tank base are compared to the case where rocking is not included. It was shown that the percent increase is higher for the case of overturning moment and can reach up to 32% for the overturning moment and 37% for the base shear. Based on the previous results, it is concluded that allowing the tank base to rock has a major impact on the behaviour and seismic quantities for steel conical tanks.

Finally, a mechanical model that includes the effect of base rocking motion is developed using a frequency analysis approach. The proposed model takes into consideration the impulsive component of the hydrodynamic pressure, deformability of the tank walls, and the hydrodynamic pressure acting on the tank base. The model is validated through comparison with a mechanical model for cylindrical tanks that include the rocking base motion found in the literature. The parameters of the mechanical model are presented in the form of charts for different dimensions of steel conical tanks. The proposed mechanical model can be used for either ground or elevated steel conical tanks undergoing horizontal translation and base rotation. Finally, a numerical example to illustrate how the proposed mechanical model can be used to estimate the base forces for an elevated steel conical tanks is presented.

5.9 References

(API), A.P.I., 2005. *Welded Storage Tanks for Oil Storage*. Washington D.C, USA: American Petroleum Institute Standard.

(AWWA), A.W.W.A., 2005. *Welded Steel Tanks for Water Storage*. Denver, CO, USA.

Chaduvula, U. et al., 2013. Fluid-Structure-Soil Interaction Effects on Seismic Behaviour of Elevated Water Tanks. In *2012 Nirma University International Conference on Engineering (NUiCONE)*., 2013.

Chopra, A.K., 2001. *Dynamics of structures: theory and applications to earthquake engineering*. Englewood Cliffs, NJ: Prentice-Hall.

El Damatty, A.A. et al., 1998. Inelastic stability of conical tanks. *Thin-Walled Structures*, 31, pp.343-59.

El Damatty, A.A. et al., 1997a. Stability of Imperfect Conical Tanks under Hydrostatic Loading. *Journal of Structural Engineering*, 123(6), pp.703-12.

El Damatty, A.A. et al., 1997d. Large displacement extension of consistent shell element for static and dynamic analysis. *Computers and Structures*, 62(6), pp.943-60.

El Damatty, A.A. et al., 1999. Simple Design Procedure For Liquid-Filled Steel Conical Tanks" Journal of structural engineering. *Journal of structural engineering*, 125(8), pp.879-90.

El Damatty, A.A. et al., 1997c. Stability of elevated liquid-filled conical tanks under seismic loading, Part II-Applications. *Earthquake Engng. Struct. Dyn.*, 26, pp.1209-29.

El Damatty, A.A. et al., 1997b. Stability of elevated liquid-filled conical tanks under seismic loading, Part I-Theory. *Earthquake Engng. Struct. Dyn.*, 26, pp.1191-208.

El Damatty, A.A. et al., 2005. Dynamic characteristics of combined conical-cylindrical shells. *Thin-Walled Structures*, 43, pp.1380-97.

El Damatty, A.A. et al., 2005. Experimental study conducted on a liquid-filled combined conical tank model. *Thin-Walled Structures*, 43, pp.1398-417.

El Damatty, A.A. and Sweedan, A.M., 2006. Equivalent mechanical analog for dynamic analysis of pure conical tanks. *Thin-Walled structures,* 44, pp.429-40.

Hafeez, G. et al., 2010. Stability of combined imperfect conical tanks under hydrostatic loading. *Journal of Constructional Steel Research*, 66, pp.1387-97.

Haroun, M.A., 1980. *Dynamic analyses of liquid storage tanks*. Pasadena, CA: California Institute of Technology.

Haroun, M.A. and Ellaithy, H.M., 1985a. Model for Flexible Tanks Undergoing Rocking. *Journal of Engineering Mechanics*, 111(2), pp.143-57.

Haroun, M.A. and Ellaithy, H.M., 1985b. Seismically Induced Fluid Forces on Elevated Tanks. *Journal of Technical Topics in Civil Engineering*, 111, pp.1:15.

Haroun, M.A. and Housner, G.W., 1981. Seismic design of liquid storage tanks. *Journal of the Technical Councils*, 107(TC1), pp.191-207.

Haroun, M.A. and Housner, G.W., 1982. Dynamic Characteristics of Liquid Storage Tanks. *Journal of the Engineering Mechanics Division*, 108(5), pp.783-800.

Housner, G.W., 1957. Dynamic Pressures on Accelerated Fluid Containers. *Bulletin Seism. Soc. America*, 47(1), pp.15-35.

Housner, G.W., 1963. The Dynamic Behavior of Water Tanks. *Bulletin Seism. Soc. America*, 53(1), pp.381-87.

Jacobsen, L.S., 1949. Impulsive Hydrodynamics of Fluid Inside a Cylindrical Tank and of a Fluid Surrounding a Cylindrical Pier. *Bulletin Seism. Soc. America*, 39, pp.189-204.

Koizey, B. and Mirza, F.A., 1997. Consistent thick shell element. *Computer & Structures*, 65(12), pp.531-41.

NBCC, 2010. *National Building Code of Canada*. Ottawa, ON, Canada: National Research Council of Canada.

Sweedan, A.M.I. and El Damatty, A.A., 2002. Experimental and analytical evaluation of the dynamic characteristics of conical shells. *Thin-Walled Structures*, 40, pp.465-86.

Sweedan, A.M. and El Damatty, A.A., 2005. Equivalent Models of Pure Conical Tanks under Vertical Ground Excitation. *Journal of Structural Engineering, ASCE*, 131(5), pp.725-33.

Sweedan, A.M. and El Damatty, A.A., 2009. Simplified procedure for design of liquid-storage combined conical tanks. *Thin-Walled structures*, 47, pp.750-59.

Sweedan, A.M. and El Damatty, A.A., 2009. Simplified procedure for design of liquid-storage combined conical tanks. *Thin-Walled structures*, 47, pp.750-59.

Vandepitte, D., 1999. Confrontation of shell buckling research results with the collapse of a steel water tower. *Journal of Constructional Steel Research*, 49, pp.303-14.

Vandepitte, D. et al., 1982. Experimental investigation of hydrostatically loaded conical shells and practical evaluation of the buckling load. In *Proc. State of the Art Colloquium*. Universitat Stuttgart, Germany, 1982.

Veletsos, A.S., 1974. Seismic Effects in Flexible Liquid Storage Tanks. In *International Association for Earthquake Engineering. Fifth World Conference*. Rome, Italy, 1974.

Veletsos, A.S. and Tang, Y., 1987. Rocking Response of Liquid Storage Tanks. *Journal of Engineering Mechanics*, 113(11), pp.1774-92.

Chapter 6

6 Conclusions and Recommendations

6.1 Summary

The current thesis is related to the seismic behaviour and design of steel liquid conical tanks. The study is conducted numerically using in-house nonlinear finite element model. Chapter 1 covers a literature review for the research conducted on liquid tanks subjected to seismic loading.

In Chapter 2, the capacity of steel conical tanks under hydrodynamic pressure resulting from horizontal ground excitation using non-linear static pushover analysis is evaluated. Two capacities are obtained corresponding to the impulsive and sloshing components of the hydrodynamic pressure including the effect of geometric imperfections. The capacities expressed in terms of base shear values at failure are presented in chart form for different geometries and imperfections' level. The obtained capacities are then compared to the seismic demand obtained using a previously developed mechanical model found in the literature for different seismic zones. The same procedure is followed in Chapter 3 for steel conical tanks under hydrodynamic pressure resulting from vertical ground excitation. The capacities expressed in terms of total vertical force values at failure are presented in chart form for different geometries and imperfections' level.

In Chapter 4, a design approach for liquid steel conical tanks subjected to ground excitations including both horizontal and vertical components is proposed. This approach is based on satisfying a design interaction which is a function of the conical tank capacities obtained in the previous two chapters in addition to the seismic demands obtained based on previously developed equivalent mechanical models found in the literature. The design procedure is validated using the outputs of nonlinear time history analyses.

The effect of the base rocking motion for elevated steel conical tanks on their seismic behaviour when subjected to horizontal excitations is studied in Chapter 5. First, a fluid-added mass matrix that simulates the induced hydrodynamic pressure including the effect

of rocking motion using a coupled shell element-boundary element formulation is derived. This derived fluid-added mas matrix is then incorporated in dynamic and free-vibration analyses in order to assess the effect of including the base rocking motion on the seismic response and the vibration characteristics of the steel conical tanks. Finally, a mechanical model that takes into consideration the effect of the base rocking motion on the hydrodynamic pressure is developed. The parameters of this mechanical model are firstly validated using results from previous studies related to cylindrical tanks and then presented in chart form showing their variations with the geometric parameters of conical tanks.

6.2 Conclusions

The following conclusions are drawn from the first part of the thesis related to seismic loading:

- Based on the comparison between the conical tank capacities and seismic demands for horizontal excitations, it is concluded that for the impulsive hydrodynamic pressure component, the initial design under hydrostatic pressure is found to be adequate for the majority of perfect and good tanks corresponding to Toronto and Montreal seismic zones. However, it is not adequate for poor tanks corresponding to the two seismic zones. With regards to the Vancouver seismic zone, the initial design under hydrostatic pressure has been found to be adequate only for the case of perfect tanks.

- For sloshing hydrodynamic pressure component, the initial design under hydrostatic pressure only is considered satisfactory for most of the cases, with the exception of some good and poor imperfect conical tanks.

- The reduction in the normalized total vertical force capacity Nh/W_cR_b is found to increase with the angle θ_v. The average percentage of the reduction for good tanks is found to be 40%, 53%, and 63% for θ_v=30, 45, and 60, respectively, while for poor tanks, the average percentage of the reduction is found to be 69%, 83%, and 95% for θ_v=30, 45, and 60, respectively.

- The design of the steel conical tanks under hydrostatic pressure only is considered enough to resist the total vertical forces induced by the vertical excitation for the three seismic zones except for poor tanks with $\theta_v=45^o$ corresponding to Montreal seismic zone with h/R_b more than 1.5 and Vancouver seismic zone with h/R_b more than 1.2; good tanks with $\theta_v=60^o$ corresponding to Vancouver seismic zone with h/R_b more than 1.2, poor tanks with $\theta_v=60^o$ corresponding to Toronto seismic zone with h/R_b more than 1.4 and Montreal and Vancouver seismic zones.

- Regarding the time history analysis outputs, it is found that: (1) Impulsive base shear is more critical compared to the sloshing base shear especially for the cases of $\theta_v=30^o$, 45°; (2) The maximum impulsive base shear is reduced as the tank becomes more inclined, while the sloshing base shear is increased for higher θ_v values; (3) The overturning moment is higher for more inclined tanks due to the longer moment arm; (4) The total vertical force is found to be higher for more inclined tanks due to the larger horizontal projection for the inclined wetted surface; (5) The maximum horizontal and vertical impulsive pressure is located in the lower half of the tank height and is shifted upward for more inclined tanks, while the maximum sloshing pressure occurs at the liquid free surface.

- For steel conical tanks designed under hydrostatic pressure, the following is noted regarding the final state at the end of the time history analysis: (1) Perfect tanks corresponding to the three seismic zones and good tanks corresponding to Toronto and Montreal seismic zones behaved elastically and survived the corresponding ground motions; (2) Majority of the good tanks corresponding to Vancouver seismic zone survived the ground motions either elastically or inelastically; (3) Over 90% of the poor tanks with $\theta_v=30^o$, 45° corresponding to Toronto seismic zone survived the ground motions elastically, while the remaining tanks survived inelastically; (4) Majority of the poor tanks with $\theta_v=60^o$ corresponding to Toronto seismic zone survived the ground motions inelastically with some tanks failing due to buckling; (5) Over 90% of the poor tanks with $\theta_v=30^o$ corresponding to Montreal seismic zone did not survive the ground motions elastically, while none of the tanks with $\theta_v=45^o$, 60° survived the ground motions elastically; (6) All poor tanks

corresponding to Vancouver seismic zone did not survive the ground motions elastically with more than 90% of the tanks failing due to buckling.

- For the effect of allowing the tank base to rock on the natural frequency of the $\cos\theta$ impulsive mode, it is found that the percent reduction in the natural frequency is higher for thicker tanks. The percent reduction in the natural frequency is almost constant for the cases of 30º and 45º, while it is lower for θ_v=60º.

- Comparing the resulting base shear and overturning moment acting on the tank base to the case where rocking is not included, it is shown that the percent increase is higher for the case of overturning moment and can reach up to 32% for the overturning moment and 37% for the base shear.

6.3 Recommendation for Future Work

The following recommendations are added for future work which would extend the results presented in this thesis:

- Develop capacity charts for the case of combined conical tanks similar to those obtained in the current study for the case of pure conical tanks.

- Extend the proposed design procedure to be applicable for the case of combined conical tanks.

- Study the effect of residual stresses on the capacity of conical tanks when subjected to hydrodynamic pressure.

- Check the proposed design procedure for the case of elevated conical tanks where the base rocking motion is allowed.

Appendix D
Derivation of Hydrodynamic Pressure

For irrotational flow for an incompressible inviscid liquid, the hydrodynamic pressure, $P_d(r,\theta,z,t)$ satisfies the Laplace equation within the liquid volume represented by ($0 \le r \le$ ($R_b + z \tan \theta_v$), $0 \le \theta \le 2\pi$, $0 \le z \le h$)

$$\nabla^2 P_d = 0$$

where

$$\nabla^2 = \frac{\partial^2}{\partial r^2} + \frac{1}{r}\frac{\partial}{\partial r} + \frac{1}{r^2}\frac{\partial^2}{\partial \theta^2} + \frac{\partial^2}{\partial z^2}$$

The function P_d must satisfy that the velocities of the liquid and the vessel normal to their mutual boundaries should be matched. As the velocity vector of the liquid is the gradient of the velocity potential $\emptyset$ which is related to the hydrodynamic pressure as $P_d = - \rho_l \, \partial\emptyset/\partial t$ where ρ_l is the liquid density, the liquid-container boundary conditions can be expressed as follows:

1. At the rigid tank bottom, $z = 0$, the liquid velocity in the vertical direction is zero

$$\frac{\partial P_d}{\partial z}(r,\theta,0,t) = 0$$

2. The velocity of the liquid adjacent to the vessel wall and the wall itself are compatible in the direction normal to the vessel wall

$$\frac{\partial P_d}{\partial n}(R,\theta,z,t) = - \rho_l \frac{\partial^2 u}{\partial t^2}(\theta,z,t).n$$

where $u(\theta,z,t).n$ is the vessel displacement normal to the vessel wall.

At the liquid free surface, $z = h + \xi(r, \theta, t)$, two boundary conditions must be imposed with ξ represents the sloshing wave height. The first condition is that a fluid particle on the free surface will always remain on the free surface. The second condition is that the pressure

on the free surface is zero. Assuming small-amplitude waves, the free surface boundary conditions can be expressed as

$$\frac{\partial P_d}{\partial z}(r,\theta,h,t) = -\rho_l \frac{\partial^2 \xi}{\partial t^2}(r,\theta,t)$$

$$-P_d(r,\theta,h,t) + \rho_l g \; \xi(r,\theta,t) = 0$$

in which the second-order terms are neglected. The two conditions can be combined to yield the following boundary condition

$$\frac{\partial^2 P_d}{\partial t^2}(r,\theta,h,t) + g\frac{\partial P_d}{\partial z}(r,\theta,h,t) = 0$$

The solution of the Laplace equation $\nabla^2 P_d = 0$ can be obtained by the method of separation of variables and the possible solutions for the Laplace equation, that are nonsingular at $r = 0$ and have vanishing derivative with respect to z at $z = 0$, can be given by

$$P_d(r,\theta,z,t) = \widehat{T}_n(t) \cos(n\theta) \begin{cases} J_n(kr) \cosh(kz) \\ I_n(kr) \cos(kz) \\ r^n \end{cases}$$

where $I_n(kr)$ and $J_n(kr)$ are the modified Bessel functions and Bessel functions, respectively, k is a separation constant, and n is the circumferential wave number.

The solutions of $P_d(r, \theta, z, t)$ should be superimposed to satisfy the boundary conditions at the liquid-shell interface, and at the liquid free surface.

$$P_d(r,\theta,z,t) = -\rho_l \sum_{n=1}^{\infty} \left[\sum_{i=1}^{\infty} A_i(t) \; I_n(\alpha_i r) \cos(\alpha_i z) \cos(n\theta) + \sum_{j=1}^{\infty} B_j(t) \; J_n(k_1 r) \cosh(k_1 z) \cos(n\theta) \right]$$

The first term represents the impulsive component as the separation constant $\alpha_i = (2i-1)\pi/2h$ is chosen to satisfy the condition of zero pressure at the surface, while the second term represents the sloshing component.

Curriculum Vitae

Name: Ahmed Musa

Post-secondary Education and Degrees:
Bachelor of Engineering Science 2003-2008
Department of Civil Engineering
Faculty of Engineering
Cairo University
Cairo, Egypt

Masters of Engineering Science 2008-2011
Department of Civil Engineering
Faculty of Engineering
Cairo University
Cairo, Egypt

Doctor of Philosophy 2011-2016
Department of Civil and Environmental Engineering
Faculty of Engineering
Western University
London, Ontario, Canada

Honours and Awards:
Faculty of Engineering, Cairo University Scholarship
2003-2008

NSERC IPS Scholarship
2012-2015

Related Work Experience
Structural Engineer
ACE Moharram.Bakhoum
Cairo, Egypt
2008-2011

Teaching Assistant
Western University
2011-2016

Assistant Wind and Structural Engineer
Boundary Layer Wind Tunnel Laboratory
Western University
London, Ontario, Canada
2012-2016

Publications:

- Musa, A. and El Damatty, A.A., (2016), "*Capacity of Liquid Steel Conical Tanks under Hydrodynamic Pressure Due to Horizontal Ground Excitations*", Thin-Walled Structures, 103, pp.157-70.
- Musa, A. and El Damatty, A.A., (2016), "*Capacity of Liquid-Filled Steel Conical Tanks under Vertical Excitation*", Thin-walled structures, 103, pp.199-210.
- Musa, A. and El Damatty, A.A., *(2013),"Evaluation of the Buckling Capacity of Steel Conical Tanks Due to Hydrodynamic Pressure"*, Proceeding of the General Conference of the Canadian Society of Civil Engineering, Montreal, QC.
- Musa, A. and El Damatty, A.A., (2014), "*Seismic Behaviour of Steel Liquid-Filled Conical Tanks Initially Designed under Hydrostatic Pressure*" Proceeding of ASCE conference, Hamilton, ON.